ELECTROSLAG CASTING OF VALVE BODIES

by

DEEPAK GUPTA

B.Tech., Indian Institute of Technology, Kanpur, India, 1979

A THESIS SUBMITTED IN PARTIAL FULFILMENT OF

THE REQUIREMENTS FOR THE DEGREE OF

MASTER OF APPLIED SCIENCE

in

THE FACULTY OF GRADUATE STUDIES

Department of Metallurgical Engineering

We accept this thesis as conforming

to the required standard

THE UNIVERSITY OF BRITISH COLUMBIA

January 1982

In presenting this thesis in partial fulfilment of the requirements for an advanced degree at the University of British Columbia, I agree that the Library shall make it freely available for reference and study. I further agree that permission for extensive copying of this thesis for scholarly purposes may be granted by the head of my department or by his or her representatives. It is understood that copying or publication of this thesis for financial gain shall not be allowed without my written permission.

Department of Metallurgical Engineering.

The University of British Columbia
2075 Wesbrook Place
Vancouver, Canada
V6T 1W5

Date Jan. 18., 1982

ABSTRACT

The Electroslag Casting (ESC) process has been widely used in the Soviet Union for the production of high quality steel castings. This work presents the results of an examination of the ESC process for the production of simple shaped valve bodies. Stainless steel (AISI 316 and ACI CF-8M) and low alloy steel (AISI 4340) valve bodies were made at U.B.C. and tested by non-destructive and destructive methods. It is concluded that this technique offers distinct quality and production advantages and the properties easily meet the required ASME/ASTM specifications. Therefore they are equivalent to or better than the conventional castings and forgings. However, there may be difficulties in reconciling the method with present code qualification requirements.

TABLE OF CONTENTS

Chapter | Page

LIST OF TABLES

Tables

LIST OF FIGURES

Figure | Page

Figure | Page

Figure | Page

ACKNOWLEDGEMENTS

I would like to thank sincerely my research supervisor, Professor Alec Mitchell, for his friendly assistance and guidance throughout the course of this research project.

Thanks are extended to my fellow graduate students of the Department of Metallurgy for their helpful suggestions. The assistance of the technical staff of this department, in particular Mr. Gus Sidla, is greatly appreciated.

And finally, I am thankful for the financial assistance of the Natural Sciences and Engineering Research Council of Canada and of the American Iron and Steel Institute.

Chapter 1

INTRODUCTION

With the growth and expansion of the aerospace and nuclear industry, the demand for specialty metals with exceptionally high standards of quality and reliability has increased tremendously. The specifications for the components are becoming more and more rigid. The result is, as might be expected, a high rate of rejection of conventionally made products which fail to pass rigorous testing prior to installation and fail when in service. Although the Vacuum Arc Remelting (VAR) process was conceived as early as the mid-nineteenth century, it has only been used extensively in the last thirty years. Electroslag Remelting (ESR) process, on the other hand, is relatively new. Over the last fifteen years, ESR has been established as an industrially-viable process for the production of high quality material in a wide composition range. The common objective behind the development of both these remelting processes was that of producing high quality material by chemical refining and controlled solidification. The possible high cost of remelting is offset by the processes' advantages of increased service life of the components, very low rejection rates, and high overall yield.

Initially, the ESR process was widely used in U.S.S.R. for upgrading the air-melted quality material. Then the use of ESR was extended to forging applications and the process gained prominence in other countries also. During recent years it became evident that the cast ESR material was equivalent to or better than the conventional castings and forgings. This led to speculation as to whether or not the ESR process can be extended to produce shapes very close to the final cast or forged product (near net shapes). The next step in this logical sequence was the emergence of the Electroslag Casting (ESC) process.

Generally, the conventionally cast components are associated with defects such as shrinkage, porosity, large non-metallic inclusions, segregation and hence have poor and anisotropic mechanical properties. Although with recent casting techniques, such as squeeze-casting, it is possible to produce better quality castings, these are limited to a small scale only and involve heavy capital expense. The hot working processes (forging and rolling) can be applied to eliminate the casting defects and produce a better quality material, but the increase in anisotropy of the mechanical properties and extra cost makes this step unattractive. However, with the ESC process it is not only possible to produce large castings with the same ease as the small ones, but they are free from most of the defects mentioned above and are manufactured

at a comparatively low cost.

The E.O. Paton Institute in Kiev, U.S.S.R. has extensively used the ESC process to produce components for a wide variety of applications. These range from dentures weighing a few grams to very large valve bodies, rolls, pressure vessels, crankshafts, gears, etc. weighing several tonnes[1-2] (see Figure 1). Numerous examples of these are published in the literature.[3-23] The production of fuel-handling components like valves, pumps, and steam fittings for boiling water reactor nuclear power plants and the petrochemical industry has been reported by the Soviets on several occasions.[3-9] ESC tubes and fittings for the petrochemical industry have been manufactured by the Mitsubishi Corporation of Japan.[10-12] They have used the ESC method (YOZO) to produce reformer tubes in HK alloys, (see Figure 2). Tubes with varying section, elbows, oval sections, header tubes and some 'I' beam sections have been produced.[11] Another area of ESC application is in the manufacture of crankshafts, rolls and gears. The production of diesel engine crankshafts up to 160 tonnes in weight has been reported[4-7,9] and they are presently in use in the Soviet Union. Heavy duty kiln-ring gears in sizes up to 150 tonnes for 6-7 meter diameter kilns are reported to be in service.[1,8,13] Paton also reports of the manufacture of ESC rolls for use in the rolling of steel.[5-8,14]

Other reported ESC applications include die blocks in

alloys similar to H11 and H13, cast close to the finished shape,[15,16] hobbing cutters made from T1 and M2 tool steels cast by ESC to the semi-finished shape,[17] gun tubes,[18] precision dentures in austenitic stainless steel,[8] and nozzles cast on pressure vessels.

It is evident from the above list that ESC indeed offers a promising prospect for producing finished shape components without any hot or cold working operation. It is also obvious that most of reports available are of Soviet origin and little or no work has been done in this field in North America. Hence it is of considerable importance to investigate this promising aspect of the Electroslag Remelting process and to determine if the properties of the ESC products qualify under the ASME/ASTM codes, given North American economic manufacturing constraints.

Chapter 2

PROCESS DESCRIPTION AND CHARACTERISTICS

The electroslag remelting process is similar to the vacuum arc remelting process in that both processes use a solid consumable electrode and melt it through a high-temperature process region into a water-cooled mold. However, they differ in the heating mechanism. Unlike VAR, where heating is through an arc, the ESR process utilizes resistance heating of a liquid slag between the electrode and the ingot surface. Detailed accounts of the operation of the ESR process are available in literature.[24-29] The concept of the ESC process is the same as the ESR process except that the ESC process uses a shaped water-cooled mold. This is illustrated schematically in Figure 3. A consumable electrode of desired composition is made as one pole of a high current source and a water-cooled copper or aluminum shaped mold is the other pole. The Joule heat generated in the slag pool melts the electrode tip and molten metal drops fall through the liquid slag into the molten metal pool from which the casting solidifies in the water-cooled mold in a directional, progressive manner. Effective refining of the metal with respect to sulphur, phosphorus and non-metallic inclusions takes place during the formation of the metal drop, as it traverses through the slag pool, and in the liquid metal pool. A continuous shell of

solid slag forms between the mold and the solidifying casting and this provides smooth surfaces to the casting. A sound casting is built up progressively by a nearly vertical solidification pattern. All this effectively eliminates macrosegregation; brings microsegregation to a minimum; and removes porosity, shrinkage, hot cracks and other defects related to conventional castings.

2.1 Electroslag Remelting Process Characteristics Which Affect the Properties of the Materials

Almost all the existing literature on ESR, has, at one point or another, extolled the virtues of the process. Of these the ones which affect the mechanical properties can be broadly classified under the following two categories:

- those related to chemical refining.
- those related to solidification structure.

2.1.1 Characteristics Related to Chemical Refining

The ESR process has earned its name from the inherent refining characteristics. The most important is the removal of large quantities of sulphur, even when the level of this is low in the starting material.[30,31] Very low sulphur levels can be obtained by using highly basic slags. It is well established that one of the most effective ways of obtaining good and reasonably isotropic mechanical properties is through

sulphur control.[32-35] Figure 4 shows the fracture toughness results of a series of ESR 4340 steels containing varying amounts of sulphur.[2] Since sulphides are initiation sites for fracture in many cases, control of their shape and size results in uniform fracture characteristics in three primary directions. It is noteworthy that with the recent advances in ladle steelmaking technologies, it is possible to achieve low sulphur levels and sulphide inclusion shape control. Hence sulphur control is no longer considered to be an important factor deciding for or against the ESR process.

However, although lowering of the overall sulphur level of the steel provides the most significant improvement, desulphurisation is only the first step. Removal of other inclusions and detrimental residual impurities, and controlling the shape and distribution of sulphide inclusions are also of considerable importance in obtaining the optimum mechanical properties. Although many references are available in the literature which deal with the type, size, content and distribution of inclusions in ESR material, very few refer to the actual mechanism by which the non-metallic inclusions are removed from the material during electroslag remelting. As the casting is solidified in a water-cooled metal mold, the chance of exogenous inclusions being present in the remelted material is very low. However, indigenous inclusions of either deoxidation (formed by dissolved oxygen and the deoxidants)

and/or solidification (formed by precipitation during solidification) are present in ESR material. Some of the early work shows that the electrode inclusion content affects the inclusion content of the ingot,[36] but it is well accepted now, as Mitchell[37] points out, that 'virtually no ingot inclusions are identifiable as unreacted electrode relics.' In the liquid metal pool there are few inclusions present, unless very high deoxidation rates are used. The liquid has only dissolved oxygen and deoxidants in near equilibrium with the slag. When the liquid metal freezes, inclusions characteristic of the oxygen and deoxidant content of the liquid are nucleated and grown in the ingot liquid-solid zone.[25,30,37] This process gives rise to a fine background of small, globular and dispersed inclusions. The total volume fraction in ESR is much lower than the best air-melting practice.

Generally, inclusions have a greater effect on non-uniform deformation (percent reduction in area) than upon uniform deformation (percent elongation). If the inclusions have an anisotropic shape (e.g. elongated sulphide inclusions in rolled material), ductility will be anisotropic. Therefore, the non-metallic inclusion content of remelted steels is of prime importance in determining their mechanical behaviour.

2.1.2 Characteristics Related to Solidification Structure

Contrary to the conventional casting processes in which

melting and casting represent two separate and different operational steps, the ESR process is characterized by addition of heat during the solidification step. Hence the temperature gradients and the solidification rate can be controlled to establish a progressive and directional solidification condition (obtained by high thermal gradients and low growth rates). Such slow melt rates are possible firstly due to the insulating character of the slag pool which levels off the thermal gradients across the pool and secondly due to the formation of the thin slag skin between the mold wall and the metal. These solidification conditions lead to a structure which is practically free of porosity, shrinkage, hot-cracks, etc. This also effectively eliminates macroscopic inhomogenities such as banded structure or freckles, macroscopic spot segregation, and brings microsegregation to a minimum.

Although low melt rates lead to a fine dendritic structure, microsegregation is pronounced as the system deviates from equilibrium solidification. Also very high melt rates lead to an equiaxed structure with increased microsegregation. An optimum melt rate leads to least microsegregation and hence good mechanical properties.[38]

In conclusion, it can be said that the enhanced mechanical properties and isotropic behaviour of the ESR material are due to good chemical refining and solidification structure.

Chapter 3

PRESENT WORK

In the latter part of 1974, a program was initiated among Dr. Alec Mitchell, Professor of Metallurgy U.B.C., Westinghouse Electro-mechanical Division (WEMD) and Dr. Boris Medovar, Director of ESR Technical Development at Paton Institute, Kiev, U.S.S.R. A 10-inch ESC valve body was made in the U.S.S.R. and sent for evaluation at U.B.C. and WEMD. Evaluations of destructive and non-destructive testing of the valve body are available.[39,40] The results indicate that the casting quality failed chemically and mechanically to meet ASME requirements as originally predicted by the Soviet workers.

Hence to study in-depth the properties and the process viability of ESC products, a simple and inexpensive ESC furnace was installed at U.B.C. The furnace is capable of making castings up to one tonne. The furnace has made valve-body castings in alloy and stainless steels from both wrought and cast electrodes.

3.1 Furnace Design

Detailed account of the design and operation of this furnace has been reported previously.[41]

The mechanical part of the design consists of a water-cooled electrode holder carriage which can move vertically using aluminium rail guides. These guides are fixed to the inside of a vertical I-beam framework. The carriage is suspended from a single chain drive having a variable speed reductor and this in conjunction with a speed controller gives a range of electrode speeds from 0-163 mm/min (see Figure 5).

The electrical part consists of two step down transformers. The first one is rated at 250 KVA with 12500 V input and 600 V output. The second transformer is single phase dry type and is also rated at 250 KVA with input voltage of 600 V and output voltage variable over a range of 25V - 60V in steps of about 2.5 V.

The operating parameters can be monitored from the control panel which not only shows the primary and secondary current and secondary voltage but also has a digital counter to measure the electrode travel. Also, a multichannel thermometer shows the mold cooling water temperatures.

3.2 Valve Mold Design

Smooth surface finish, flat tops and bottoms, controlled vertical solidification and shaped products are some of the discussed unique features of ESR ingots. All of these are directly attributable to or are strongly influenced by mold design

and operating parameters. The optimum mold design is associated with the manner in which the mold assembly dissipates the heat primarily from the slag layer, molten pool and solidified ingot casting. ESR mold design has been discussed to some extent by Mitchell[25] and Cremesio et al.[42]

Most of the ESR molds used are made out of copper because of its high thermal conductivity. This adds substantially to the overall cost of the product. Fabrication of a copper mold also presents a problem as the metal has to be formed and welded into the mold shape. This is particularly difficult for ESC molds with contoured sections. Since the inventory costs and fabrication make copper molds unattractive, a cast-to-shape mold of less costly aluminum was considered to be a viable alternative.

Gear castings using a cast aluminum mold were made successfully in U.B.C. The water channel positions and dimensions in the gear mold were roughly calculated to give a maximum hot-face temperature of 300°C during the ESC process.[43] Following this, an aluminum mold for casting of valve bodies was manufactured.

The valve mold was cast out of aluminum using a steel pattern. The orthogonal views of the valve body are given in Figure 6. Accordingly the complete valve mold was divided into

four segments - two plate molds for the flat sides of the valve and two molds with cupped depressions to accommodate the inlet/outlet sections of the valve. The sectional drawings of these segments are given in Figure 7a-b. Figure 8 shows the assembled valve mold. Besides this, two round section molds were used - one on top and the other at the bottom of the valve mold.

3.3 Melting Procedure

The valve mold is placed between two round molds and the whole assembly is placed on a water-cooled copper base plate. To prevent any damage to the base plate due to arcing with the electrode at the initiation of the process, a starter block is used. There are two different practices employed to initiate the process. One is known as 'molten-slag' start and the other is the 'dry-slag' start. Both the processes were tried and they worked equally well.

In the 'molten-slag' start the main slag component, i.e. CaF_2, is melted in a slag melting furnace (see Figure 9). This furnace has a graphite crucible and employs a single-phase graphite electrode system. CaF_2 is added to the furnace and power is applied to initiate an arc which forms a small pool of molten CaF_2 and then the heating is through resistance heating of the slag. When all the slag (CaF_2) has melted, it is poured into the water-cooled mold and the electroslag furnace

is energized. After this the remaining slag components are added slowly.

In the 'dry-slag' start, a bed of turnings of a metal similar to the electrode is placed between the starter plate and the electrode. Alternatively a pellet of compressed mixture of CaF_2 and metal turnings can be used. Either one of these is used and the electrode is lowered such that it presses the turnings against the starter plate. Then the dry CaF_2 is poured into the surrounding annulus between the electrode and the mold walls. When the furnace is energized, power is applied across the short-circuit current path established by the turnings under the electrode. This causes melting of the slag and continues till a large enough volume of molten slag is generated to sustain resistance heating. After all the CaF_2 is melted, the remaining slag components (CaO, Al_2O_3, La_2O_3 etc.) are added.

The electrode is lowered as it melts and the mold is slowly filled up with resolidified metal. At the end of the run, power is terminated and the electrode is withdrawn from the mold, the casting being taken out after about thirty minutes. The castings have a smooth surface due to a thin, continuous shell of solid slag which forms between the mold and the solidifying metal (see Figure 10).

The main operating parameters established during the production of valve castings were as follows:

- operating voltage 36-39V
- primary current 200-260 A
- secondary current 3000-4000 A
- melt rate 0.8-1.0 kg/min.

3.4 Selection of Slags for ESC Process

The slag pool is perhaps the most important component in the electroslag remelting process. It is required to 'fill a number of simultaneous functions - it must act as a heat source, heat-transfer medium, metal container and metal refiner.'[44] Therefore the correct choice of slag composition is of prime importance for successful ESR operation.

The choice rests upon the following:

a) heat generation and transfer characteristics of the slag - (electrical conductivity, thermal capacity and thermal conductivity).

b) slag phase properties - (vapour pressure, liquidus temperature, viscosity, surface tension and density).

c) metal refining characteristics (chemical composition).

The more important of the above points are discussed below with reference to slag selection.

The ternary CaF_2 - CaO - Al_2O_3 system is the most important and universally applicable slag system in the field of ESR. Fluoride generally decreases the solidus and liquidus temperatures and viscosity, and increases electrical conductivity of CaF_2 + Al_2O_3. It has been observed that relatively small additions of Al_2O_3 to pure CaF_2 produces a substantial decrease in the conductivity of the liquid. The work of Mitchell and Cameron[45] showed that this occurs because the fluoride ion contribution to the total ionic mobility is reduced by complexing it in $AlOF_2^-$ and $AlO_2F_2^{3-}$. This would be through the reaction:

$$Al_2O_3 + 4F^- \longrightarrow AlO_2F_2^{3-} + AlOF_2^-$$

This effect is also seen in the addition of silicates and of rare earth oxides. However, addition of CaO replaces the fluoride part of the complex ions by oxide ions thus releasing fluoride ions as charge carriers, e.g.,

$$AlO_2F_2^{3-} + O^{2-} \longrightarrow AlO_3^{3-} + 2F^-$$

and

$$AlOF_2^- + O^{2-} \longrightarrow AlO_2^- + 2F^-$$

This produces an increase in electrical conductivity but this increase is not substantial.[44] Low electrical conductivity by the addition of Al_2O_3 leads to higher melt rates and higher efficiency.

It has also been noted[46] that the rate of dissolution of Al_2O_3 in CaF_2 is higher in the presence of CaO. This is because Al_2O_3 dissolves essentially by an acid/base reaction:

$$Al_2O_3 + O^{2-} \rightleftharpoons 2AlO_2^-$$

and hence is dissolved much faster by a slag containing CaO than CaF_2 alone. This decreases the overall melting time and thus also increases the efficiency.

Due to the high temperatures attained during the melting, expecially in the region directly below the electrode, the thermal stability of the slag components should be high i.e. the slag components should have a low vapour pressure. Also it has been noted[44] that production of CaO due to volatility of CaF_2 through the reaction

$$Al_2O_3 + 3CaF_2 \rightleftharpoons 2AlF_3 + 3CaO$$

can cause significant shift in Al_2O_3/CaO ratio. Presence of SiO_2 and H_2O will have similar effects.

An essential requirement for the slag to be a suitable melting medium is that it must have a liquidus temperature at least 100°C below that of the metal, but must also form a solid phase on freezing which has a melting point higher than that of the metal.[44,47] These conditions lead to good surface quality of the castings.

The phase diagram for CaF_2-$A\ell_2O_3$-CaO is shown in Figure 11.[48] From this it can be seen that for low liquidus temperatures of the slag, approximately equal proportions of $A\ell_2O_3$ and CaO should be present in the ternary slag system.

The metal refining characteristics are a complex function of the slag composition, power mode (a.c. or d.c.), melting conditions, deoxidation, and of course the metal that is being refined. CaO is primarily used as a desulphurising agent. It has been suggested[44] that addition of a rare-earth-oxide (RE_2O_3) to the ternary system of CaF_2+CaO+$A\ell_2O_3$ leads to wide regions in the phase diagram where the physical properties are compatible with ESR processing. Besides strongly complexing O^{2-} and F^- (hence increasing the electrical resistivity), the presence of $(RE\text{-}O\text{-}S)^{n-}$ complexes also leads to a strongly basic behaviour with respect to sulphur reactions. Both these conditions are highly desirable for ESR.

Taking the above points in consideration, two different slag compositions were selected for stainless steel and low alloy steel castings. For stainless steel we had

$$70\%\ CaF_2\ ,\ 15\%\ CaO\ ,\ 15\%\ A\ell_2O_3$$

and for low alloy steel (AISI 4340) where a very low sulphur content is required we had

$$50\%\ CaF_2\ ,\ 15\%\ CaO\ ,\ 15\%\ A\ell_2O_3\ ,\ 20\%\ La_2O_3$$

As the slags used were highly basic and the fact that the castings were deoxidised, careful control of residual hydrogen content in the castings was of prime importance. Three main sources of hydrogen in ESR are the hygroscopic, basic slag, the humidity of the atmosphere from which hydrogen is transported through the slag into the liquid metal pool, and the hydrogen content of the electrode. Of these the last one is not so serious as the first two because sufficiently low electrode hydrogen contents can be obtained by today's steel melting practice. Highly basic slags (e.g. slags containing CaO) hydrate easily. Also hydrogen pick-up from the atmosphere is increased if basic slags are used because such slags promote the formation of OH^- ions -

$$O^{2-} + H_2O \rightleftharpoons 2OH^- \quad \text{(at the slag surface)}$$

and this is subsequently transferred to the metal.

$$2OH^- \rightleftharpoons O^{2-} + [O] + [2H] \quad \text{(at the slag-metal interface)}$$

According to this a low partial pressure of O_2 in Fe (as in the deoxidised condition) would promote transfer of hydrogen to the metal

Careful storage, preheating, prefusing, and using the molten slag start technique are a few ways to avoid hydrogen

in the slag. Hydrogen from the atmosphere can be reduced by creating a dry atmosphere by simply protecting the surface of the slag by a shielding hood. Application of superimposed d.c. on a.c. melting has also been claimed to reduce the hydrogen content during electroslag remelting,[49,50] but these were an ambiguous series of experiments.

Utilizing the molten-slag start technique, hydrogen problems were not encountered in the castings. However, when the dry slag-start technique was used, the problem of hydrogen was severe enough to create several longitudinal holes in the bottom half of the castings. Using prefused or even double prefused slag in dry start did not solve the problem. The ternary diagram of CaF_2-$A\ell_2O_3$-CaO (shown in Figure 11) showed that 70%CaF_2/15%CaO/15%$A\ell_2O_3$ slag composition could precipitate some CaO when solidified and this could easily rehydrate. Therefore prefusing the slag did not eliminate hydrogen in the casting.

To avoid hydrogen problems due to moisture in the slag in the dry-slag start, the components were heated to sufficiently high temperatures. CaF_2 and $A\ell_2O_3$, which are not so susceptible to moisture, were preheated to 500°C while CaO was preheated and $La_2(CO_3)_3$ was calcined at 800°C. These were used directly in the hot condition. No traces of moisture related porosity were observed.

Although it was a clear indication that the holes in the castings were due to the moisture in the slag, precaution was taken to avoid hydrogen from the atmosphere. A shielding hood made of stainless steel and lined with saffil (Al_2O_3 fibrous sponge) was used. This had a hole in the middle for the electrode and two more small holes at the side - one for addition of deoxidant and alloying additions and through the other hole argon was passed during the melting operation.

Several valve castings were made in low alloy steel (AISI 4340) and cast stainless steel (CF-8M). All the valves were subjected to non-destructive testing (NDT), macroexamination, microexamination and mechanical testing.

The next section deals with the evaluation of valve castings and has been divided into two parts. Part A deals with the stainless steel valve castings while part B deals with low alloy steel (AISI 4340) valve castings.

Chapter 4

EVALUATION OF ESC VALVE CASTINGS

A. STAINLESS STEEL VALVE CASTINGS

Five stainless steel valves were made. Out of these two were made from CF-8M (0.08% max. C, 1.5% max. Mn, 1.5% max. Si, 0.04% max. S, 0.04% max. P, 18.0-21.0% Cr, 9.0-12.0% Ni, 2.0-3.0% Mo) electrode, one from 316 (0.08% max. C, 2.0% max. Mn, 0.03% max. S, 0.04% max. P, 1.0% max. Si, 10.0-14.0% Ni, 16.0-18.0% Cr, 2.0-3.0% Mo) rolled bar, one from 316 rolled bar with controlled addition of chromium chips and the last one with 316 rolled bar from controlled additions of ferro-chrome and ferro-molybdenum powder. The alloying was done to change the 316 bar chemistry to CF-8M composition. This was done keeping in view that even a manufacturer who does not have electrode casting facility can produce CF-8M castings with the readily available 316 rolled bar composition.

Besides this, a CF-8M block (12" x 16½" x 17") was conventionally cast after refining in AOD. The heat treatment given was a double quenching treatment from 1094°C (2000°F). The properties of this conventional casting were compared with ESC valves.

A typical electroslag casting of a valve body made in stainless steel is shown in Figure 12.

4.1 Remelting Log for Stainless Steel ESC Valves

Table I gives the melting conditions for 5 stainless steel valves made by the ESC process. Some of the special characteristics noticed during the melt or in the castings are as follows:-

Valve No. 5 - Melting had to be interrupted abrubtly (hence no hot topping cycle) because of a minor explosion heard towards the end of its run. This will be discussed in section 4.3.7. To avoid any porosity due to the moisture in the slag components (particularly CaO), the slag was prefused and crushed for use. However, when the casting was sectioned, large holes (about the diameter of a pencil) running longitudinally from the bottom for a distance of about 8 inches were observed (see Figure 13). As the slag was prefused, the chances of moisture being responsible for the holes were low. They could also be due to carbon monoxide evolution due to insufficient deoxidation.

Valve No. 6 - The casting was incomplete because the electrode was not long enough. Extra aluminum powder was added in the beginning of the run to avoid CO evolution Also the mold was covered from the top and argon was passed over the slag. The sectioned casting again showed

longitudinal holes. At this point it was certain that the holes were due to moisture.

Valve No. 7 - Electrolytic chromium chips were added to increase the chromium content of the casting. The slag was prefused twice to avoid the moisture problem but again there were some holes. However, the size and density of these holes had decreased considerably. As mentioned in section 3.4 the holes were due to rehydration of precipitated CaO in the fused slag.

Valve No. 9 - Heating the slag components to high temperature (mentioned before) avoided the problem of moisture in the slag. No trace of moisture related porosity was observed. The casting was sound and complete.

Valve No. 10 - 70% Fe-Cr and 65% Fe-Mo powder was added to increase the chromium and molybdenum contents of the casting. The feeding rate was uneven because of an inadequate feeding arrangement which probably resulted in clusters of ferroalloy powder segregated in pockets in the casting. No porosity was observed in this casting.

4.2 Non-Destructive Testing (NDT)

As U.B.C. does not have the facility for radiography and the appropriate ultrasonic testing for heavy sections, two

CF-8M valves were externally evaluated - one for radiography and one for ultrasonic testing.

4.2.1 Dye Penetrant Test

The stainless valves were sectioned longitudinally and a conventional dye-penetrant system was used. It showed that the internal surface was sound.

4.2.2 Ultrasonic Test

Ultrasonic testing was performed on a full ESC valve and then on a sectioned half casting. The testing was done according to the ASME SA-388 (ASTM A 388-71) specification for heavy section steel forgings. Test results indicate that 'no useable ultrasonic response was received from the austenitic (CF-8M) stainless steel valve casting at depths of 7-3/4 inches...' The ASME specifications also note that the 'heavy austenitic stainless steel forgings are more difficult to penetrate ultrasonically than similar carbon or low-alloy steel forgings. The degree of attenuation normally increases with section size; and the noise level, generally or in isolated areas, may become too great to permit detection of discrete indications. In most instances this attentuation results from inherent coarse grained microstructure of these austenitic alloys.' Following this a three inch thick section with one machine cut surface was tested with the 1 MH_z - 3/4 inch diameter transducer. The

penetration direction was transverse to the grain orientation. It was still questionable whether or not fine defects could be detected.

Although a better penetration could have been accomplished in the direction of the grain in a three inch section, these results indicate that ultrasonic testing is not suitable for austenitic stainless steel ESC valves.

4.2.3 Radiography Test

Radiography was performed in accordance with ASTM E 94-77 specification using a cobalt-60 source. No apparent defects could be detected.

4.3 Destructive Testing (DT)

The conventional and ESC valve castings were sectioned longitudinally through the middle and half inch thick plates were cut out (see Figure 14) for destructive tests.

4.3.1 Macrostructures

The half inch thick plates were surface ground and macro-etched in an acid solution (38% HCℓ, 12% H_2SO_4, 50% H_2O) at about 65-70°C for 1-2 hours. The macrostructures obtained are shown in Figures 15-19. The grain structure clearly shows the chilling effect of the water-cooled mold and almost

vertical solidification pattern. Also, the structures are essentially free of solidification defects although some peculiarities do exist. Figure 16 shows a slag inclusion at the top of the casting. This was due to an interrupted hot-topping cycle and can be corrected easily. Figure 17 shows a change of pool profile in the top right hand corner and a peculiar structure in the centre. This is believed to be a piece of electrode which dropped during the melting operation. Figure 18 shows some big inclusions scattered in the casting. This casting was made with the addition of ferro-chrome and ferro-molybdenum powders during the melt and these inclusions are believed to be due to the ferro-alloy additions. These two cases will be identified and discussed subsequently.

The macrostructure of the top quarter part of the longitudinal section of the conventional CF-8M casting is given in Figure 19. Most of the area is covered by equiaxed grains though there is some columnar structure near the edge of the casting. This macrostructure also shows a banded structure between the columnar and the equiaxed zones and at an angle to the top surface. This is thought to be due to either a feeder or a riser placed at this position.

The macro-etched plates were then cut up for micro-examination and other tests.

4.3.2 Microstructures

The austenitic cast stainless steel designated as CF-8M by ACI closely corresponds to the wrought grade AISI type 316 stainless steel. The silicon and chromium contents of the cast alloy are higher and the nickel content lower than in the wrought alloy. The variations in chemistry may be small but they are not trivial - they provide for optimum forgeability and considerable ductility for hot and cold working on one hand and optimum castability on the other. Depending principally on composition, but also on thermal history to a lesser extent, microstructures ranging from non-magnetic (fully austenitic as in Type 316) to perceptibly magnetic (due to substantial amounts of ferrite phase present in the austenitic matrix, as in CF-8M) can be produced.

Besides production of sound castings, presence of delta-ferrite improves weldability and improves the resistance to hot cracking during casting operation.[51] It also improves resistance to corrosive media such as sulphurous and acetic acids, to intergranular attack,[52] and to chloride stress corrosion cracking.[53] Delta ferrite also increases the proof stress and tensile strength values by a dispersion-strengthening effect[54] (this will be discussed later). This is the real reason for higher chromium content in CF-8M.

From the above we see that presence of delta-ferrite in CF-8M castings is essential to obtain good corrosion

resistance and mechanical properties. However, the presence of delta-ferrite in austenitic stainless steels has been shown to accelerate the formation of an intermetallic sigma phase.[55] Sigma phase was first detected in Fe-Cr-Ni alloys and reported in 1927.[56] It has been identified as a hard, brittle, non-magnetic, intermediate phase with a tetragonal crystal structure occurring in many binary and ternary alloys of the transition elements and has been well documented in the literature.[47,58,59] The formation of sigma phase is enhanced by addition of ferrite-stabilizers such as chromium, molybdenum and silicon. Although this phase forms most readily from ferrite, it can also form from austenite.[60] Sigma formation is time- and temperature-dependent and can be described on a transformation diagram by a typical 'C' curve.[61] The temperature range of sigma formation is regarded as about 600°C to 950°C and in alloys of the 18-8 type with 2 to 3 percent molybdenum and retained delta-ferrite, the maximum rate of formation occurs at about 850°C with ferrite transforming to sigma and austenite in less than one-half hour.[62] It has been reported[63,64] that delta-ferrite being a region of relatively high chromium content, forms sigma in a comparatively short time by a concentration of chromium through diffusion from adjacent chromium-rich ferrite to areas where sigma nucleated. The depletion of chromium in the surrounding ferrite eventually results in the formation of austenite. This is shown in Figure 23.

The effects of sigma on the corrosion behaviour of austenitic stainless steels are most serious in highly oxidising environments such as nitric acid.[59] In general sigma phase increases the hardness, yield strength, and tensile strength, but decreases the impact strength, both at room temperature and at elevated temperatures. Loss of low temperature ductility and corrosion resistance is particularly severe when the sigma phase forms a nearly continuous network around the austenite grains.[62]

In consequence of the above discussion, it is important to identify the ferrite and sigma phases in the stainless steel valve castings and to eliminate any sigma phase present in the as-cast condition by a suitable heat treatment. The CF-8 type cast alloys are used in the solution treated condition which involves heating at 1100 to 1150°C and quenching in water or oil. The heat treatment adopted was heating the specimens to 1120°C for 1-2 hours and quenching in water. The microstructure after heat treatment was essentially austenitic with ferrite distributed throughout the matrix in discontinuous pools. Sigma phase was eliminated.

Many techniques have been cited in the literature to identify and differentiate sigma phase from other phases occurring in austenitic stainless steels.[63,65] Two different polishing and etching procedures were used to identify the ferrite and sigma phases in ESC valves.

In the first one, the specimens were mechanically polished to 5 microns, then electro-polished in chromic-acetic solution (133 ml acetic acid, 7 ml water, 25 gms CrO_3) at 28-30 V for 8-10 minutes. Then they were electro-etched in 10 wt.% oxalic acid solution at 6 V for 20-30 seconds. This procedure was found to outline the ferrite phase clearly and the oxalic acid etch attacks the sigma phase very rapidly. Figure 20a-b shows the microstructure of a specimen from CF-8M valve in the as-cast condition. The ferrite phase shows up in relief and it is clearly outlined and the sigma phase which is predominantly present within the ferrite phase is attacked severely. The heat treated specimens show that the sigma phase is eliminated and only ferrite is left behind. Similarly Figures 21 and 22 show the microstructures from 3 different valves in the as-cast and heat-treated conditions respectively.

In the second procedure, the specimens were polished to 1 micron and etched in a mixed acid solution (HNO_3 and HCℓ in H_2O) several times to remove the disturbed metal. Then they were etched in Vilella's reagent (5 mℓHCℓ, 1 gm picric acid, 100 mℓ ethanol) to outline the sigma phase. Ferrite is faintly outlined. Then the specimens were electro-etched in 10N KOH solution (56 gms KOH, 100 mℓ water) at 2.5 V for a few seconds. This stains the sigma phase yellow to reddish-brown and the ferrite to bluish-grey. Austenite is not attacked. One specimen from the conventional CF-8M casting was kept at 850°C for

14 hours to promote sigma formation and then it was etched with the above procedure. Figure 23 shows the microstructure of this specimen. The black regions are the sigma-phase, the dark grey regions are the untransformed ferrite phase, and the light grey area is the austenite. The austenite which has been transformed from ferrite is also seen. As the conventional casting was received in the solution-treated condition, the microstructures given in Figure 24 shows that only ferrite and austenite are present. Figure 25 shows the microstructure of a CF-8M ESC valve No. 9 in the as-cast condition. Sigma phase within the ferrite boundaries is easily detected. Figure 26 shows the specimens from the same valve but in the solution-treated condition. Sigma phase is completely eliminated.

Microhardness tests on sigma and austenite were also carried out to confirm that what has been distinguished to be sigma phase from metallography is actually the hard and intermetallic sigma phase. Figure 27 shows the identation of the diamond pyramid hardness indentor on sigma and austenite phases. The relative DPH values calculated from these are -

sigma phase - 643.3 DPH

austenite phase - 255.0 DPH

The microhardness value obtained for sigma phase is somewhat lower than the value quoted in literature which is 750 DPH.[63] This difference could be because the indentation taken

here is over a network of sigma particles while the literature value is within a large isolated sigma particle.

4.3.3 Delta Ferrite Measurements

The importance of delta ferrite in austenitic stainless steel cast alloys has been discussed briefly in the last section. It becomes essential, therefore, to determine the ferrite content of the castings. The ferrite content was measured by three different instruments - a Ferrite Indicator, a Magne Gage, and a Quantimet. Ferrite content was also estimated from the Schoefer's[66] diagram.

The Ferrite Indicator uses magnets calibrated to known ferrite numbers to 'bracket' the ferrite content of the test piece between two ferrite numbers. The ferrite number has been adopted as the accepted index which quantifies the ferrite content. Although closely related to actual percentage ferrite content, particularly at low ferrite contents, the ferrite number does not correspond precisely to percent ferrite. Measurements were done on the specimens used for microexamination. The surface was rough polished to avoid erroneous results due to oxidation. Table II shows the ferrite numbers obtained from different locations in the castings.

As the Ferrite Indicator only 'brackets' the ferrite content, a Magne-Gage was used to find out the specific

ferrite content of the castings. This instrument also works magnetically and has a calibrated coil spring attached to a pointer which moves on a dial. The dial reading indicates the ferrite content of the test specimen in ferrite numbers. The specimens were polished to 320 grit to provide an even, clean and similar surfaces to all specimens. The ferrite contents obtained from various locations in the castings are given in Table II. Table III gives the average ferrite number of each casting in the as-cast and heat-treated conditions. From this table it can be noticed that for valve numbers 5, 6 and 7, the ferrite contents in the heat-treated condition are lower than in the as-cast condition. Normally, an opposite result would be expected due to the presence of sigma phase within the ferrite boundaries in the as-cast condition. This anomaly can be explained by the thermal history of the heat-treated specimens. The specimens from these three valves were heat-treated in stainless steel bags to avoid excessive oxidation. It was found that quenching of the specimens was not fast enough as it was difficult to cut open the bags before quenching. Hence the microstructure still showed some sigma phase. Therefore the specimens were heat treated again without the stainless bags and quenched in water. It seems that this particular thermal cycle resulted in lower ferrite content. It has been indicated[67] that the residual ferrite content of duplex alloys is strongly influenced by the solutioning temperature and the subsequent cooling rate.

Another point which emerges from the ferrite measurements is that the ferrite content of the topmost part of the casting is much lower than the bulk of the casting. This is probably due to the very slow cooling rate of the top part of the casting. Towards the end of the run, there is a brief hot topping cycle and after the run has been terminated the slag blanket solidifies slowly and acts as a thermal insulator for the last part of metal to freeze.

Ferrite measurements were also done by using the Quantimet. A stain etch was done using the technique described in the last section. It was found that it was difficult to get a good accuracy in the Quantimet. The ferrite forms a net work particularly at higher ferrite contents and it is difficult to cut out the 'snow' or noise in the normal mode. The 'snow' can be reduced by using the 'ground cut' mode and lower resolution, but this mode makes it difficult to set the threshold values which in turn leads to variable results. The use of any other more sophisticated technique was not considered to be necessary in this study.

Theoretical estimation of the ferrite content was also carried out using the Schoefer's diagram. Schoefer[66] has developed a one-line constitution diagram for cast Fe-Cr-Ni alloys with which the ferrite content of the

alloy can be estimated accurately knowing only the alloy composition. It was derived from Schaeffler's diagram for weld metal. The Schoefer's diagram requires the conversion of all ferrite-promoting elements into 'chromium equivalents' and all austenite promoting elements into 'nickel equivalents' through the use of coefficients representing the ferritising or austenitising power of each element. The diagram is shown in Figure 28. Table III also gives the calculated ferrite contents using the Schoefer's diagram. It can be seen the ferrite numbers estimated from Schoefer's diagram are higher than those obtained by Magne Gage particularly at higher ferrite contents.

Tensile data generated by other workers[62] on CF-8M shows that the strength levels are directly related to the ferrite content. Comparison of the strength levels obtained on conventional CF-8M casting showed that the ferrite content obtained by Magne Gage is similar to that found by those workers. Also, Schoefer's diagram is applicable to as-cast rather than heat-treated condition. As mentioned earlier the residual ferrite contents are greatly affected by the solutioning temperature. Quenching from 1300°C results in twice as much ferrite as quenching from 1150°C.[67]

4.3.4 Interdendritic Microsegregation

It has been frequently claimed[68,69] that interdendritic microsegregation in electroslag remelted material is greatly

reduced from that in the equivalent section in conventional casting. In general, low melt rates and small cross sections lead to low microsegregation. As mentioned in Section 2.1.2 an optimum melt rate is needed to achieve least microsegregation.

Microsegregation was studied by electron microprobe analysis of samples from two CF-8M valve castings (in the as-cast condition) and the conventional CF-8M casting (in the heat-treated condition). Line scans were performed in selected areas and across the dendritic direction. Before analysis the samples were etched and the lines to be traversed were marked with microhardness indentations such that they were 5 mm apart. After photographing the samples in the etched and marked condition, they were repolished before the analysis. The 'segregation ratio' (defined as the ratio of maximum composition to minimum composition) of three alloying elements (Cr, Ni, Mo) was determined in all the samples. Figures 29a, b and 30 a-c show the line scan of the microprobe along with variation of solute concentration along the line, while Table IV gives the segregation ratios obtained from the analyses. The results show that -

a) Out of elements analysed, molybdenum is the most highly

segregated element followed by nickel and then chromium.

b) Interdentritic microsegregation or the segregation ratio increases from the edge to the centre of the castings.

c) Microsegregation is much lower in the ESC valves than in the conventional castings for an equivalent distance from the edge. This is clearly depicted from the segregation ratio of molybdenum which is a heavily segregating element.

The segregation ratio, as defined here, does not represent the true interdendritic microsegregation because the alloy in consideration has a duplex structure with delta ferrite forming interdendritically during solidification process. Three stages of solidification in 18-8 stainless steels have been reported.[70] The first precipitation of delta ferrite is interrupted by the precipitation of austenite and at the end of solidification there is a transition back to precipitation of delta ferrite. Austenite grows into and consumes most of the dendrites which form initially as ferrite and then at the end of solidification ferrite is precipitated from the residual melt in the interdendritic areas. So the segregation value determined here includes the partioning of alloying elements between the austenite and ferrite phases and hence does not present a true picture of microsegregation due to solidification directly from the liquid. From the line scans it can be seen that an enrichment of nickel shows a corresponding depletion of chromium as one would expect in the austenite phase. In the ferrite phase an opposite effect

is noticed. Therefore, the segregation ratio should be determined from the segregation occurring within austenite or ferrite.

4.3.5 Composition Analysis and Macrosegregation

Top to bottom and side to side composition analysis of the ESC valves and the conventional casting was carried out using optical emission spectrograph. Tables V-X show the average composition of different regions of the castings along with the electrode composition for comparison. It can be seen that there is a negligible composition difference between the electrode and the casting.

The advantage of ESR for as-cast material is the rather small pool volume which approximately gives the same solidification conditions at the centre and surface in these relatively small sections. This results in low radial macrosegregation. However, longitudinal segregation might occur because of the change in the slag composition and oxygen potential during the melting operation.[71] Generally this is also small.

Macrosegregation in the ESC valves and the conventional casting was determined by the composition analysis mentioned above. The results with respect to top to bottom and side to side composition variation of chromium, nickel, molybdenum, and carbon are given in Figures 31-36. No definite macrosegregation trend is observed in the castings and the

variation of elements is very small. The only point which can be noticed is that wherever there is a positive deviation of chromium from the mean content, there is a corresponding negative deviation of nickel from the mean content and vice versa.

From the variation of chromium in Valve No. 7 (see Figure 33) it can be seen that composition uniformity can easily be obtained by controlled addition of chromium during the melting operation. However, a reasonable variation in composition with respect to chromium and molybdenum was observed in Valve No. 10. In this valve ferro-chrome and ferro-molybdenum powder was added during the melt (see Figure 35).

The variation is due to the inadequate feeding mechanism which resulted in unstable feeding of the powders. Two magnetic vibrator feeders set at a predetermined feeding rate were used. A funnel with a long tube was used to feed the powders from the vibrators to the ESC mold. During the melting operation it was noticed that the funnel was small to handle the volume flow and the powder was frequently jammed in the funnel and had to be dislodged manually. This led to an uneven feeding rate and probably resulted in sudden additions of large quantities of the powders. This not only resulted in a composition variation but also agglomerated into clusters of powders which could not melt completely and appeared as large inclusions in pockets in the solid casting. The latter point is discussed

in detail later in section 4.3.6.

The use of a better feeding arrangement would easily overcome this problem and a sound casting with uniform composition can be produced (as in Valve No. 7 with the addition of chromium chips). It is firmly believed that converting of AISI 316 composition to ACI CF-8M composition by addition of chromium and molybdenum will not present any insuperable production problems.

4.3.6 Problems With Alloying During the ESC Operation

As outlined above controlled addition of chromium and molybdenum was made during the electroslag casting operation of Valve Nos. 7 and 10. Chromium chips were added in Valve No. 7 while ferro-chrome and ferro-molybdenum were added in Valve No. 10. Although a sound, solid casting with uniform composition could be made with the addition of chromium chips, the same could not be achieved with ferro-chrome and ferro-molybdenum additions. In the macrostructure of Valve No. 10 (Figure 18), large inclusions can be seen and these have been marked on the photograph for easy identification. Observing these areas under the Scanning Electron Microscope (SEM) it became obvious that they were clusters of the ferro alloy powder. The SEM photographs of areas 1 and 2 at different magnifications are shown in Figures 37(a-d) and 38(a-d). From these it can be seen that the ferro alloy powder did not melt completely but instead

were loosely sintered together forming 'small pockets' in the cast material. The powder seems to have been partially molten as a dendritic structure can be observed at 2000 X magnification in Figure 38(d). To identify whether it is Fe-Cr or Fe-Mo powder, the areas shown were analysed with Energy Dispersive X-ray Analyser (EDXA). The results of EDXA on the 'parent metal' and areas 1 and 2 are shown in Figure 39. Areas 1 and 2 both show very distinct peaks for Mo and Cr. Although the 'parent metal' shows both Cr and Mo peaks, they are not as pronounced as the ones from areas 1 and 2. From this it is obvious that areas 1 and 2 are much richer in Cr and Mo than the parent metal.

To determine whether the material in the 'pockets' is Fe-Cr or Fe-Mo powder, the non-metallic inclusions present in areas 1 and 2 and also in the original Fe-Cr and Fe-Mo powder were analysed in the SEM. The EDXA graphs for the inclusions present in area 1 and 2, in Fe-Cr powder and in Fe-Mo powder are shown in Figure 40. From these it can be seen that the composition of inclusions present in areas 1 and 2 is very similar to the ones present in Fe-Cr powder. The inclusions in Fe-Mo are of completely different composition. This could be expected as Fe-Cr and Fe-Mo are produced by two entirely different processes. Fe-Cr is produced generally in an electric-arc furnace with basic dolomite lining and hence the inclusions contain Ca and Mg. Fe-Mo, on the other hand is produced by

aluminothermic reduction process and hence the inclusion morphology and composition is completely different. This shows that the material present in the pockets basically consists of Fe-Cr powder.

To confirm this by another method, areas 1 and 2 were analysed in the electron microprobe. The results obtained for Cr and Mo are shown in Table XI. The Cr and Mo contents of the parent metal are also given for comparison. Initially, the ferro-chrome powder had about 70% Cr and the ferro-molybdenum powder had about 65% Mo. The results show that areas 1 and 2 have about 54% Cr and 13% Mo. From this it is certain that areas 1 and 2 contain much more Cr than Mo and that it is the ferro-chrome powder which did not melt completely and formed pockets in the valve casting.

One would normally expect that Fe-Mo would not go in solution as compared to Fe-Cr because of its higher melting point (m.p. of 65% Fe-Mo = 1900°C, m.p. of 70% Fe-Cr = 1650°C) and also because it is heavier. So the question as to why Fe-Cr powder did not melt and formed agglomerates in preference to

Fe-Mo can only be answered by the fact that the particle size of the Fe-Cr powder used was larger than Fe-Mo powder and also that the feeding rate was much higher for Fe-Cr than for Fe-Mo (30.5 gms/min. vs. 4.5 gms/min). These inclusions occurred because of the unstable feeding of the powders as described earlier in Section 4.3.5.

4.3.7 Problems With Using Cast Electrodes in ESC Operation

Towards the end of the melting operation of Valve No. 5, there was a minor explosion inside the mold. The melting was immediately terminated as a leak in the water-cooled mold could have caused this effect. After removing the casting the mold surfaces were cleaned and inspected for leaks. However, no trace of any leaks were found. Another source of the explosion could have been a macro porosity in the electrode. Therefore the electrode was sectioned near the tip and indeed there was a porosity probably due to secondary piping in the cast electrode (see Figure 41). When the porosity was exposed, the entrapped pressurised gases must have been released under the slag layer causing the explosion. Although this does not present a threat to the safety of the ESR operation, however, it does cause certain instabilities in the melting process and should be avoided.

Another problem which is much more serious was encountered

when a cast electrode was used. After sectioning and macro-etching Valve No. 9, an unusual pool profile was noticed in the top right part and also a foreign body having a different structure was observed in the centre of the casting (see Figure 17).

Taking the latter point into consideration, it is thought that a foreign body (possibly an electrode piece) had dropped into the liquid metal pool during the melting operation. To confirm this speculation a piece was cut from this area and repolished and etched to reveal the structure. This structure is shown in Figure 42. It can be seen from this photograph that the structure of the electrode piece is entirely different to the parent casting. The electrode piece is composed of re-crystallised polygonal grains while the 'parent casting' has the normal dendritic structure. Although the cast electrode has a coarse dendritic structure (see Figure 43), the thermal cycle which this electrode piece went through is enough to convert the dendritic structure into polygonal grains.

The composition of the electrode is more or less similar to the casting and therefore chemistry alone cannot distinguish between the electrode piece and the casting. However as the electrode was cast by a conventional method, the morphology of non-metallic inclusions in the electrode piece would be much different than the parent electroslag casting but similar to the ones present in the electrode, particularly at the electrode tip.

So the inclusions from three areas (electrode piece, parent casting, and the electrode tip) were examined in an optical microscope and the SEM. Figure 44 shows the inclusions from the electrode piece and the electrode tip as observed through optical microscope. All the inclusions have a composite (multi-phase) and similar morphology although the average size of the inclusions from the electrode tip is larger.

The three areas mentioned above were also examined under the SEM and the composition of the inclusions was determined by EDXA. The kind of inclusions found in the electrode piece, the electrode tip and the parent casting are given in Figure 45. The corresponding compositions are given in Figure 46. The following can be deduced from these figures -

a) The type of inclusions observed from the electrode piece and the electrode tip are very much alike except that they are bigger in the latter.

b) The shape of the inclusions observed in the parent casting is entirely different and the size is much smaller. Also they appear to have nucleated and grown in the interdendritic region because they intersect delta ferrite which forms interdendritically.

c) However, the point which confirms that it is actually a piece of electrode sitting in the middle of the valve casting is the composition of these inclusions. Figure 46

shows that both the electrode piece and the electrode tip have inclusions which are significantly rich in silicon and manganese. In fact their overall composition is very similar. The composition of the inclusions from the parent casting, on the other hand, is entirely different. They are basically alumina-type inclusions. Silicon is completely absent.

All these points confirm the speculation that the foreign body observed in the electroslag casting is actually a piece which has dropped from the electrode during the melting operation.

The peculiar pool profile observed in the casting is thought to be an event which occurred as a result of the fallen electrode piece. The probable events which took place before and after the dropping of th electrode piece are shown schematically in Figure 47(a-c). The electrode was not in the centre of the mold during the melting process and this resulted in an asymmetric poor profile as shown in Figure 47(a). Asymmetric pool profiles are common if the electrode is off-centre. This was also observed in another valve casting in AISI 4340 steel (see Figure 59). At such a time a piece from the electrode fell off. This is apparently quite common with cast electrodes. The cast electrodes invariably have a centre porosity (perhaps representing secondary piping) and this might have resulted in a piece of electrode being detached due to melting by the slag entering

the porosity. After this piece of electrode fell off, the high temperature zone was shifted more towards the centre (see Figure 47(b). As a result of this the liquid metal pool on the right side was suddenly cooled and the liquidus and solidus advanced rapidly. The oriented dendritic growth was cut off and the liquid pool solidified with a fine and randomly oriented dendritic structure. The pool profile was shifted to the left and it made little or no difference to the liquidus and solidus on the left side (see Figure 47(c)). The affected pool profile area is shown in Figure 48. One can notice that the oriented dendritic crystals have stopped growing and there is a band of unresolved structure which represents the solidification front position change through the event. Above this, a fine and random dendritic structure is observed. It has been pointed out by Jackson and Mitchell[72] that there is a structure refinement due to the sudden increase in growth rate and changes in primary direction due to the change in the heat flow pattern. Metals with low anisotropy of growth direction (e.g. 300 series stainless steels) will renucleate in the new heat-flow direction immediately after the change in heat flow. Composition changes due to sudden growth rate occur only in the case of elements having small segregation coefficients (e.g. C,S,P and O). However the segregation of these elements would be difficult to detect in CF-8M as they are present in very small quantities.

It would be worthwhile to mention here that the presence

of the electrode piece inside the valve casting would not be detected by the NDT tests (e.g. Radiography and Ultrasonic test), which are generally used to qualify the valve castings for nuclear applications. In fact such an electrode piece would be removed when the valve is machined, but even if it is present it would not be detrimental to the properties of the valve. However if such a 'defect' occurs in a component which would be subjected to fatigue stressing (e.g. a landing gear of an aircraft), it might be a potential site for the nucleation of a fatigue crack as the fatigue properties of the electrode piece and the parent casting would be very different.

4.4 Mechanical Properties

4.4.1 Tensile Testing

Tensile tests were carried out on samples from the ESC valves and the conventional casting. The tests conformed to the ASTM standards (ASTM A370-376). The samples were 0.25" in gauge diameter (see Figure 49) and they were tested in the solution-treated condition (given before in section 4.3.2). Tests were carried out both in the longitudinal and the transverse directions. The results of these tests for Valve Nos. 5, 6 and 7 are given in Table XII while those for Valve No. 9 and the conventional casting are given in Table XIII. The tensile requirements for ferritic and austenitic steel castings (ASME SA-351/ASTM A351-72 for CF-8M) and for forged or rolled alloy

steel valves etc. for high temperature service (ASME SA-182/ ASTM A182-74 for 316) are also given in Table XIII. The complete specifications are given in Appendix 1.

From the results given in these tables, it can be seen that all the ESC valves except for the 316 valve (Valve No. 6) satisfy the tensile requirements of ASME and ASTM code for forgings and castings for valve bodies and their parts used in high-temperature service. The 316 valve falls short by about 2000 psi in tensile strength. The following two points should be noted in reference to this -

1) The ASTM/ASME specifications for valve bodies and parts made out of 316 stainless steel are for rolled or forged condition. Hence the specified strengths are for a fine sized and worked material and not for a cast material (low in delta-ferrite content).
2) The cast counterpart of the rolled or forged 316 is CF-8M where the composition has been altered to give a large amount of delta-ferrite in order to increase the strength values and thus compensate for the loss in strength due to the non-worked condition.

These two points adequately explain the lower tensile strength observed in the 316 ESC valve. So it can be concluded that tensile properties of the ESC valves lie well within the ASME/ASTM specification provided the composition requirements are met. This is also evident if we consider the

properties of Valve No. 7 where the chromium content was increased from the 316 specification to CF-8M specification (i.e. the delta ferrite content was increased).

The tensile properties of the conventional casting are also within the specifications. If the results of Valve No. 9 (CF-8M) and the conventional CF-8M casting are compared, it can be seen that on average the tensile strength of the latter is higher by about 2000 psi while the yield strength is higher by about 4000 psi. This can be due to two things. Firstly the delta-ferrite content of the conventional casting is higher than ESC valve No. 9 by about 24% and secondly the grain size of the conventional casting is smaller. The latter point accounts for the higher yield strength. On the other hand the ductility (as demonstrated by percent elongation and percent reduction in area) of the conventional casting is significantly lower than the ESC Valve No. 9 and although part of this can be due to the difference in delta ferrite content, the rest can only be explained by the fact that the electroslag casting is much cleaner (w.r.t. non-metallic inclusions), has less microsegregation and has a better solidification structure. This can also be seen by considering the percent reduction in area which is more sensitive to non-metallic inclusion content. There is a sharp decrease in percent reduction in area from the edge to the centre of the conventional casting while no such decrease is observed in the ESC Valve No. 9.

From the tensile results it also became evident that the delta-ferrite content of the castings greatly influences the proof stress and tensile strength values. Irvine et al.[73] conclude that delta-ferrite increases the proof stress and tensile strength by a dispersion strengthening effect. The ferrite has a higher yield stress than the austenite and the strain concentration in the softer austenite phase causes it to work harden to a strain greater than the nominal 0.2%, and therefore gives a higher proof stress value. In the case of the tensile strength, about 80% of the strengthening due to delta-ferrite increases is due to partitioning of carbon and nitrogen to the austenite, thereby increasing the work hardening rate.

Beck, Schoefer et al.[62] concluded from the results from about 62 CF-8M and 277 CF-8 heats that the tensile and yield strengths are directly related to the ferrite content. Figure 50 shows the variation of longitudinal tensile and yield strengths with ferrite number for the ESC valves. It can be seen that the strength is a direct function of the ferrite content. However, ductility (as determined by percent elongation) does not show any definite relation to the ferrite content. When the average tensile and yield strengths of the conventional casting are plotted on the graph, the former lies about 1000 psi below the line while the latter show a positive deviation of about 4000 psi from the line. This higher value of the yield strength is quite significant and could be explained by the fact that the conventional casting has a much smaller grain size than the

electroslag casting and this results in a higher yield stress. This is also obvious from the fact that the yield strength of the samples from the edge of the conventional casting is about 21.5% higher than the samples away from the edge.

The fractured and deformed areas of the 0.25 inch diameter tensile samples exhibited the characteristics of a large grain sized material (see Figure 51). Coarse grain materials approach more closely the behaviour of single crystals.[64] To present a valid result, a sufficient number of grains in the cross section of the specimen are required so that the relatively free grains near the surface are too few in number to affect appreciably the properties of the whole aggregate of grains. In the case of tin, Pell-Walpole[74] found that the tensile strength of rolled material increases by 60-100% with increase in the number of grains for 1 to 20-30, and very slightly increased by further refinement. He also concluded that it is the number of grains in the cross-section rather than the absolute grain size which controls the grain size/ultimate tensile strength relationship. Work done on polycrystalline aluminum also shows that the coarse grained specimens work harden substantially less than the finer grained speciments, although the general form of the stress-strain curves is similar, and the effect of grain size on the elastic limit is particularly marked.[75]

It became obvious, particularly from the 316 tensile

samples, that the grain size of the ESC valves was large and there were very few grains in the cross-section of 0.25 inch diameter samples. As a result the tensile properties of the small specimens did not represent the bulk tensile properties. To overcome this problem, it was decided to test larger specimens.. Large size specimens with a gauge diameter of 1 inch and a gauge length of 4 inches (see Figure 49) were machined from Valve No. 6 (316) and Valve No. 9 (CF-8M). These were solution treated (in the same way as mentioned before) prior to the final machining operation and were tested in the MTS machine. These specimens were 16 times larger in the cross-sectional area than the smaller specimen and therefore should have about 16 times more grains in the cross section. The results of these specimens are given in Table XIV. The deformed region near the fractured surface still shows the presence of large grains and the slip lines on the grains are clearly visible. The fractured surface shows an irregular outline. A close up of one of the broken tensile samples is shown in Figure 52. To measure the projected area of the fractured surface, both the ends of the sample were photographed and then the area was measured by a planimeter. The average value of both the ends was taken as the fractured area for that sample.

Comparison of the tensile results of the large and small specimens (see Tables XII, XIII and XIV) shows that the yield

as well as the tensile strength of the larger specimens were lower than the smaller specimens for both 316 and CF-8M. The percent elongation of the larger specimens was similar to the smaller specimens in the case of 316 and much lower in the case of CF-8M, while the reduction in area for CF-8M was similar for both sized specimens. This is completely opposite to what was expected. It is possible that because of the difference in the size of the samples, there was a variation in the heat treatment which could have occurred during the heating or quenching of the specimens, and that this had a much greater influence in the mechanical properties than the number of grains in the cross section. So to investigate this possibility small samples were machined from the undeformed region in the threaded grip section of the large tensile specimens from Valve No. 9 (CF-8M). In all three tensile samples (two from the edge and one from the centre) were tested. The results (given in Table XIV) show that the yield and ultimate tensile strength and percent reduction in area are only marginally higher than the large samples. This shows that the difference in heat treatment of the small and large specimen is responsible for the difference in mechanical properties rather than the number of grains in the cross section.

In conclusion it can be said that the tensile properties of the ESC valves can easily meet the required ASME/ASTM codes if the chemical composition is controlled within the required range.

B. LOW ALLOY STEEL VALVE CASTINGS

Six valves were made using AISI 4340 (0.38-0.43% C, 0.6-0.8% Mn, 0.04% P, 0.04% S, 0.20-0.35% Si, 1.65-2.00% Ni, 0.70-0.90% Cr and 0.20-0.30% Mo) rolled bar as electrode.

4.5 Remelting Log for AISI 4340 ESC Valves

Table XV gives the melting conditions for the ESC valves. Towards the end of the melting in Valve No. 3, the cables connected to the top mold were heated up and started smoking. This was because the casting lost contact with the base plate and so most of the current was carried by the cables. These cables were not designed to carry such high currents and so they were heated. The inside of the mold (where the cables were connected) was not damaged. In all further castings, this problem was overcome by joining the base plate and starter plate with screws. The slag composition was changed after Valve No. 3. A rare earth oxide (La_2O_3) was used. Valve No. 8 was made without any problems and the casting was sound. However, Valve Nos. 11 and 12 had to be rejected because of porosity due to moisture. Only dimensional measurements could be done on these valves. Valve Nos. 13 and 14 were also sound.

A typical electroslag casting of a valve body in AISI 4340 steel is shown in Figure 53.

4.6 Non-Destructive Testing (NDT)

4.6.1 Dye Penetrant Test

As Valve Nos. 11 and 12 showed porosity due to moisture, the other valves were sectioned and tested for cracks. Valve Nos. 3, 8 and 13 did not show any crack. However, Valve No. 14 showed cracks all over the section (see Figure 54). This valve was heat treated as one whole piece and these cracks were due to improper heat treatment. This point will be discussed later in this chapter.

4.6.2 Ultrasonic Test

Unlike CF-8M valve castings, AISI 4340 valve castings did not present any problems in ultrasonic testing. The full section thickness could be penetrated. The results of ultrasonic testing on two castings showed that they were sound.

4.6.3 Radiography Test

Radiography was performed using the cobalt-60 source. The radiographs obtained were satisfactory and no flaws could be detected. The radiographs of Valve No. 3 are shown in Figure 55.

4.7 Destructive Testing (D.T.)

The sectioning procedure has been mentioned in Section 4.3.

4.7.1 Macrostructures

The AISI 4340 steel was macroetched in an acid solution (50% HCℓ, 50% H_2O) at about 65-70°C for 1-2 hours. The macrostructures of longitudinal sections from Valve Nos. 3, 8, 13 and 14 are shown in Figures 56-59. One-half of the section from Valve No. 3 was etched in 10% animonium persulphate solution. Figure 60 shows a transverse section through a mild steel ESC valve. All the macrostructures are free of defects except the one from Valve No. 14 as shown in Figure 59. Cracks running longitudinally (probably inter-dendritic) can be seen. The top part (which was etched for a longer time) clearly shows the cracks. Also a slag entrapment on the top indicates insufficient hot-topping cycle. The macrostructure also shows that the pool profile was assymmetric and this must be due to the electrode being off-centre with respect to the mold. Some indications of this are also noticed from the macrostructure of Valve No. 8 (shown in Figure 57). From the macrostructure of the transverse section it can be seen that the grain size near the edge (surface of the casting) is smaller than in centre.

Specimens from edge, mid-radius, centre and top of Valve No. 3 were etched in Oberhoffer's solution (30 gms $FeCℓ_3$, 2 gm $CuCℓ_2$, 0.5 gms $SnCℓ_2$, 50 mℓ HCℓ, 500 mℓ ethyl alcohol, 500 mℓ distilled water) to reveal the dendritic structure. These are shown in Figure 61(a-d). The dendrites are fine at the edge and become coarser towards the centre, but they are all

oriented directionally. However, the photograph of the specimen from the top shows coarse dendrites in random orientation forming equiaxed grains (due to very slow cooling at the top.)

4.7.2 Sulphur Prints

Sulphur printing reveals the distribution of sulphur in ingots as well as rolled or forged products. Sulphur prints were taken from Valve Nos. 3 and 8 along with a piece of electrode. These are shown in Figures 62 and 63. The valves do not show any sulphur segregation and the prints are lighter than those from the electrode indicating that the sulphur content of the valve castings is much lower than that of the electrode.

4.7.3 Interdendritic Microsegregation

Using the same technique as described in Section 4.3.4, microsegregation at the centre of the AISI 4340 ESC valves was determined. The line scans of the microprobe along with variation of solute concentration of Cr, Ni, and Mo are shown in Figures 64-66. Also Table XVI gives the segregation ratios obtained from the analyses. From this we see that the segregation ratio is maximum for Mo. Also, the segregation ratio of Mo in Valve No. 13 is low while no value could be given for Valve No. 14 as the minimum count was similar to the background count. The low segregation ratio of Mo in Valve No. 13 could

be due to the heat-treatment and/or the fact that the specimen was located away from the centre due to the machined hole.

4.7.4 Composition Analysis and Macrosegregation

Composition variation of chromium, nickel, molybdenum and carbon was studied in the AISI 4340 ESC valves. The variation of these elements along the height and width of the castings are shown in Figures 67-70, while Tables XVII to XX give the complete composition analyses of the starting electrode and the castings. No appreciable change in chemistry due to remelting is observed except in the case of sulphur. Besides using optical emission spectroscopy, the sulphur content of the valve castings and the electrode was also determined by "combustion analysis" using Leco Sulphur Analyser. The results are shown in Table XXI. From this we can see that the sulphur content is decreased by about 70% through electroslag processing of the material, even when the sulphur content of the starting material was low.

4.7.5 Heat Treatment and Microstructures

The mechanical properties of steel are greatly affected by the heat treatment and hence the resulting microstructure. All the mechanical tests were done in the heat-treated condition. Unmachined individual specimens from Valve Nos. 3

and 8 were austenitised at about 845°C and oil quenched. They were tempered at about 480°C and 550°C. The exact heat treatment done for each set of tests are given in the mechanical property section.

Valve No. 13 was machined with a vertical hole of 3 inch diameter and a horizontal hole (through the side protrusions) of 2 inch diameter. The machined valve is shown in Figure 71(a), while Figure 71(b) shows a longitudinal section of this valve. Valve No. 14 was not machined. Instead of heat treating individual specimens (for mechanical testing) from Valve Nos. 13 and 14, both these valves were heat treated as a whole prior to the sectioning step. Both these valves were austenitised in a salt bath at 845°C and oil quenched. They were tempered at 560°C. After the heat treatment, the valves were sectioned for the destructive tests.

When Valve No. 14 was cut longitudinally, very fine cracks were observed. These cracks showed up clearly when a dye penetrant test was done (see Figure 54) and also when the plates were macroetched (see Figure 59). Macroetching also revealed that the cracks were interdendritic and they were concentrated inside the casting rather than on the surface. A bar with 0.5 inch square cross section cut from this valve separated along a crack without much force. The separated surfaces were smooth and shiny and the dendritic structure was revealed (see Figure 72). The machined casting did not show any such cracks.

From the above results it can be said conclusively that the cracks in Valve No. 14 were caused due to improper heat treatment.

Hardness measurements were done to find out the variation of hardness along the height and width of the heat-treated valves. These are shown in Figures 73 and 74. Valve No. 14 shows a large variation in hardness, particularly along the width of the casting. The surface shows a higher hardness than the centre. In Valve No. 13 the hardness variation is not as large. This is due to the difference in cross section between the two valves. Valve No. 14 had a section thickness of about 8 inches compared to 2½ inches in Valve No. 13 (due to the machined hole).

The above points strongly suggest that valve castings should be rough machined to their final shape prior to heat treatment. Beside these, other advantages include reduced heat treating cycle due to smaller cross section and weight, and that it would be easier to machine the valve in the as-cast condition because it is softer than in the heat-treated condition.

For microstructural examination, the specimens were polished and etched in 2% nital. The microstructures obtained in as-cast and heat-treated conditions are shown in Figure 75(a-d).

The as-cast condition has a coarse bainitic structure while the quenched and tempered condition shows a structure composed entirely of tempered martensite. Same is true for the quenched and tempered specimen from the electrode. The microstructure of a specimen from Valve No. 13 showed a different structure. Figure 76. shows that the microstructure in the interdendritic area is different than that in the dendrites. At higher magnification it is seen that the light areas (dendrites) have a bainitic structure while the darker areas shows the presence of martensite. Some ferrite is also present. This mixed microstructure resulted is low ductility when tensile test was done on this material (see Table XXIII). This microstructure is largely due to improper heat treatment, but interdendritic segregation has also contributed to it. This suggests that 'normalising' might become an important step in heat treatment process. Heat treatment of AISI 4340 steel (homogenising effects on mechanical properties, overheating during normalising, etc.) is well documented in the literature, and we believe that heat treatment of ESC valve would not present any problems.

4.7.6 Dimensional Measurements

Dimensional measurements were done on the mold and valve casting Nos. 11, 12 and 13. After the mold has been assembled, the inner dimensions between certain points were taken. After the casting was made, measurements between the same points were again taken. Also the slag thickness at these points was

determined. From these data, 'real percent shrinkage' and 'pseudo percent shrinkage' were obtained. These are defined below and are listed in Table XXII.

$$\text{real percent shrinkage} = \left[\frac{Di - Df - 2Ts}{Di}\right] 100$$

$$\text{pseudo percent shrinkage} = \left[\frac{Di - Df}{Di}\right] 100$$

where

Di - inner dimension of the mold

Df - final dimension of the casting

Ts - slag thickness.

The 'pseudo percent shrinkage', as determined here, is of practical significance and importance to foundrymen. The maximum value for this is around 4.6%. It was found that the maximum 'shrinkage' is at the corners and edges of the castings. This is because of the very high heat transfer and hence large slag thickness at these points.

4.8 Mechanical Properties

4.8.1 Tensile Testing

As mentioned in Section 4.4, tensile tests were carried out on AISI 4340 ESC Valve Nos. 3, 8 and 13. Both the longitudinal and transverse samples were tested in the quenched and tempered condition. The details of the heat treatment have

been mentioned before. The results are given in Table XXIII. Tests were also done on AISI 4340 rolled bar and the results are given in Table XXIV. Some tensile results which have been quoted in literature for air melted, vacuum arc remelted and electroslag remelted AISI 4340 have also been included in Tables XXV to XXVII for comparison. The yield and tensile strengths are not so important as different strength levels can be achieved by suitable heat treatments. However, ductility at a certain strength level is important, particularly for transverse specimens. In ESC valves, the ductility (as represented by percent reduction in area and percent elongation) of the longitudinal specimens is more or less similar to that of the transverse specimens. However if we consider the conventional rolled bar, the longitudinal values of % RA and % Elongation are 150% and 90% higher respectively than the transverse values at the same strength level. Obviously the bar had been subjected to extensive plastic deformation and hence the ductility is anisotropic.

The mechanical properties (particularly ductility) can drop drastically if AISI 4340 steel is subjected to improper heat treatment. When the tensile specimens from Valve No. 13 were tested, they exhibited very poor ductility values even at much lower strength (Table XXIII). The drop is directly related to the microstructure. As mentioned earlier, Valve No. 13 was heat treated as one piece and due to inadequate heat-treatment it showed the presence of bainite, tempered martensite and

some ferrite (see Figure 76). When individual tensile specimens were re-heat treated (austenitised, quenched and then tempered) the tensile properties were recovered because the microstructure showed that only tempered martensite was present.

Considering the tensile properties of the AISI 4340 ESC valves in general, and comparing them to the longitudinal tensile properties of hot-rolled ESR 4340 steel (given in Table XXVI) and to the transverse tensile properties of forged ESR 4340 steel (given in Table XXVII), it can be seen that the ESC specimens show slightly lower ductility values than the longitudinal specimens but similar ductility values as the transverse specimens. It is noteworthy that the transverse tensile properties given in Table XXVII for forged AISI 4340 steel are perhaps the best one can obtain.

For the same reasons as stated in Section 4.4, larger tensile specimens of 0.75 inch gauge diameter (see Figure 49) and therefore having 9 times larger cross-sectional area than the small specimens, were also tested in the MTS machine. The optical fractographs of these large specimens are shown in Figure 77. The results (given in Table XXVIII(a)) do not show any improvement in tensile properties over the small specimens. To eliminate any possible effect of heat-treatment, orientation etc. on the mechanical properties, small specimens were cut from the threaded region of the large tensile specimens.

The results are given in Table XXVII(b), and they are similar to the rest. This shows that number of grains in the cross-section does not have significant effect on the tensile properties.

4.8.2 Impact Testing

Standard Charpy V-Notch impact tests conforming to ASTM E23-72 specifications were carried out on ESC Valve Nos. 3, 8 and 13 and also on AISI 4340 rolled bar electrode. The tests were done in the quenched and tempered condition. Specimens from both longitudinal and transverse directions were tested in Valve Nos. 3 and 13 and in the AISI 4340 rolled bar electrode while in Valve No. 8 specimens from longitudinal, transverse (having a longitudinal and transverse notch) and from the edge were tested. Figure 78 shows the specimen and notch orientation of the charpy specimens. The results of all these tests are presented in Figures 79-81. Each point represents an average of at least 3 tests. It was difficult to estimate the percent brittle fracture from the broken charpy specimens as the fracture surface was very irregular. Hence it was also difficult to plot percent brittle fracture versus temperature and thus determine the Fracture Appearance Transition Temperature (FATT).

From Figure 79 which shows the charpy results of Valve No. 3 and the electrode, it can be seen that at the same hardness

level, the longitudinal specimen from the electrode exhibit better toughness values than the longitudinal specimens from the ESC valve. However, the transverse values of the electrode are much lower than the ESC valve. Also the transition temperature for the longitudinal specimens from the electrode seems to be higher than for the longitudinal specimens from the ESC valve.

Figure 80 shows the Charpy results of Valve No. 8. The longitudinal specimens seem to have higher energy values than the transverse specimens with a longitudinal notch. Although the transverse specimens with transverse notch (TT) show better toughness than the transverse specimens with longitudinal notch (TL), nothing conclusive can be said as this difference could entirely be due to the difference in hardness. However, the ductile-brittle transition characteristics of the specimens from the edge are much superior as it shows reasonable toughness at very low temperatures. This could again be due to the small grain size at the edge.

The ductile-brittle transition characteristics of Valve No. 13 are shown in Figure 81 and they are similar to Valve No. 8, but the curves seem to have shifted to the right.

Table XXIX gives the FATT valves estimated from the

ductile-brittle-transition characteristics. They show that the FATT is lower for the ESC material.

The optical fractographs of the specimens from ESC Valve No. 8 with various notch orientations are shown in Figures 82(a-d) and the longitudinal and transverse specimens from the electrode are shown in Figure 83. There is a great difference in fractography between the ESC valve and the electrode specimens. The longitudinal specimens from the electrode show an even, smooth fractured surface with large shear lips characteristic of high energy fracture. The transverse samples from the electrode, on the other hand show an irregular laminated structure and shear lips are absent even at 100°C. The specimens from the ESC valve, on the other hand, exhibit entirely different fracture characteristics. The fracture surface is very irregular and there are areas where vertical ridges are present and the surface is smooth and shiny. This is clearly shown in Figure 84(a). These ridges are predominantly present at low temperatures.

To distinguish the mode of failure in different regions of the same specimen, the specimens were examined under the SEM. The general appearance of a broken charpy specimen is shown in Figure 84(a). Areas where 'cracks' or very small ridges appear are shown in Figure 84(b). The cleavage fracture is quite apparent. Four different areas with different fracture

characteristics were identified. Instead of characterising them as ductile/brittle fractures, they have been termed as 'low', 'intermediate' or 'high energy' fractures. The different areas are shown in Figures 85(a-d) and identified below:-

Area 1 - This is the region on the vertical sides of the ridge area. This represents 'low energy fracture' as flat and faceted fracture mode is seen. There are also some round areas where tearing is observed (probably large dimples).

Area 2 - This is the region at the base of the ridge area. The fractograph from this area shows very coarse dimples with some flat areas. This can be termed as the 'transition zone' with 'intermediate energy fracture'.

Area 3 - This represents the general area (all except the ridge and the shear lip areas) and shows that fracture is due to microvoid-coalescence but here also the dimples are still coarse. This is the 'high energy fracture' area.

Area 4 - This comprises of the shear lips area on the specimen. The fracture is very much like Area 3, but here the dimples are much finer. This is also the 'high energy fracture' area.

These areas are representative of all the charpy specimens from ESC valves. This kind of fracture is probably due to firstly the large grain size and secondly due to the cast structure of the ESC material.

Chapter 5

OTHER TRIALS AND FUTURE WORK

Although the present work shows that the electroslag casting of valve bodies is a viable process, some more work is needed in two major areas which might lead to lower costs and improved capabilities of the process.

The first area of interest is the manufacture of hollow electroslag cast valves (i.e. valves with the centre hole). Much of the work done on this aspect of ESC is again of Soviet origin and Paton and other workers have shown the feasibility of the process.[3-5,77] Figure 86 shows the hollow ESC valve made in the Paton Institute, U.S.S.R., and sent here for evaluation. The two methods used by the Soviets are the fixed mandrel with the valve being cast in an inverted position and the moving mandrel with the valve in the upright position. These are shown in Figure 87. The problems associated with casting of hollow ingots (not valves) with different techniques have been discussed to some extent by Bhat[78,79] and Hoyle,[80] and these might provide some useful information as to which of the two methods mentioned above would be better. A comparative study of properties of hollow and solid ESC ingots of the same size has been done by Paton et al.,[81] and their results show that the hollow ingots have a better structure and mechanical properties. Also, hollow valves would lower the machining cost. Comparative

studies should therefore be conducted on hollow and solid ESC valves taking into account the economics of both the process routes.

The other area where investigations are required is the technique whereby separately prepared auxiliary parts are joined or fusion welded to the main body during the casting process. By using this technique it is possible to join inlet/outlet flanges (which have been made by the ESC process or otherwise) to the main valve body. Hence more complicated shapes which are close to the final product could be made. The Soviets have used this technique to produce very large crankshaft (with a pin diameter of 480 mm.) for diesel engines used in ships.[8]

Some preliminary work was done here to study this aspect of the ESC process. A flange mold was used to make flange castings joined to a thick plate. This is shown in Figure 88. Then the segment of the valve mold which had the cupped side was replaced with a similar segment but with a hole in the side. An electrode piece was placed in this hole to act as an insert and the valve casting was made. This casting is shown in Figure 89. The macrostructure of the longitudinal section of this casting is shown in Figure 90. From this it can be seen that the fusion of the insert to the main valve

body is possible. The incomplete fusion at the top can probably be corrected. A flange casting could therefore be placed instead of the insert and hence joined to the main valve. More work is needed in this area and the soundness and mechanical properties of the weld region should be studied.

Both these techniques warrant further investigation and if they appear to be acceptable from the point of view of properties and economics, they would certainly widen the scope of the ESC process and make it more versatile.

Chapter 6

SUMMARY AND CONCLUSIONS

The results reported above clearly indicate that the electroslag casting process is a viable technique to produce valve bodies. Non-destructive tests show that although ultrasonic testing can be used in the case of low alloy steel ESC valves, the same cannot be applied to austenitic stainless steel valves due to their inherent large grain size. Radiography would thus become an important tool to qualify the stainless steel castings.

The macrostructures show that the castings are essentially free of solidification defects. However special precautions are required firstly to avoid moisture related porosity in the castings and secondly when cast electrodes are used. Heat treatment also becomes an important step to achieve the desired microstructure resulting in optimum mechanical properties. Chemical composition of stainless steel castings greatly affects the ferrite content, the presence of which is essential to obtain good mechanical properties and corrosion resistance.

Although the interdendritic microsegregation increases

from the edge to the centre of the valve castings, it is reduced from that in the equivalent section in conventional casting. This is particularly true for Mo in stainless steel castings. It is noteworthy that the CF-8M valve casting was tested in the as-cast condition while the conventional CF-8M casting was tested in solution treated condition. The segregation ratio in stainless steel castings, however, should be determined from the segregation occuring within austenite or ferrite phases.

Macrosegregation studies show that the variation of elements (Cr, Ni, Mo, C) along the height and width of the valve castings is small. Composition uniformity can be achieved by controlled addition of alloying elements during the melting operation with a proper feeding arrangement.

The tensile properties of the stainless steel valves can easily meet the required ASME/ASTM codes if chemical composition is controlled within the required range. Although the strength values of the ESC valves were slightly lower than that of conventional CF-8M casting, the ductility values were significantly higher. Strength of these valves was found to be a direct function of the ferrite content. At about the same strength level, the longitudinal and transverse ductility of AISI 4340 ESC valves was significantly

higher than the transverse ductility of the conventional rolled bar and equivalent to the transverse ductility of the forged ESR steel. Increasing the cross-sectional area of the tensile specimens did not alter the measured properties showing that the number of grains in the cross-section does not have a significant effect on the measurement of tensile properties in these samples. The impact results show that the ductile-brittle-transition characteristics of the ESC material are better than the conventional rolled material. The impact strength of the ESC material was much higher than the transverse impact strength of the rolled material. Also the estimated FATT was lower for the ESC material. The fractured surface of the ESC material was very irregular due to large grain size and as-cast structure.

Electroslag casting of hollow valves and joining of individually cast components to the main valve body during the casting operation are promising potential applications of the process and need further investigation.

At this point two problems need attention: The problem of code qualification for the ESC material must be resolved. Although it is a casting, it has been shown to be of a high quality and therefore should be permitted to be used in applications where codes presently require forgings. Also,

if fabrication of the final shape is done with simultaneous casting and welding, the codes should accommodate this.

However, the real problem does not lie in the product but in the process control. The question is - can the ESC process be controlled such that the electroslag casting can be qualified by a generic test on the electrode stock rather than on the individual castings? This might be difficult if alloying additions are made during the casting operation because there will be appreciable differences between the electrode and the ESC analyses. However, if such a code qualification cannot be established, the process might become economically less feasible due to high testing costs.

In conclusion, we may say that electroslag casting process can be used to cast simple valve-body shapes in stainless and low alloy steel from cast or wrought electrodes. The properties of the ESC valves can easily meet the required specifications with proper heat treatment. The ESC valves are therefore equivalent to or better than commercial castings and forgings and can be substituted for them without any penalty.

REFERENCES

1. A. Mitchell: 'Modern Casting', Nov. 1978, p.86.

2. A. Mitchell and A. Akhtar: ASME MPC-6, 'Effects of Melting and Processing Variables on the Mechanical Properties of Steel: ed., G.V. Smith, 1977, p.1.

3. V. I. Rabinovich et al.: 'Special Electrometallurgy', 1972, Kiev. p.231.

4. B.E. Paton et al.: ibid, p.169.

5. B.E. Paton et al.: Proc. 3rd International Symposium on ESR, Pittsburgh, 1971, p.135.

6. B.E. Paton et al.: Report of E.O. Paton Electric Welding Institute, Kiev, U.S.S.R.

7. B.E. Paton et al.: Proc. 5th International Symposium on ESR, Pittsburgh, eds. G.K. Bhat and A. Simkovitch, 1974, p.239.

8. B.E. Paton et al.: Proc. 4th International Symposium on ESR, Japan, June 1973, p.209.

9. E.F. Dubrovskaya et al.: 'Vest Mashinost ', 1975, IV, p.62 (cited as Ref. 17 in Ref.2).

10. A. Ujiie et al.: 'Electroslag Refining', Iron and Steel Institute, London, 1973, p.113.

11. A. Ujiie et al.: Proc. 4th International Symposium on ESR, Japan, June 1943, p.168.

12. A. Ujiie et al.: Proc. 5th International Symposium on ESR, Pittsburgh, eds. G.K. Bhat and A. Simkovitch, 1974, p.251

13. M. P. Braun et al.: 'Electroslag Casting', Kiev, Na kova Dumka, 1976, p.44 (cited as Ref. 21 in Ref. 2).

14. B.E. Paton et al.: 'Fonderie', 1974, vol. 29, no. 340, p.435.

15. Demidov et al.: Issled Protsessov Obrabch Metall Davleniem, 1969, vol. III, p.173 (cited as Ref. 23 in Ref. 2).

16. G.A. Boiko et al: 'Rafinivuynshchie Pereplary', 1974, vol. I, p.138.

17. I. Petram: Proc. 3rd International Symposium on ESR, Pittsburgh, 1971, p.108.

18. H.J. Wagner and K. BarAvi: 'Metals Technology', Nov. 1979, p.420.

19. A. Mitchell et al.: Conf. Proc., Institute of Mechanical Engineers, London, 1980, p.87.

20. A. Ujiie et al.: U.S. Pats. #3,683,997: #3,878,882: #3,892,271: #3,894,574.

21. B.I. Medovar et al.: U.S. Pats. #3,896,878: #3,878,882: #3,892,271: #3,894,574.

22. D.M. Longbottom: U.S. Pats. #3, 902,543.

23. A. Schneidholfer: U.S. Pats. #3,804,148.

24. W.E. Duckworth and G. Hoyle: 'Electroslag Refining', Chapman and Hall Ltd., 1969.

25. A Mitchell: 'Electroslag and Vacuum Arc Remelting Processes', to be published in Electric Furnace Steelmaking, AIME publication.

26. National Materials Advisory Board: 'Electroslag Remelting and Plasma Arc Remelting', NMAB Publ., 324, National Academy of Sciences, Wash. D.C. 1975.

27. R.H. Nafziger and others: 'The Electroslag Remelting Process', Bulletin 669, U.S. Bureau of Mines, 1976.

28. B.I. Medovar et al.: 'Electroslag Remelting' JPRS Report 22217, JPRS, Wash. D.C., 1963.

29. U. Yu. Latash et al.: 'Electroslag Remelting', NTIS Translation AD 730371, U.S. Dept. of Commerce, Springfield, Virginia, 1971.

30. D.A.R. Kay: 'Special Electrometallurgy', 1972, Kiev, p.63.

31. A. Mitchell: 'Journal of Vacuum Science and Technology', Vol. 7, no. 6, p.563.

32. A.D. Wilson: ASM Technical Report System No. 76-02.

33. A.D. Wilson: Proc. Conf. TMS-AIME Ferrous Met. Committee, 106th Annual Meeting, Georgia, March 1977.

34. R.S. Cremisio et al.: Proc. 3rd International Symposium on ESR, Pittsburgh, 1971.

35. R.H. Elwell et al.: ASME-MPC-6, 'Effects of Melting and Processing Variables on the Mechanical Properties of Steel', ed. G.V. Smith, 1977, p.41.

36. V.L. Myzetsky et al.: 'Special Electrometallurgy', 1972, Kiew, p.119.

37. A. Mitchell: Ironmaking and Steelmaking (Quarterly), 1974, no. 3, p.172.

38. W. Holzgruber: Proc. 5th International Symposium on ESR, Pittsburgh, eds. G.K. Bhat and A. Simkovitch, 1974, p.70.

39. Westinghouse Electric Corporation Report on 'The Qualification of an ESC Valve' 1980.

40. L.M. Jose: U.B.C. Met. 499 Project Report, 1980.

41. G. Sidla and A. Mitchell: 'The Design, Construction and Operation of an ESC Installation', Special Report to DREP/DSS, June 1980.

42. R.S. Cremisio and E.D. Zak: Proc. 4th International Symposium on ESR, Japan, June 1973, p.137.

43. A. Mitchell et al: Paper presented at Warwick Conference, England, Sept. 1980.

44. A. Mitchell: 'Canadian Metallurgical Quarterly', vol. 20, no. 1, 1981, p.101.

45. A. Mitchell and J. Cameron: 'Metallurgical Transactions', vol. 2, Dec. 1971, p.3361.

46. A. Mitchell and R.M. Smailer: 'International Metals Reviews', nos. 5 and 6, 1979, p.231.

47. A. Mitchell and M. Etienne: Trans. of the Metallurgical Society of AIME', vol. 242, July 1968, p.1462.

48. K.C. Mills and B.J. Keene: 'International Metals Reviews, no. 1, 1981, p.21.

49. W. Hotzgruber et al.: 'Special Electrometallurgy', 1972, Kiev, p.161.

50. H. Jaeger et al.: Proc. 5th International Symposium on ESR, Pittsburgh, eds. G.K. Bhat and A. Simkovitch, 1974, p.306.

51. R.F. Steigerwald: 'Corrosion', vol. 33, no. 9, Sept. 1977, p.338.

52. ASM Metals Handbook, 8th Edition, vol. 1, p.433.

53. J.W. Flowers et al.: 'Corrosion', vol. 19, 1963, p.186t.

54. F.B. Pickering: 'The Metallurgical Evolution of Stainless Steels', ASM Metals Science Source Book, p.1.

55. F.R. Beckitt: 'Journals of The Iron and Steel Institute', May 1969, p.632.

56. E.C. Bains and W.E. Griffiths: Transactions AIME, vol. 75, 1927, p.166.

57. E.O. Hall and S.H. Algie: 'Metallurgical Reviews', vol. 11, 1966, p.61.

58. L. Smith and K.W.J. Bowen: Journal of The Iron and Steel Institute, March 1984, p.295.

59. A.J. Lena: 'Metal Progress', July 1954, p.86.

60. C.E. Spaeder, Jr. and K.G. Brickner: Advances in Technology of Stainless Steels', ASTM-STP369, 1965, p.143.

61. R. Blower and G.J. Cox: Journal of Iron and Steel Institute', Aug. 1970, p.769.

62. F.H. Beck et al.: 'Advances in Technology of Stainless Steels', ASTM - STP 369, 1965, p.159.

63. E.J. Dulis and G.V. Smith: 'The Nature, Occurrence, and Effects of Sigma Phase', ASTM STP 110, 1950, p.3.

64. ASM Metals Handbook, 8th Edition, vol. 1, p.419-422.

65. R.J. Gray et al.: 'Journal of Metals', Nov. 1978, p.18.

66. 'Handbook of Stainless Steels', eds. D. Peckner and I.M. Bernstein, published by McGraw-Hill, p.10-10.

67. L. Colombier and J. Hochniaun: 'Stainless and Heat Resisting Steels', published by Edward Arnold Ltd., 1965, p.109.

68. W. Holzgruber: Proc. 5th International Symposium on ESR, Pittsburgh, eds. G.K. Bhat and A. Simkovitch, 1974, p.70.

69. R.P. DeVries: Proc 2nd International Symposium on ESR, Pittsburgh, 1969.

70. H. Fredriksson: 'Metallurgical Transactions', vol. 3, Nov. 1942, p.2989.

71. H. Fredriksson and O. Jarleborg: Journal of Metals, Sept. 1971, p.32.

72. R.O. Jackson and A. Mitchell: 'Journal of Vacuum Science and Technology', vol. 9, no. 6, Nov.-Dec. 1972, p.1301.

73. K.J. Irvine et al.: 'The Metallurgical Evolution of Stainless Steels', ASM Metals Science Source Book, p.379.

74. W.T. Pell-Walpole: 'Journal, Institute of Metals', vol. 69, 1943, p.131.

75. ASM Metals Handbook, 9th Edition, vol. 1, p.427-428.

76. ESR 4340 steel data from Cabot Corporation, Texas, 1977.

77. B.E. Paton et al.: Proc. 2nd International Symposium on ESR, Pittsburgh, 1969.

78. G.K. Bhat: Proc. 3rd International Symposium on ESR, Pittsburgh, 1971, p.241.

79. G.K. Bhat: Proc. 4th International Symposium on ESR, Japan, June 1973, p.196.

80. G. Hoyle: 'Electroslag Refining', Iron and Steel Institute, London, 1973, p.136.

81. B.E. Paton et al.: 'Special Electrometallurgy', 1972, Kiev, p.174.

TABLES

TABLE I Remelting Log for Stainless Steel ESC Valves

	Valve No. 5	Valve No. 6	Valve No. 7	Valve No. 9	Valve No. 10
Electrode Material	CF-8M	Rolled 316	Rolled 316	CF-8M	Rolled 316
Electrode Diameter	3.5" (88.9 mm)	3.0" (76.2 mm)	3.0" (76.2 mm)	3.5" (88.9 mm)	3.0" (76.2 mm)
Slag Composition	70%CaF_2/15%Al_2O_3/15%CaO	70%CaF_2/15%Al_2O_3/15%CaO	70%CaF_2/15%Al_2O_3/15%CaO	70%CaF_2/15%Al_2O_3/15%CaO	70%CaF_2/15%Al_2O_3/15%CaO
Slag Weight	6.8 kgs	6.8 kgs	6.6 kgs	6.8 kgs	6.8 kgs
Slag Condition	Hot, dry, prefused	Hot, dry, prefused	Hot, dry, prefused	Hot and dry	Hot and dry
Average Secondary Current	3.72 KA	2.41 KA	3.50 KA	4.04 KA	3.71 KA
Average Voltage	37.4V	38.0 V	38.0 V	33.4 V	37.0 V
Average Melt Rate	0.942 kg/min	0.833 kg/min	0.868 kg/min	0.866 kg/min	0.888 kg/min
Total Melt Time	86 mins	101 mins	93 mins	117 mins	97 mins
Hot Topping Cycle	None	6.8 mins at 2.3 KA	6.9 mins at 2.1 KA	6.1 mins at 2.2 KA	5 mins at 2.2 KA
Deoxidant	Al powder	Al powder	Al powder	Al powder	Al powder
Rate of Deoxidation	1.2 gms/min	1.5 gms/min	1.6 gms/min	1.2 gms/min	1.3 gms/min
Melting Atmosphere	Air	Partial Argon	Partial Argon	Partial Argon	Partial Argon
Alloying Additions	None	None	Cr chips at 22.3 gms/min	None	FeCr-30.4 gms/min FeMo-14.5 gms/min

TABLE II Ferrite Numbers of Stainless Steel Castings

Valve No. 5 - CF-8M (i)

Specimen Location	Ferrite Indicator		Magne-Gage (F.N.)*	
	As Cast	Heat Treated	As Cast	Heat Treated
Top	10<F.N.<15	10<F.N.<15	9.1	1.56
Centre	15<F.N.<20	7.5<F.N.<10	16.51	10.6
Edge	15<F.N.<20	10<F.N.<15	17.18	11.5

*F.N. - Ferrite No.

Valve No. 6 - 316 (ii)

Specimen Location	Ferrite Indicator		Magne-Gage (F.N.)	
	As Cast	Heat Treated	As Cast	Heat Treated
Top			0.91	0.55
Centre	F.N.<2	F.N.<2	0.61	0.16
Mid-Radius	Everywhere	Everywhere	0.94	0.43
Edge			0.40	0.47

Valve No. 7 - 316 + Cr (iii)

Specimen Location	Ferrite Indicator		Magne-Gage (F.N.)	
	As Cast	Heat Treated	As Cast	Heat Treated
Top	2<F.N.<5	F.N<2	3.34	1.37
Centre	2<F.N.<5	5<F.N.<7.5	5.56	5.29
Bottom	5<F.N.<7.5	5<F.N.<7.5	4.31	5.75
Mid-Radius	5<F.N.<7.5	5<F.N.<7.5	4.72	5.05
Edge	5<F.N.<7.5	2<F.N.<5	5.68	3.28

TABLE II Ferrite Numbers of Stainless Steel Castings (Continued)

Valve No. 9 - CF-8M (iv)

Specimen Location	Ferrite Indicator		Magne-Gage (F.N.)	
	As Cast	Heat Treated	As Cast	Heat Treated
Top	5<F.N.<7.5	5≤F.N.<7.5	6.33	5.00
Centre	15<F.N.<20	15<F.N.<20	14.85	15.35
Bottom	15<F.N.<20	10<F.N.<15	14.71	12.62
Mid-Radius	15<F.N.<20	20<F.N.<25	16.09	19.46
Edge	15<F.N.<20	15<F.N.<20	14.75	15.81

Conventional Casting - CF-8M (v)

Specimen Location	Ferrite Indicator	Magne-Gage (F.N.)
	Heat Treated	Heat Treated
Top	20<F.N.<25	20.57
3/4 Height	20<F.N.<25	20.67
Centre	20<F.N.<25	20.45
1/4 Height	20<F.N.<25	18.99
Bottom	F≤N.<25	26.78
Mid-Radius	15<F.N.<20	16.99
Edge	20<F.N.<25	28.70

TABLE III Average Ferrite Numbers of Stainless Steel Castings Determined by Magne-Gage and Schoefer's Diagram

Casting	As Cast	Heat Treated*	Schoefer's Diagram
Valve No.5 - (CF-8M)	16.85	10.80	16.8
Valve No.6 - (316)	0.65	0.35	<0
Valve No.7 - (316+Cr)	5.07	4.84	4.5
Valve No.9 - (CF-8M)	15.10	15.81	22
Conv.Cast - (CF-8M)	-	19.53	32
*From Magne-Gage			

TABLE IV Interdentritic Microsegregation Ratios of CF-8M Castings

Casting and Position	Segregation Ratio (C max/C min)		
	Chromium	Nickel	Molybdenum
Valve No. 5* (CF-8M)			
Centre	1.349	2.37	2.10
Valve No. 9* (CF-8M)			
Edge	1.25	2.19	1.74
Centre	1.18	2.48	2.60
Conv. Casting**(CF-8M)			
Edge	1.167	1.625	3.568
Mid-Radius	1.305	2.178	3.859
Centre	2.337	2.587	3.299

* in as-cast condition

** in solution-treated condition

TABLE V Chemical Composition of Valve No. 5 (CF-8M) (wt.%)

	C	Mn	Si	P	S	Ni	Cr	Cu	Mo	Aℓ	Nb	Co	Ti	Zr
Electrode	0.066	0.33	1.19	0.027	0.016	10.19	20.31	0.44	2.51	-	0.073	0.108	0.008	0.006
Top	0.086	0.34	1.06	0.021	0.010	10.08	19.48	0.37	2.55	-	0.065	0.115	NA*	NA*
Centre	0.063	0.26	0.74	0.019	0.010	9.80	19.86	0.15	2.53	-	0.060	0.150	"	"
Side (L)	0.055	0.25	0.73	0.019	0.009	9.88	19.39	0.16	2.55	-	0.060	0.150	"	"
Side (R)	0.056	0.26	0.73	0.220	0.010	9.91	19.72	0.16	2.58	-	0.061	0.158	"	"

N.A. - not analysed

TABLE VI Chemical Composition of Value No. 6 (316) (wt.%)

	C	Mn	Si	P	S	Ni	Cr	Cu	Mo	Aℓ	Nb	Co	Ti	Zr
Electrode	0.049	1.89	0.67	0.030	0.031	11.60	17.56	0.09	1.98	-	0.062	0.445	0.008	0.006
Top	0.072	1.89	0.64	0.031	0.011	11.91	16.84	0.13	2.11	-	0.061	0.278	N.A.*	N.A.*
Centre	0.073	1.85	0.64	0.030	0.011	11.80	16.89	0.12	2.09	-	0.059	0.266	"	"
Bottom	0.075	1.84	0.64	0.033	0.011	11.65	17.09	0.12	2.12	-	0.059	0.263	"	"
Side (L)	0.069	1.84	0.63	0.034	0.011	11.42	16.74	0.12	2.05	-	0.061	0.258	"	"
Side (R)	0.070	1.86	0.65	0.031	0.011	11.80	17.08	0.13	2.08	-	0.060	0.283	"	"

*N.A. - not analysed

TABLE VII Chemical Composition of Valve No. 7 (316+Cr) (wt.%)

	C	Mn	Si	P	S	Ni	Cr	Cu	Mo	Aℓ	Nb	Co	Ti	Zr
Electrode	0.049	1.89	0.67	0.030	0.031	11.60	17.56	0.09	1.98	-	0.062	0.495	0.008	0.006
Top	0.074	1.87	0.61	0.035	0.012	11.48	18.94	0.12	2.01	-	0.061	0.285	N.A.*	N.A.*
Centre	0.078	1.80	0.58	0.029	0.012	11.37	18.93	0.02	1.98	-	0.61	0.264	"	"
Bottom	0.072	1.79	0.54	0.036	0.011	11.43	19.25	0.12	2.00	-	0.60	0.256	"	"
Side (R)	0.062	1.84	0.57	0.056	0.013	11.26	19.88	0.12	2.01	-	0.61	0.290	"	"

*N.A. - not analysed

TABLE VIII Chemical Composition of Valve No. 9 (CF-8M) (wt.%)

	C	Mn	Si	P	S	Ni	Cr	Cu	Mo	Aℓ	Nb	Co	Ti	Zr
Electrode	0.066	0.33	1.19	0.027	0.016	19.19	20.31	0.44	2.51	-	0.073	0.108	0.008	0.006
Top	0.058	0.35	1.04	0.028	0.009	10.33	19.87	0.40	2.51	-	0.068	0.089	0.013	0.005
Centre	0.036	0.19	0.66	0.018	0.009	10.15	19.67	0.13	2.55	-	0.060	0.159	0.005	0.004
Bottom	0.037	0.27	0.67	0.021	0.009	9.73	20.12	0.15	2.41	-	0.063	0.176	0.005	0.006
Side (L)	0.039	0.21	0.72	0.021	0.009	9.63	20.51	0.13	2.49	-	0.064	0.185	0.005	0.006
Side (R)	0.041	0.20	0.70	0.020	0.009	9.90	20.19	0.13	2.51	-	0.063	0.193	0.004	0.006

TABLE IX Chemical Composition of Valve No. 10 (316+Cr+Mo) (wt.%)

	C	Mn	Si	P	S	Ni	Cr	Cu	Mo	Aℓ	Nb	Co	Ti	Zr
Electrode	0.049	1.89	0.67	0.030	0.031	11.60	17.56	0.09	1.98	-	0.062	0.445	0.008	0.004
Top	0.055	1.69	0.43	0.030	0.010	12.10	18.47	0.10	2.32	-	0.063	0.102	0.007	0.005
Centre	0.046	1.65	0.41	0.027	0.011	11.91	19.14	0.07	2.32	-	0.064	0.134	0.007	0.005
Bottom	0.051	1.62	0.28	0.027	0.009	12.11	18.78	0.10	2.26	-	0.064	0.127	0.007	0.005
Side (L)	0.048	1.65	0.40	0.028	0.011	11.96	19.22	0.08	2.33	-	0.065	0.133	0.007	0.005
Side (R)	0.040	1.61	0.39	0.024	0.010	11.90	19.05	0.09	2.51	-	0.065	0.135	0.007	0.006

TABLE X Chemical Composition of the Conventional Casting (CF-8M) (wt.%)

	C	Mn	Si	P	S	Ni	Cr	Cu	Mo	Aℓ	Nb	Co	Ti	Zr
Top	0.029	0.61	1.24	0.027	0.010	9.13	19.41	0.25	2.02	-	0.087	0.067	0.009	0.003
Centre	0.023	0.62	1.21	0.026	0.010	8.90	19.80	0.22	2.00	-	0.086	0.071	0.009	0.003
Bottom	0.019	0.65	1.24	0.031	0.010	9.34	19.67	0.23	2.06	-	0.089	0.068	0.008	0.003
Mid-radius	0.024	0.63	1.25	0.029	0.010	9.05	19.85	0.23	2.04	-	0.087	0.072	0.008	0.003
Side (R)	0.020	0.63	1.24	0.031	0.010	9.57	19.36	0.23	2.10	-	0.087	0.066	0.008	0.003

TABLE XI Percent composition of Cr and Mo in areas 1 and 2 and the Parent Valve No. 10

Area Analysed	Chromium (wt.%)	Molybdenum (wt.%)
Area 1	54.88	12.56
Area 2	54.21	13.12
Parent	22.10	1.79

TABLE XII Tensile Properties of Valve Nos. 5, 6 and 7

Casting No. and Test Direction	Elongation In 1 inch (25.4 mm) %	Yield Strength, 0.2% offset, Ksi(MPa)	Ultimate Tensile Strength Ksi(MPa)
Valve No. 5 (CF-8M)			
Longitudinal - 1	45.3	36.5 (251.7)	77.2 (532.3)
- 2	51.3 47.3†	35.8 (246.8) 37.0†	74.1 (510.9) 77.8†
- 3	45.2	38.6 (266.1) 255.1	82.1 (566.4) 536.4
Transverse - 1	46.3	36.2 (249.6)	71.7 (494.4)
- 2	53.4 50.1†	39.0 (268.9) 36.9†	75.3 (519.2) 72.6†
- 3	50.6	35.5 (244.8) 254.4	70.7 (487.5) 500.6
Valve No. 6 (316)			
Longitudinal - 1	62.1	34.1 (235.1)	71.1 (494.4)
- 2	68.8 64.8†	31.7 (218.6) 32.5†	69.7 (480.6) 68.3†
- 3	63.6	31.1 (214.4) 224.1	64.1 (442.0) 470.9
Transverse - 1	69.6	32.3 (222.7)	68.0 (468.9)
- 2	62.4 65.4†	34.0 (234.4) 32.5†	69.4 (475.8) 69.3†
- 3	64.1	31.2 (215.1) 224.1	70.6 (486.8) 477.8
Valve No. 7 (316+Cr)			
Longitudinal - 1	51.1	34.9 (240.6)	73.6 (507.5) 71.7†
- 2	68.6 57.9†	35.2 (242.7) 34.7†	68.4 (471.6) 494.4
- 3	54.0	33.9 (233.7) 239.3	73.2 (504.7)
Transverse - 1	56.0	34.0 (234.4)	66.3 (457.1)
- 2	53.4 61.3†	39.0 (268.9) 35.7†	75.3 (519.2) 70.8†
- 3	74.5	34.2 (235.8) 246.2	70.7 (487.5) 488.2

† Average value.

TABLE XIII Tensile Properties of Valve No. 9, Conventional Casting and ASME/ASTM Standards for AISI 316 and ACI CF-8M

Casting No. and Test Direction	Reduction In Area, %	Elongation In 1 inch (25.4 mm) %	Yield Strength, 0.2% offset, Ksi (MPa)	Ultimate Tensile Strength Ksi (MPa)
Valve No. 9 (CF-8M)				
Longitudinal - 1	80.0	70.7	39.3 (271.0)	82.4 (568.1)
- 2	82.0 81.0†	71.3 71.0†	42.4 (292.3) 40.9† / 282.0	82.1 (566.1) 82.3† / 567.5
Transverse - 1	82.4	70.0	41.8 (288.2)	82.3 (567.5)
- 2	78.7 79.7†	73.0 71.2†	42.1 (290.3) 42.4† / 291.0	81.1 (559.2) 82.2† / 566.8
- 3	77.9	70.5	42.6 (293.7)	83.2 (573.7)
Edge - 1	79.4	73.7	44.2 (304.8)	86.3 (595.0)
- 2	82.0 80.7†	69.0 71.4†	42.8 (295.1) 43.5† / 300.0	84.5 (582.6) 85.4† / 588.8
Conventional Cast (CF-8M)				
Longitudinal* -				
0.25 inches from the edge	74.3	46.6	57.0 (393.0)	82.5 (568.8)
2.50 " " " "	72.6	52.0	45.0 (310.3)	82.0 (565.4)
4.25 " " " "	70.1	58.9	46.7 (322.0)	85.2 (587.5)
6.00 " " " "	62.0	53.2	46.7 (322.0)	85.8 (591.6)
7.75 " " " "	63.4	56.7	45.9 (316.5)	84.6 (583.3)
Transverse*				
1.90 inches from the edge	72.2	58.3	46.4 (319.9)	84.5 (582.6)
3.75 " " " "	75.2	55.5	46.0 (317.2)	83.2 (573.7)
5.60 " " " "	65.7	55.3	46.6 (321.3)	84.7 (584.0)
ASME SA-182 or ASTM A-182-77a(316)	50 (min)	30 (min)*	30 (207) min	70 (483) min
ASME SA-351 or ASTM A-351-77(CF-8M)	not specified	30 (min)*	30 (207) min	70 (483) min

† Average value.

* Each value represents an average of 3 tests.

* Elongation in 2 inches (50.8 mm)

TABLE XIV. Tensile Properties of Large Specimens from Valve Nos. 6 and 9 and Small Specimens from a Large Specimen.

Casting No. and Test Direction	Reduction In Area, %	Elongation In 1 inch (25.4 mm) %	Yield Strength 0.2% offset, Ksi (MPa)	Ultimate Tensile Strength Ksi (MPa)
Valve No. 6 (316)				
Longitudinal - 1	78.8	70.9	32.6 (224.8)	66.8 (460.6)
- 2	82.0 $\underline{81.3}^{\dagger}$	69.3 $\underline{66.0}^{\dagger}$	29.0 (200.0) $\frac{30.9^{\dagger}}{213.1}$	61.8 (426.1) $\frac{63.7^{\dagger}}{439.2}$
- 3	83.0	57.8	31.0 (213.7)	62.6 (431.6)
Valve No. 9 (CF-8M)				
Longitudinal - 1	85.2	47.9	36.2 (249.6) $\frac{36.7^{\dagger}}{253.0}$	73.0 (503.3) $\frac{73.5^{\dagger}}{506.8}$
- 2	80.7 $\underline{83.0}^{\dagger}$	47.5 $\underline{47.7}^{\dagger}$	37.1 (255.8)	74.0 (510.2)
Valve No. 9 (CF-8M) (From large Longitudinal -1)				
Edge - 1	87.0	35.8	38.7 (266.8)	78.2 (539.2)
Edge - 2	87.1 $\underline{86.1}^{\dagger}$	73.1 $\underline{71.1}^{\dagger}$	38.4 (264.8) $\frac{38.0^{\dagger}}{262.0}$	73.0 (503.3) $\frac{75.0^{\dagger}}{517.1}$
Centre - 1	24.2	84.5	37.0 (255.1)	73.7 (508.2)

† Average value.

TABLE XV Remelting Log for AISI 4340 Steel ESC Valves

	Valve No. 3	Valve No. 8	Valve No. 11	Valve No. 12	Valve No. 13	Valve No. 14
Electrode Materiel	Rolled 4340	Rolled 4340	Rolled 4340	Rolled 4340	Rolled 4340	Rolled 4340
Electrode Diameter	3.25" (82.6 mm)	3.25" (82.6 mm)	3.25" (82.6 mm)	3.25" (82.6 mm)	3.25" (82.6 mm)	3.25" (82.6 mm)
Slag Composition	61.75%CaF_2/26.5%Al_2O_3/ 11.75%CaO	46%CaF_2/17%Al_2O_3/ 17%CaO/20%La_2O_3	46%CaF_2/17%Al_2O_3/ 17%CaO/20%La_2O_3	46%CaF2/17%Al_2O_3/ 17%CaO/20%La_2O_3	46%CaF_2/17%Al_2O_3/ 17%CaO/20%La_2O_3	46%CaF_2/17%Al_2O_3/ 17%CaO/20%La_2O_3
Slag Weight	9.1 kg	6.8 kg	6.8 kg	6.8 kg	6.8 kg	6.8 kg
Slag Condition	Liquid CaF_2, Hot Al_2O_3 and CaO	Hot and Dry	Hot and Dry	Hot and Dry	Hot and Dry	Hot and Dry
Average Secondary Current	2.73 KA	3.72 KA	3.59 KA	3.60 KA	3.55 KA	3.60 KA
Average Voltage	36.9 V	37.1 V	36.9 V	36.8 V	35.4 V	36.0 V
Average Melt Rate	1.022 kg/min	0.938 kg/mins	0.967 kg/min	0.854 kg/min	0.785 kg/min	0.812 kg/min
Total Melt Time	87 mins	98 mins	98 mins	112 mins	113 mins	110 mins
Hot Topping Cycle	3.2 mins at 2.6 KA	7.2 mins at 2.2 KA	6.7 mins at 2.2 KA	8.3 mins at 2.2 KA	6.7 mins at 2.2 KA	9.2 mins at 2.3 KA
Deoxidant	Al powder	Al powder	Al powder	Al powder	Al powder	Al powder
Rate of Deoxidation	2.4 gms/min	1.2 gms/min	1.2 gms/min	1.2 gms/min	1.4 gms/min	1.4 gms/min
Melting Atmosphere	Air	Partial Argon	Partial Argon	Partial Argon	Air	Air

TABLE XVI Interdendritic Microsegregation at the Centre of AISI 4340 ESC Valves

Valve No.	Segregation Ratio (C max/C min)		
	Chromium	Nickel	Molybdenum
Valve No. 3*	1.39	1.13	2.15
Valve No. 8*	1.34	1.14	2.21
Valve No. 13** (At mid-radius)	1.12	1.60	1.24
Valve No. 14**	1.30	1.05	-

*In as-cast condition

**The whole valve was heat-treated.

TABLE XVII Chemical Composition of Valve No. 3 (4340) (wt.%)

	C	Mn	Si	P	S	Ni	Cr	Cu	Mo	Aℓ	Nb	Co	V	B	W	Ti	Zr
Electrode	0.42	0.77	0.37	0.021	0.015	1.87	0.80	0.10	0.21	0.013	0.053	0.029	0.012	0.0006	0.018	0.011	0.003
Top	0.42	0.78	0.41	0.021	0.004	1.84	0.83	0.07	0.22	0.095	0.024	0.033	0.017	0.0014	0.026	N.A.	N.A.
Centre	0.40	0.76	0.40	0.019	0.004	1.80	0.81	0.08	0.21	0.082	0.023	0.031	0.016	0.0011	0.026	"	"
Bottom	0.40	0.73	0.37	0.018	0.004	1.79	0.80	0.08	0.21	0.127	0.020	0.028	0.016	0.0013	0.024	"	"
Side (L)	0.40	0.75	0.38	0.018	0.003	1.81	0.81	0.08	0.21	0.085	0.019	0.028	0.016	0.0009	0.022	"	"
Side (R)	0.42	0.78	0.40	0.019	0.003	1.83	0.82	0.08	0.22	0.073	0.022	0.031	0.016	0.0010	0.024	"	"

*N.A. - not analysed

TABLE XVIII Chemical Composition of Valve No. 8 (4340) (wt.%)

	C	Mn	Si	P	S	Ni	Cr	Cu	Mo	Aℓ	Nb	Co	V	B	W	Ti	Zr
Electrode	0.42	0.77	0.37	0.021	0.015	1.87	0.80	0.10	0.21	0.031	0.053	0.029	0.012	0.0006	0.018	0.011	0.003
Top	0.43	0.80	0.33	0.030	0.004	1.90	0.81	0.11	0.22	0.035	0.056	0.042	0.013	0.0007	0.024	0.005	0.004
Centre	0.41	0.77	0.34	0.028	0.004	1.86	0.80	0.11	0.22	0.048	0.056	0.039	0.012	0.0007	0.023	0.005	0.004
Bottom	0.40	0.75	0.20	0.29	0.003	1.74	0.76	0.10	0.21	0.051	0.052	0.030	0.012	0.0005	0.016	0.004	0.003
Side (L)	0.41	0.75	0.34	0.29	0.003	1.80	0.78	0.10	0.21	0.043	0.053	0.032	0.012	0.0007	0.016	0.005	0.004
Side (R)	0.41	0.79	0.34	0.28	0.002	1.87	0.81	0.11	0.22	0.045	0.051	0.024	0.012	0.0006	0.019	0.004	0.003

TABLE XIX Chemical Composition of Valve No. 13 (4340) (wt.%)

	C	Mn	Si	P	S	Ni	Cr	Cu	Mo	Aℓ	Nb	Co	V	B	W	Ti	Zr
Electrode	0.42	0.77	0.37	0.021	0.015	1.87	0.80	0.10	0.21	0.031	0.053	0.029	0.012	0.006	0.018	0.011	0.003
Top	0.43	0.84	0.18	0.030	0.003	1.89	0.86	0.31	0.21	0.020	0.053	0.055	0.011	0.0004	0.041	0.003	0.002
Centre	0.42	0.86	0.11	0.030	0.001	1.88	0.86	0.3o	0.21	0.021	0.053	0.057	0.011	0.0004	0.044	0.002	0.002
Bottom	0.42	0.76	0.04	0.030	0.001	1.79	0.83	0.30	0.21	0.017	0.052	0.059	0.010	0.0004	0.039	0.003	0.003
Side (L)	0.40	0.80	0.09	0.029	0.002	1.75	0.82	0.31	0.20	0.021	0.052	0.062	0.011	0.0004	0.033	0.004	0.003
Side (R)	0.41	0.82	0.10	0.030	0.002	1.80	0.84	0.31	0.21	0.022	0.055	0.065	0.011	0.0004	0.037	0.004	0.003

TABLE XX Chemical Composition of Valve No. 14 (4340) (wt.%)

	C	Mn	Si	P	S	Ni	Cr	Cu	Mo	Aℓ	Nb	Co.	V	B	W	Ti	Zr
Electrode	0.42	0.77	0.37	0.021	0.015	1.87	0.84	0.10	0.21	0.031	0.053	0.029	0.012	0.0006	0.018	0.011	0.003
Top	0.44	0.84	0.19	0.033	0.004	1.90	0.86	0.31	0.21	0.018	0.058	0.071	0.012	0.0006	0.050	0.003	0.004
Centre	0.45	0.88	0.14	0.032	0.002	1.98	0.88	0.30	0.22	0.022	0.057	0.066	0.012	0.0006	0.056	0.001	0.003
Bottom	0.46	0.87	0.05	0.033	0.002	2.03	9.90	0.30	0.22	0.013	0.059	0.072	0.012	0.0005	0.064	0.001	0.004
Side (L)	0.45	0.89	0.09	0.033	0.002	1.94	0.87	0.31	0.22	0.018	0.059	0.088	0.013	0.0006	0.050	0.003	0.004
Side (R)	0.45	0.89	0.09	0.032	0.002	1.97	0.88	0.30	0.22	0.016	0.060	0.090	0.012	0.0006	0.055	0.001	0.004

TABLE XXI Sulphur Contents of AISI 4340 Electrode and ESC Valves

	Electrode	Valve No. 3	Valve No. 8	Valve No. 13	Valve No. 14
Sulphur Content (wt.%)	0.0146	0.0040	0.0037	0.0055	0.0053

TABLE XXII Dimensional Measurements on Valve Nos. 11, 12 and 13

Valve No.	Shrinkage Type	% Shrinkage and Location								
		a	b	c	d	e	f	g	h	i
Valve No.11	Real	2.37	2.68	2.33	1.35	1.97	2.55	1.48	1.67	1.92
	Pseudo	3.60	4.10	3.75	3.05	3.09	4.55	4.34	4.17	4.12
Valve No.12	Real	1.87	1.07	1.72	1.29	2.34	0.47	0.97	1.27	1.61
	Pseudo	3.36	2.31	2.80	2.70	3.26	1.73	2.22	2.52	2.87
Valve No.13	Real	2.43	2.01	2.53	2.36	2.27	2.18	2.23	2.19	2.99
	Pseudo	4.64	4.26	4.25	4.22	3.30	3.36	3.30	3.37	4.17

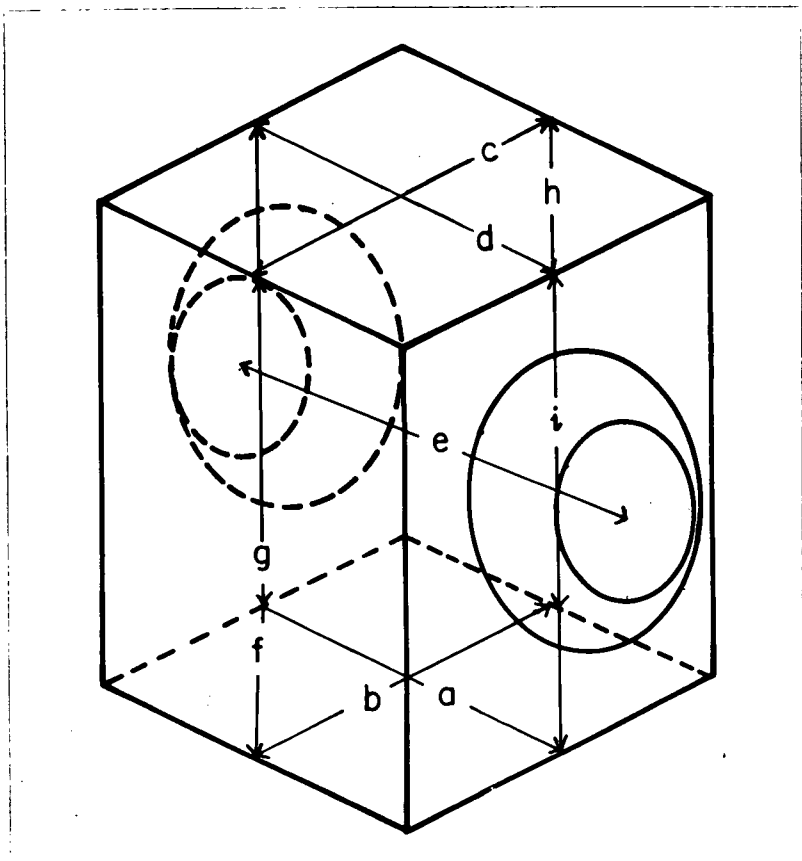

TABLE XXIII Tensile Properties of AISI 4340 Electroslag Cast Valves

Casting No. and Test Direction	Reduction in Area, %		Elongation In 1 inch (25.4 mm), %		Yield Strength 0.2% offset, Ksi (MPa)		Ultimate Tensile Strength Ksi (MPa)	
Valve No. 3 (a)								
Longitudinal - 1	48.0		10.1		174.6 (1197.0)		185.1 (1276.3)	
- 2	33.3	37.1†	7.2	8.6†	176.8 (1212.1)	176.2† / 1214.9	187.8 (1292.8)	187.0† / 1289.4
- 3	30.1		8.5		179.1 (1234.9)		188.0 (1296.3)	
Transverse - 1	33.9		9.3		174.0 (1199.7)		184.1 (1269.4)	
- 2	37.8	36.0†	11.2	9.1†	171.8 (1184.6)	172.7† / 1190.8	184.7 (1273.5)	183.8† / 1267.3
- 3	36.4		8.4		172.9 (1187.3)		182.7 (1259.7)	
Valve No. 8 (b)								
Longitudinal - 1	46.0		16.5		149.9 (1033.6)		164.7 (1130.8)	
- 2	42.2	45.3†	14.7	16.4†	149.3 (1029.4)	140.0† / 1034.3	164.3 (1132.8)	164.7† / 1135.6
- 3	47.7		17.9		150.7 (1039.1)		165.1 (1138.4)	
Transverse - 1	41.8		15.5		151.8 (1046.7)		166.3 (1146.5)	
- 2	44.2	43.6†	17.0	16.8†	153.0 (1054.9)	152.5† / 1051.5	167.2 (1152.8)	166.4† / 1147.3
- 3	44.7		17.8		152.6 (1052.2)		165.8 (1143.2)	
Edge - 1	51.3		14.1		149.1 (1028.0)		160.4 (1106.0)	
- 2	46.1	48.7†	17.5	15.8†	150.5 (1037.7)	149.8† / 1032.9	165.2 (1139.1)	162.8† / 1122.5
Valve No. 13 (c)								
Longitudinal - 1	7.1		3.7		120.1 (828.1)		142.1 (979.8)	
- 2	9.4	9.1†	4.2	4.6†	120.1 (828.1)	120.1† / 828.1	138.8 (957.0)	139.2† / 959.8
- 3	10.9		5.8		120.1 (828.1)		136.6 (941.9)	
Transverse - 1	11.7		3.5		122.4 (843.9)		134.1 (924.6)	
- 2	8.7	9.9†	4.9	4.3†	120.1 (828.1)	120.0† / 833.6	135.4 (933.6)	135.4† / 933.6
- 3	9.4		4.5		120.1 (828.1)		136.8 (943.2)	
Valve No. 13 (d)								
Longitudinal - 1	39.9	41.0†	16.7	17.6†	147.7 (1018.4)	147.5† / 1017.0	159.8 (1101.8)	159.6† / 1100.4
- 2	42.0		18.5		147.3 (1015.6)		159.3 (1098.4)	
Transverse - 1	32.9	32.3†	17.0	15.2†	146.2 (1008.0)	145.3† / 1001.8	157.9 (1088.7)	156.6† / 1079.8
- 2	31.7		13.3		144.3 (994.9)		155.3 (1070.8)	

(a) Tempered at 482°C to a hardness of 38 Rc.
(b) Tempered at 550°C to a hardness of 35 Rc.
(c) The whole valve was heat-treated and tempered at 560°C. Average hardness of the tensile specimens was 31 Rc.
(d) The specimen bars were re-heat-treated and tempered at 560°C to a hardness of 33 Rc.
† Average value.

TABLE XXIV Tensile Properties of Conventional AISI 4340 Hot Rolled Bar[a]

Specimen No. and Test Direction	Reduction In Area, %		Elongation In 1 inch (25.4 mm) %		Yield Strength at Lower Yield Point Ksi (MPa)		Ultimate Tensile Strength Ksi (MPa)	
Longitudinal - 1	57.7		19.2		150.7 (1039.1)		162.8 (1122.5)	
- 2	58.2	57.8†	19.6	18.3†	150.0 (1034.3)	150.8† / 1039.8	164.3 (1132.8)	163.6† / 1128.0
- 3	57.5		16.2		151.8 (1046.7)		163.6 (1128.0)	
Transverse - 1	21.9		9.4		150.3 (1036.3)		162.0 (1117.0)	
- 2	22.7	22.7†	9.5	9.8†	149.1 (1028.0)	150.2† / 1035.6	161.1 (1110.8)	162.0† / 1117.0
- 3	23.5		10.5		151.3 (1043.2)		162.8 (1122.5)	

(a) Tempered at 560°C to a hardness of 33.5 Rc. Diameter of the bar was 3.25 inches (82.6 mm)
† Average value.

TABLE XXV Transverse Tensile Properties of Air Melted and Vacuum Arc Melted 4340 Steels*[75]

Tempering Temperature	Reduction in Area, %	Elongation In 2 inches (50.8 mm), %	Yield Strength Ksi (MPa)	Tensile Strength Ksi (MPa)
Air Melted				
480°C	14.9	8.0	173 (1192.8)	200 (1379)
540°C	22.0	10.0	163 (1123.9)	180 (1241.1)
Vacuum Arc Remelted				
480°C	20.0	9.0	175 (1206.6)	200 (1379)
540°C	24.0	10.5	160 (1103.2)	180 (1241.1)

* Properties listed are averages of several heats from the same producer; billet size and amount of hot reduction were not available.

TABLE XXVI Longitudinal Mechanical Properties of Bar Stock Made From Remelted 4340 Steel[a] [75]

Melting Method	Reduction In Area, %	Elongation In 4D, %	Yield Strength Ksi (MPa)	Tensile Strength Ksi (MPa)	Hardness (MRc)
VAR[b]	61.2	16.4	163 (1123.9)	175 (1206.6)	37
ESR[c]	59.0	16.1	158 (1089.4)	171 (1179.0)	37

(a) Bars were normalised at 900°C, oil quenched from 845°C, and tempered 2 hrs. at 541°C. All specimens taken from mid-radius.
(b) 3.62 inch round.
(c) 4.625 inch round.

TABLE XXVII Mechanical Properties of ESR 4340 Material in the Transverse Direction Heat-Treated to Different Strength Levels.*[76]

Tempering Temperature	Reduction in Area, %	Elongation %	0.2% Yield Strength Ksi (MPa)	Tensile Strength Ksi (MPa)
538°C	45.1	12.9	169.4 (1168.0)	180.6 (1245.2)
566°C	49.2	14.6	158.3 (1091.5)	173.0 (1192.8)

* Data from Cabot Corporation.

Notes (1) Tensile data were generated from a 0.357 in. (9mm) diameter test bars machined from heat-treated 1-in. diameter transverse bars taken from a 24-in. diameter ESR ingot forged 3:1 to 14-in. diameter.

(2) All samples were normalised at 1750°F (954°C) prior to heat-treating, then austenitized at 1525°F (830°C) and tempered at various temperatures.

(3) Tensile values are average of five tests.

TABLE XXVIII(a) Tensile Properties of Large Specimen from ESC Valve of AISI 4340 Steel.

Casting No. and Test Direction	Reduction In Area, %	Elongation In 3 inches (76.2 mm) %	Yield Strength, 0.2% offset, Ksi (MPa)	Ultimate Tensile Strength, Ksi (MPa)
Valve No. 8*				
Longitudinal - 1	48.1 $\underline{47.9}^{\dagger}$	19.7 $\underline{18.1}^{\dagger}$	144.9 (999.1) $\frac{145.5^{\dagger}}{1003.2}$	160.6 (1107.3) $\frac{160.5^{\dagger}}{1106.6}$
- 2	47.6	16.5	146.0 (1006.7)	160.3 (1105.3)

* Tempered at 550°C to a hardness of 34.5 Rc.
† Average value.

TABLE XXVIII(b) Tensile Properties of Small Specimens Cut From Large Tensile Specimens

Specimen No. and Test Direction	Reduction In Area, %	Elongation In 1 inch (25.4 mm) %	Yield Strength, 0.2% offset, Ksi (MPa)	Ultimate Tensile Strength, Ksi (MPa)
Value No. 8 (From Large Longitudinal -1)				
Edge - 1	45.2	16.7	149.7 (1032.2)	164.8 (1136.3)
Edge - 2	48.6 $\underline{46.5}^{\dagger}$	17.4 $\underline{17.4}^{\dagger}$	144.7 (997.7) $\frac{146.3^{\dagger}}{1008.7}$	159.7 (1101.1) $\frac{161.4^{\dagger}}{1112.9}$
Centre - 1	45.7	18.0	144.5 (996.3)	159.7 (1101.1)

† Average value.

TABLE XXIX FATT Values Estimated from Ductile Brittle Transition Characteristics of AISI 4340 ESC Valves and Electrode.

Type and Orientation of Specimen	Estimated FATT
Valve No. 3 - Long.	-40°C
Electrode - Long.	5°C
Electrode - Trans.	45°C
Valve No. 8 - Long.	-25°C
Valve No. 8 - Trans.(T)	-30°C
Valve No. 8 - Trans.(L)	-35°C
Valve No. 8 - Edge	-32°C
Valve No. 13 - Long.	20°C
Valve No. 13 - Trans.	20°C

Notes: (1) The FATT values have been estimated according to a suggested method in ASTM E23-72.
(2) FATT has been determined as the temperature corresponding to the energy value 50% of the difference between values obtained at 100% and 0% fibrous fracture.
(3) The specimens have been assumed to be 100% fibrous at 100°C and 0% fibrous at -100°C. The latter is not exactly true as some areas were found to be ductile even at -100°C.
(4) The high FATT for Valve No. 13 is probably due to the inadequate heat treatment.
(5) These are just estimated values and not exact because of the kind of fractured surface (as mentioned in the text).

FIGURES

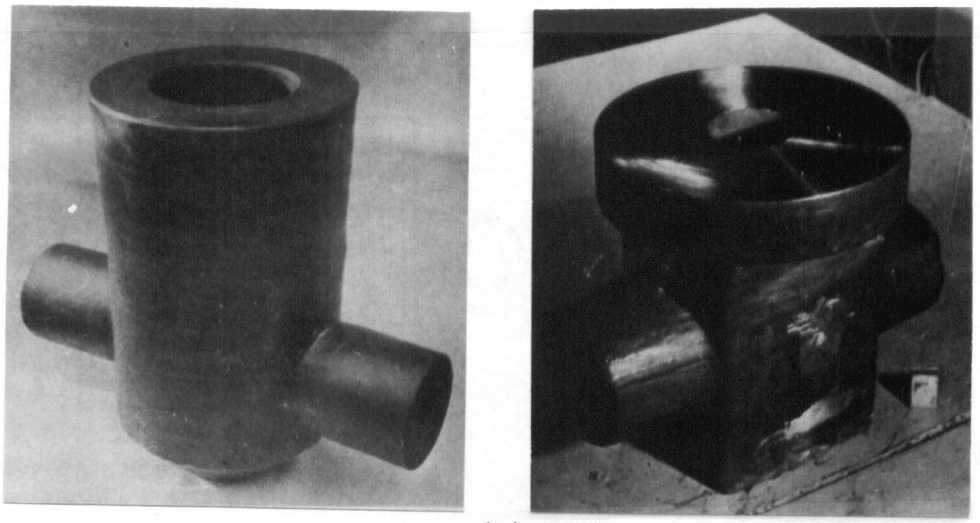

(a)

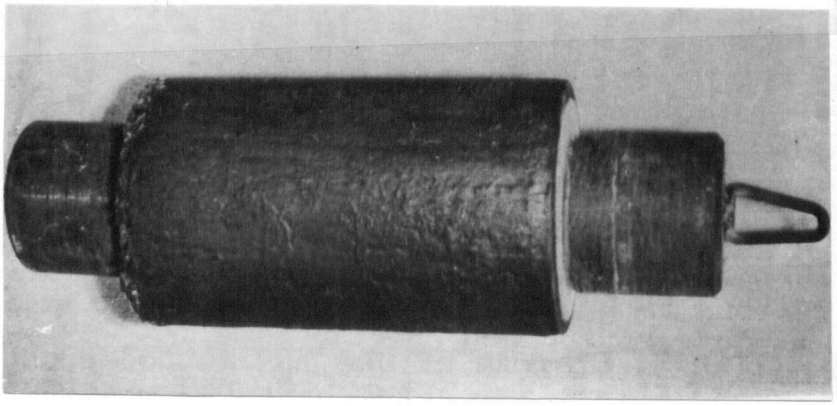

(b)

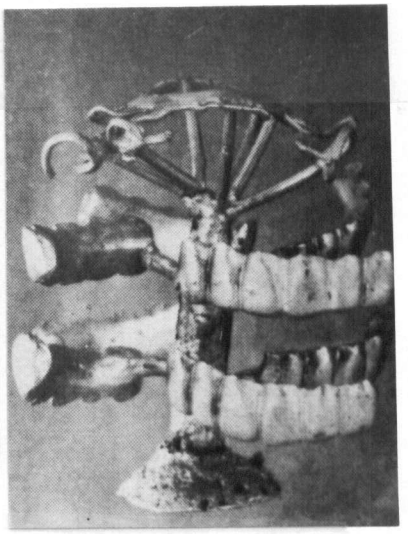

(c)

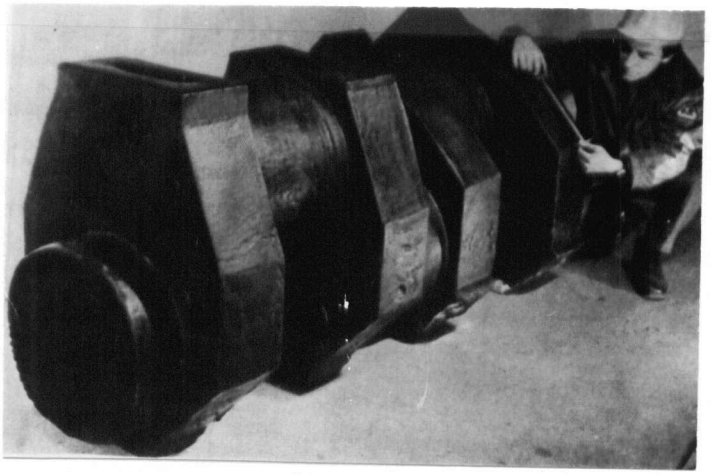

(d)

Figure 1. Electroslag Cast Products.[8]
(a) Valve Bodies; (b) Rolls; (c) Dentures
(d) Crankshaft with pin diameter of 480 mm.

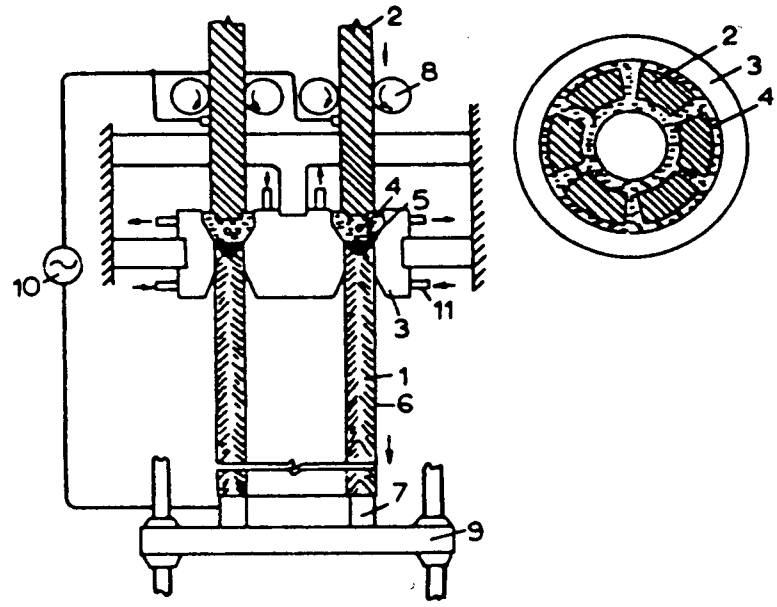

1 straight tube, 2 source material, 3 ring-type mould, 4 molten-slag bath, 5 molten-metal pool, 6 slag film, 7 start piece, 8 feed roller for source material, 9 drawing apparatus, 10 electric power source, 11 cooling water

Figure 2. 'YOZO' process of Mitsubishi Heavy Industries Ltd: products pipe, tube.[11,12]

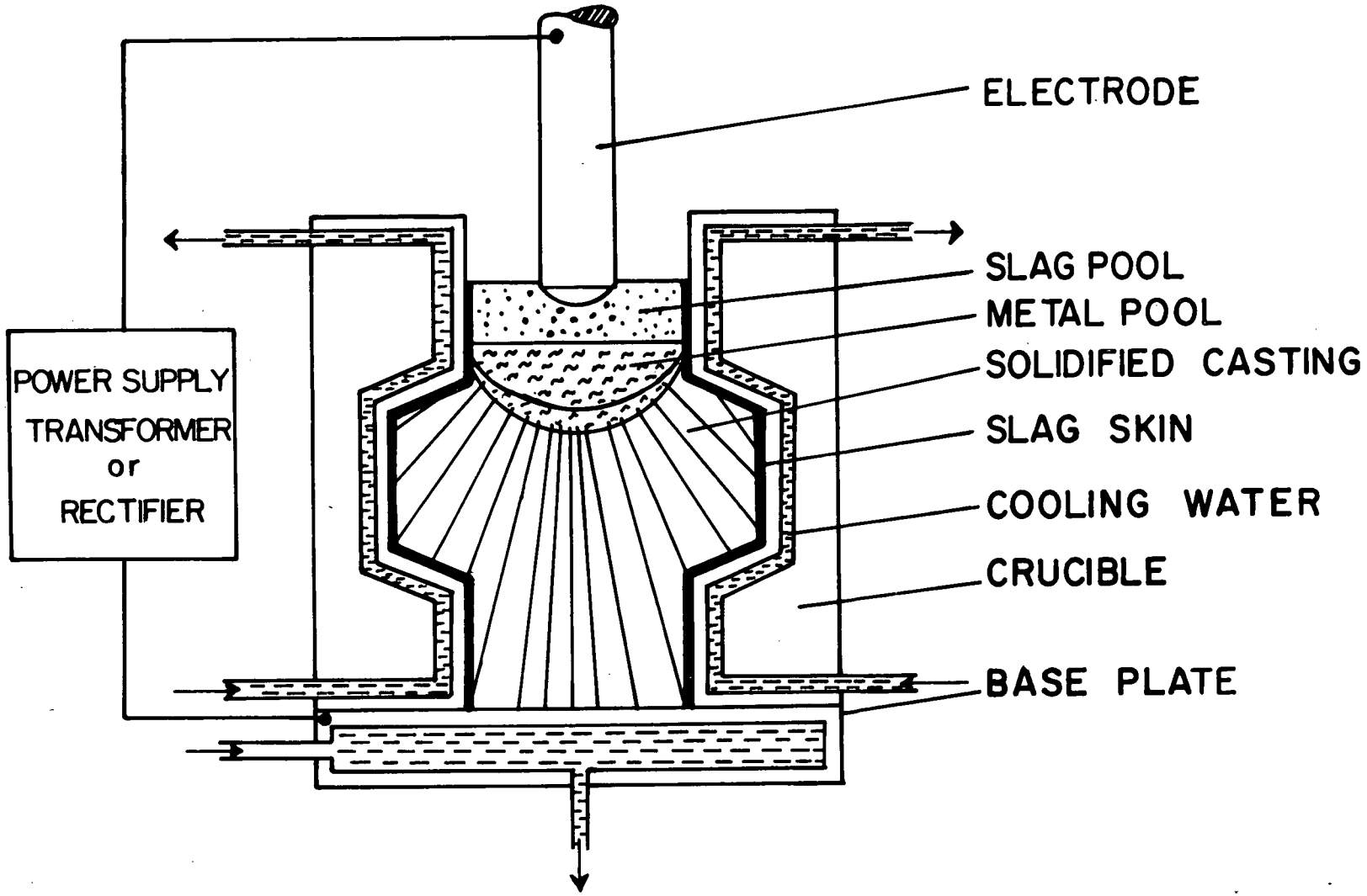

Figure 3. Schematic of the ESC process.

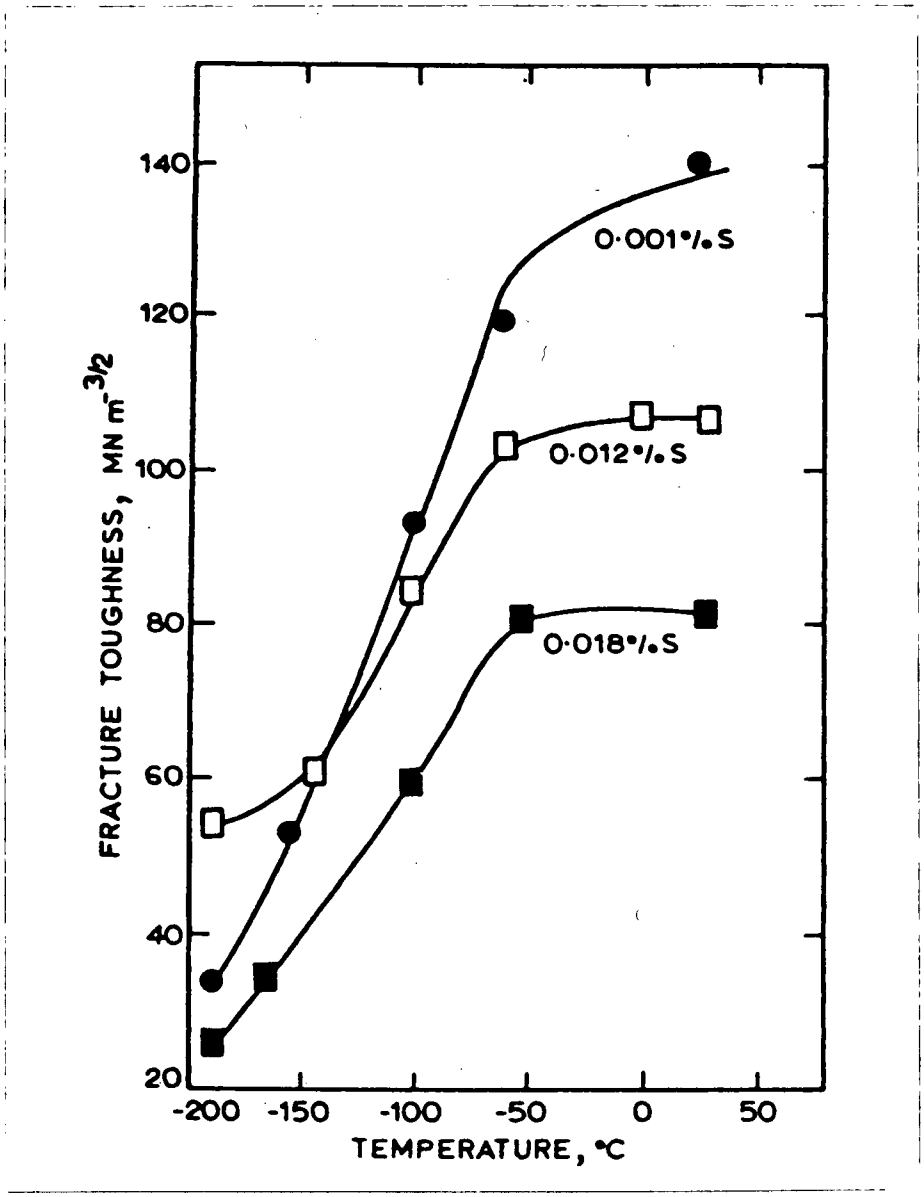

Figure 4. Fracture toughness of ESC AISI 4340 steel containing varying amounts of sulphur.[2]

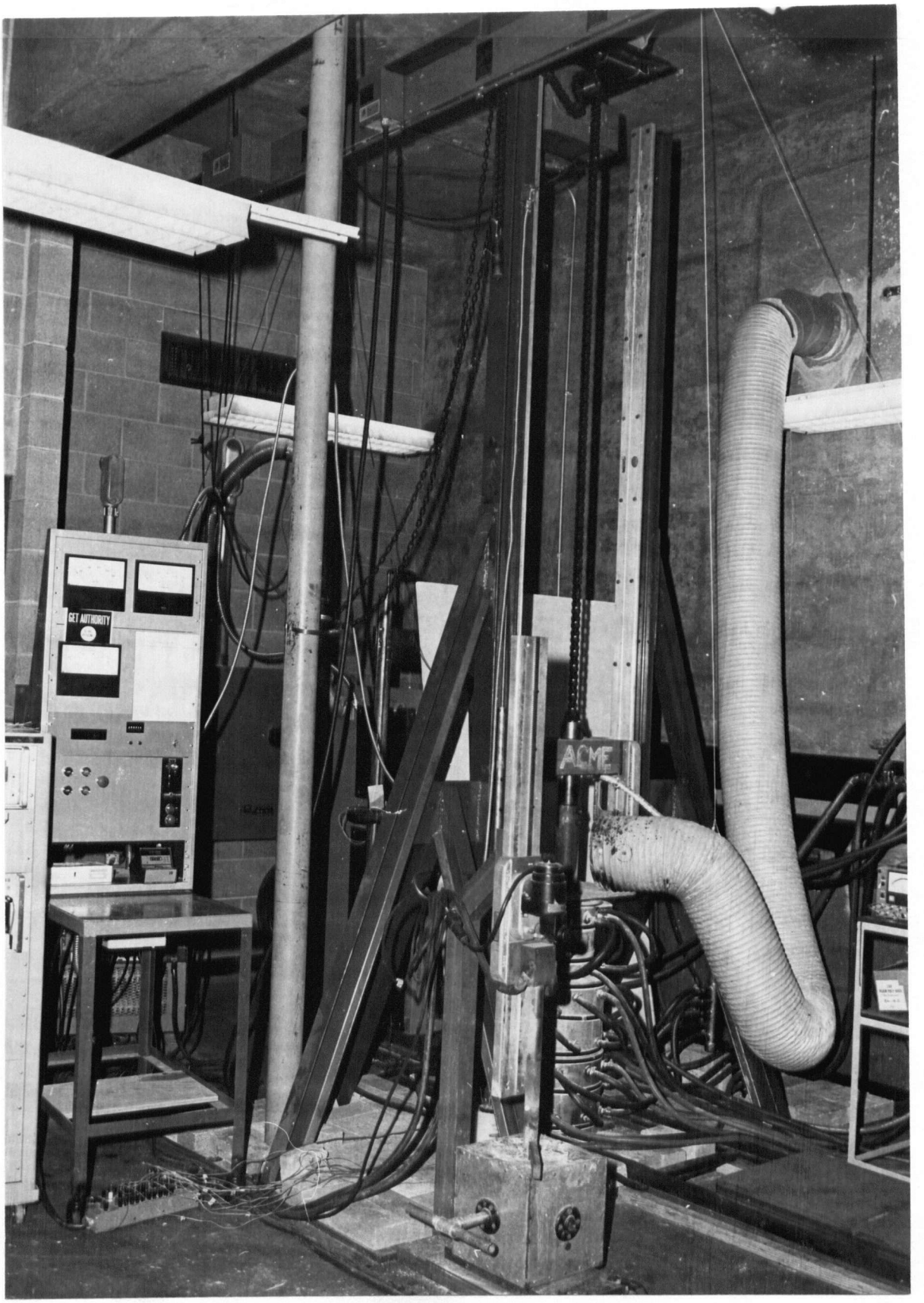

Figure 5. Electroslag casting installation at U.B.C.

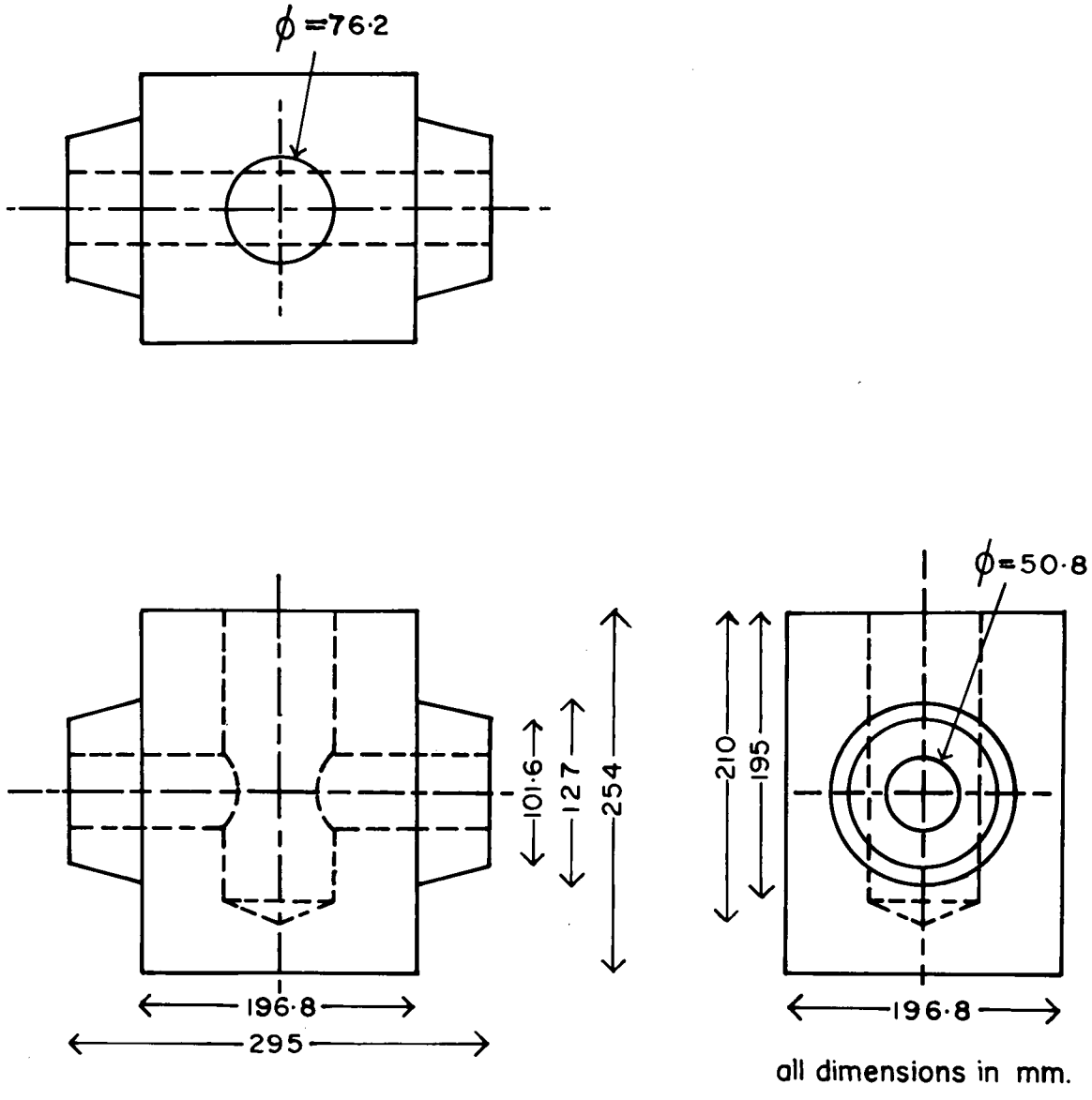

Figure 6. Orthogonal views of ESC valve body.

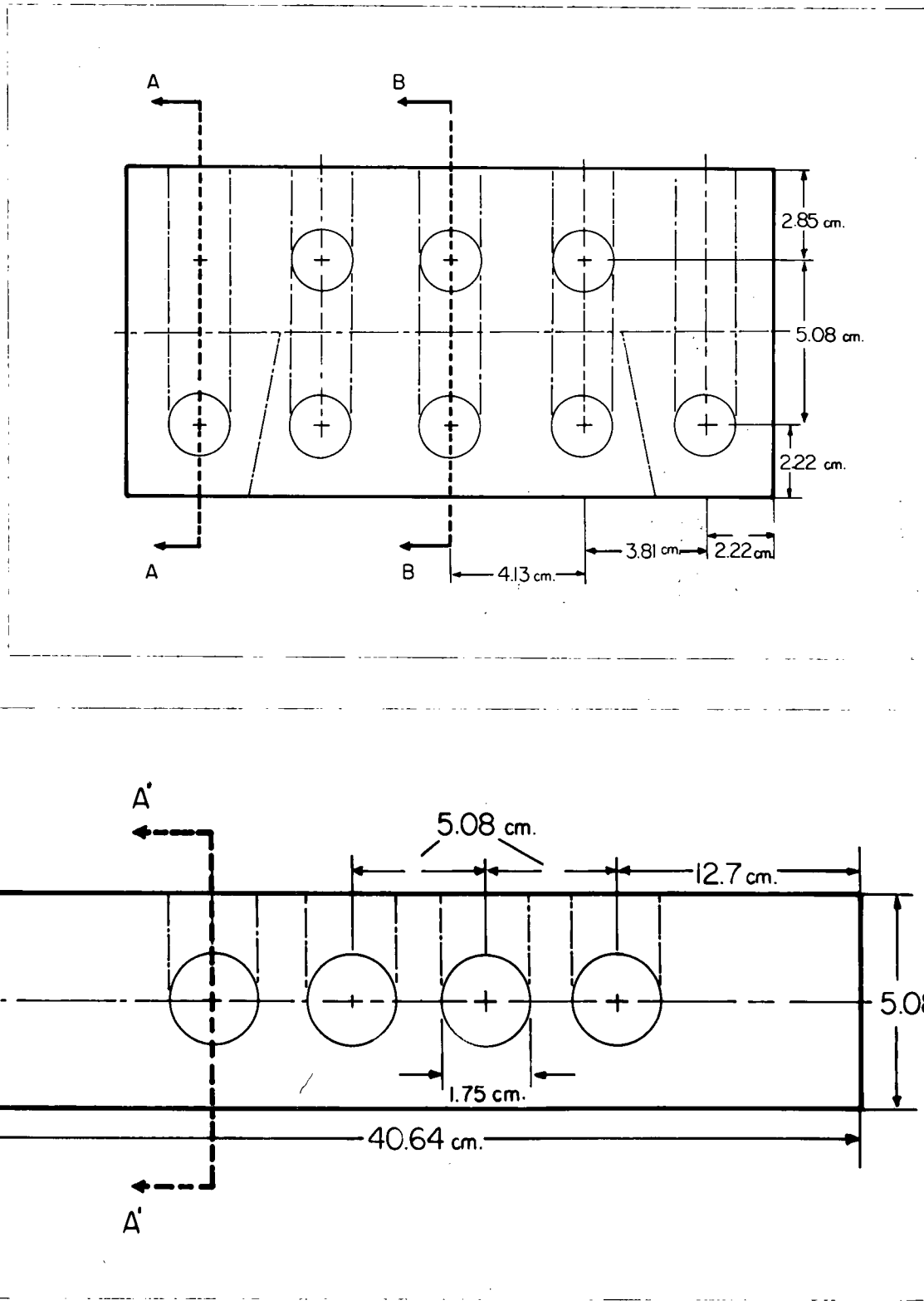

Figure 7(a). Plan views of the valve mold segments.

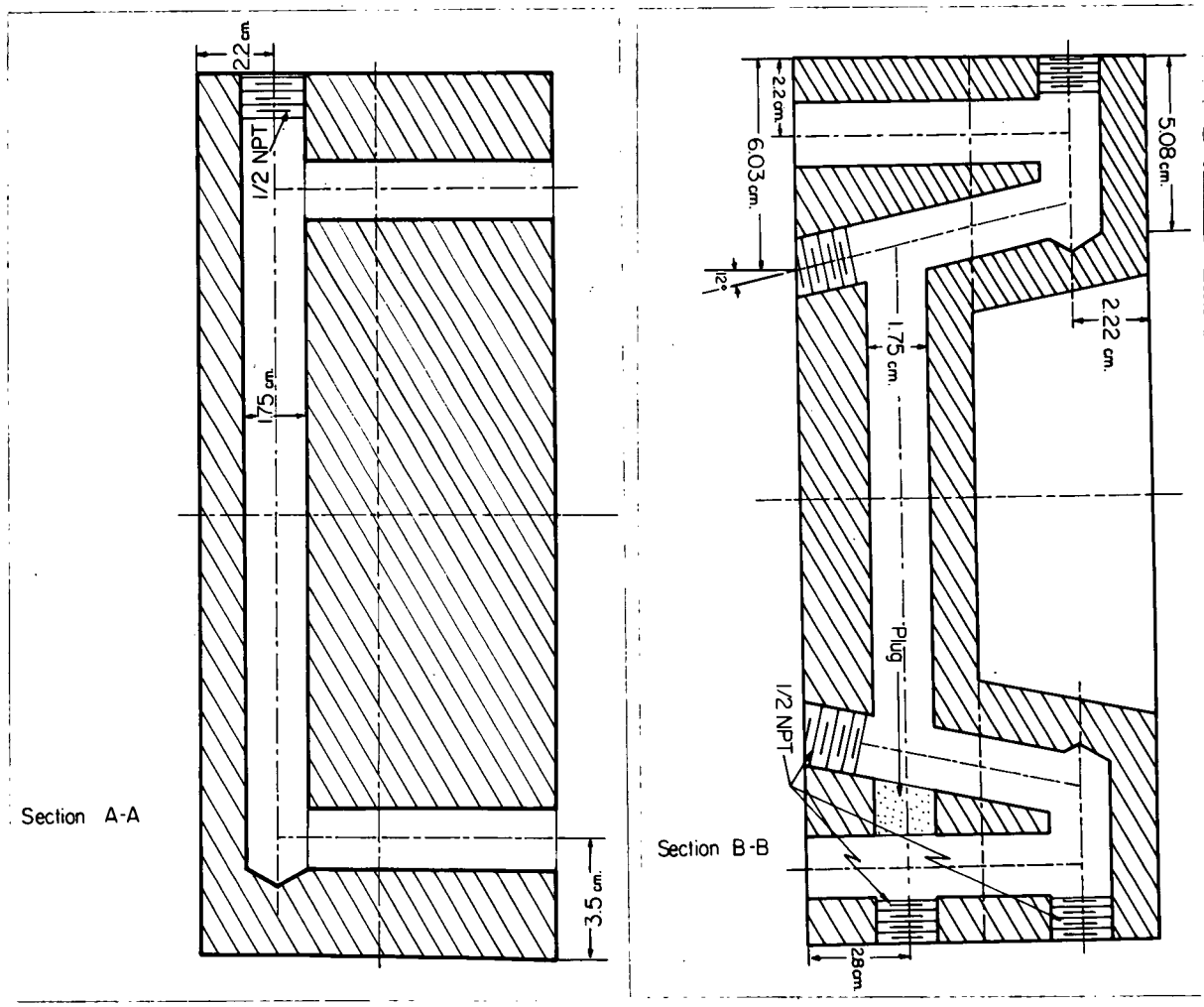

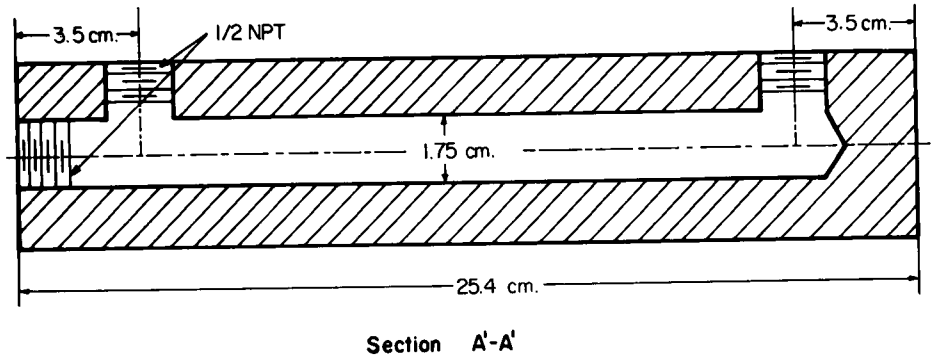

Figure 7(b). Sections through the valve mold segments.

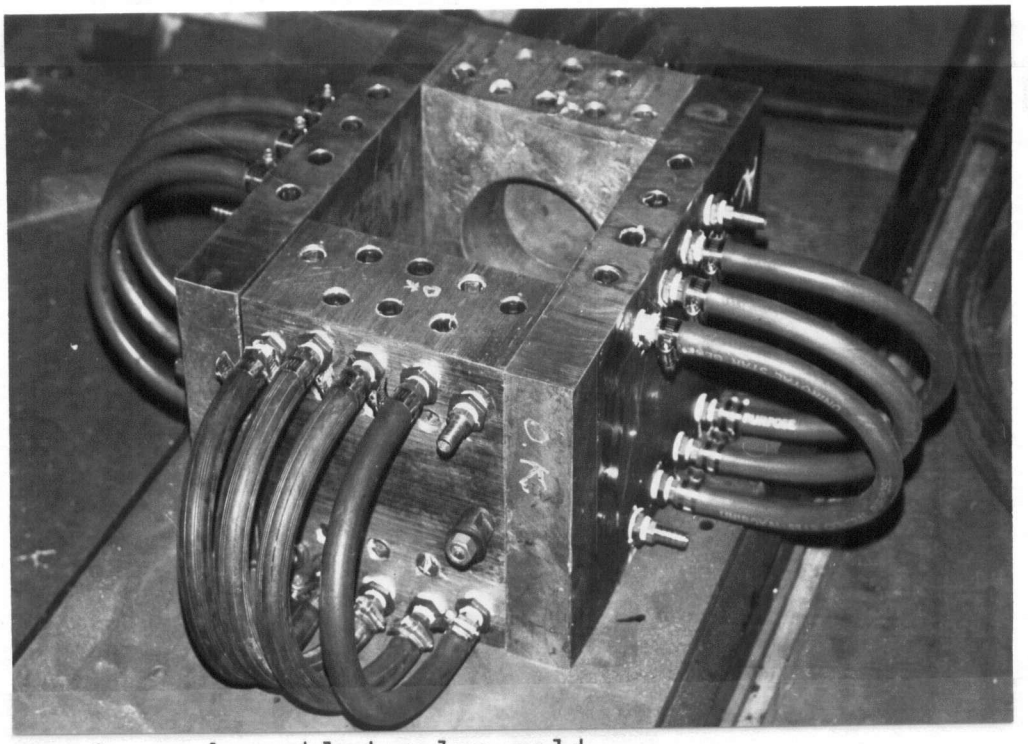

Figure 8. Assembled valve mold.

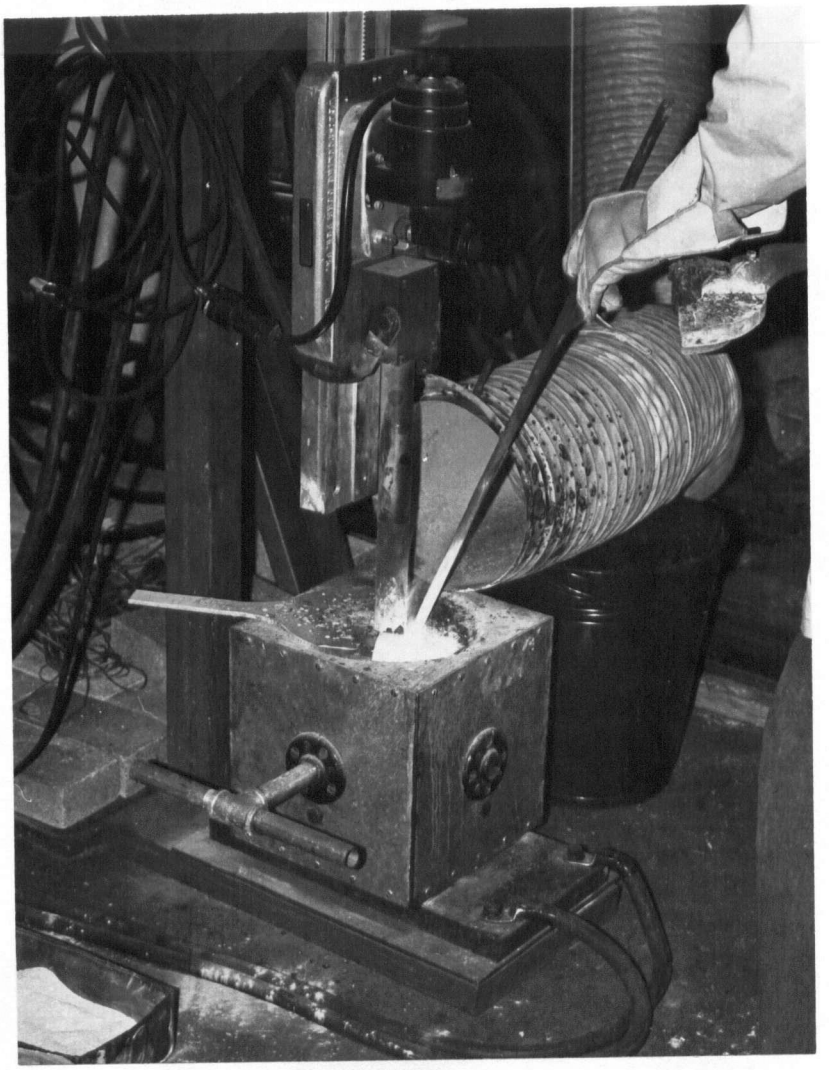

Figure 9. Slag melting furnace.

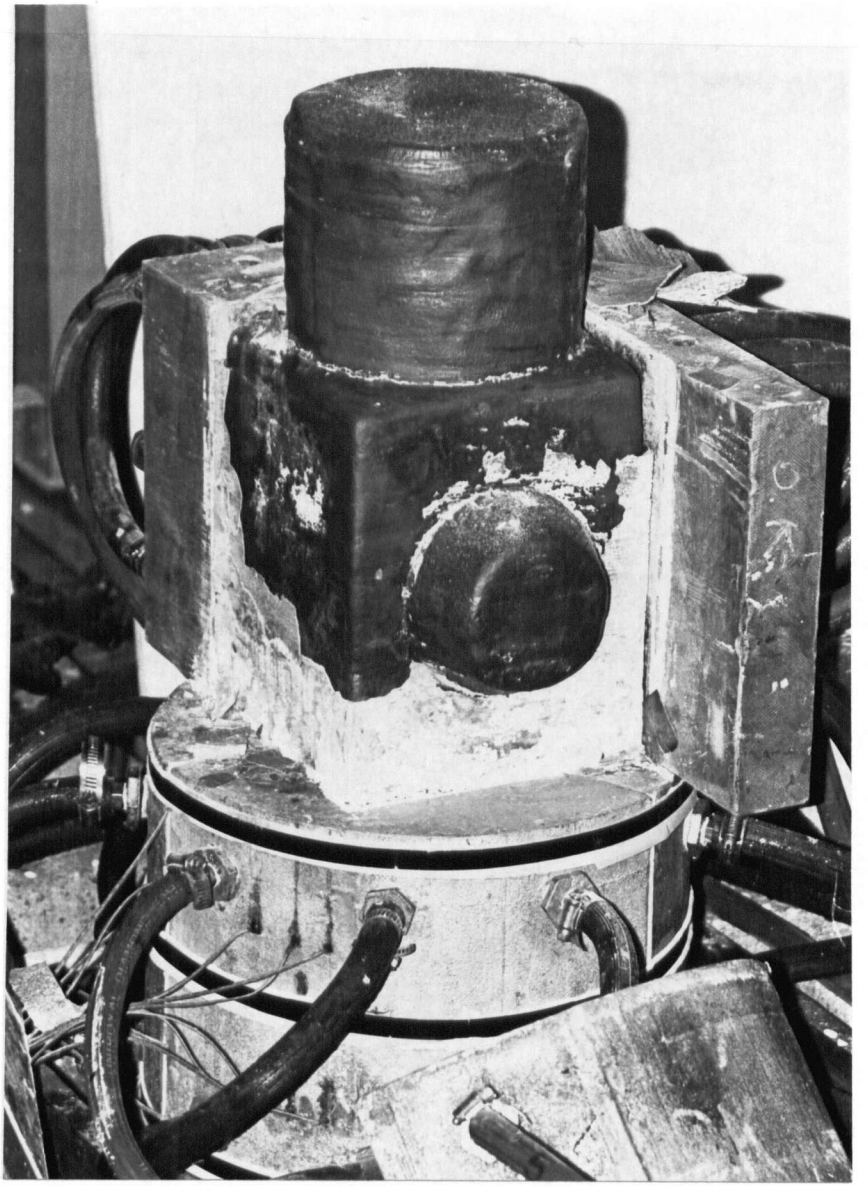

Figure 10. Solidified slag skin on the casting.

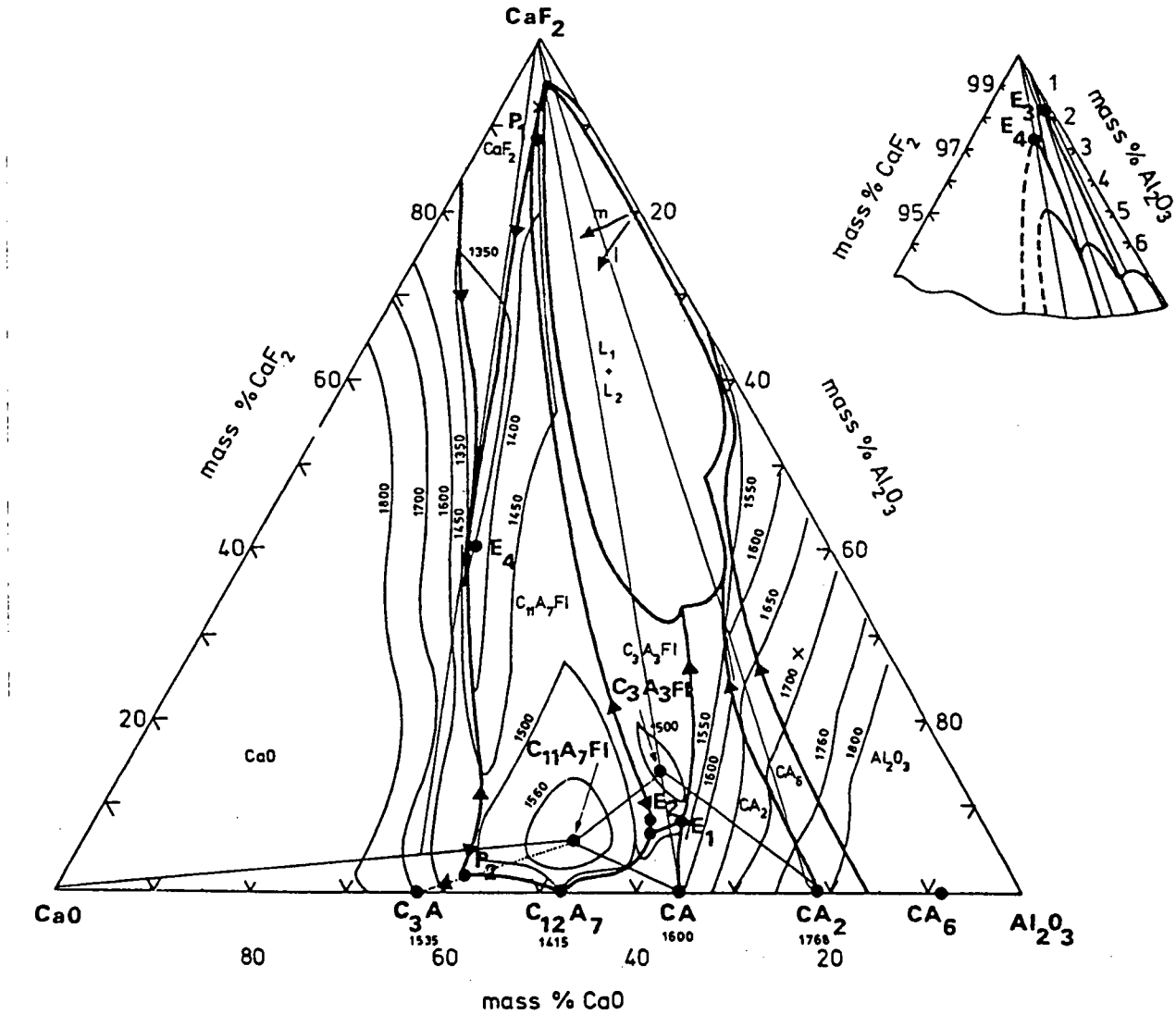

Figure 11. Phase diagram for CaF_2-Al_2O_3-CaO system.[48]

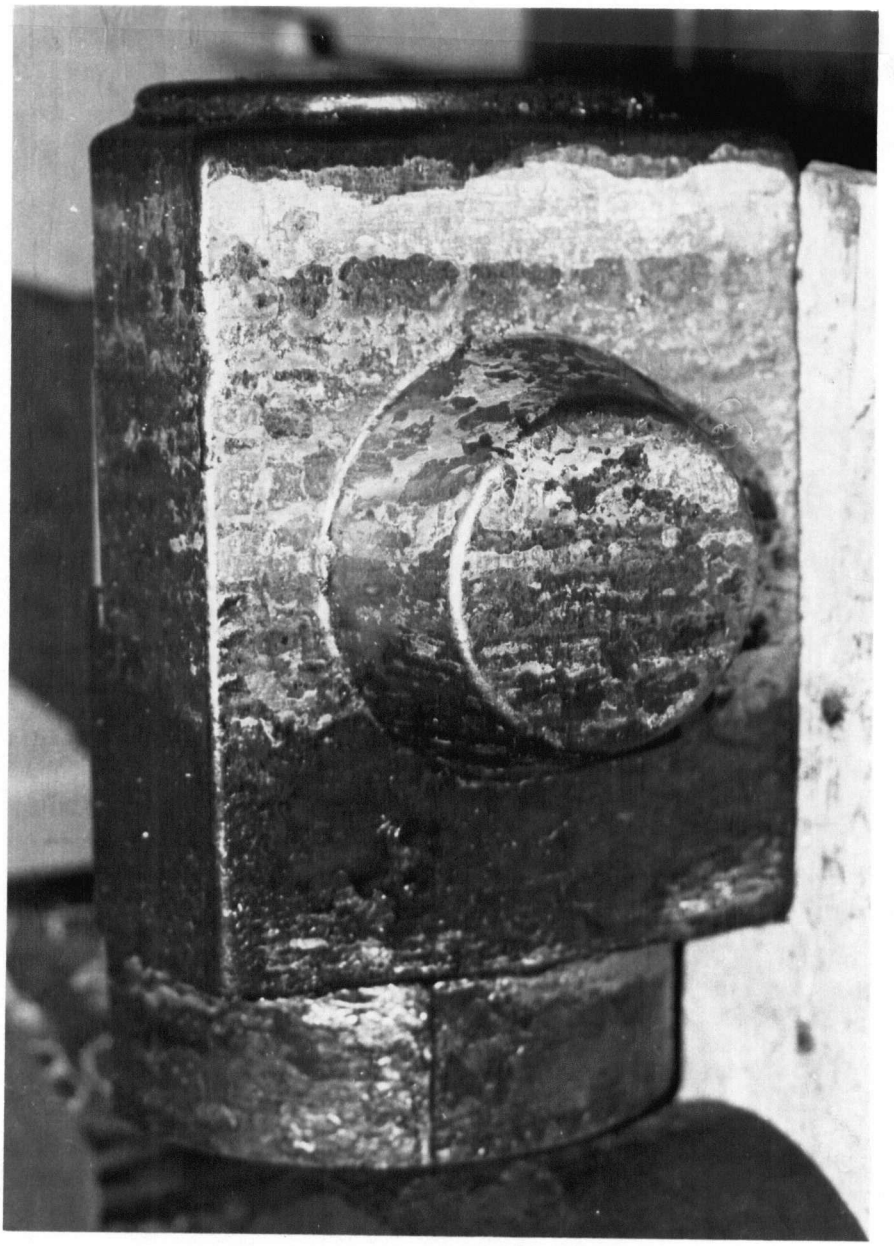

Figure 12. Stainless steel ESC valve.

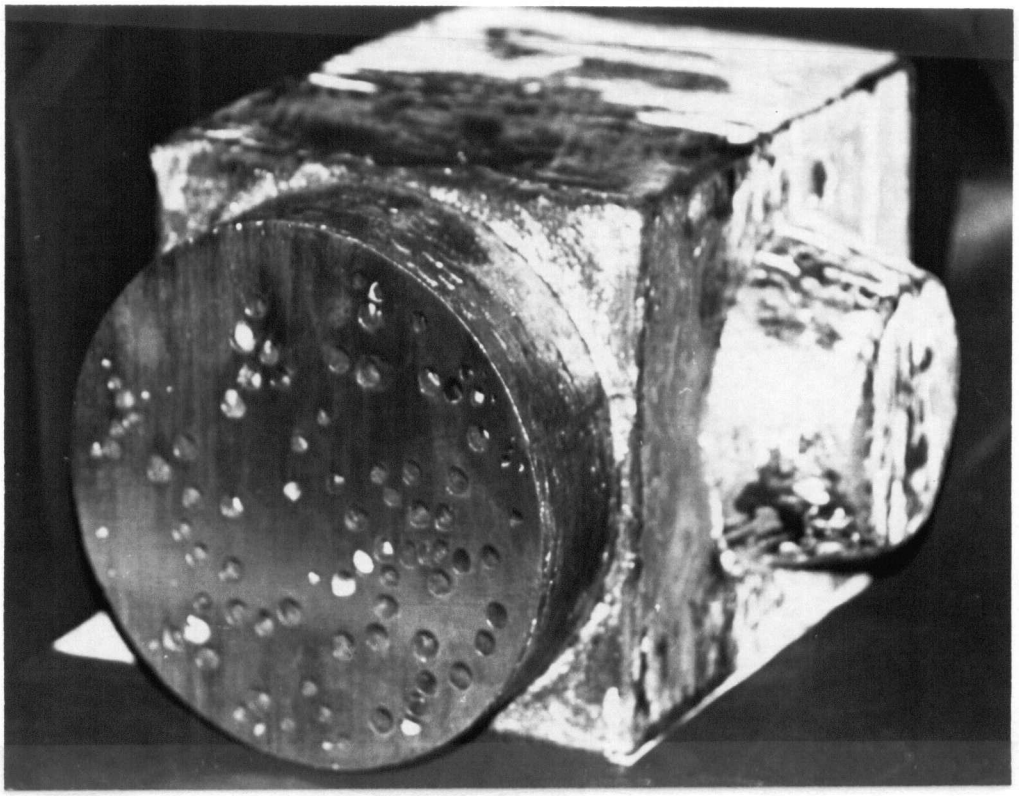

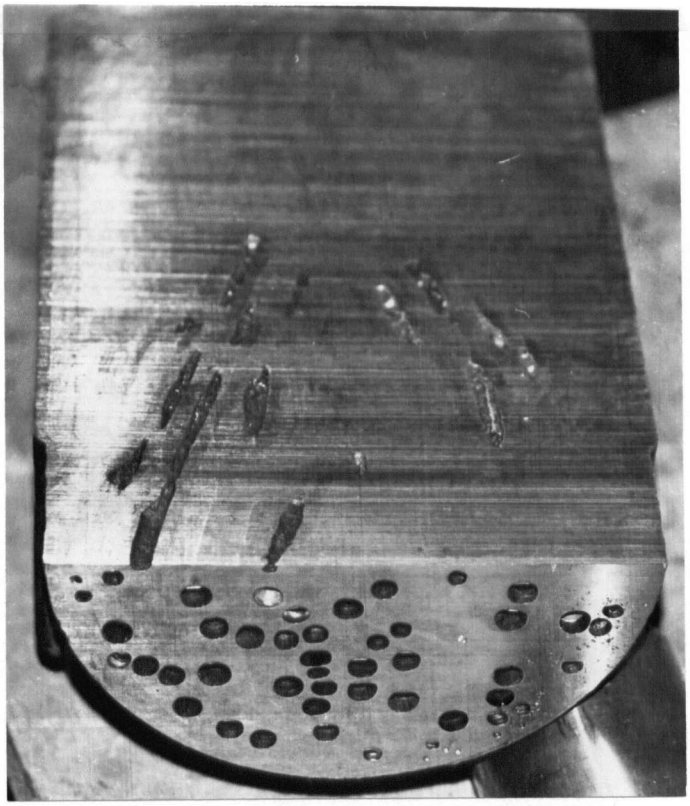

Figure 13. Longitudinal holes in the castings due to moisture.

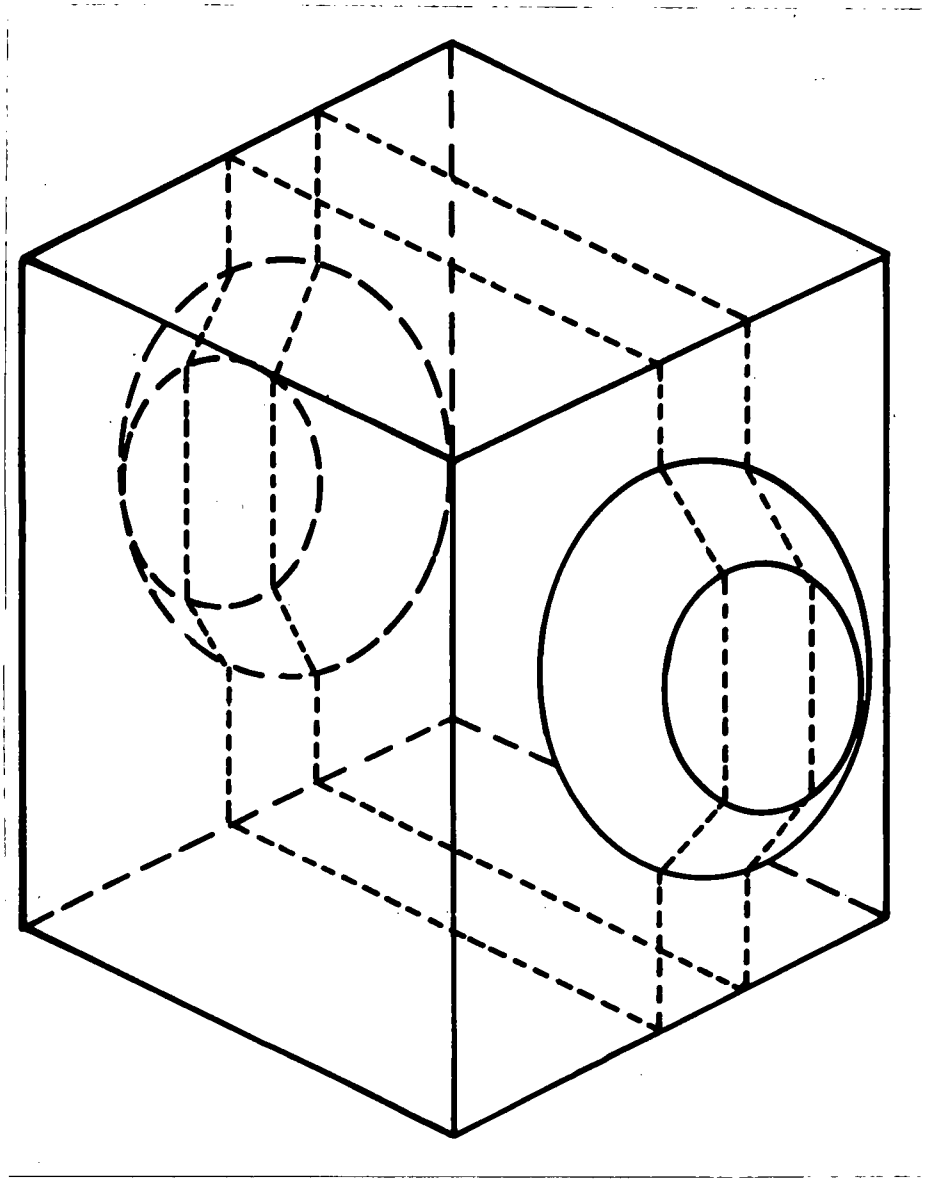

Figure 14. Schematic of the sectioning procedure of the valves.

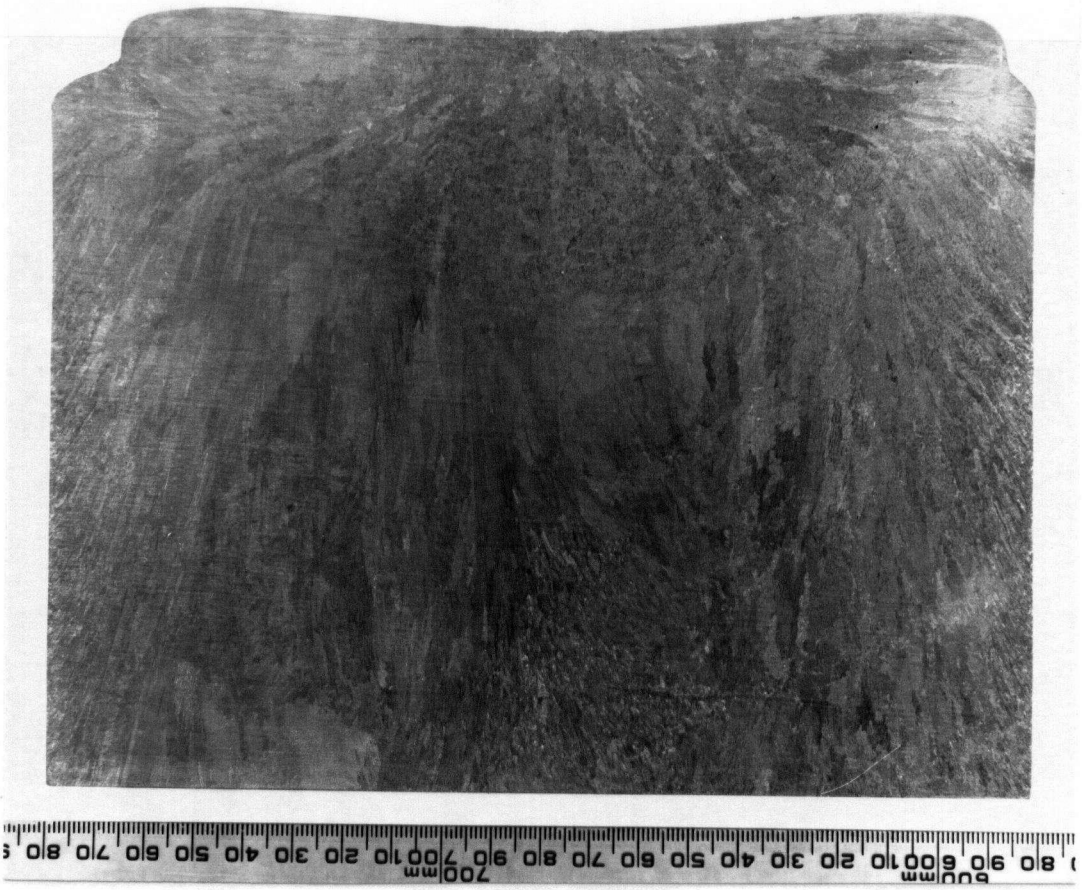

Figure 15. Macrostructure of Valve No. 5 (CF-8M).

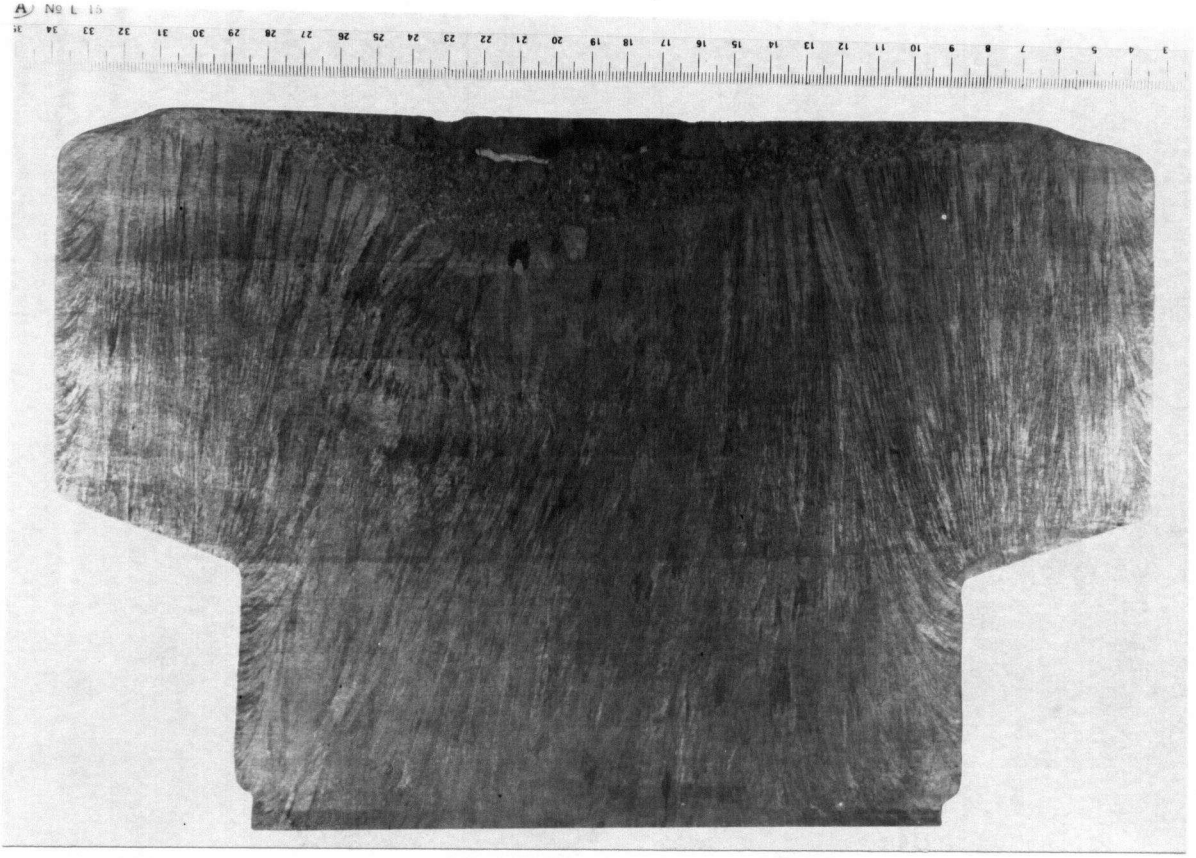

Figure 16. Macrostructure of Valve No. 6 (316).

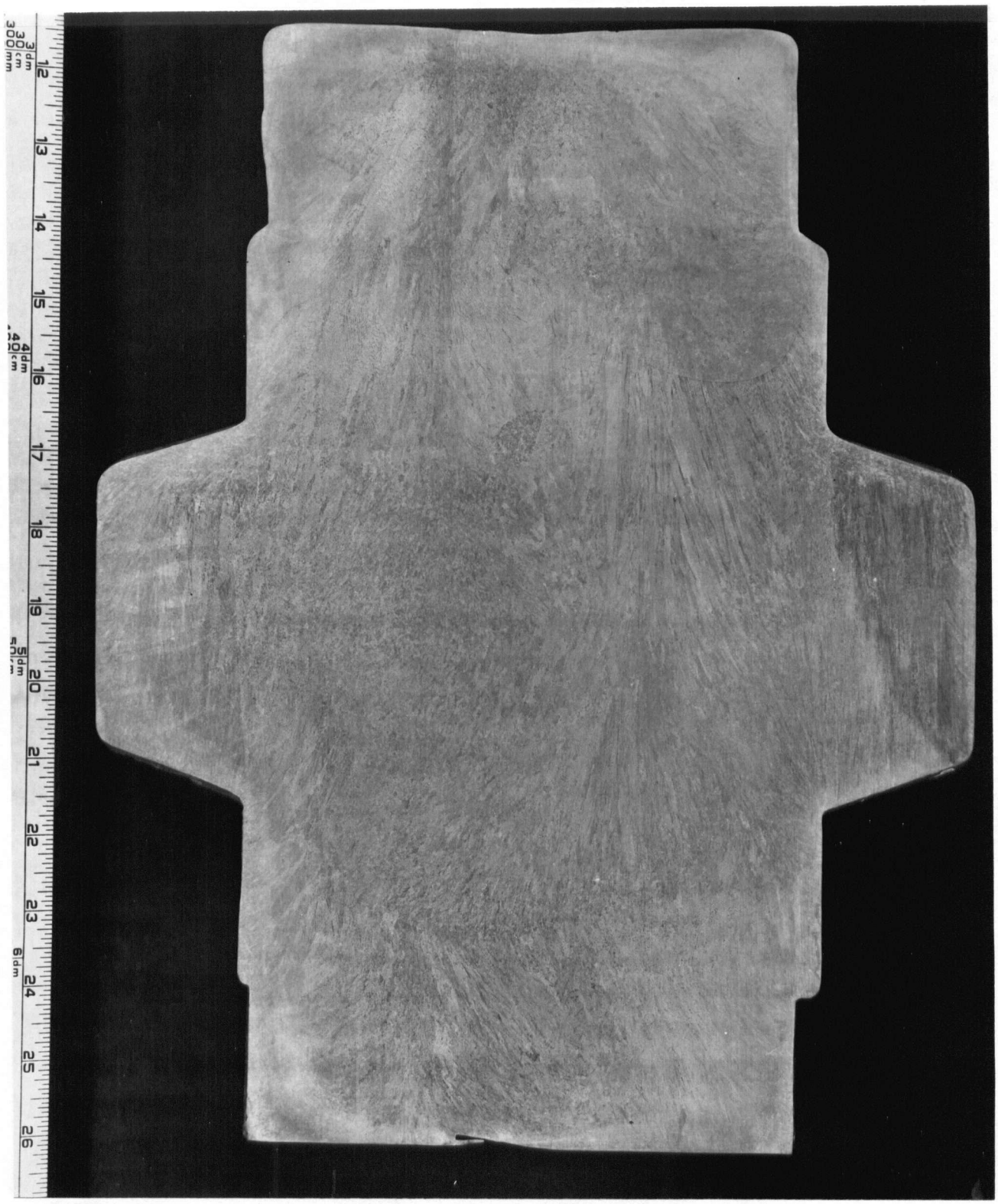

Figure 17. Macrostructure of Valve No. 9 (CF-8M).

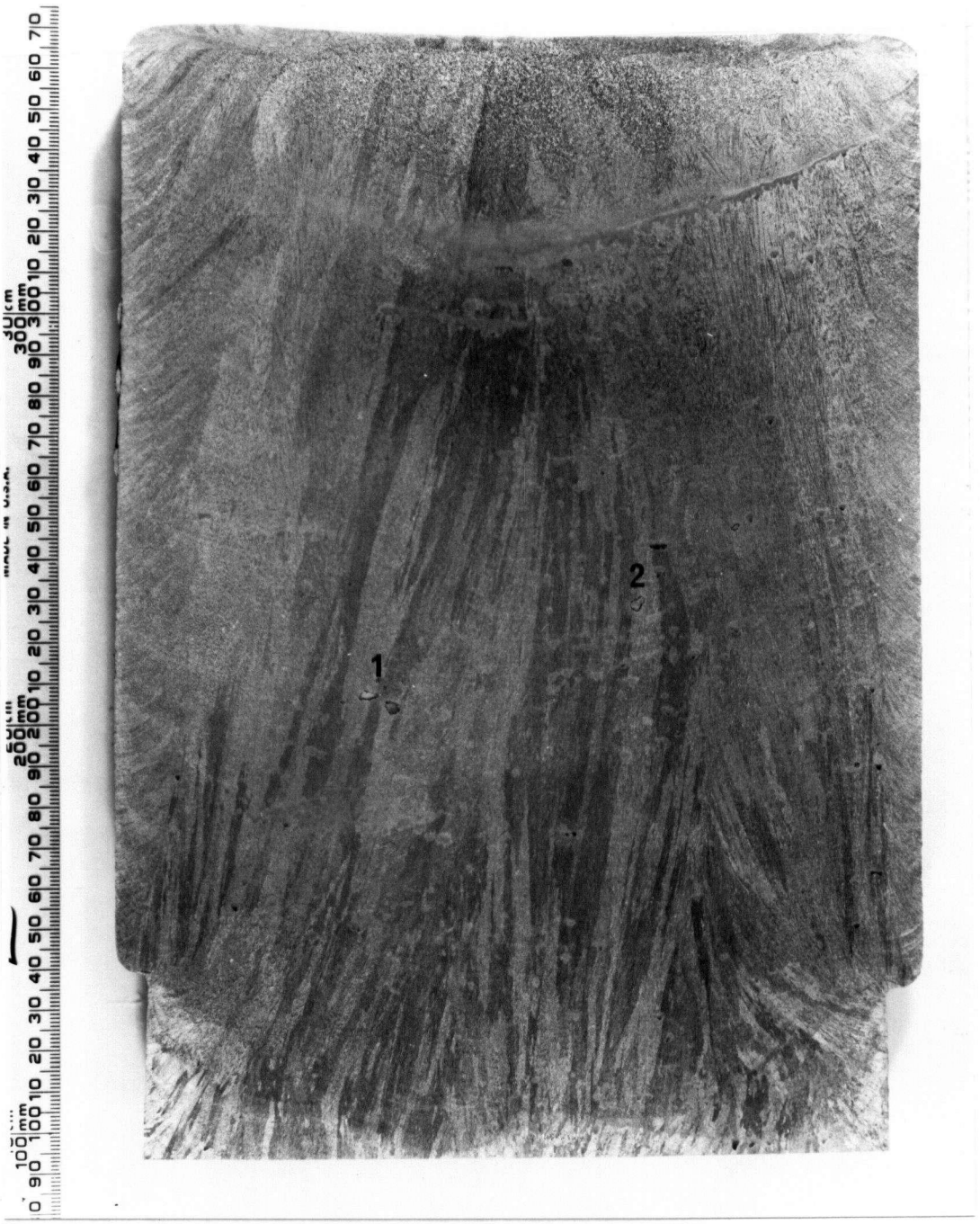

Figure 18. Macrostructure of Valve No. 10 (316+Cr+Mo).

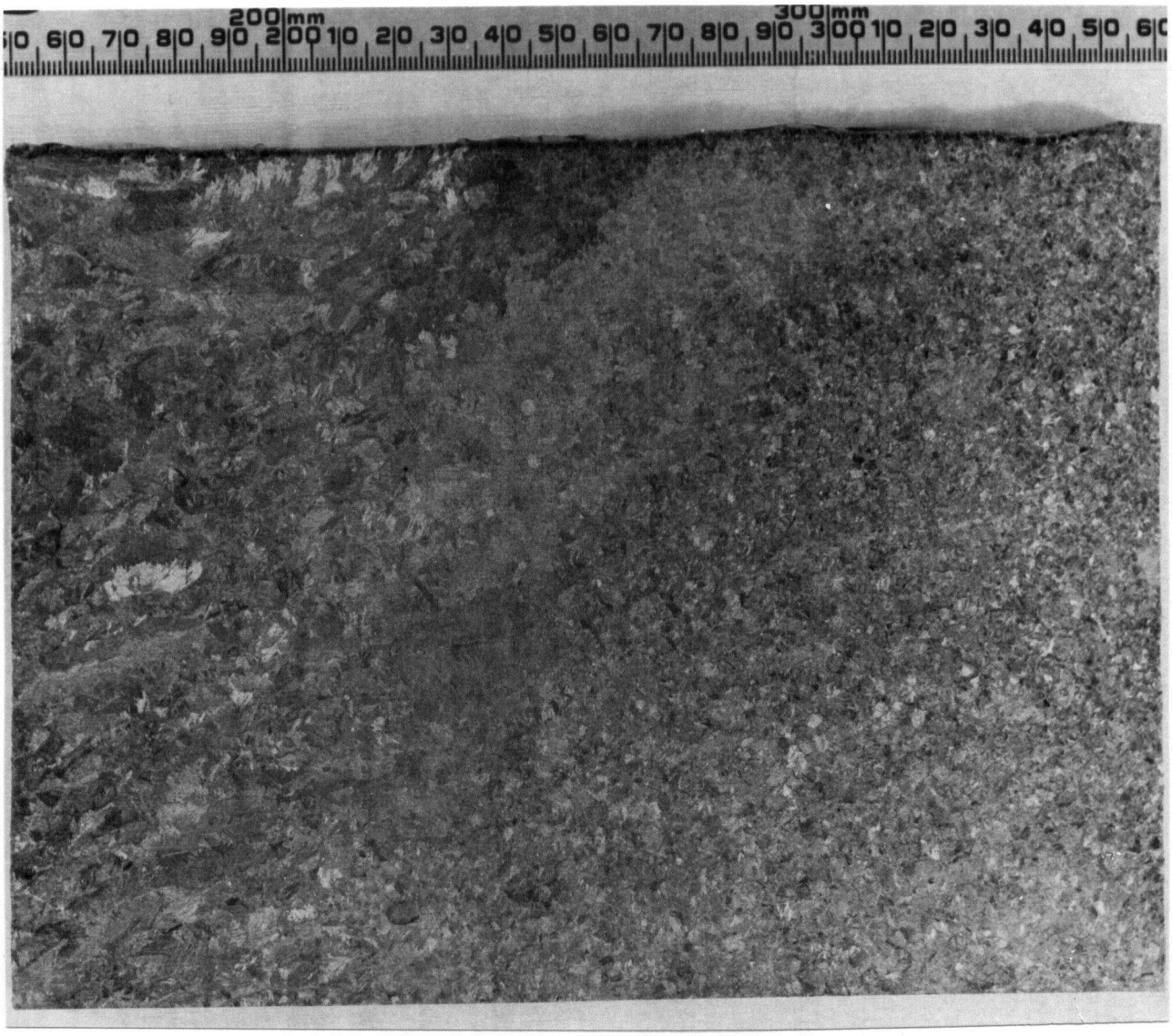

Figure 19. Macrostructure of conventional casting (CF-8M).

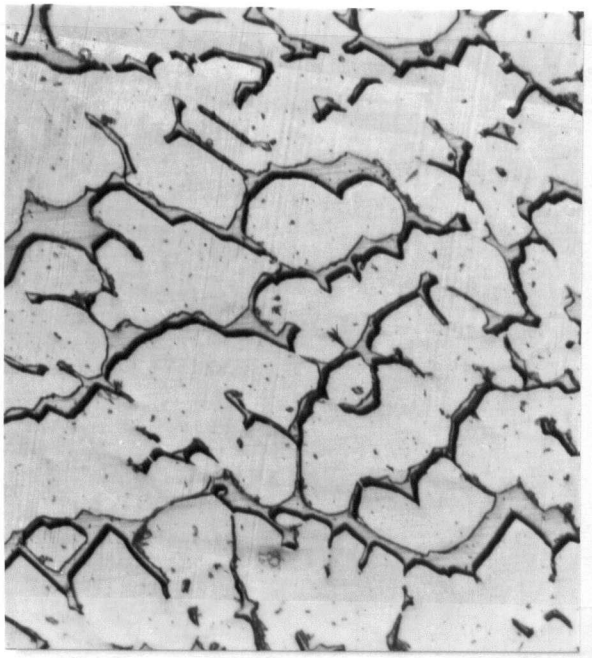

300 x

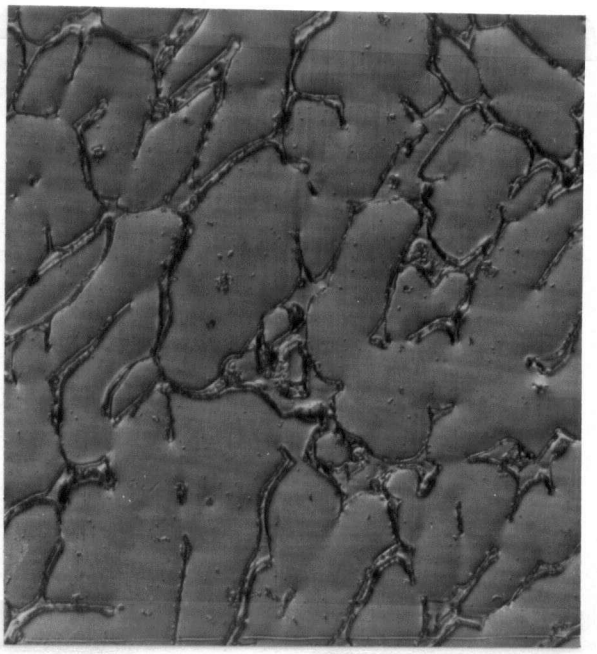

300 x

640 x

Figure 20(a). Microstructure of CF-8M ESC valves before heat treatment (etchant - oxalic acid).

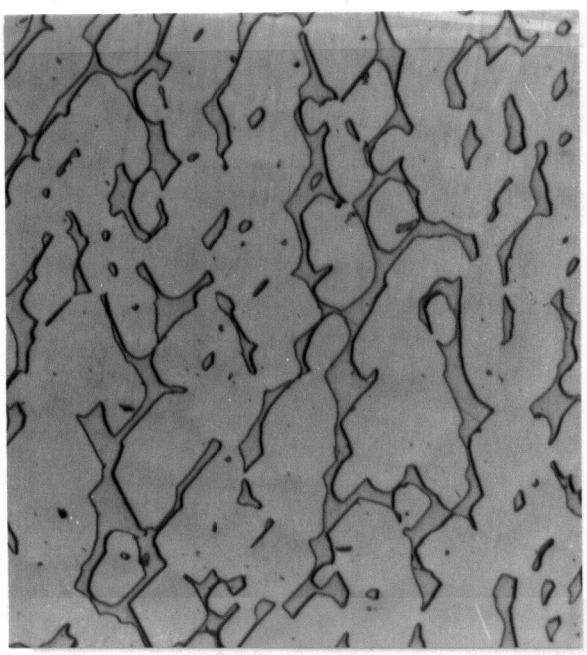

300 x

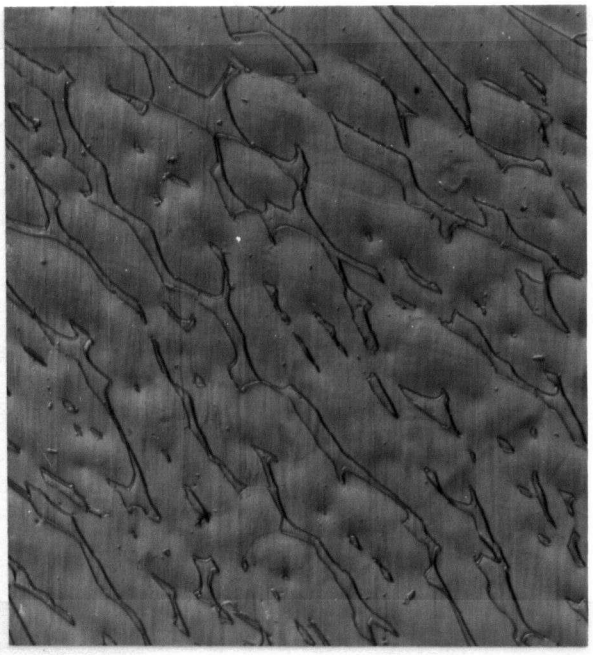

300 x

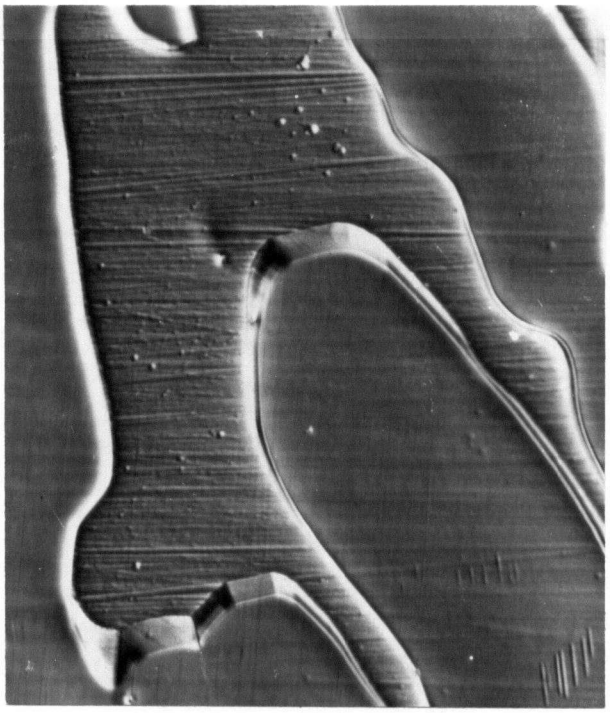

640 x

Figure 20(b). Microstructure of CF-8M ESC valves after heat treatment (etchant - oxalic acid).

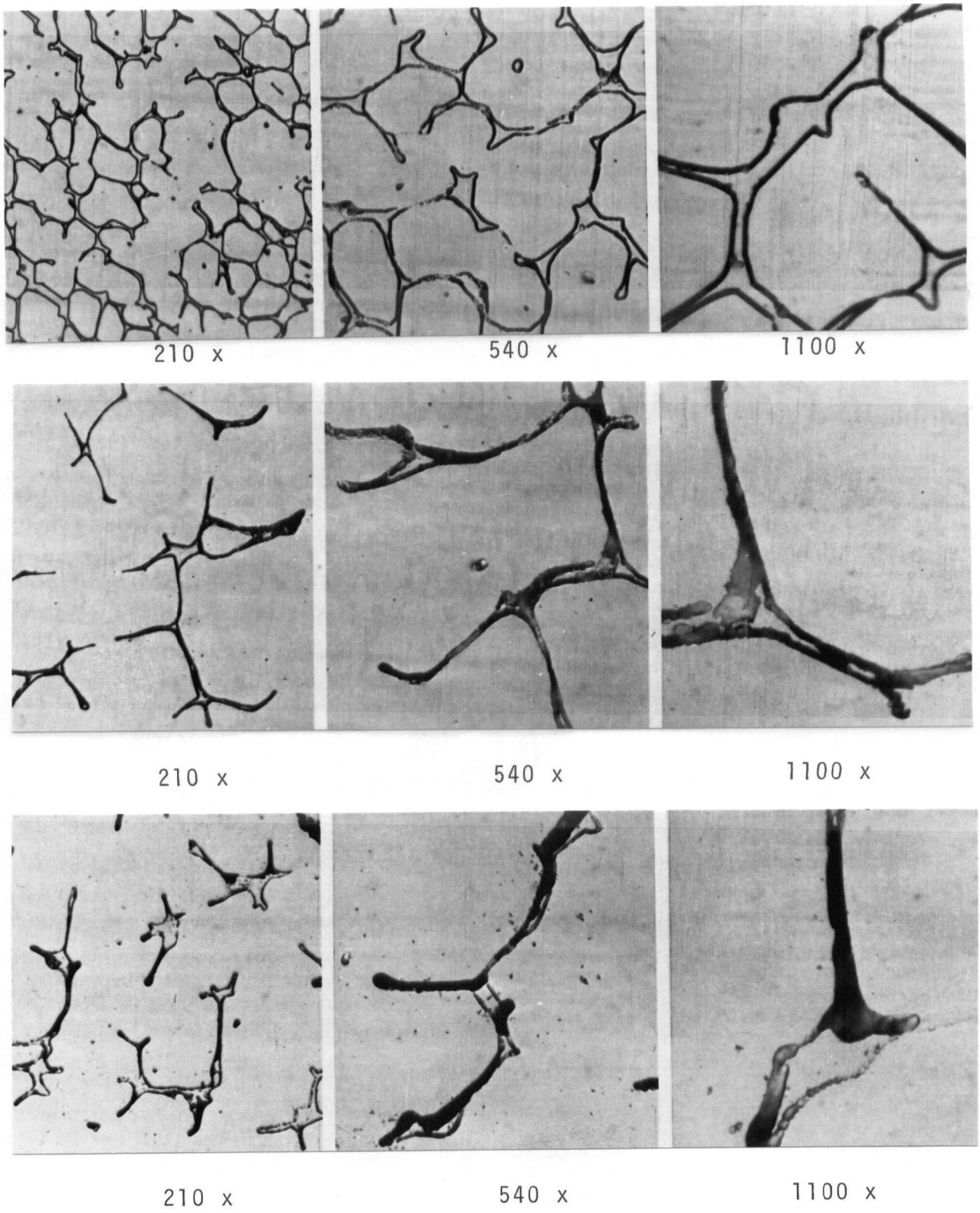

Figure 21. Microstructure of as-cast ESC Valve Nos. 5, 6 and 7 (etchant - oxalic acid).
Top Row - Valve No. 5 (CF-8M), Middle Row - Valve No. 6 (316), Bottom Row - Valve No. 7 (316+Cr).

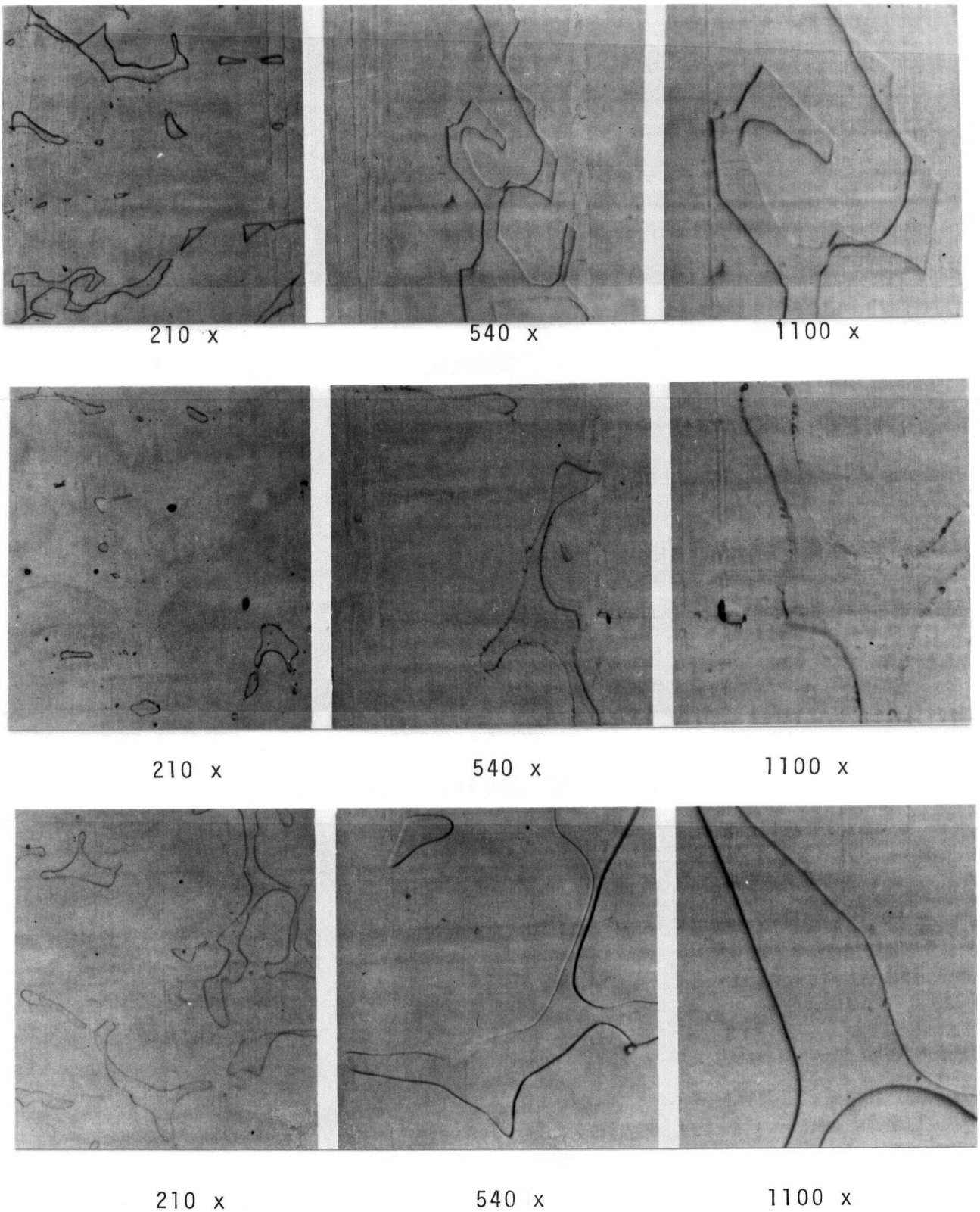

Figure 22. Microstructure of heat-treated ESC Valve Nos. 5, 6 and 7 (echant - oxalic acid).
Top Row - Valve No. 5 (CF-8M), Middle Row - Valve No. 6 (316)
Bottom Row - Valve No. 7 (316+Cr).

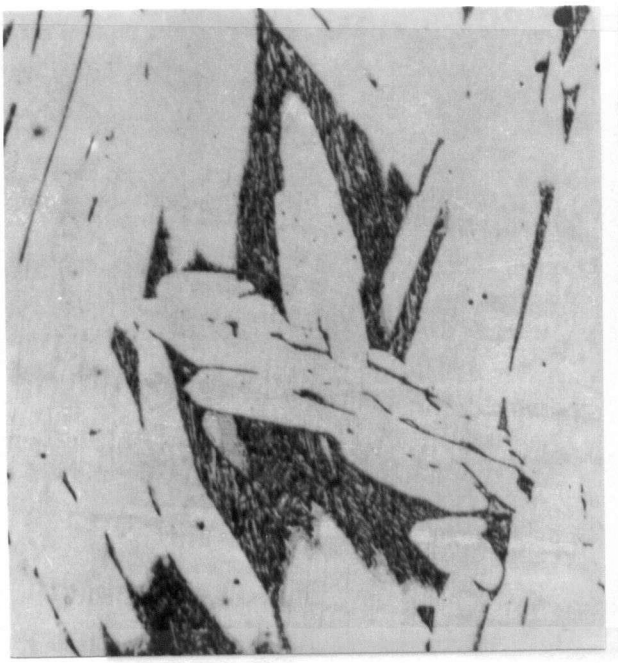

80 x

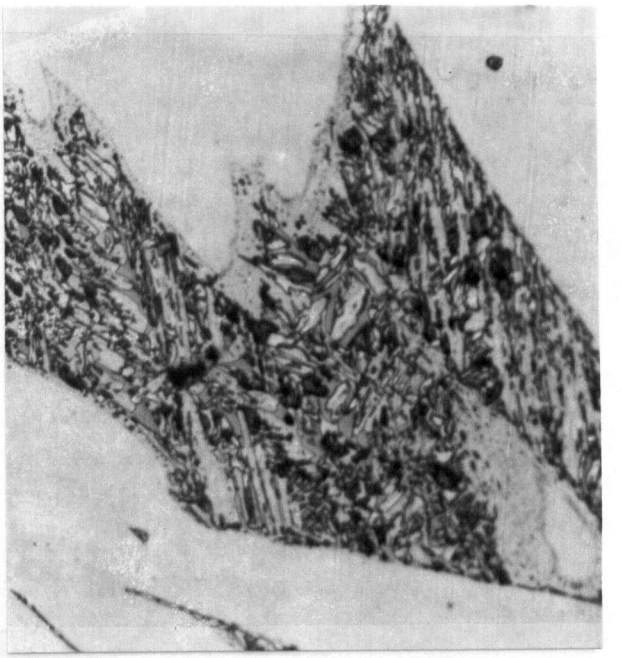

300 x

640 x

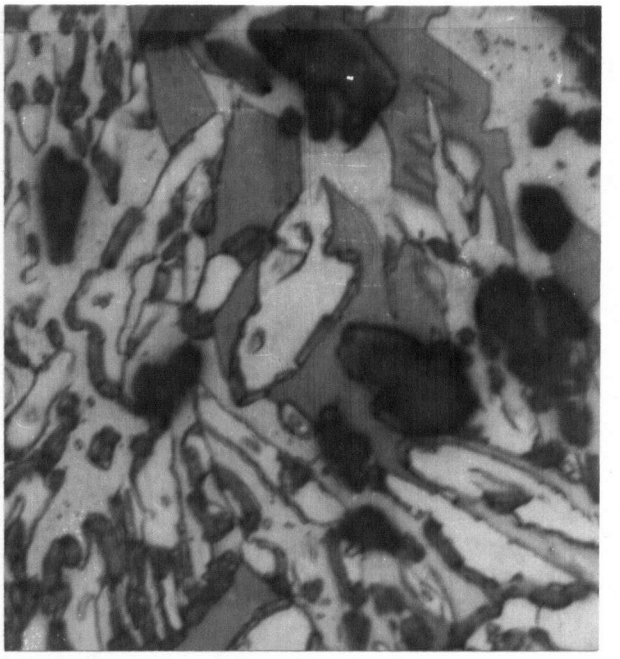

1300 x

Figure 23. Microstructure of CF-8M specimen heated to 850°C (etchant - KOH).

light grey area - austenite phase
dark grey area - ferrite phase
black area - sigma phase

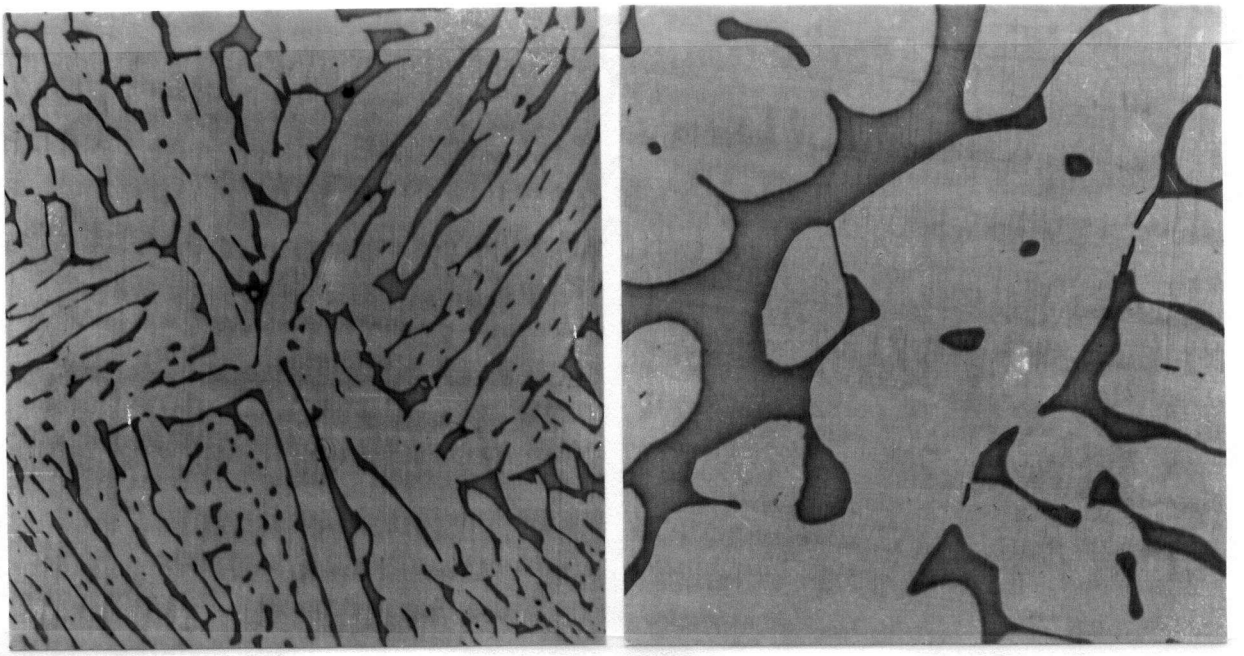

80 x

300 x

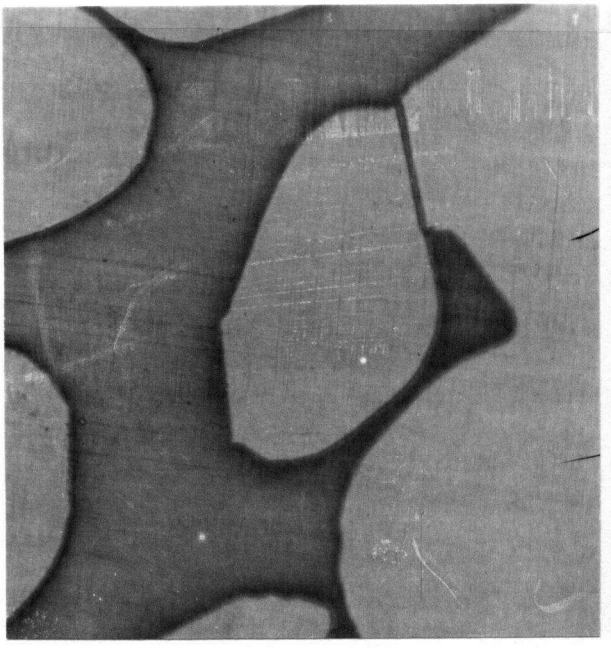

640 x

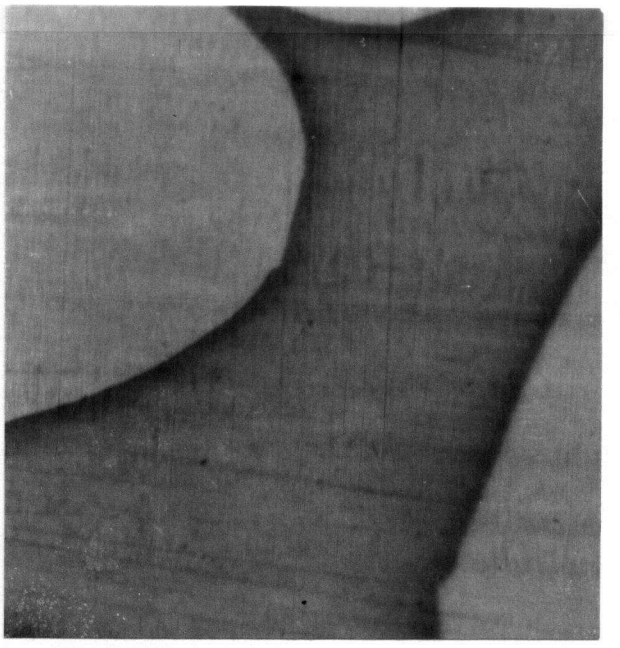

1300 x

Figure 24. Microstructure of heat-treated CF-8M conventional casting (etchant - KOH).

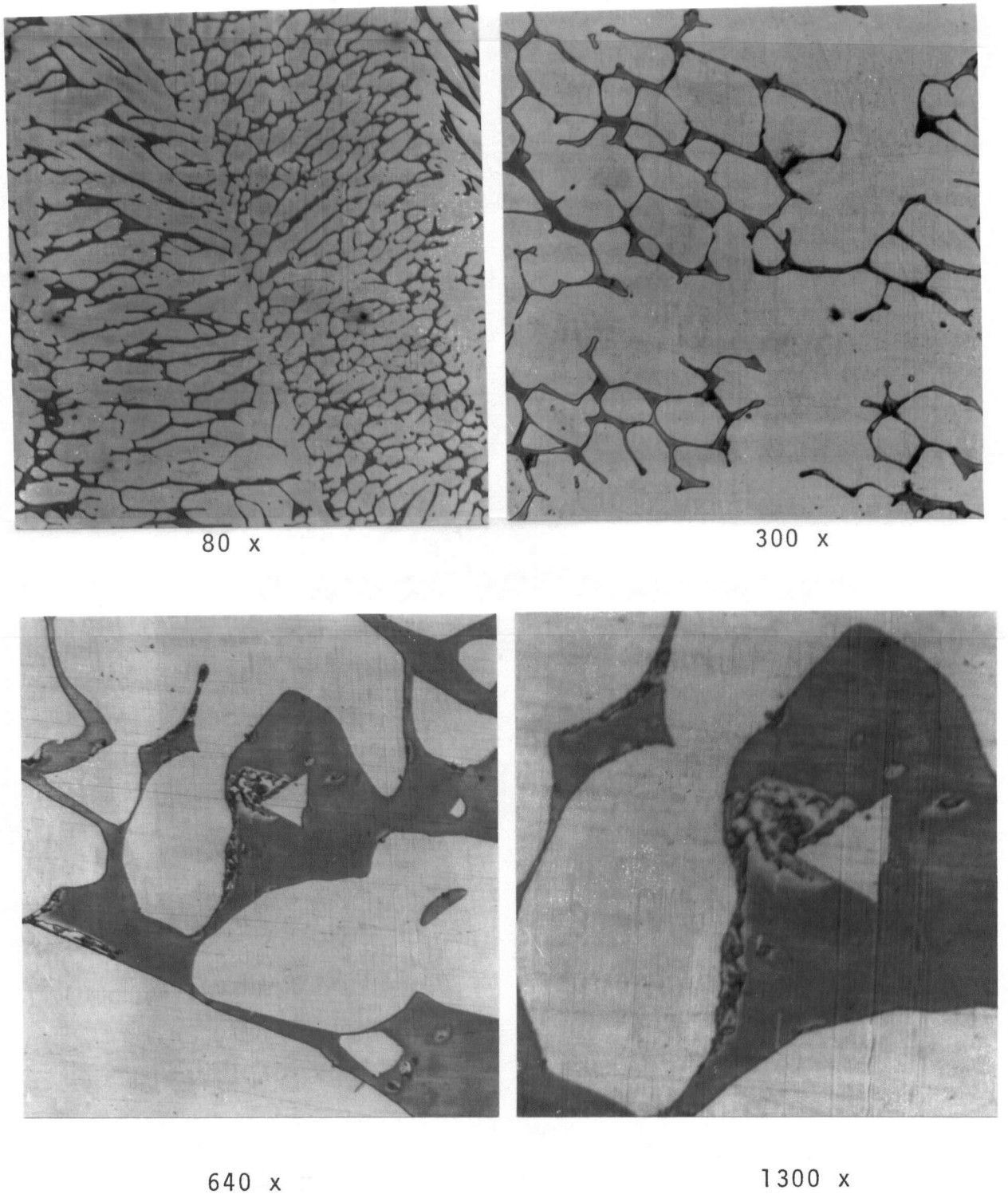

80 x

300 x

640 x

1300 x

Figure 25. Microstructure of Valve No. 9 in as-cast condition (etchant - KOH).

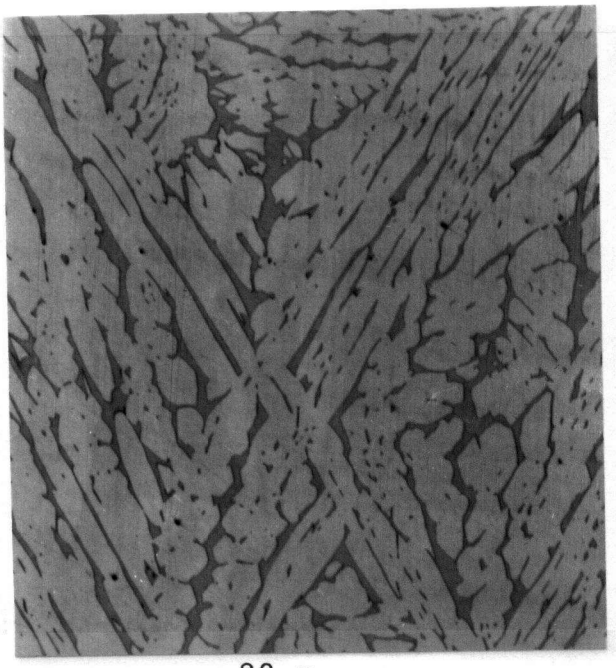

80 x

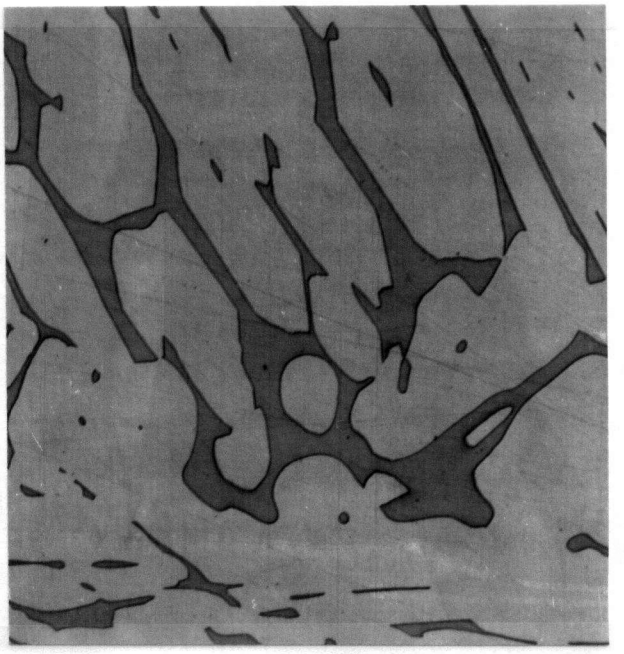

300 x

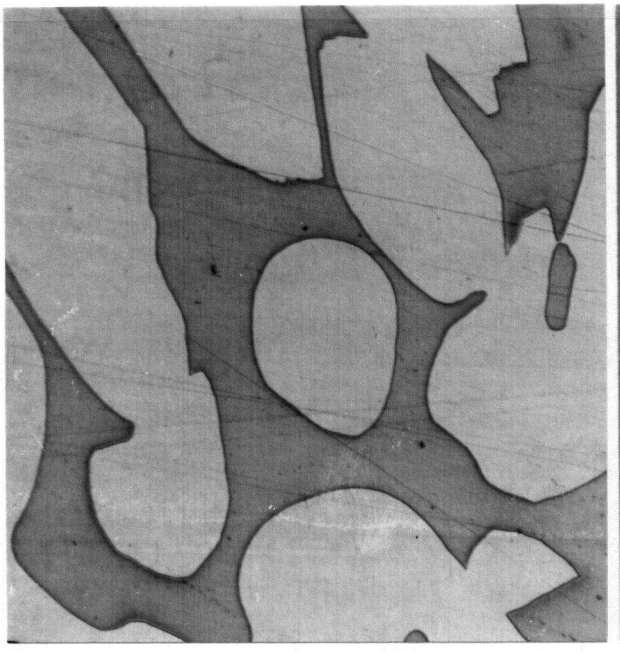

640 x

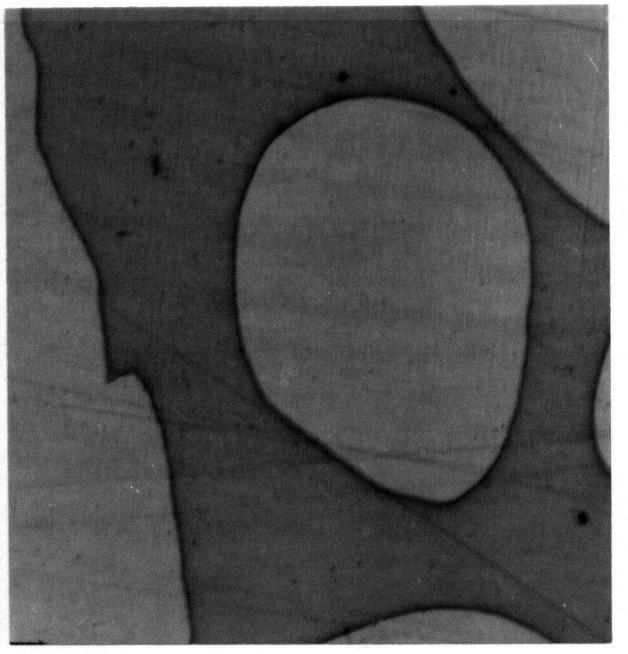

1300 x

Figure 26. Microstructure of Valve No. 9 in heat-treated condition (etchant - KOH).

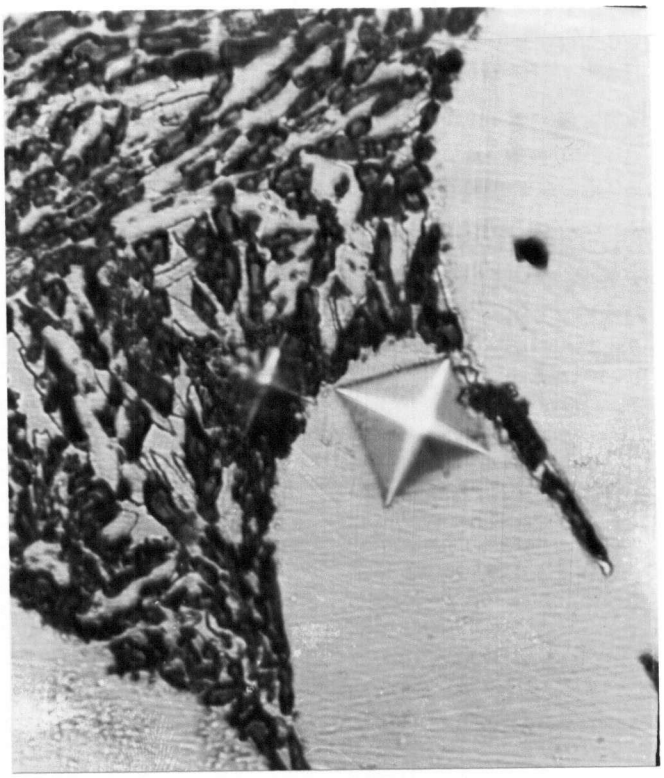

700 x

Figure 27. Microhardness indentations on sigma and austenite phases.

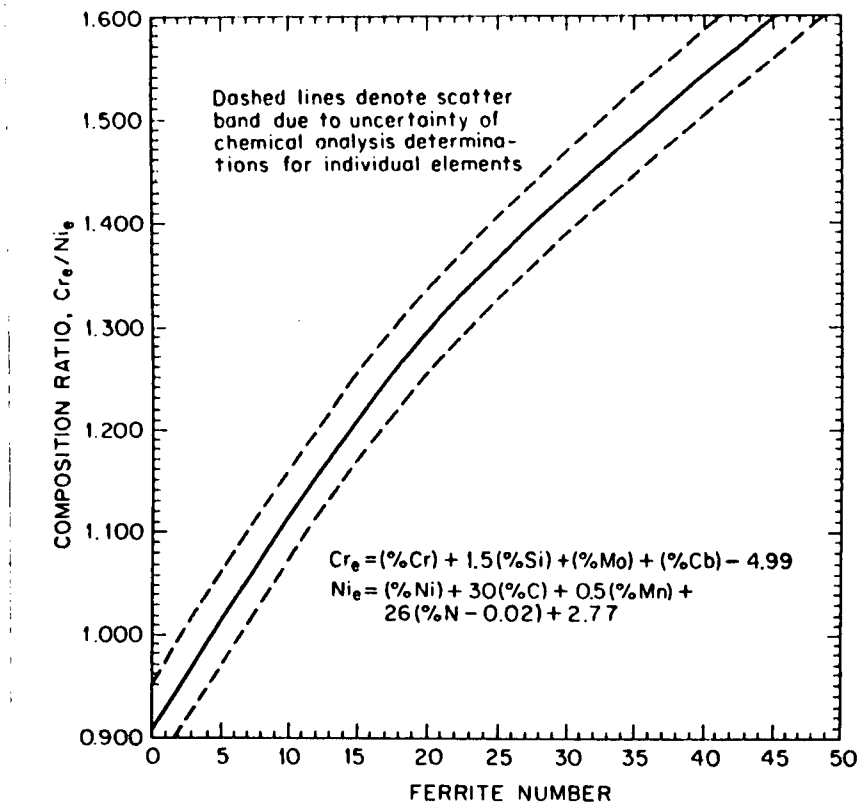

Figure 28. Schoefer's diagram for determination of ferrite numbers of stainless steel castings.[66]

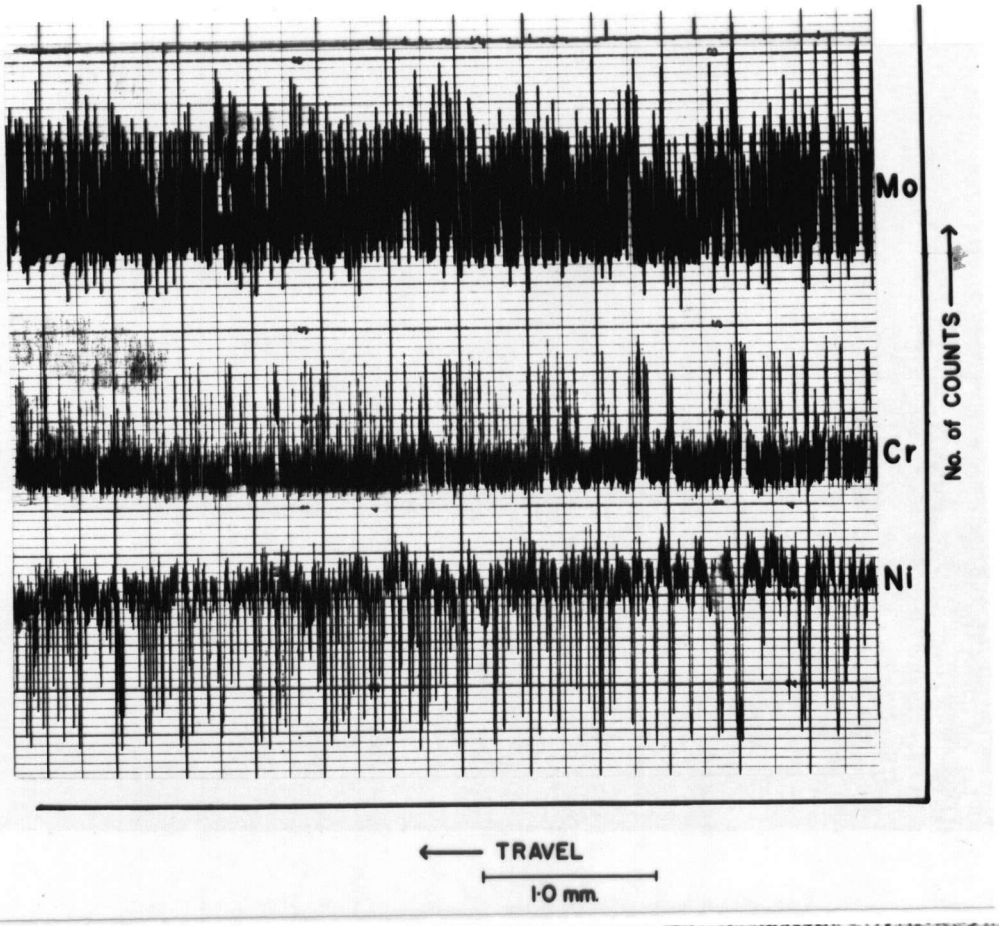

Figure 29(a). Variation of Cr, Ni and Mo across the dendritic direction in Valve No. 9 at the edge.

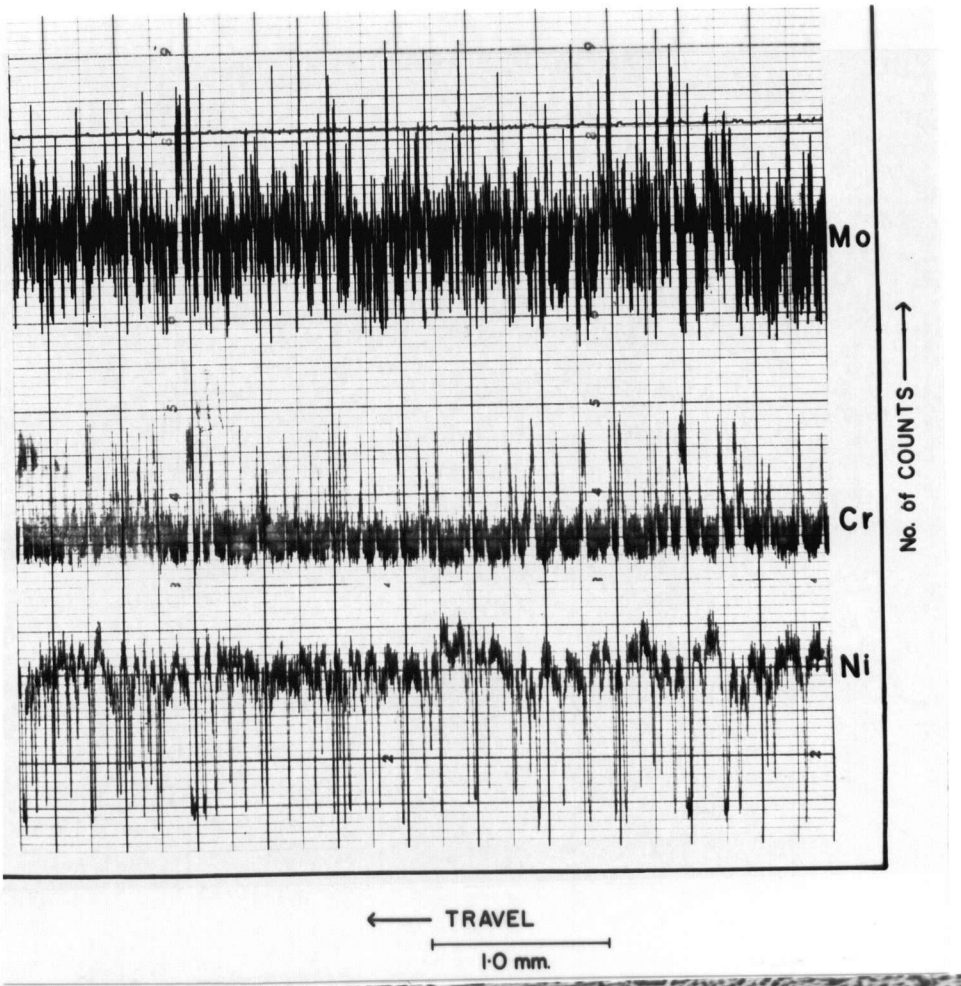

Figure 29(b) Variation of Cr, Ni and Mo across the dendritic direction in Valve No. 9 at the centre.

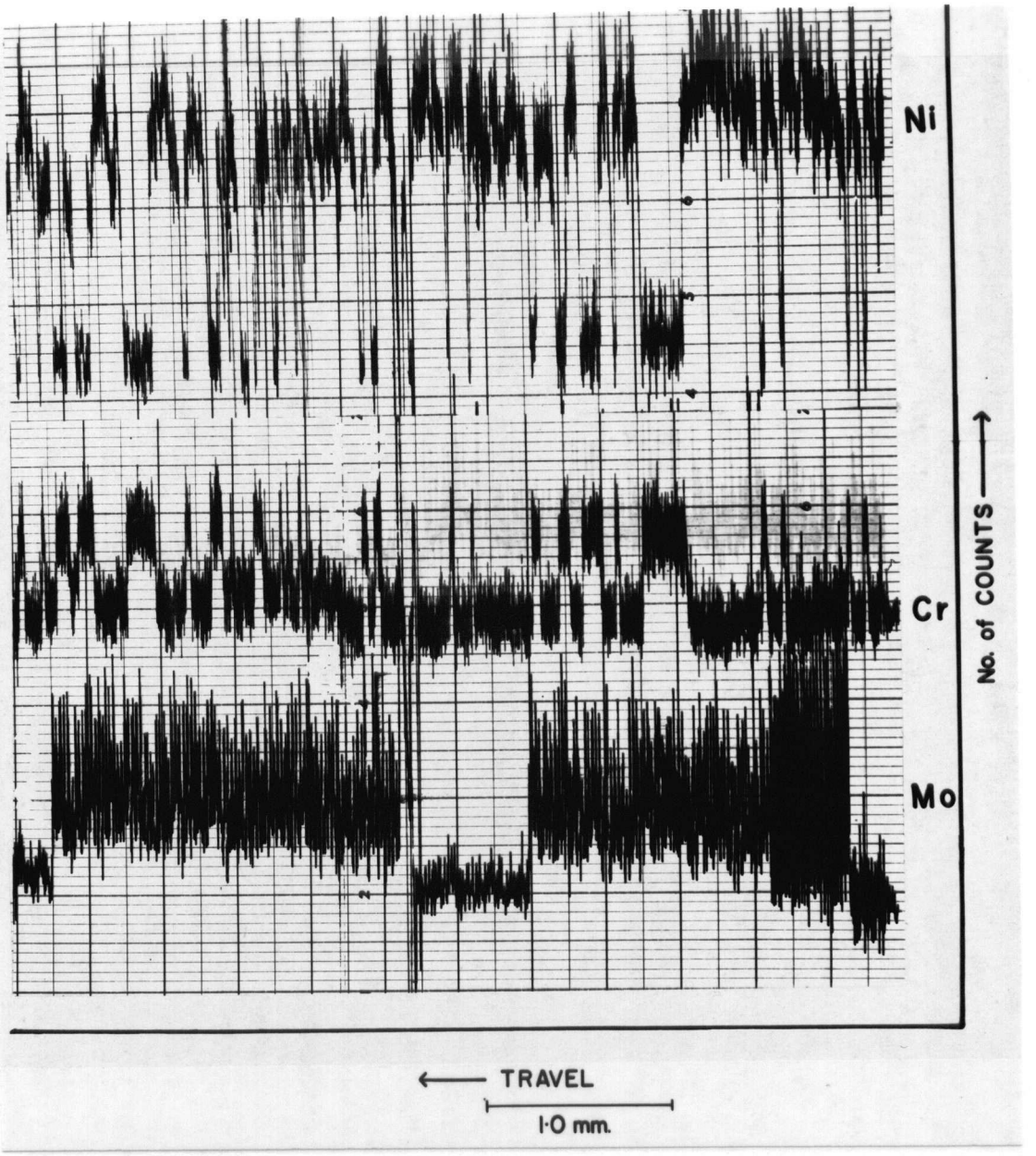

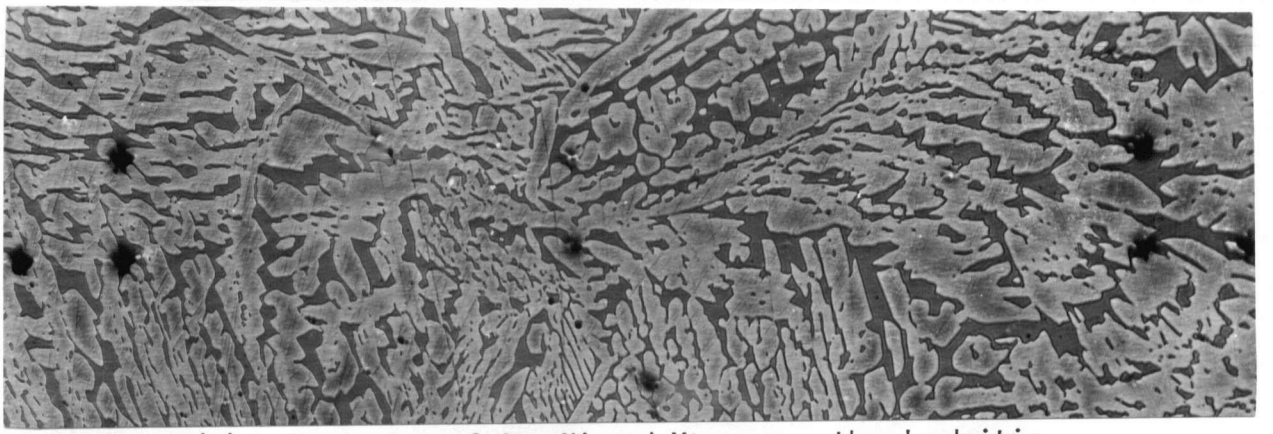

Figure 30(a). Variation of Cr, Ni and Mo across the dendritic direction in conventional casting at the edge.

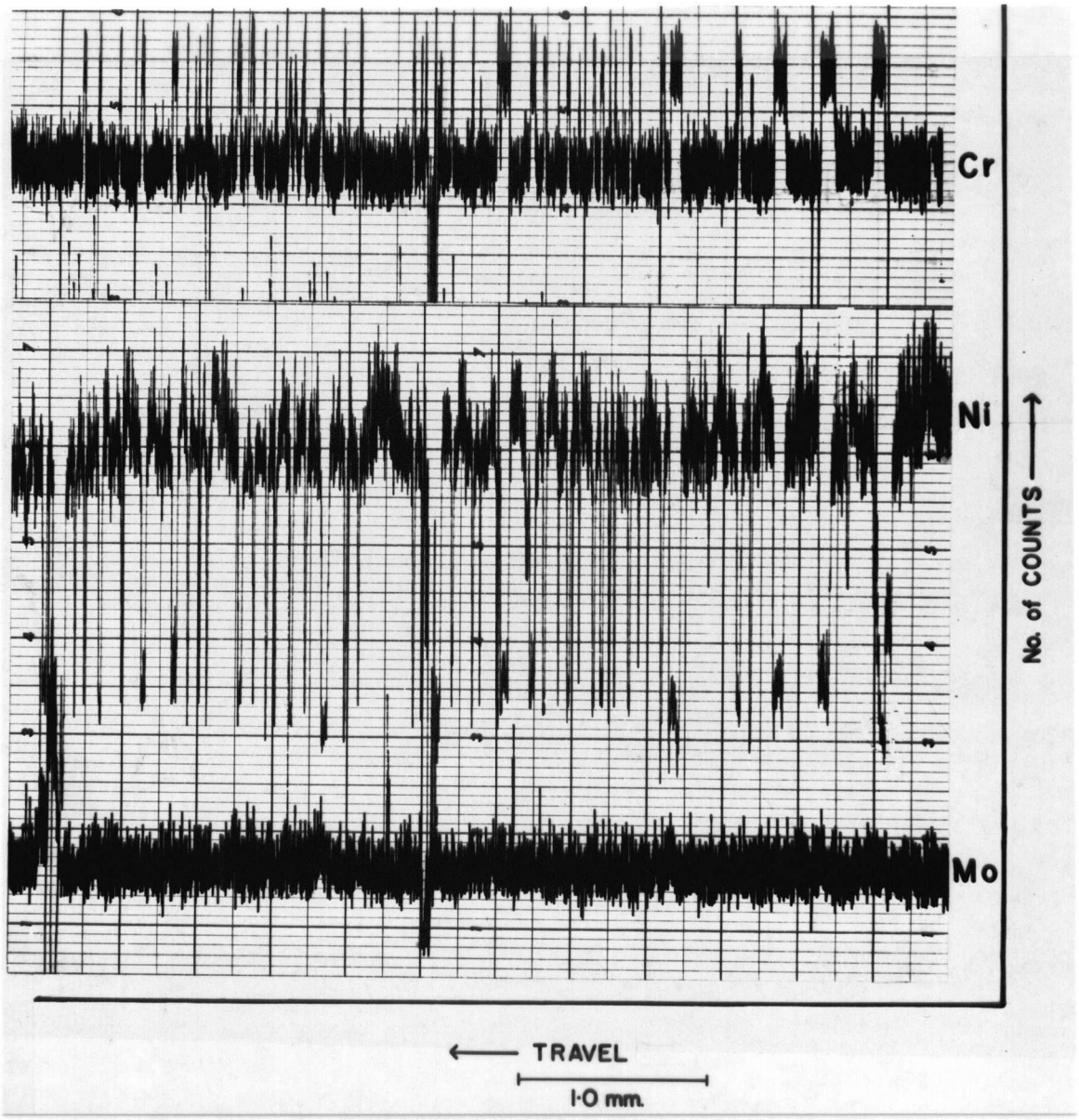

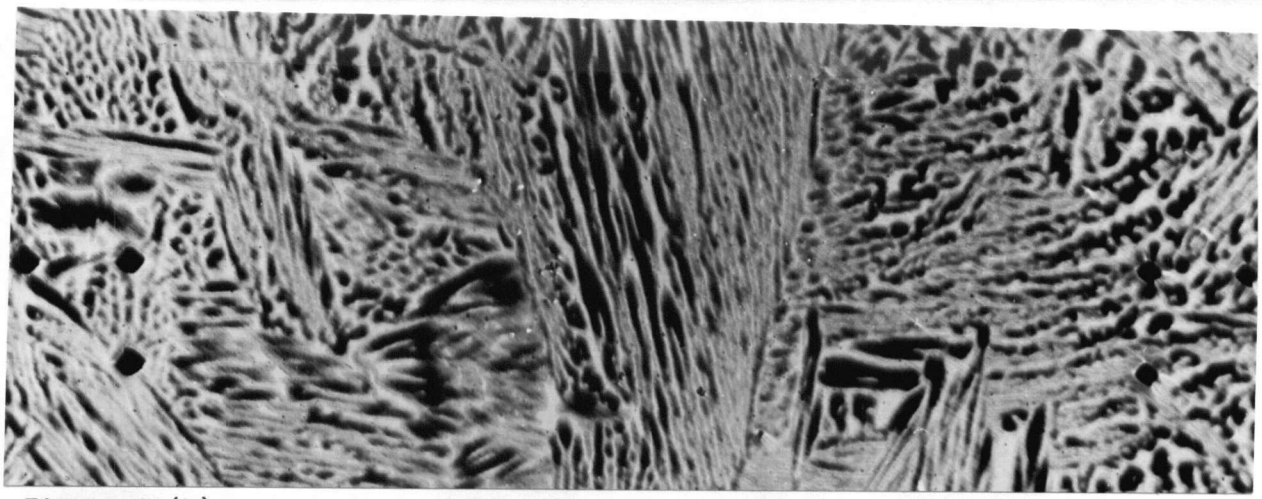

Figure 30(b). Variation of Cr, Ni and Mo across the dendritic direction in conventional casting at the mid-radius.

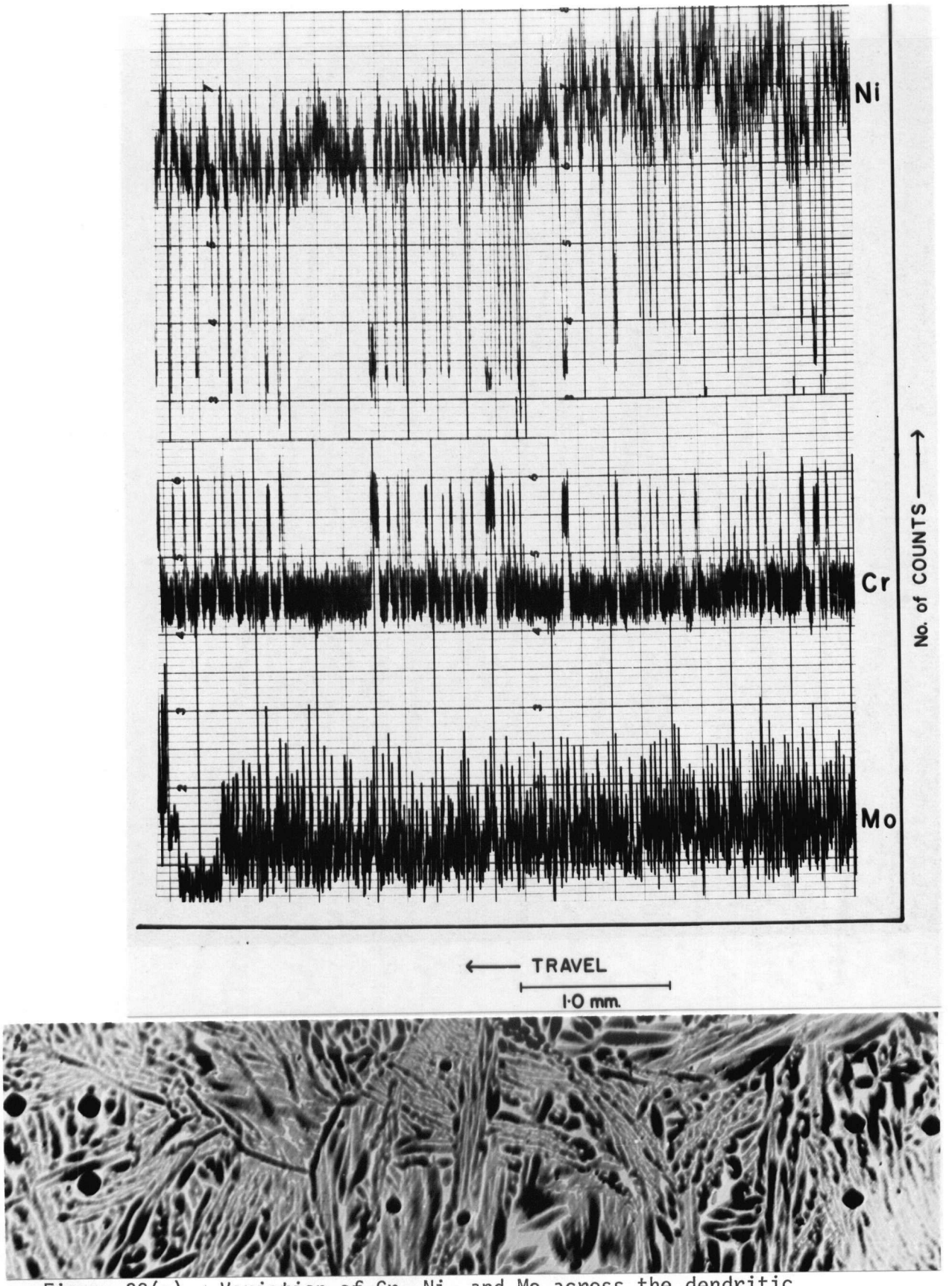

Figure 30(c). Variation of Cr, Ni, and Mo across the dendritic direction in conventional casting at the centre.

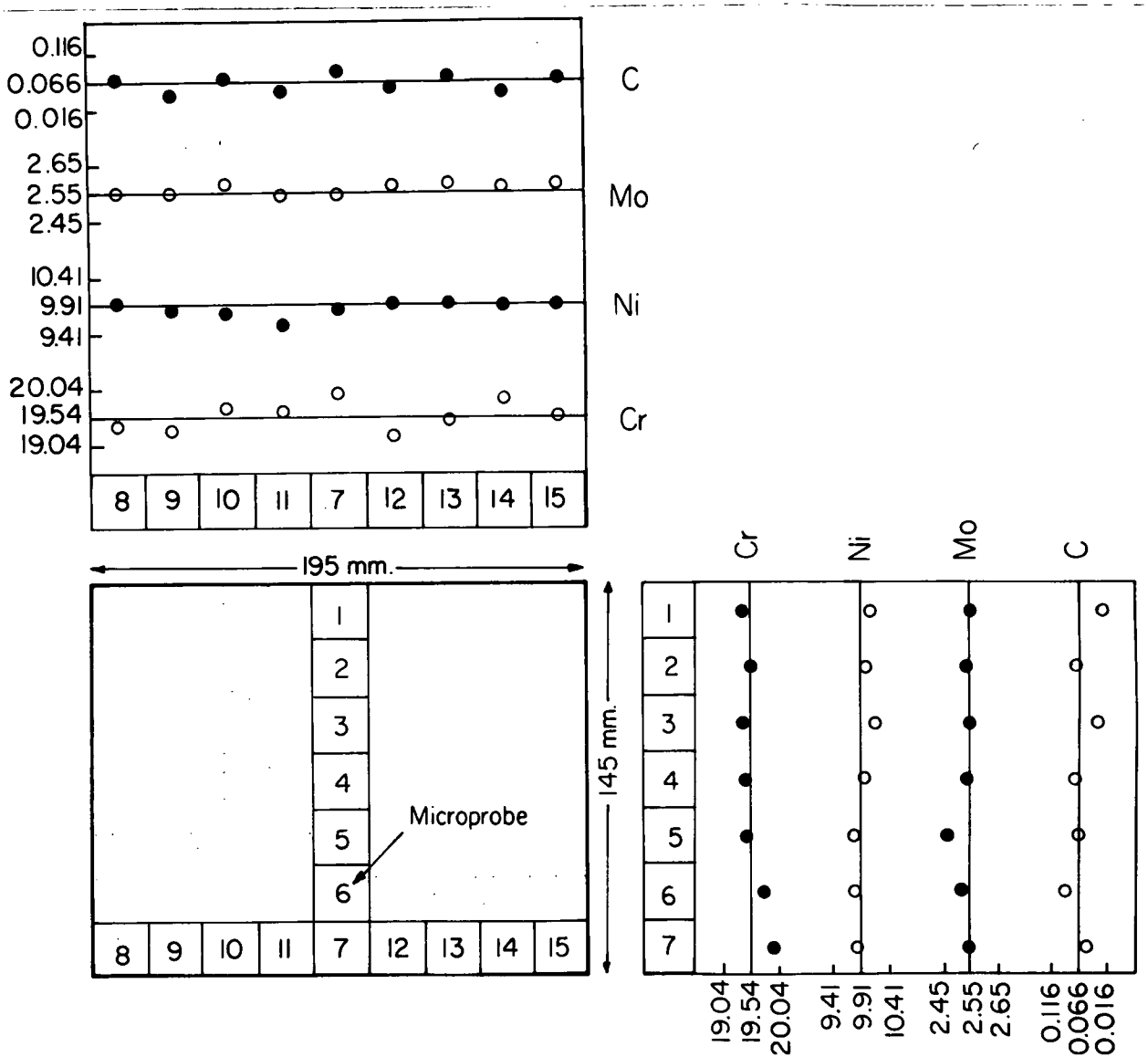

Figure 31. Composition variation in Valve No. 5 (CF-8M).
(The solid line shows the overall average composition.)

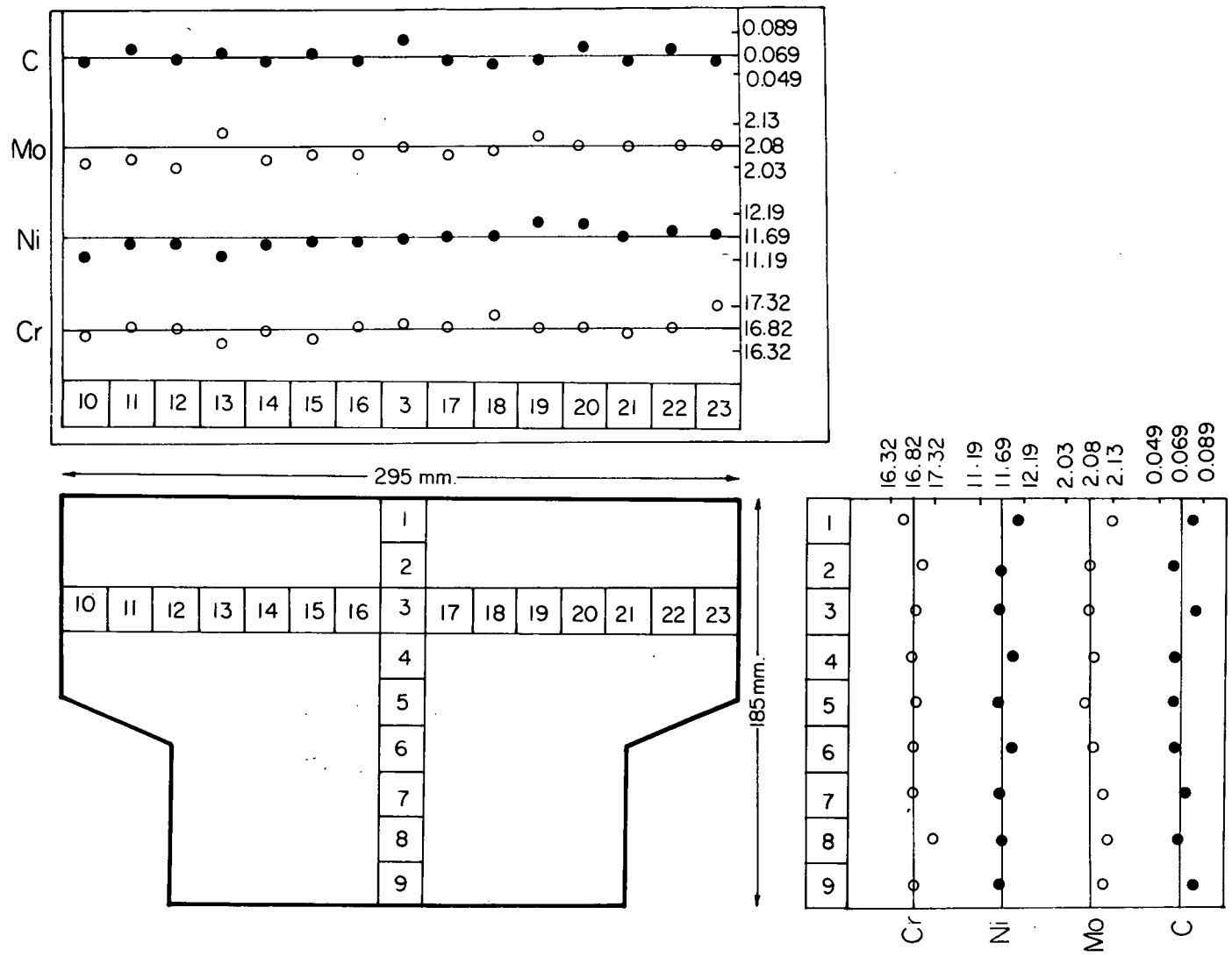

Figure 32. Composition variation in Valve No. 6 (316)
(The solid line shows the overall average composition.)

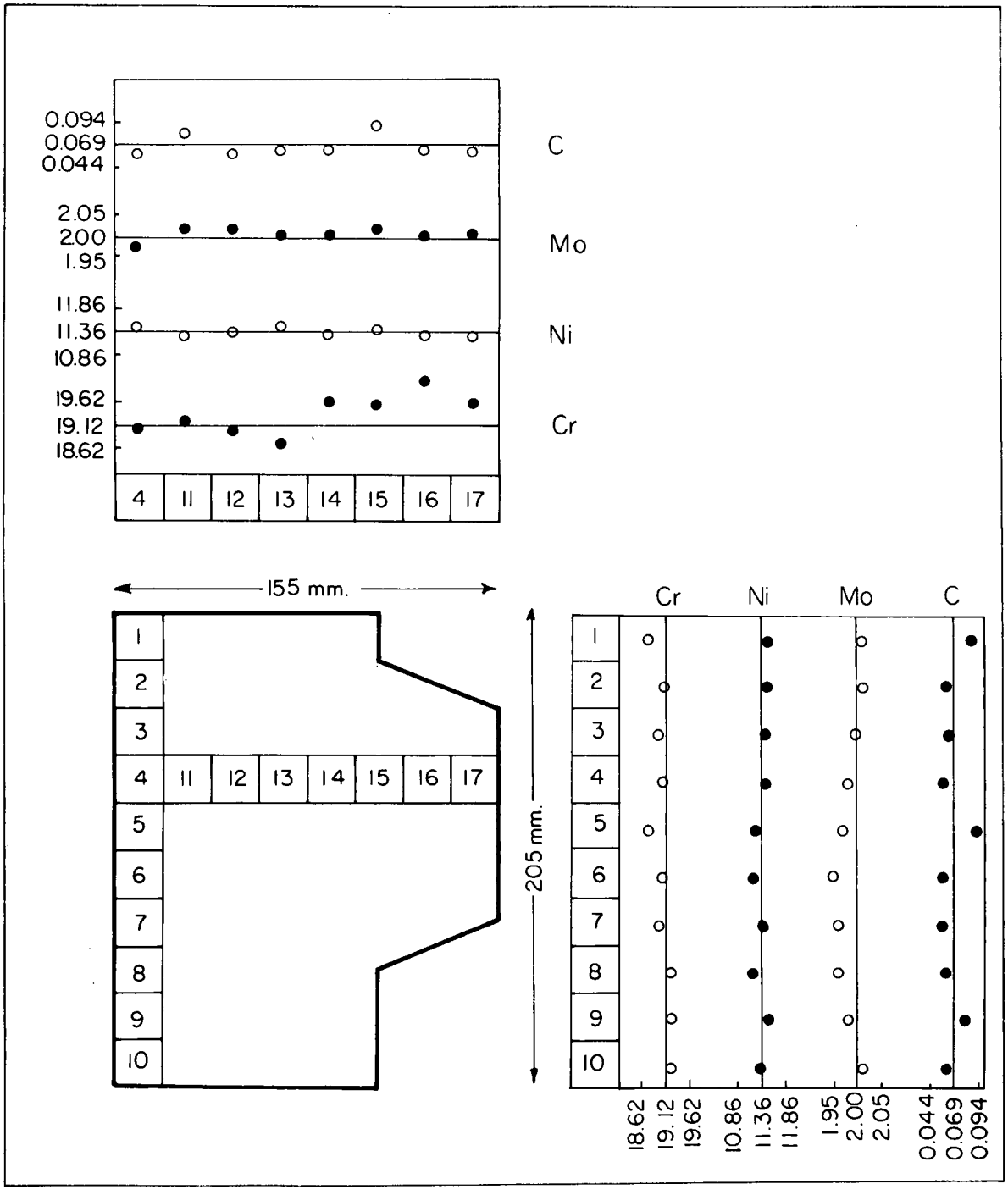

Figure 33. Composition variation in Valve No. 7 (316+Cr).
(The solid line shows the overall average composition.)

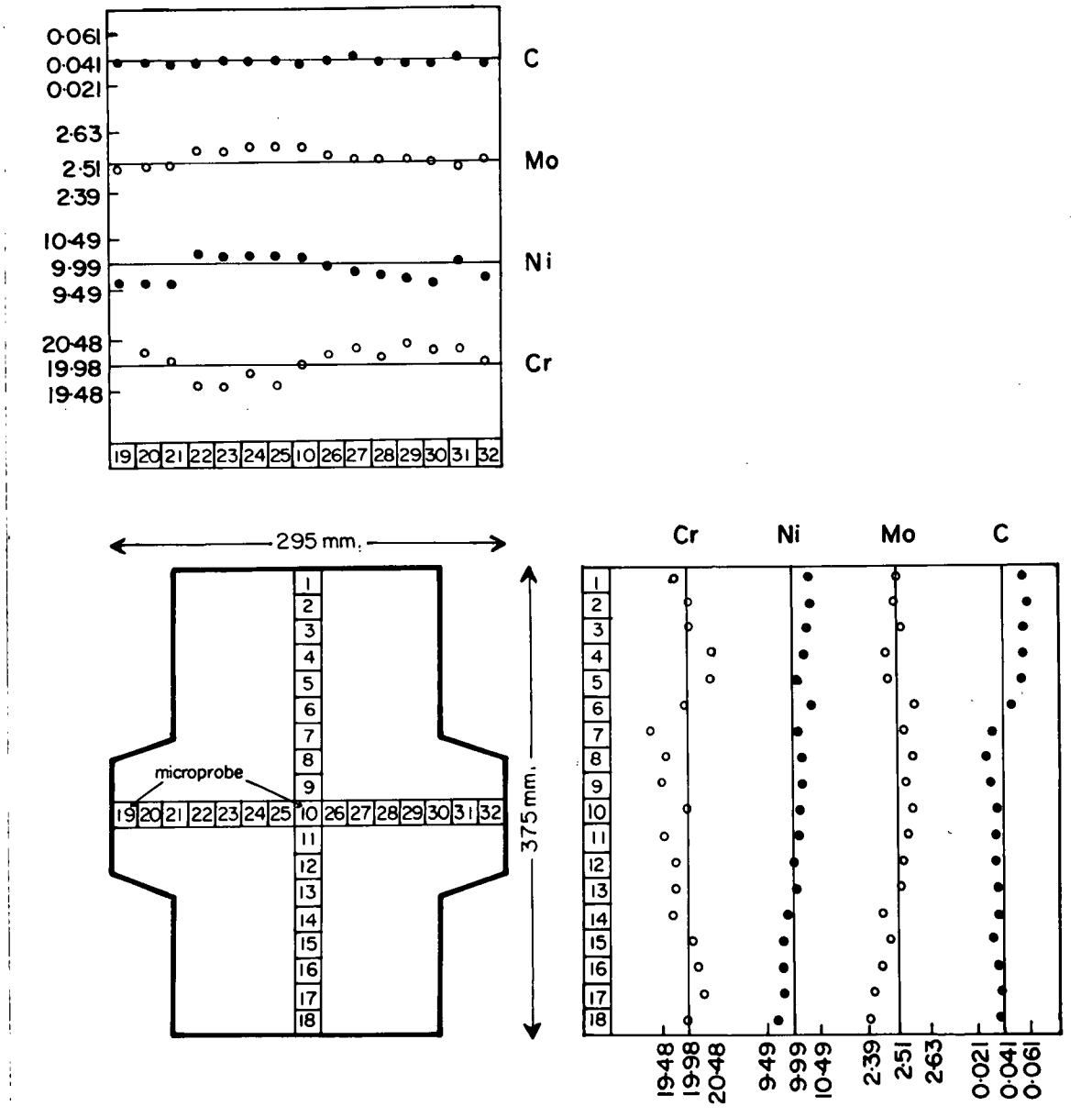

Figure 34. Composition variation in Valve No. 9 (CF-8M).
(The solid line shows the overall average composition.)

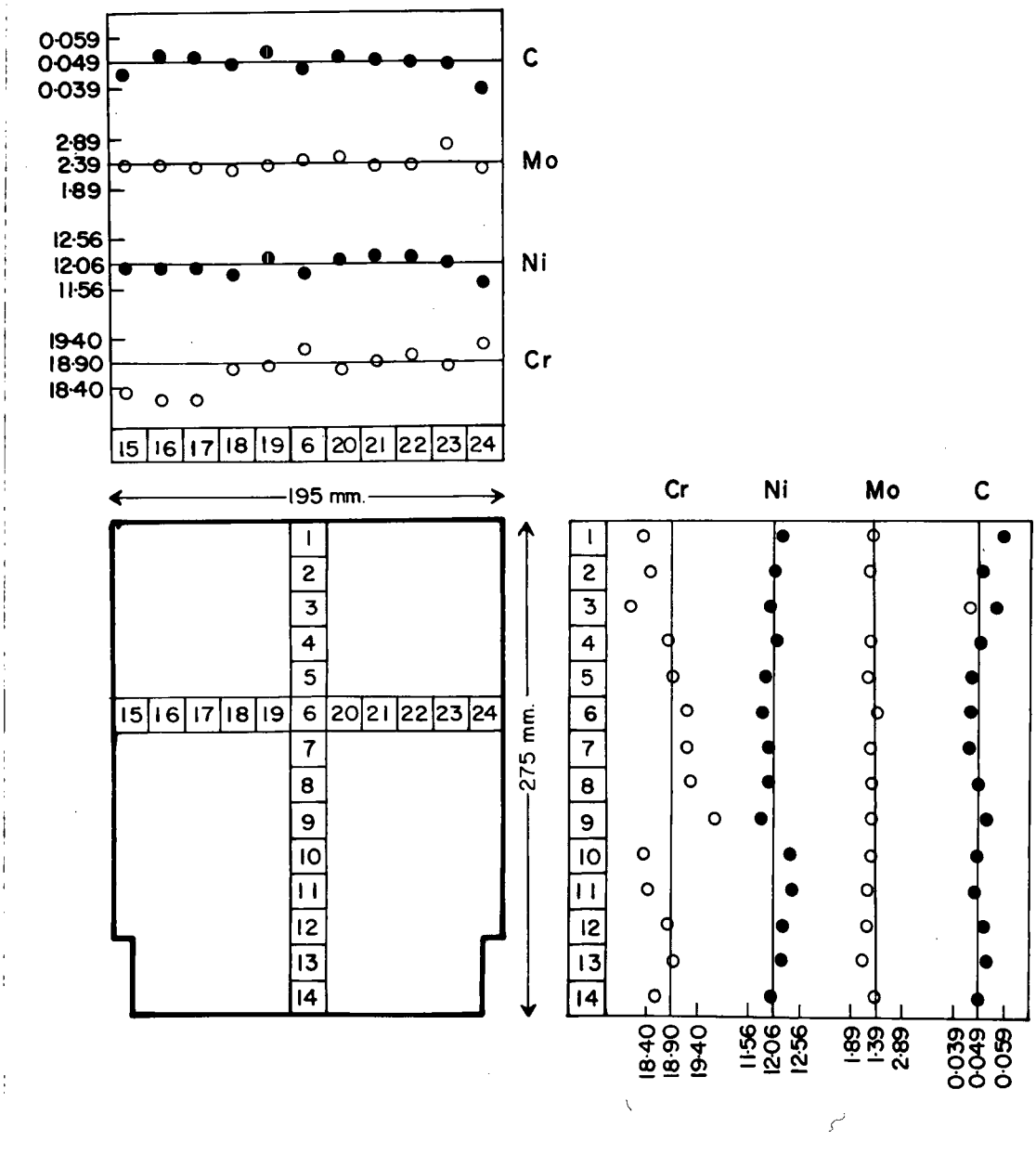

Figure 35. Composition variation in Valve No. 10 (316+Cr+Mo).
(The solid line shows the overall average composition.)

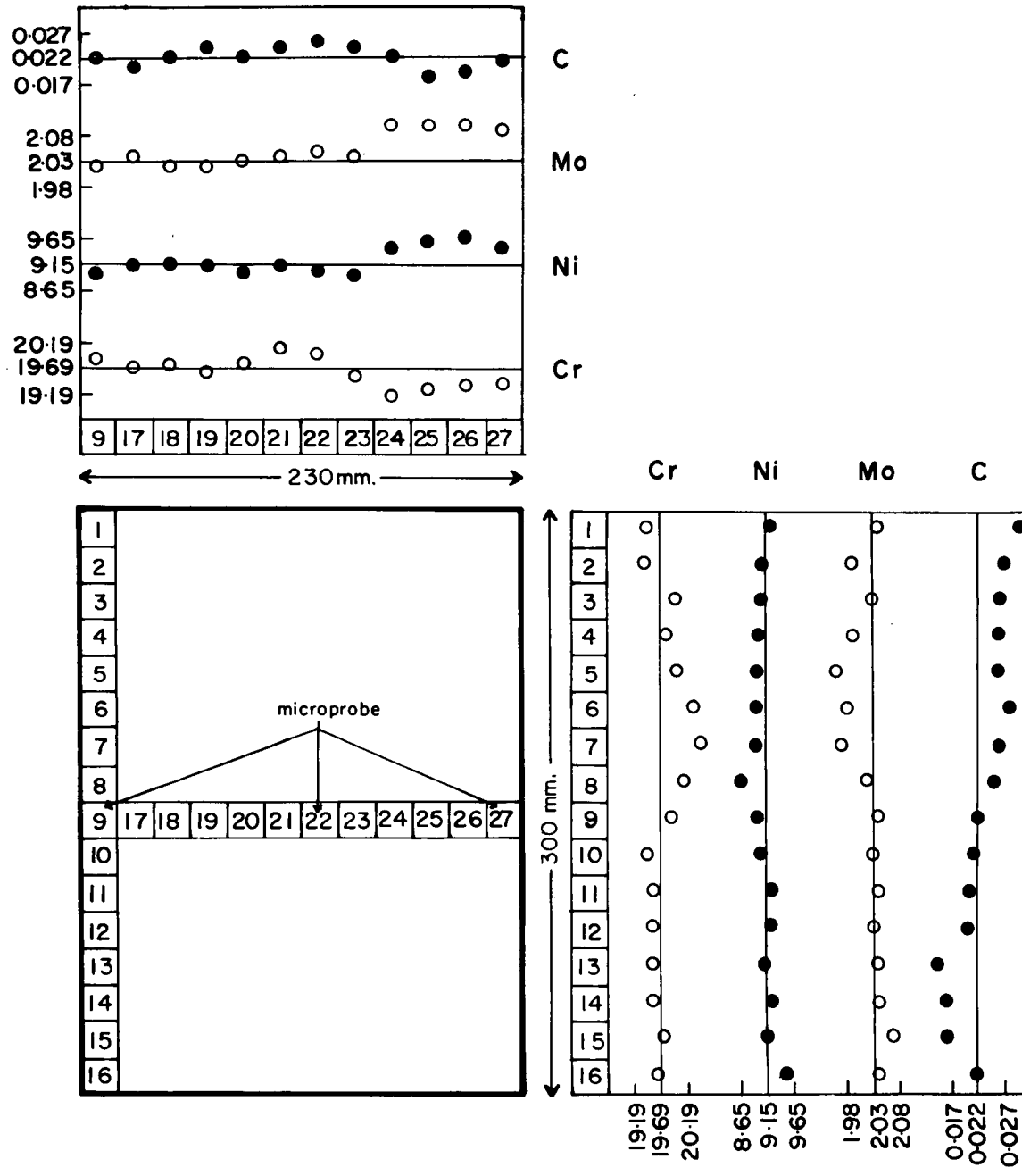

Figure 36. Composition variation in conventional casting.
(The solid line shows the overall average composition.)

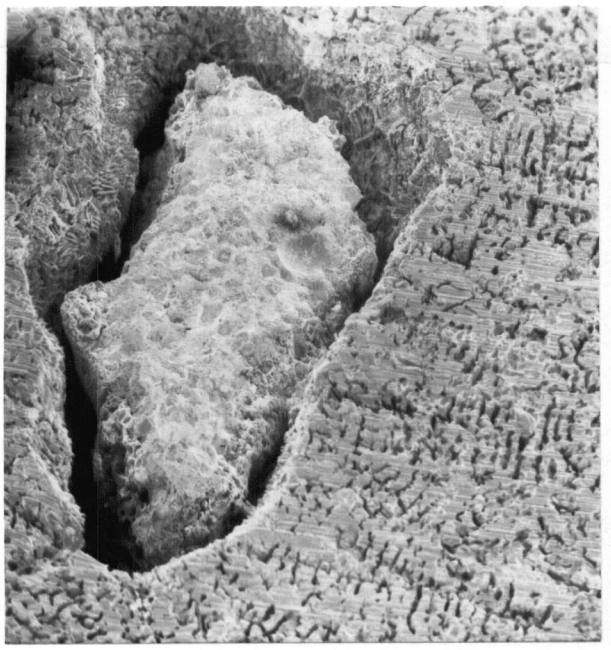

(a) 20 x

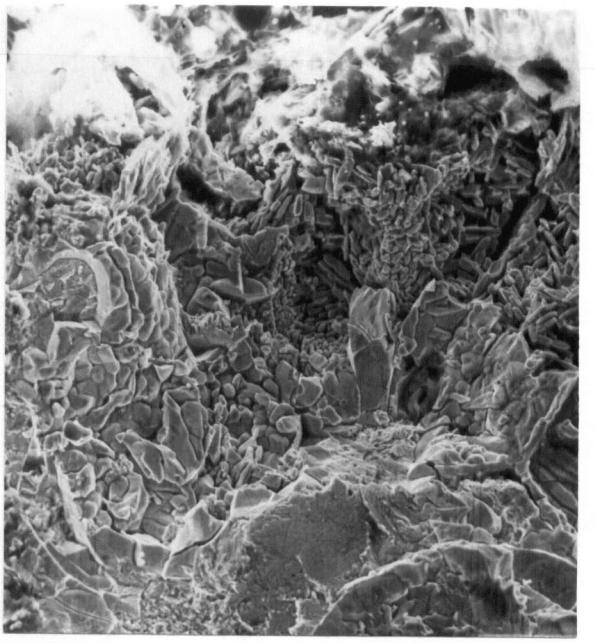

(b) 400 x

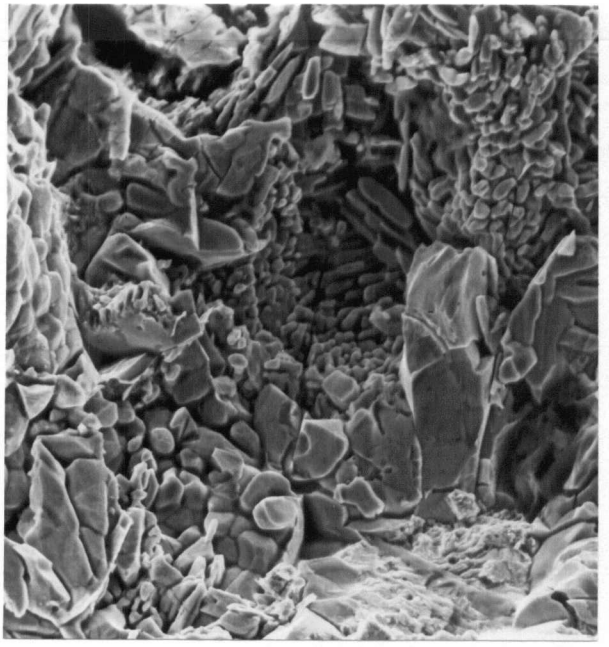

(c) 800 x

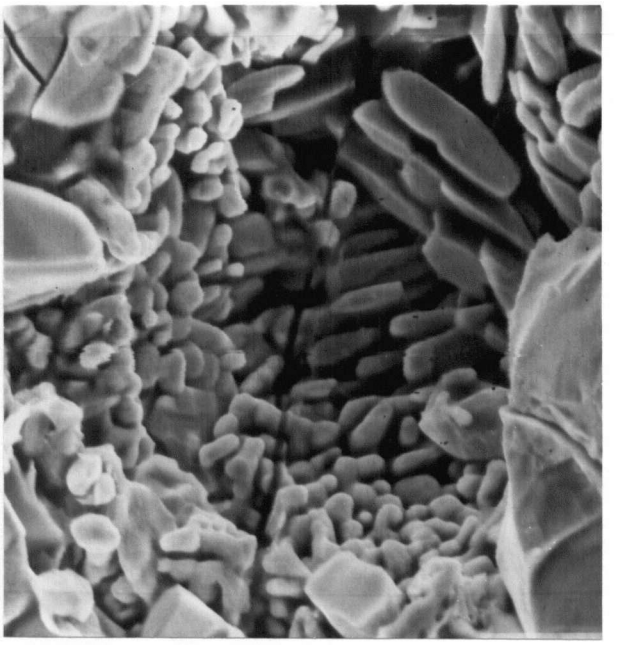

(d) 2000 x

Figure 37. SEM photographs of agglomerated ferro alloy powder in area 1 in Valve No. 10.

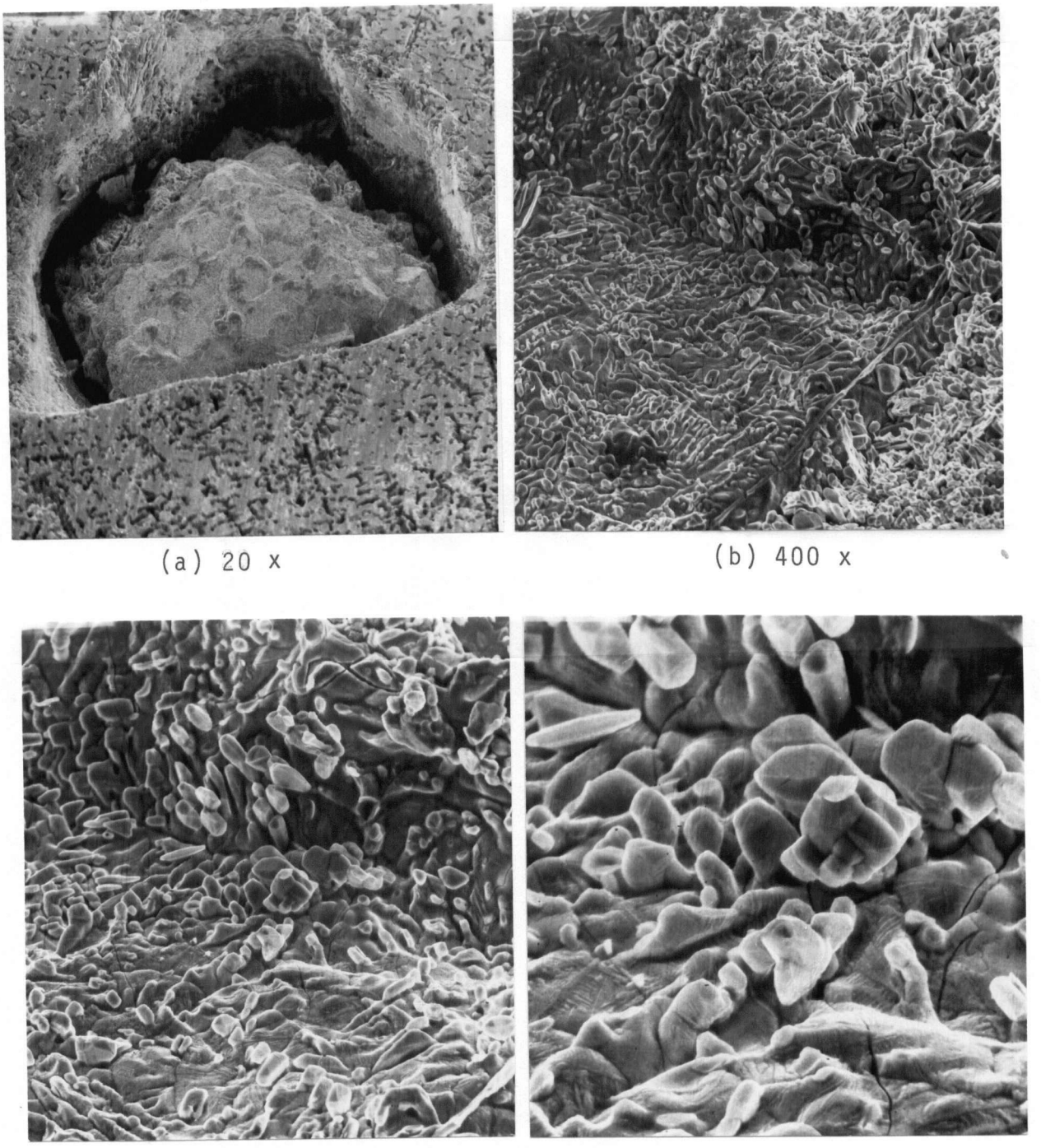

(a) 20 x

(b) 400 x

(c) 800 x

(d) 2000 x

Figure 38. SEM photographs of agglomerated ferro alloy powder in area 2 in Valve No. 10.

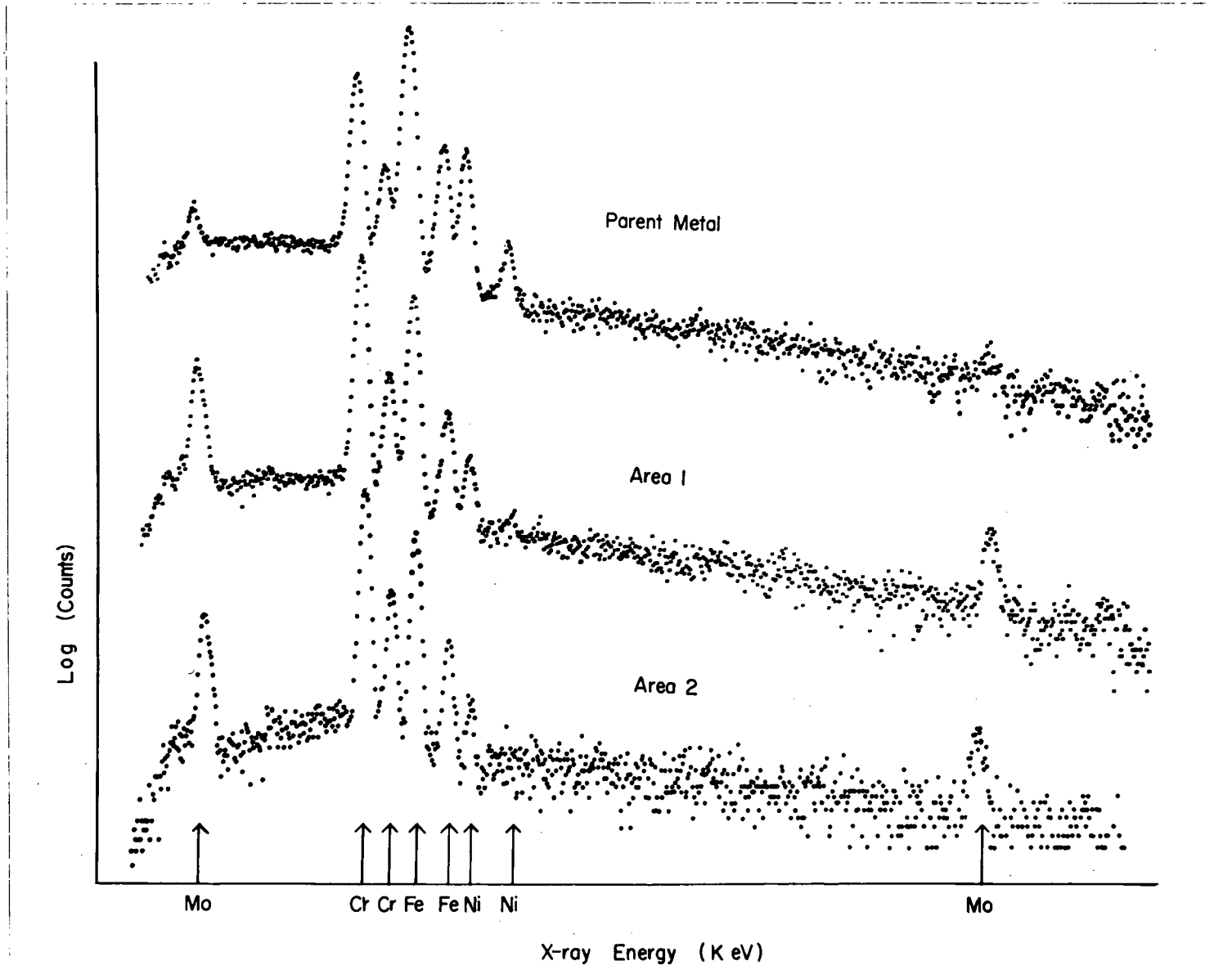

Figure 39. EDXA plots of agglomerated ferro alloy powder in areas 1 and 2 and the parent metal (Valve No. 10).

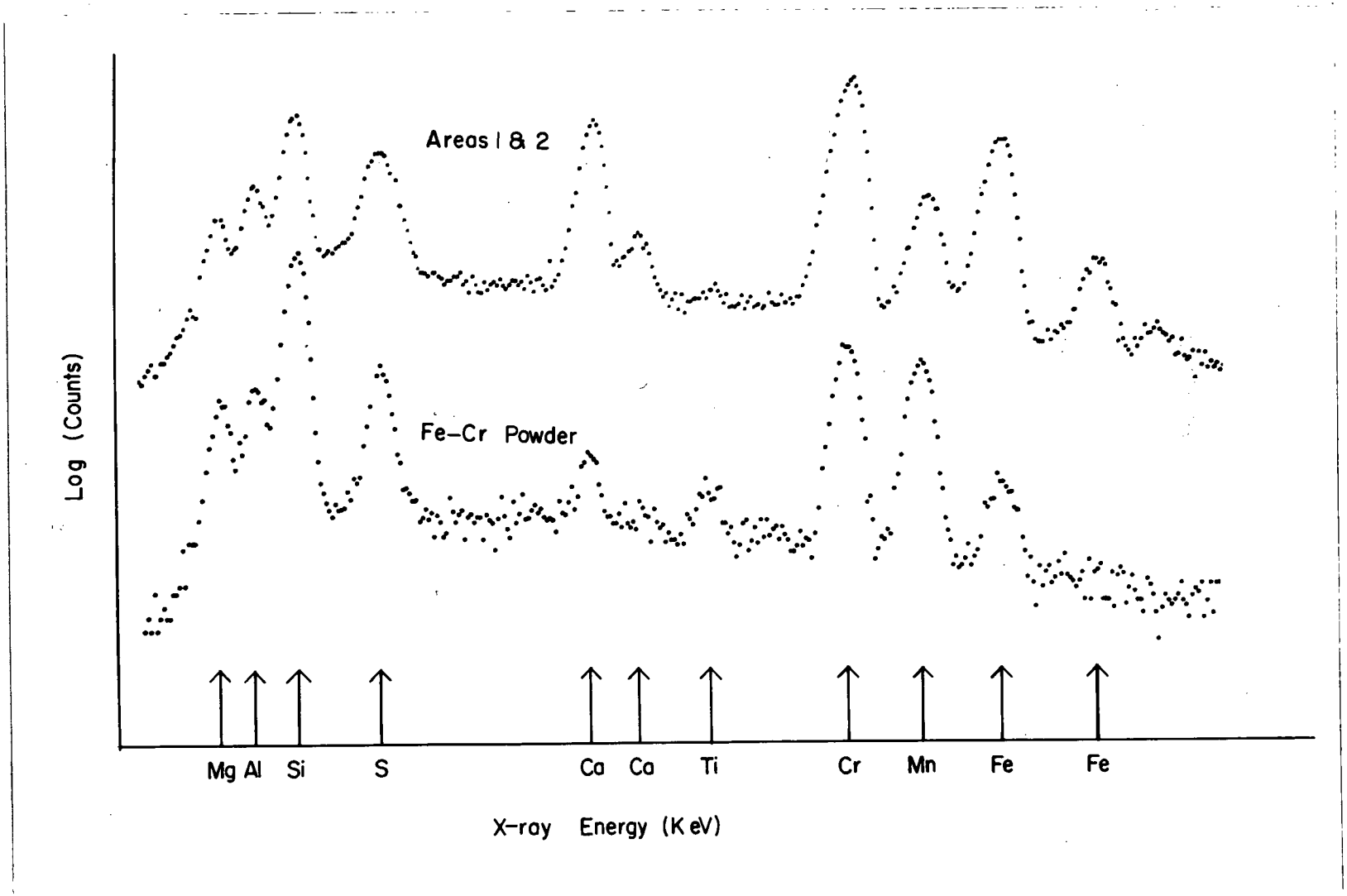

Figure 40 (a). EDXA plots of inclusions in areas 1 and 2 and Fe-Cr powder.

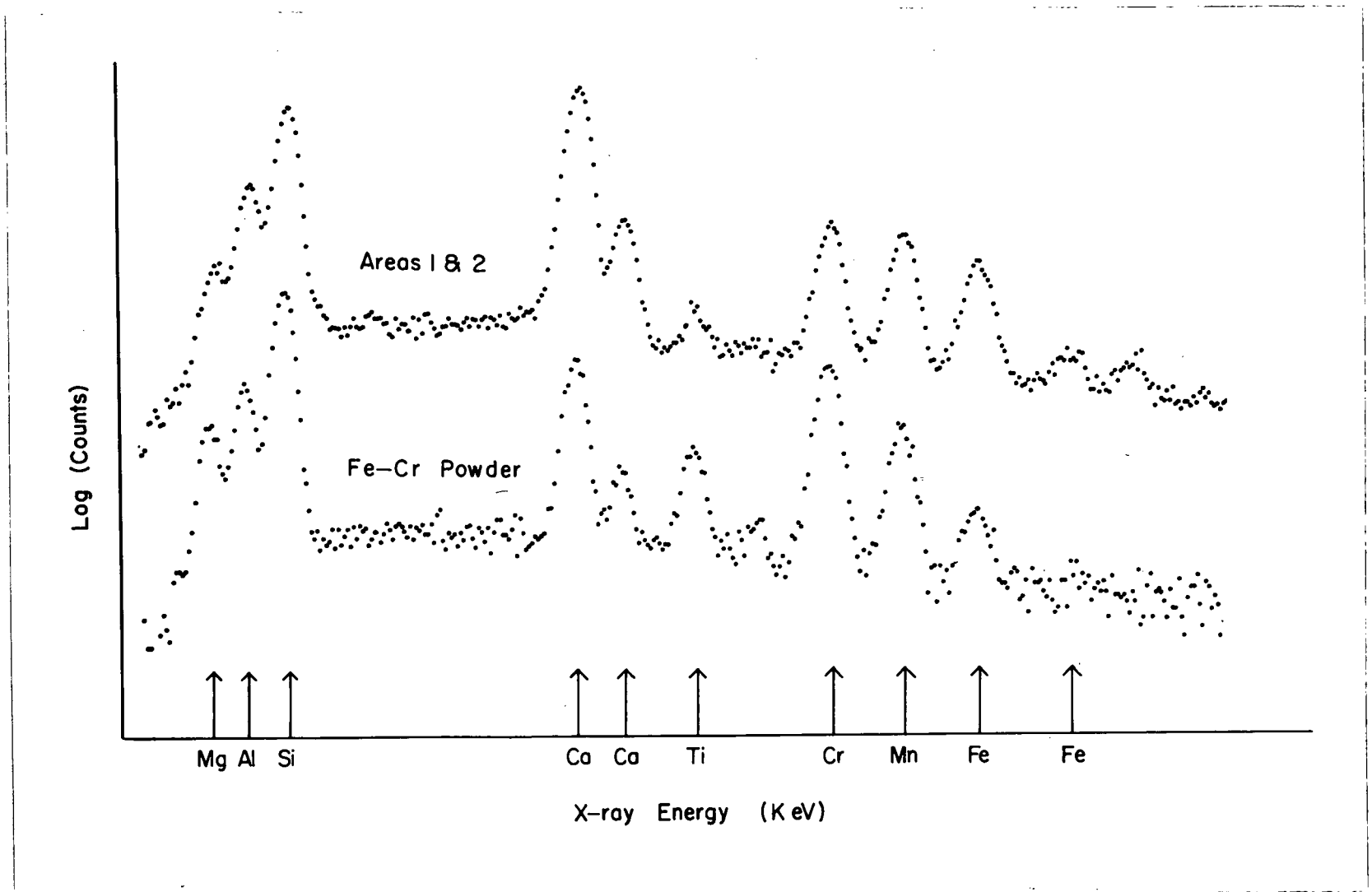

Figure 40(b). EDXA plots of inclusions in areas 1 and 2 and Fe-Cr powder.

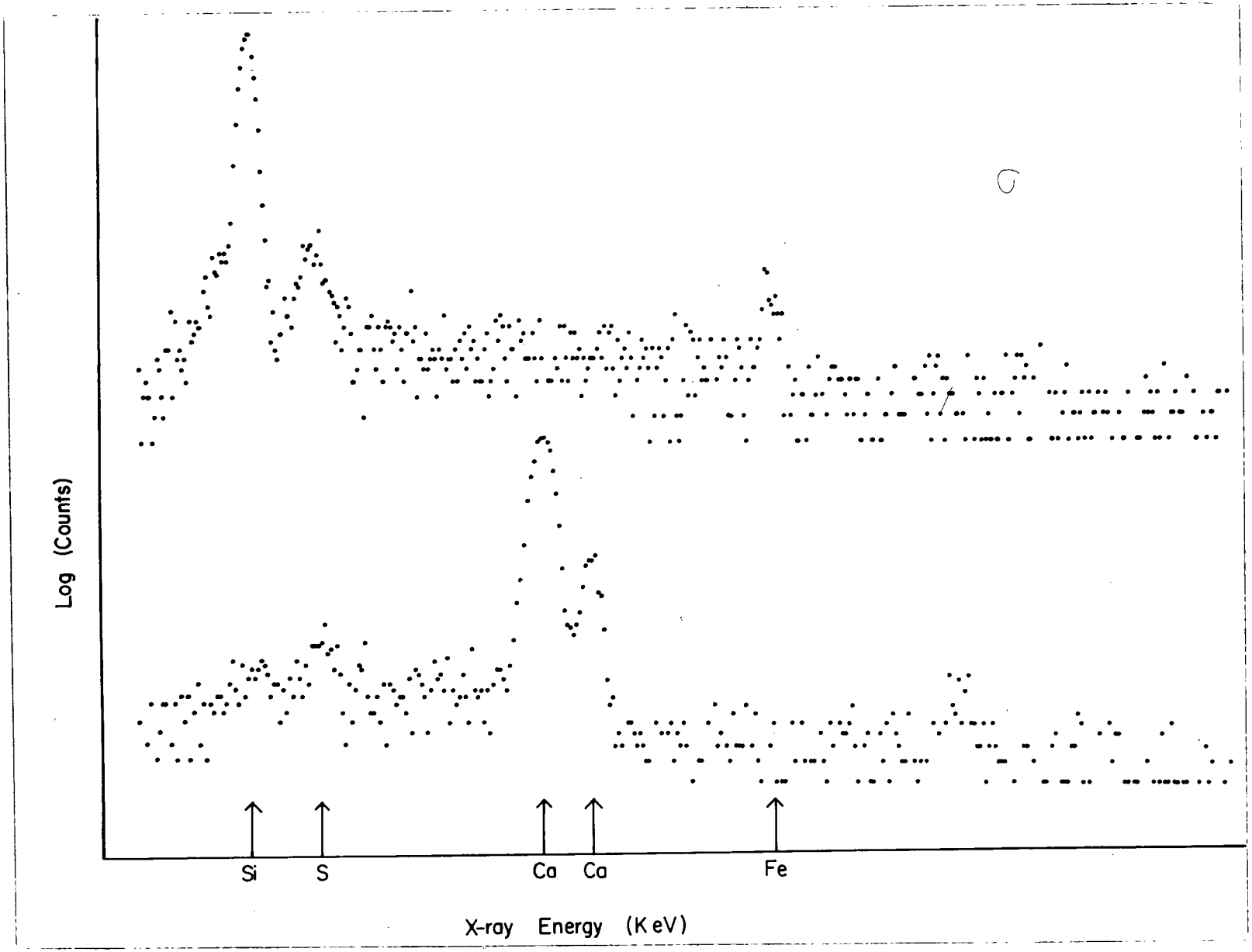

Figure 40(c). EDXA plots of inclusions in Fe-Mo powder.

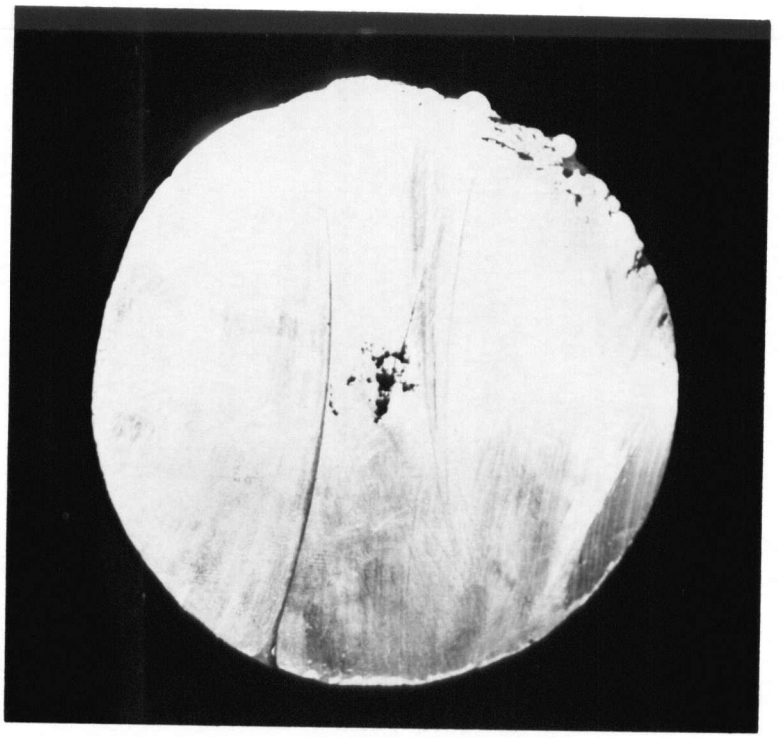

Figure 41. Macroporosity in the Centre of the CF-8M electrode.

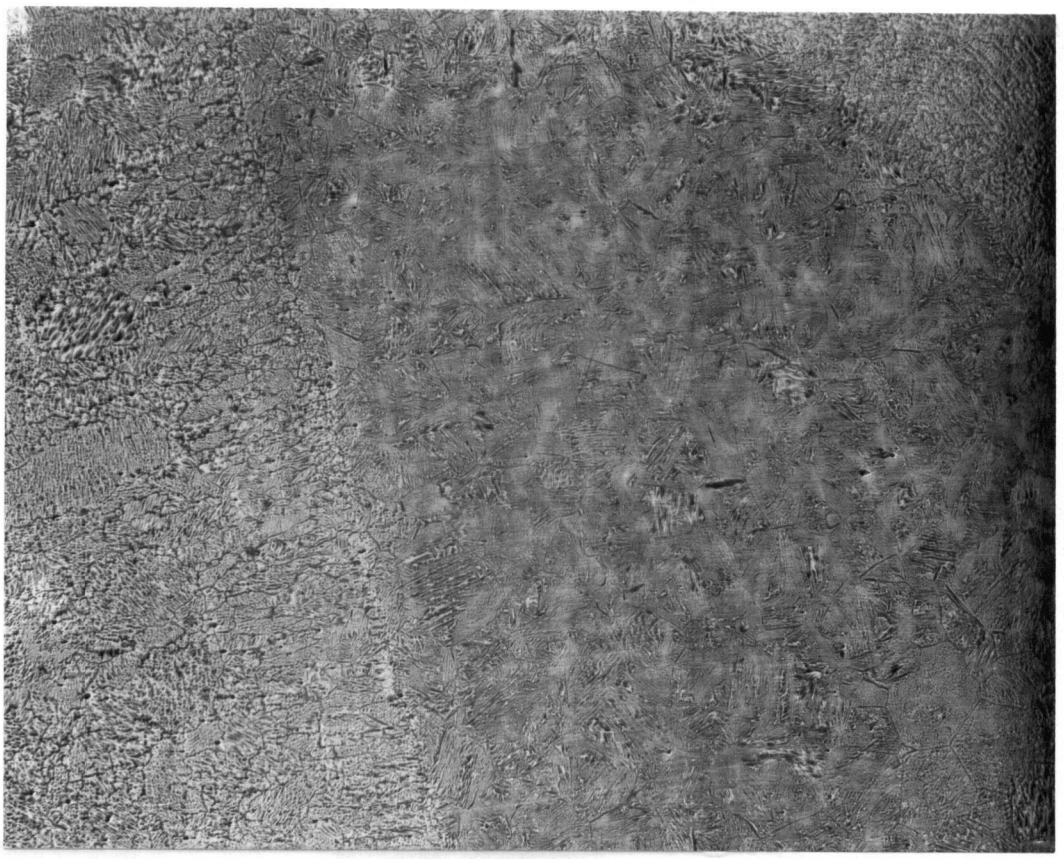

Figure 42. Macrostructure of the electrode piece that dropped in Valve No. 9. (5.5 x)

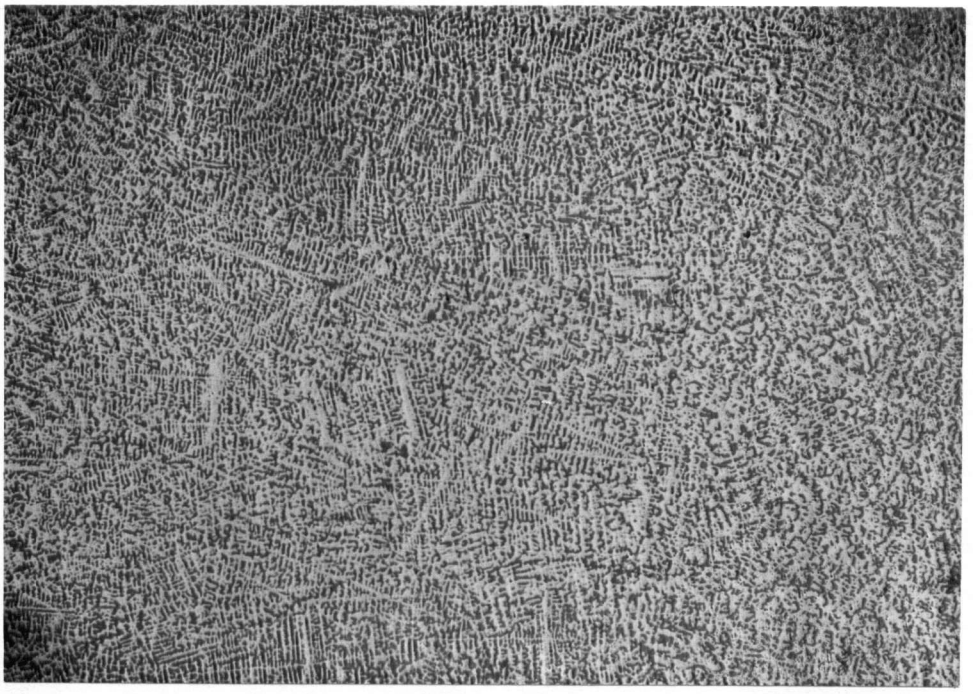

Figure 43. Macrostructure of the CF-8M electrode. (5.5 x)

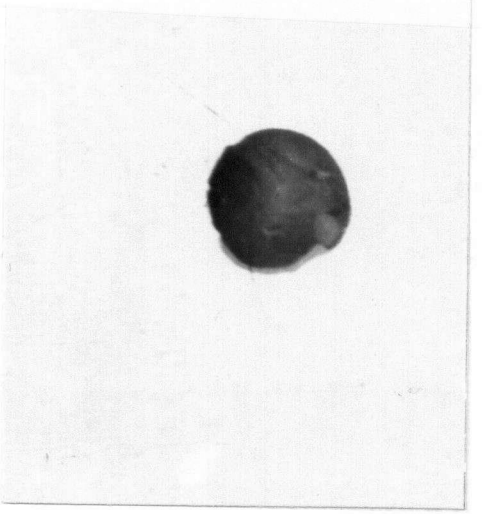

Electrode Piece 1300 x

Electrode Piece 1300 x

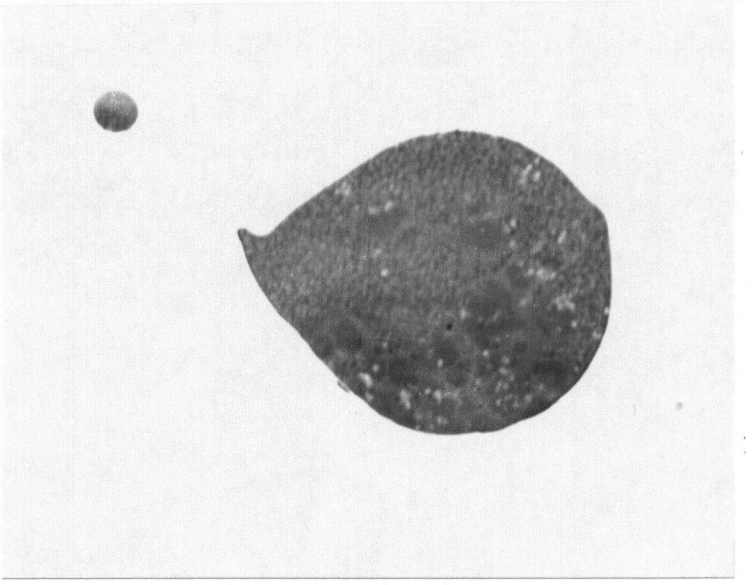

Electrode Tip 1300 x

Figure 44. Inclusions in the electrode piece dropped in Valve No. 9 and electrode tip (optical photographs).

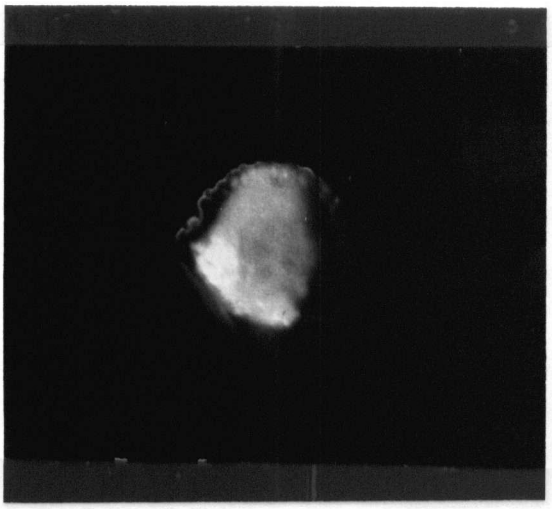

Electrode Piece 2000 x

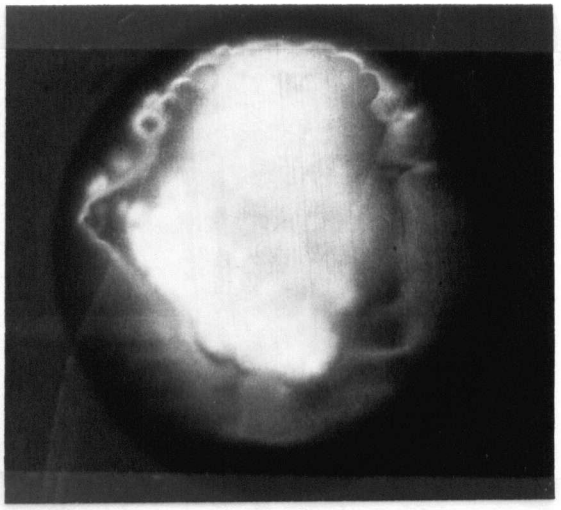

Electrode Piece 4000 x

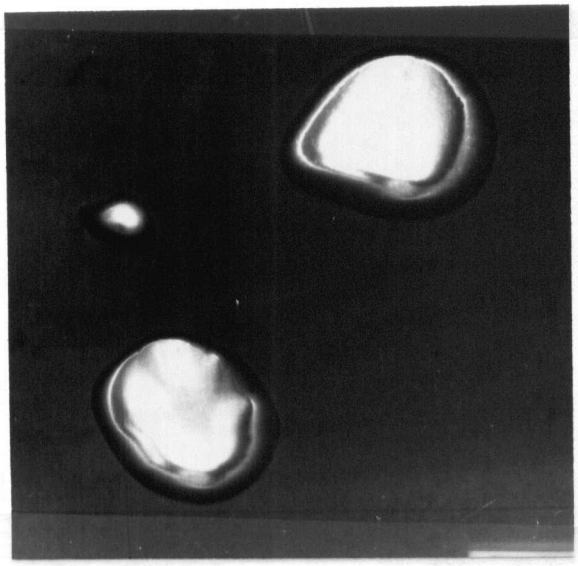

Electrode Tip 950 x

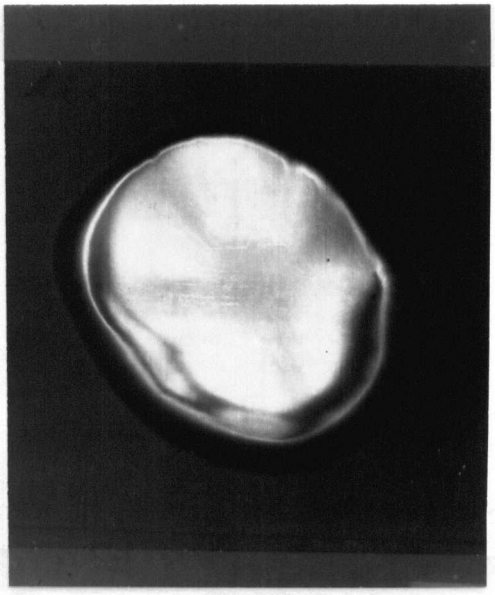

Electrode Tip 1900 x

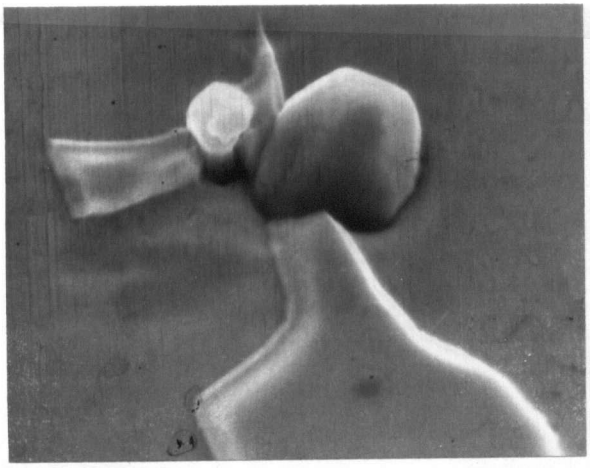

Parent Casting 4000 x

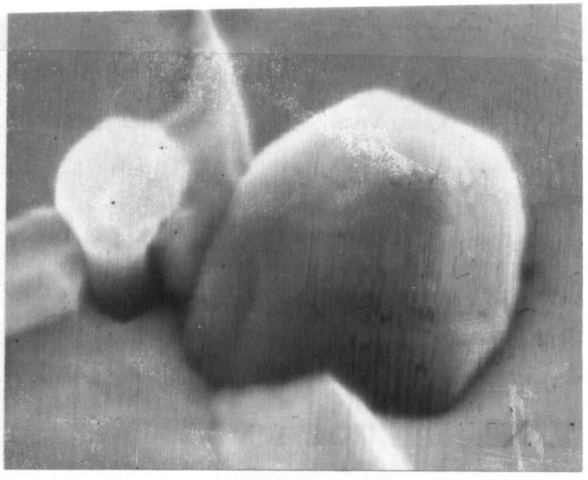

Parent Casting 8000 x

Figure 45. Inclusions in the electrode piece dropped in Valve No. 9, electrode tip and the parent casting (Valve No. 9).

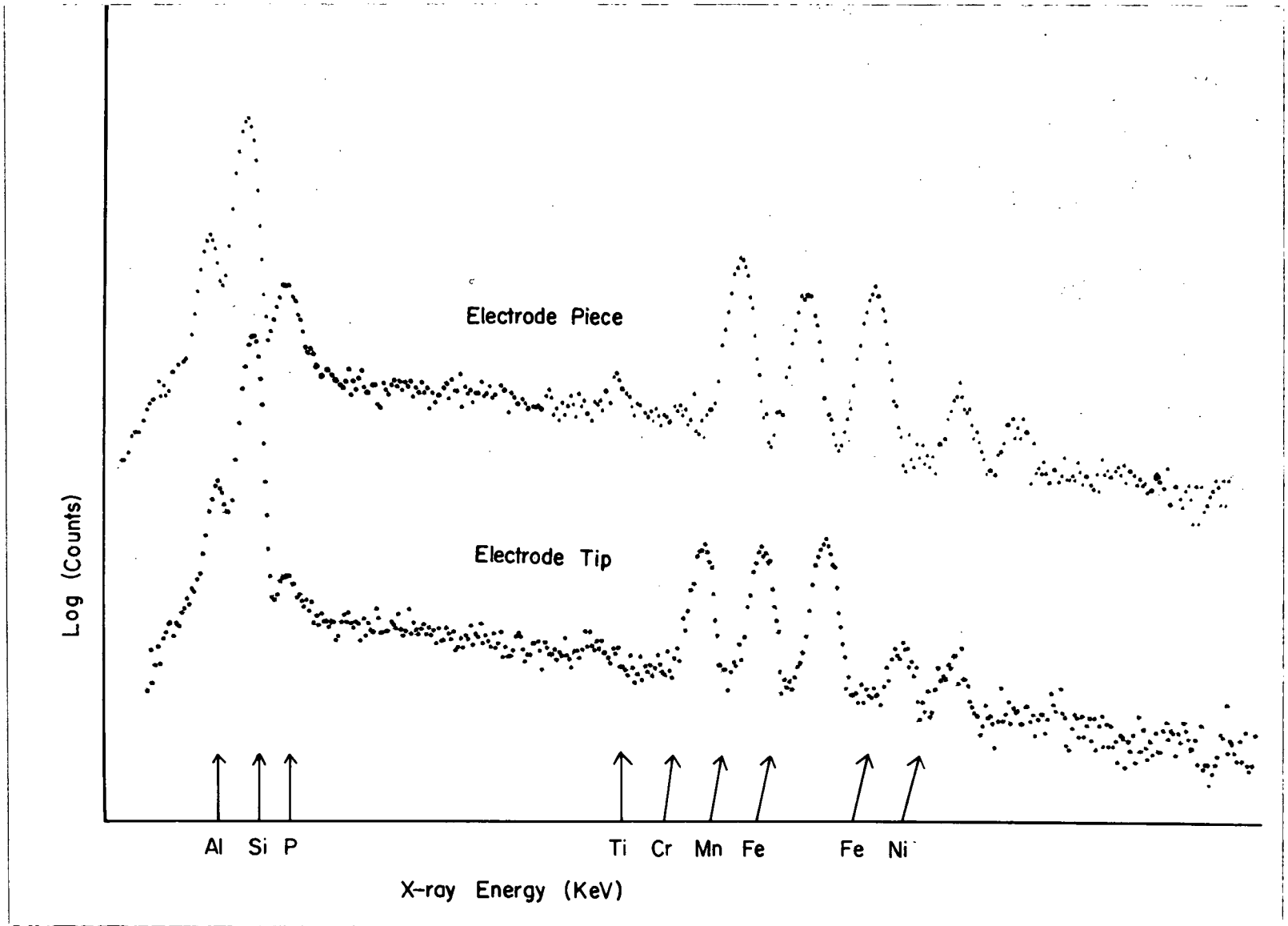

Figure 46(a). EDXA plots of inclusions in the electrode piece dropped in Valve No. 9 and the electrode tip.

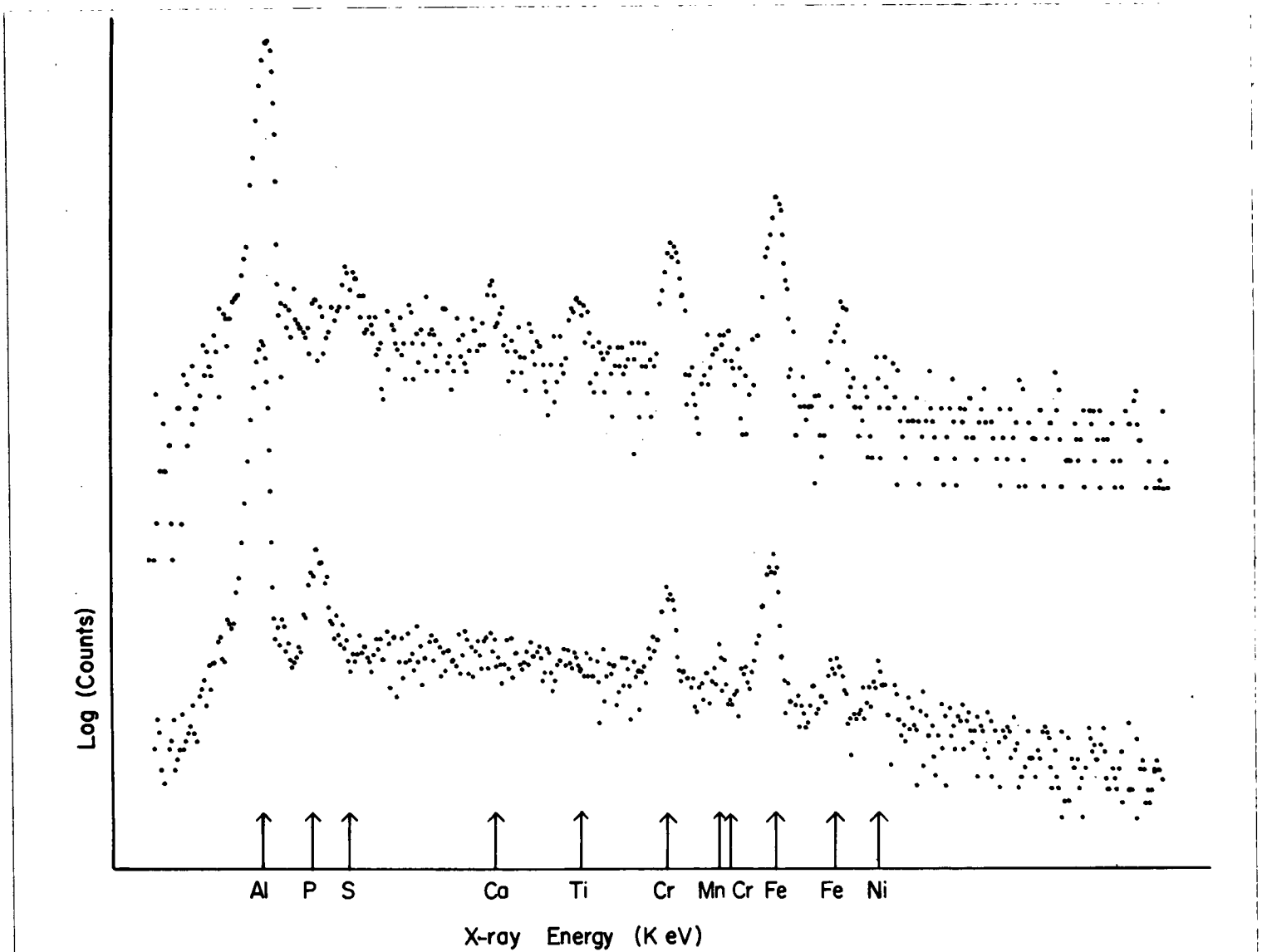

Figure 46(b). EDXA plots of inclusions in the parent casting (Valve No. 9).

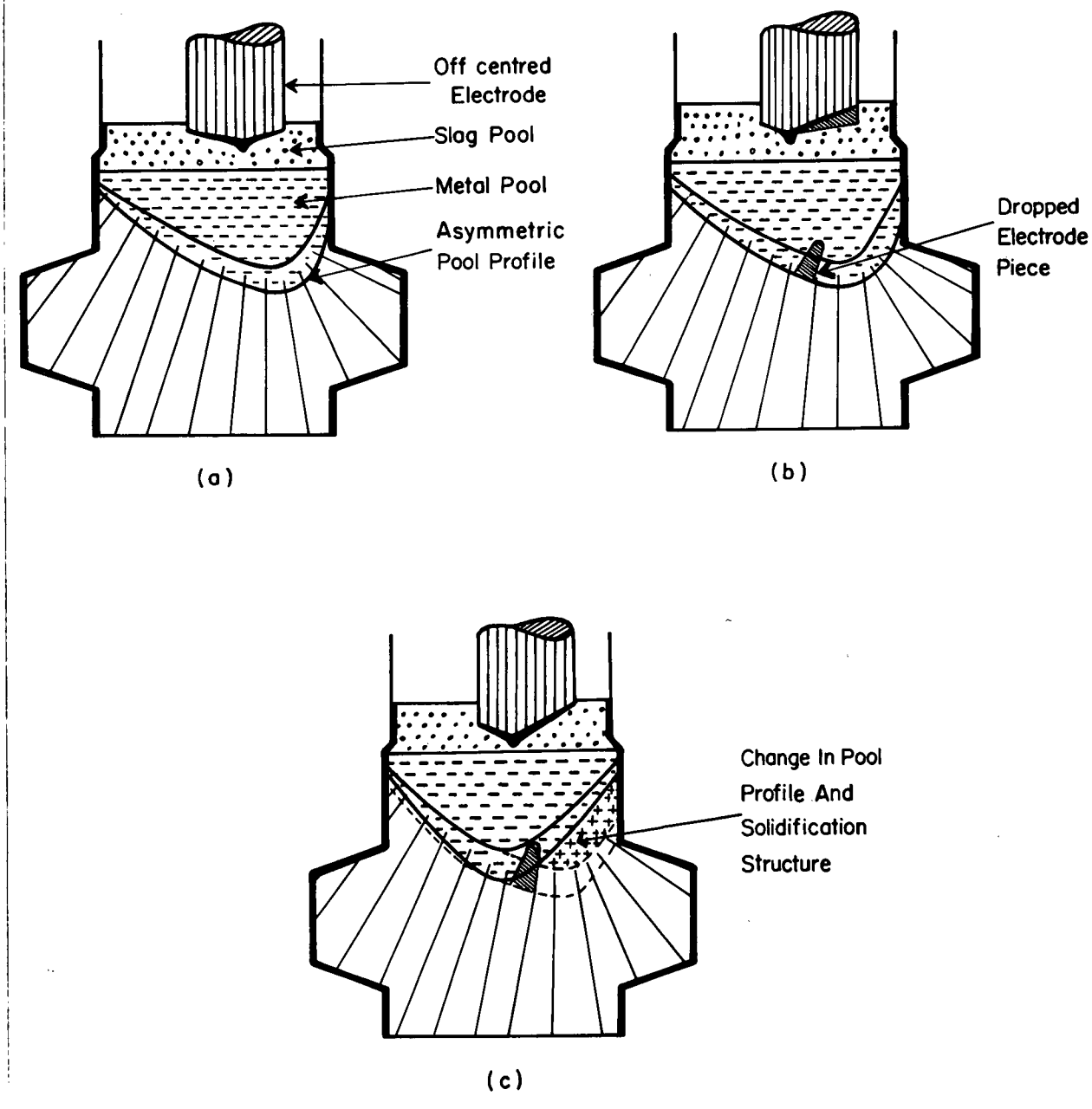

Figure 47. Schematic to explain the peculiar pool profile observed in Valve No. 9.

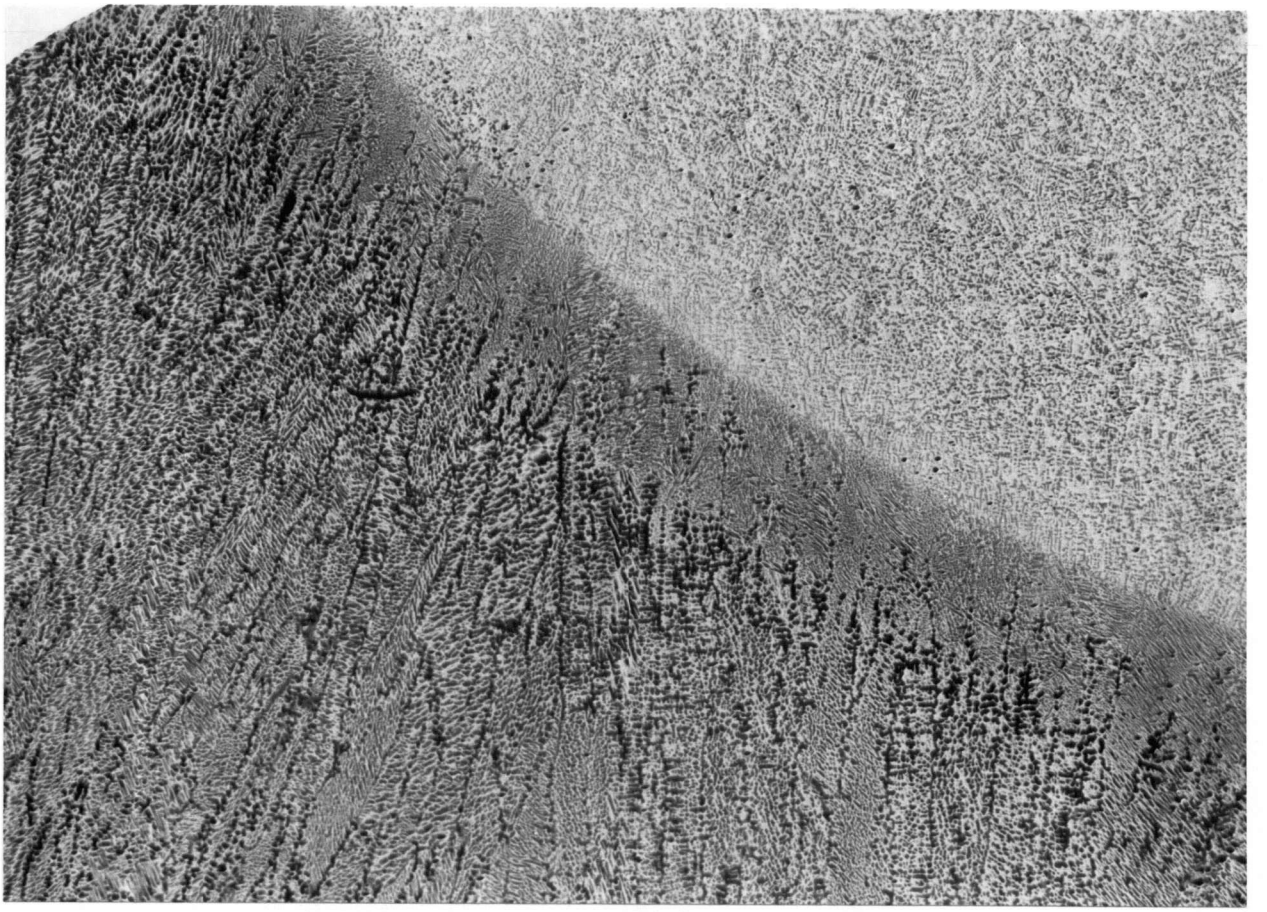

Figure 48. Macrostructure of the peculiar pool profile observed in Valve No. 9. (5.5X)

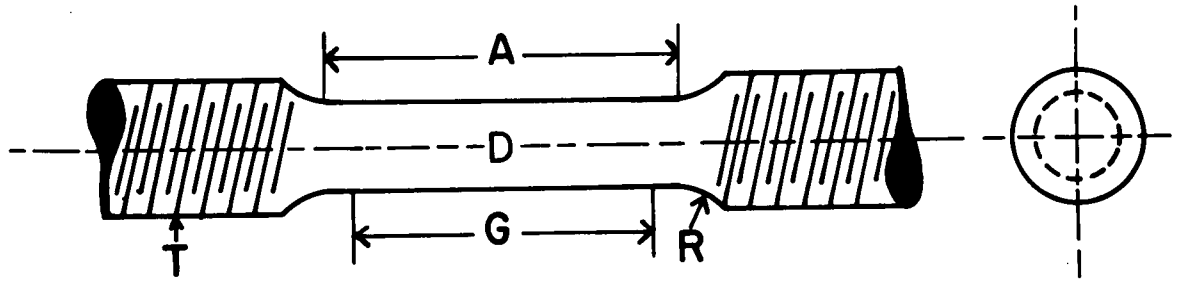

	Small Specimen (316,CF-8M and 4340)	Large Specimen (316 and CF-8M)	Large Specimen (4340
D	0.25 inches	1.00 inches	0.75 inches
G	1.00 "	4.00 "	3.00 "
A	1.25 "	5.00 "	3.75 "
R	3/16 "	3/4 "	9/16 "
T	3/8 "	2 "	2 "

Figure 49. Schematic of the tensile specimens used.

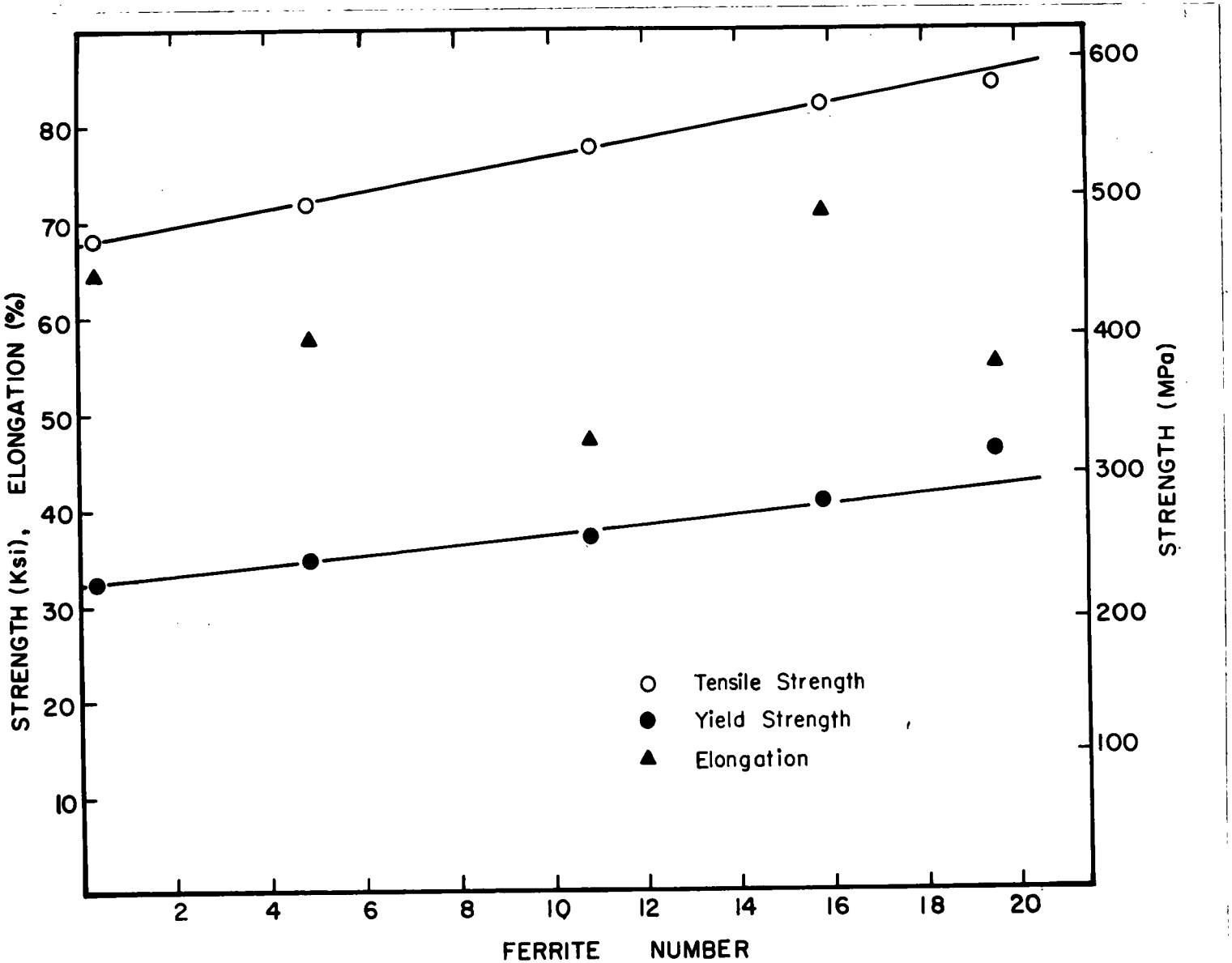

Figure 50. Variation of tensile properties with ferrite number of stainless steel castings.

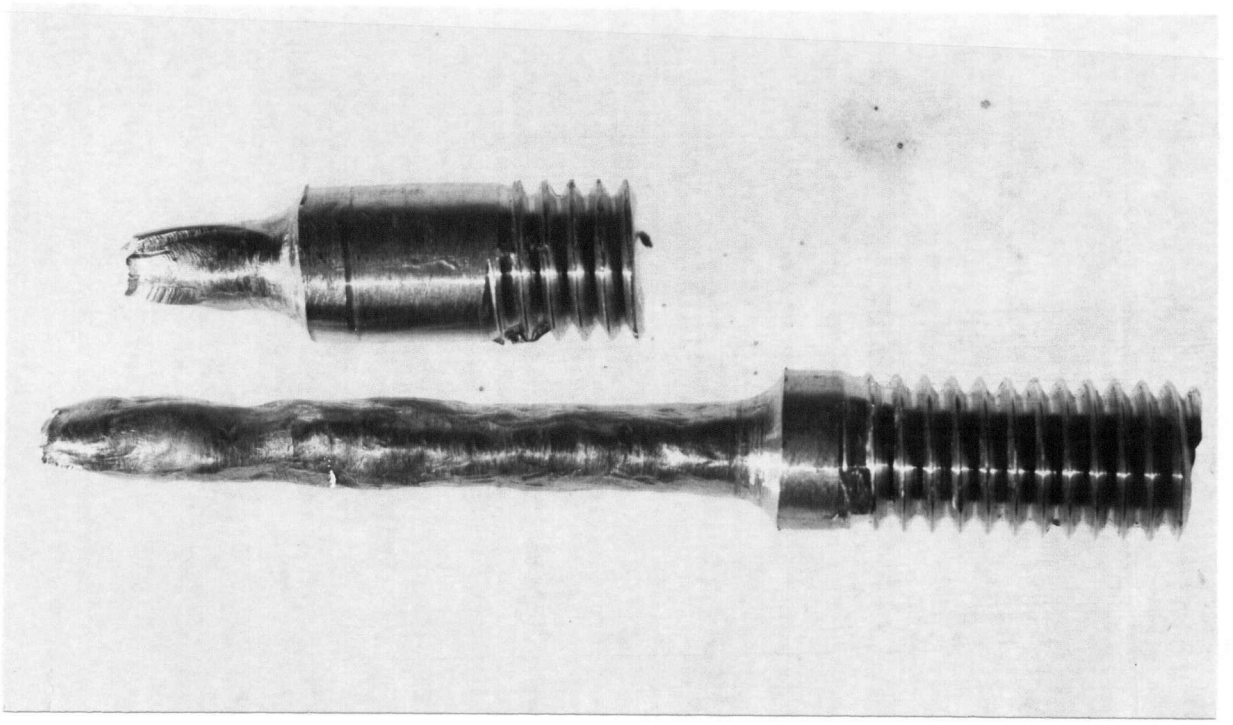

Figure 51. Photograph of the deformed and fractured areas of small tensile specimen from Valve No. 6.

Figure 52. Photograph of the deformed and fractured areas of large tensile specimen from Valve No. 6.

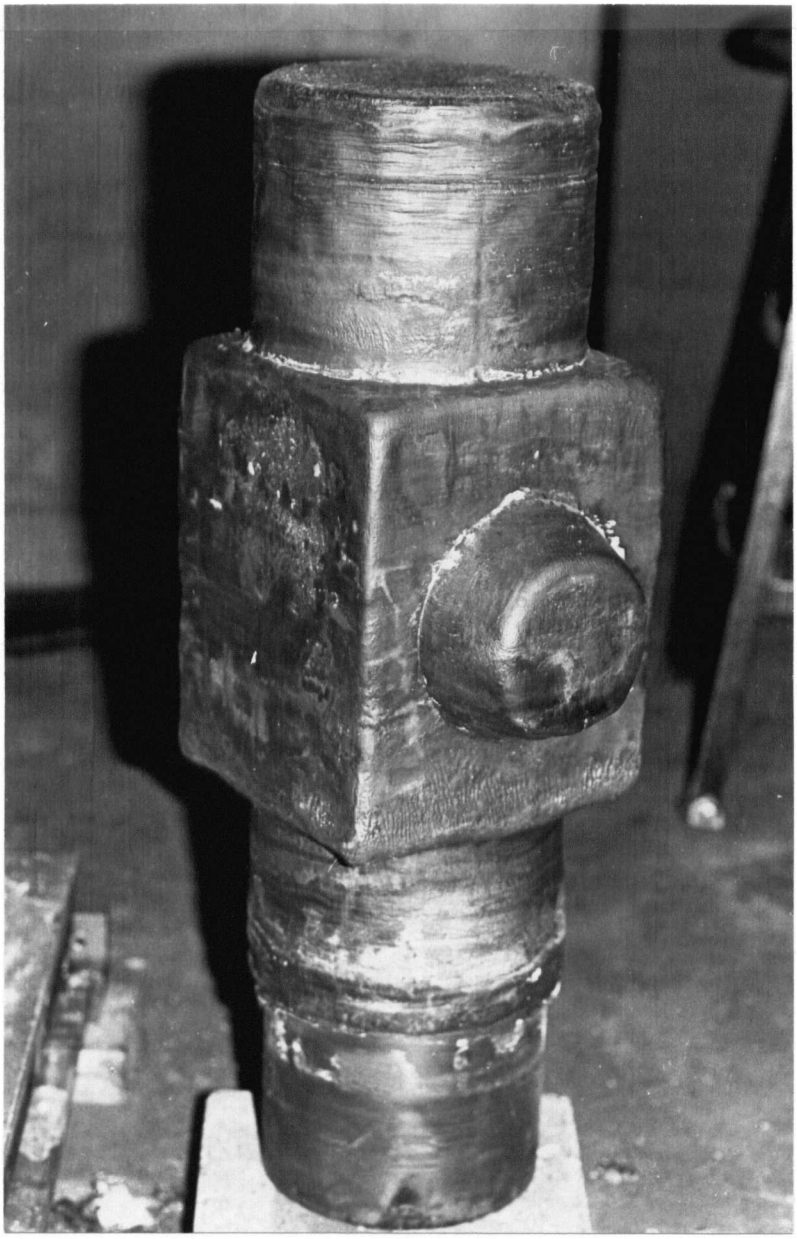

Figure 53. AISI 4340 ESC valve.

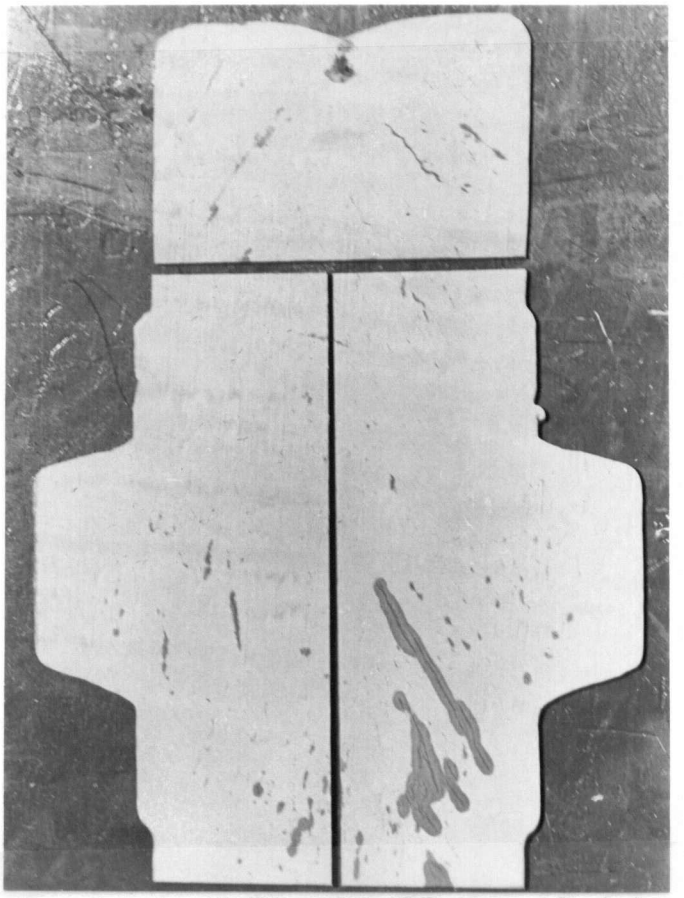

Figure 54. Cracks in Valve No. 14 revealed by dye-penetrant test.

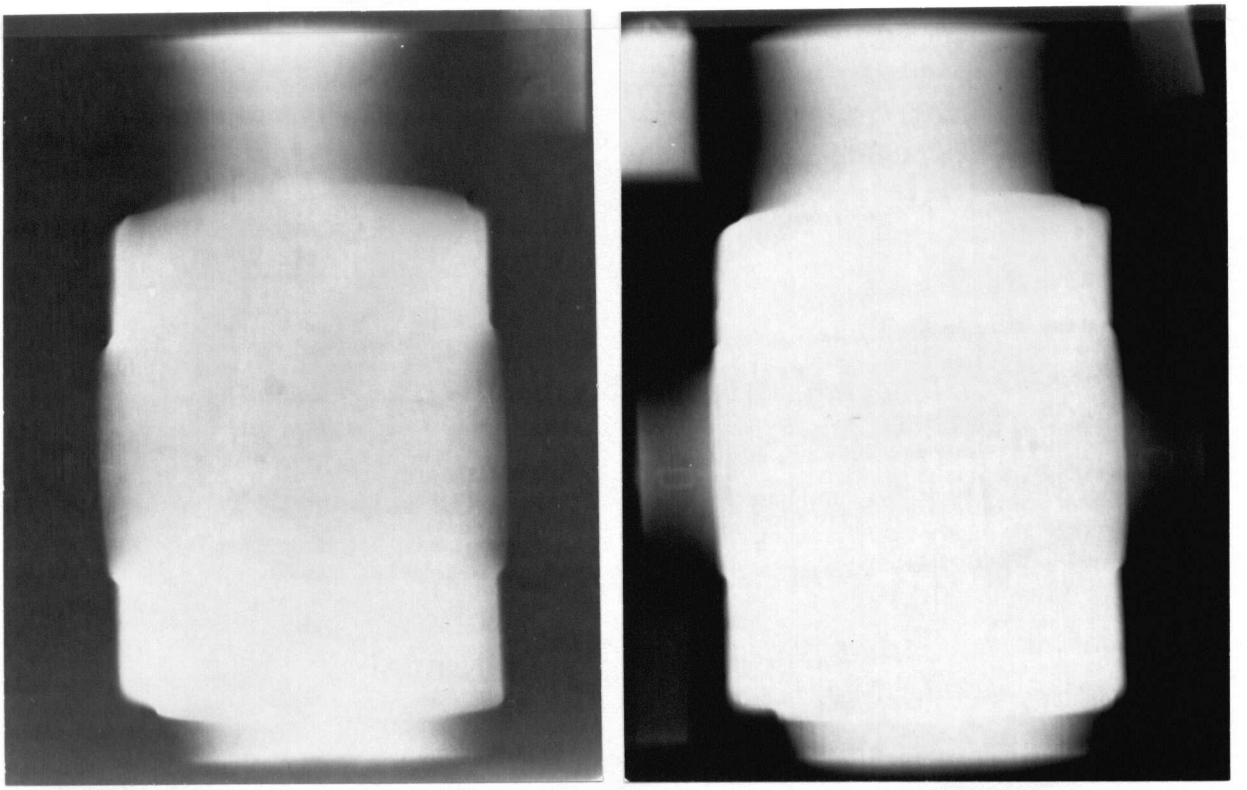

Figure 55. Radiographs of Valve No. 3.

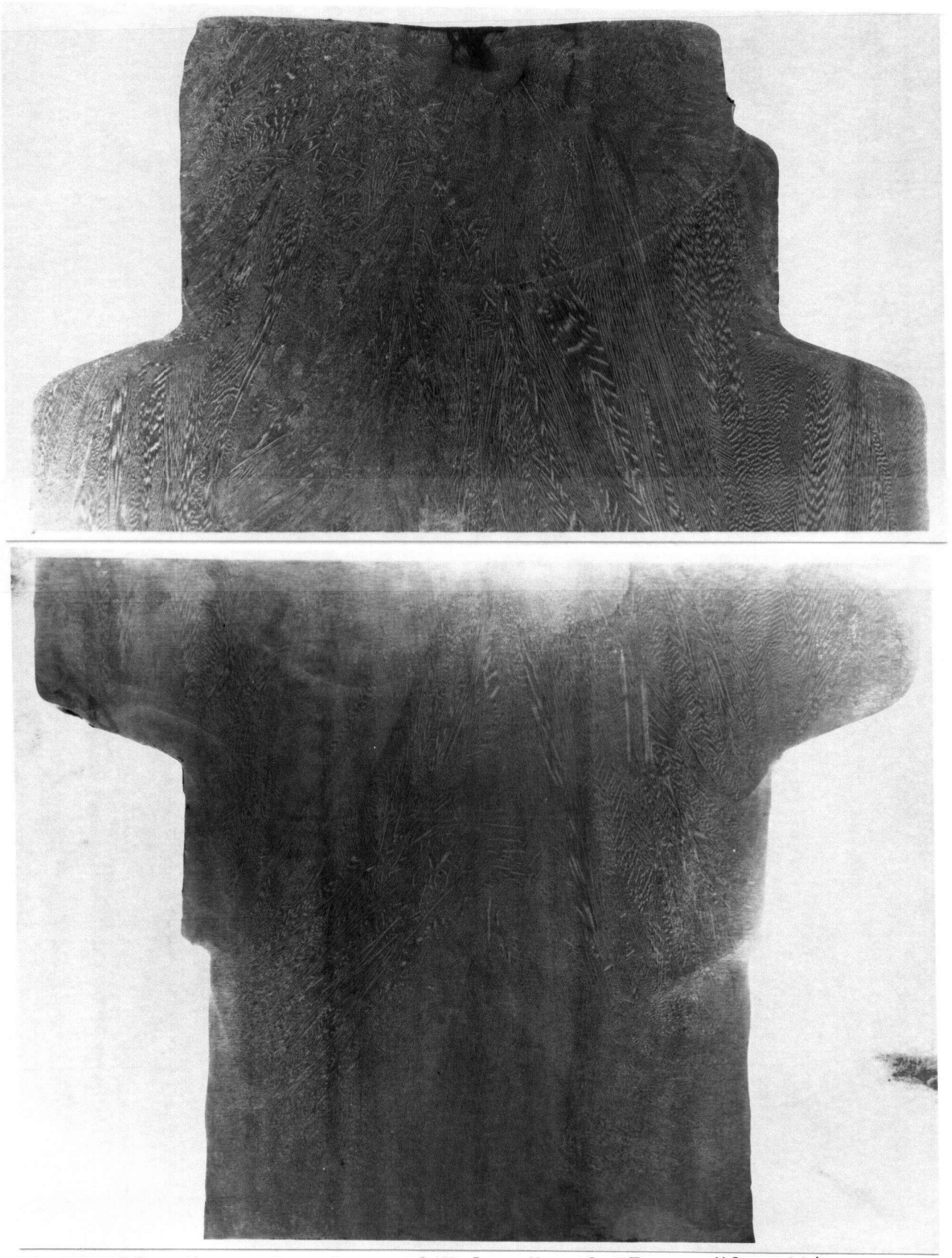

Figure 56. Macrostructure of Valve No. 3 Top - HCℓ etch. Bottom - $(NH_4)_2\ SO_4$ etch.

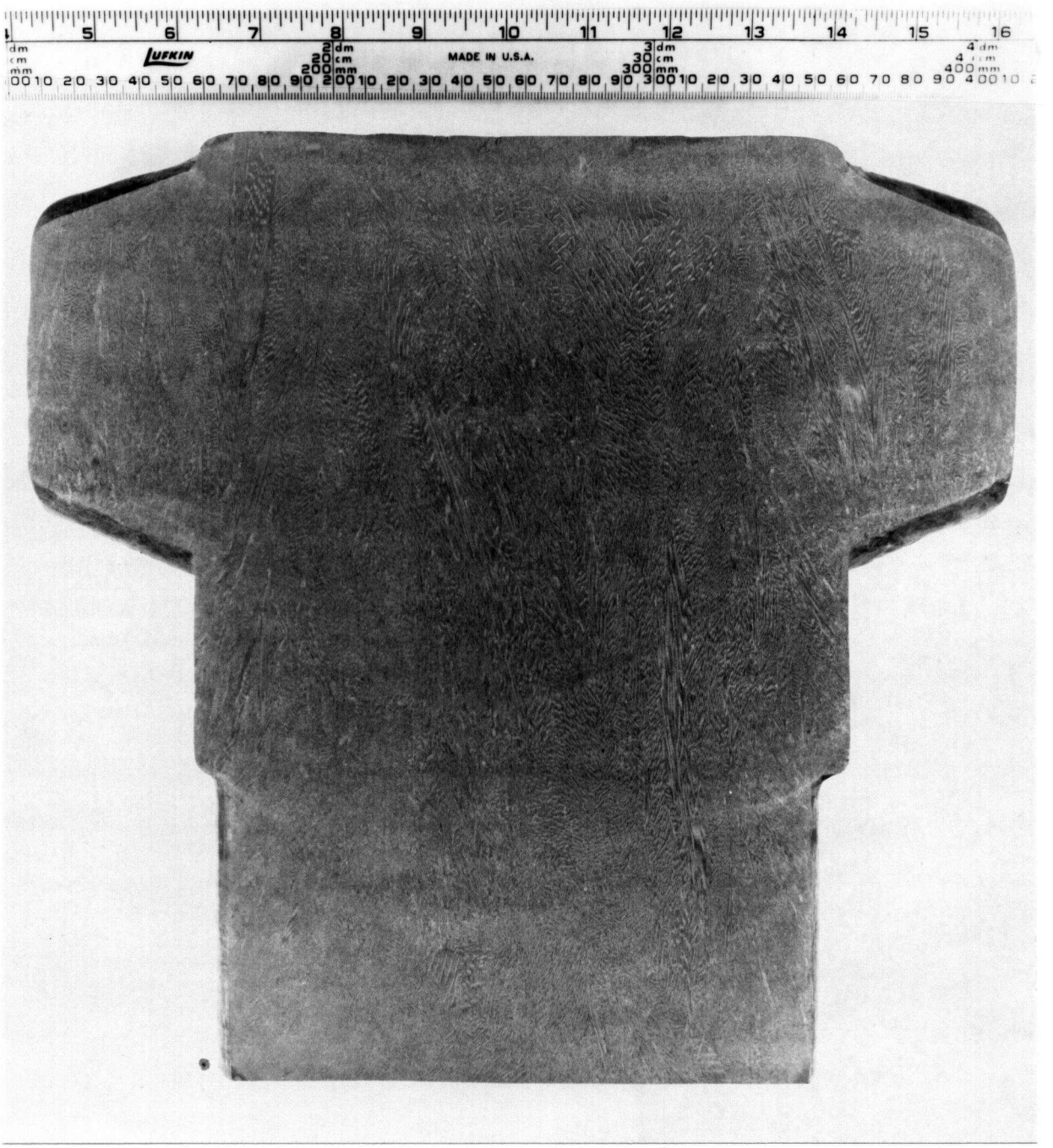

Figure 57. Macrostructure of Valve No. 8 (HCℓ etch).

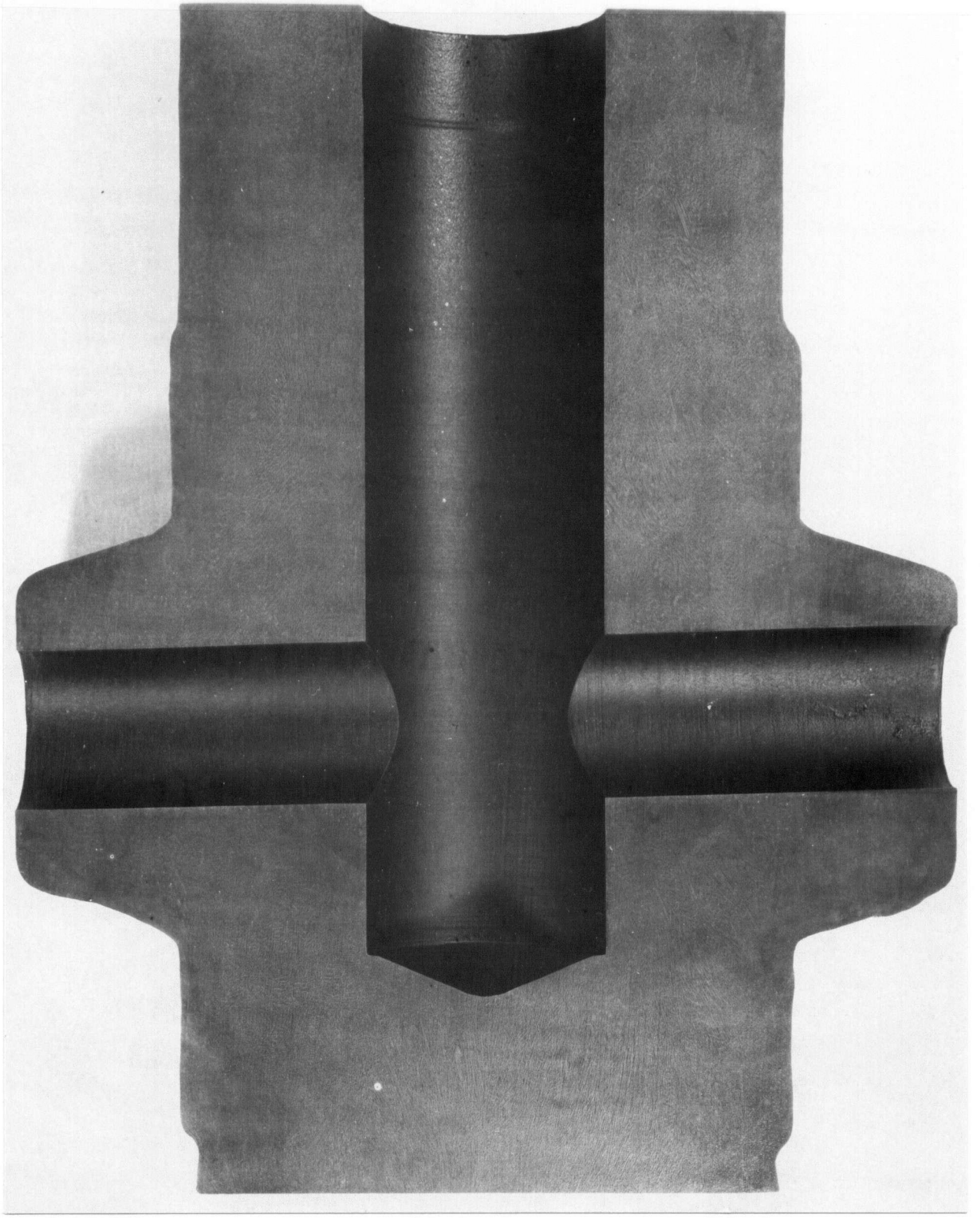

Figure 58. Macrostructure of Valve No. 13 (HCℓ etch).

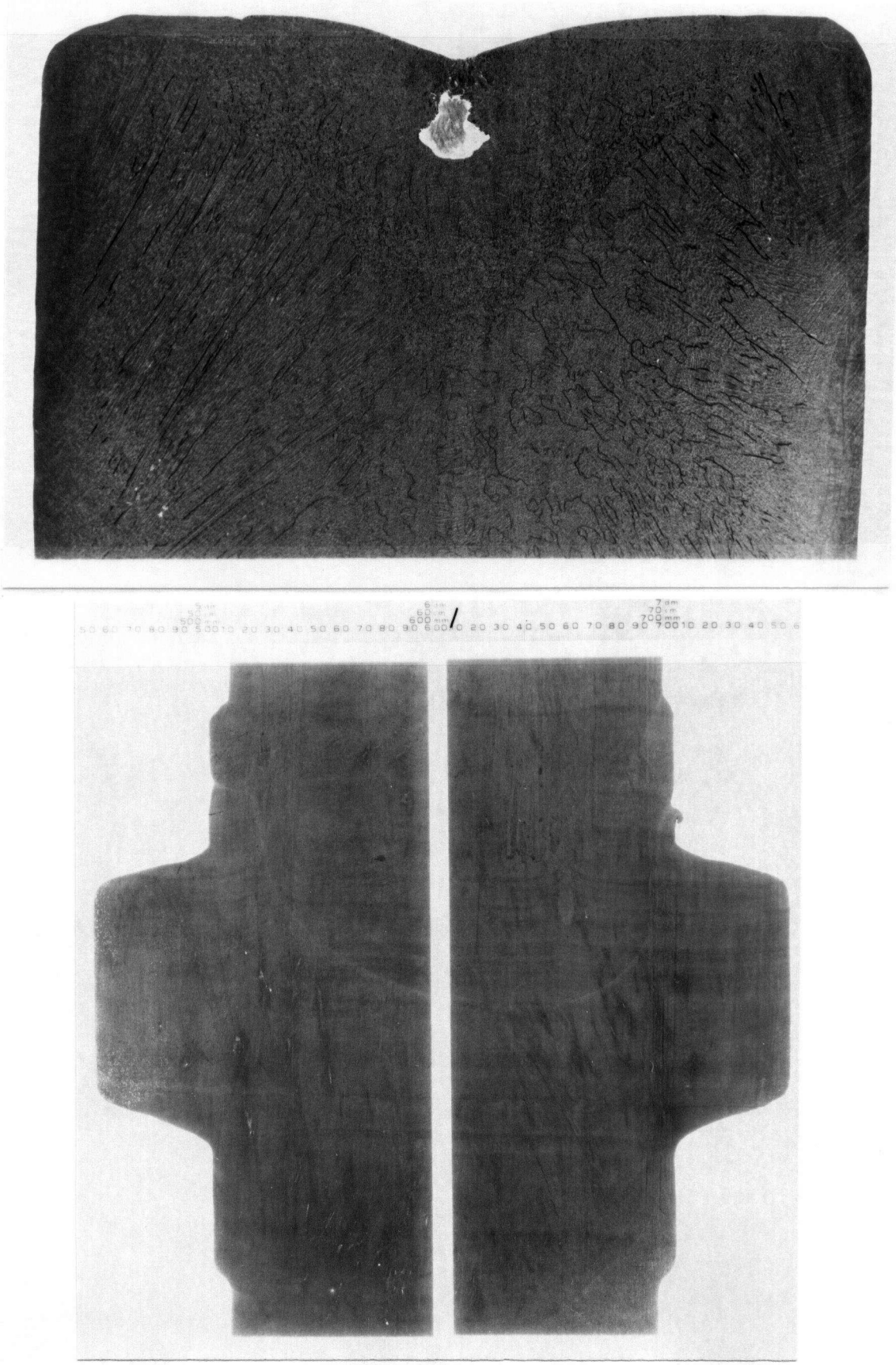

Figure 59. Macrostructure of Valve No. 14 (Hcℓ etch)
(top part etched for a longer time).

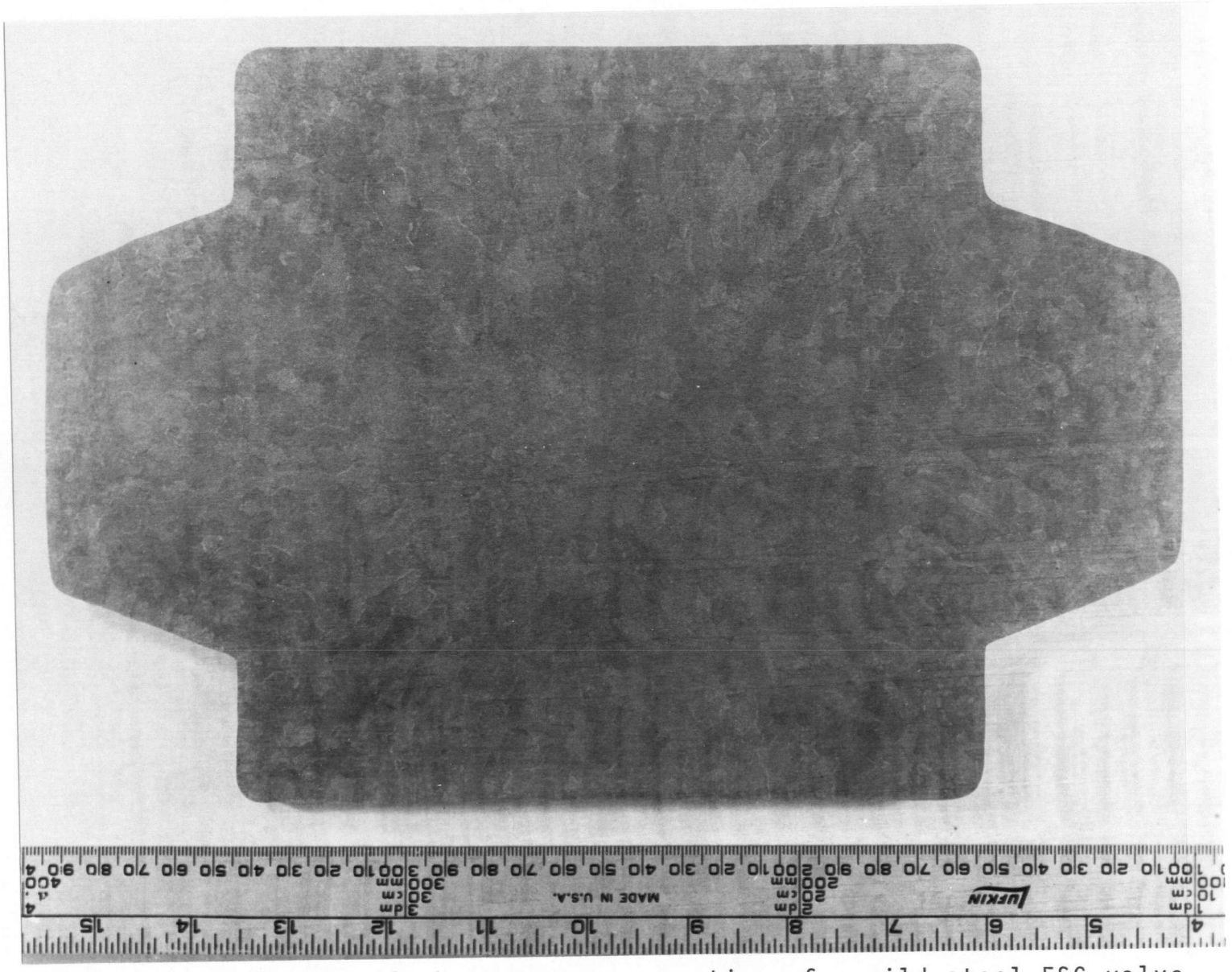

Figure 60. Macrostructure of the transverse section of a mild steel ESC valve ($HC\ell$ etch).

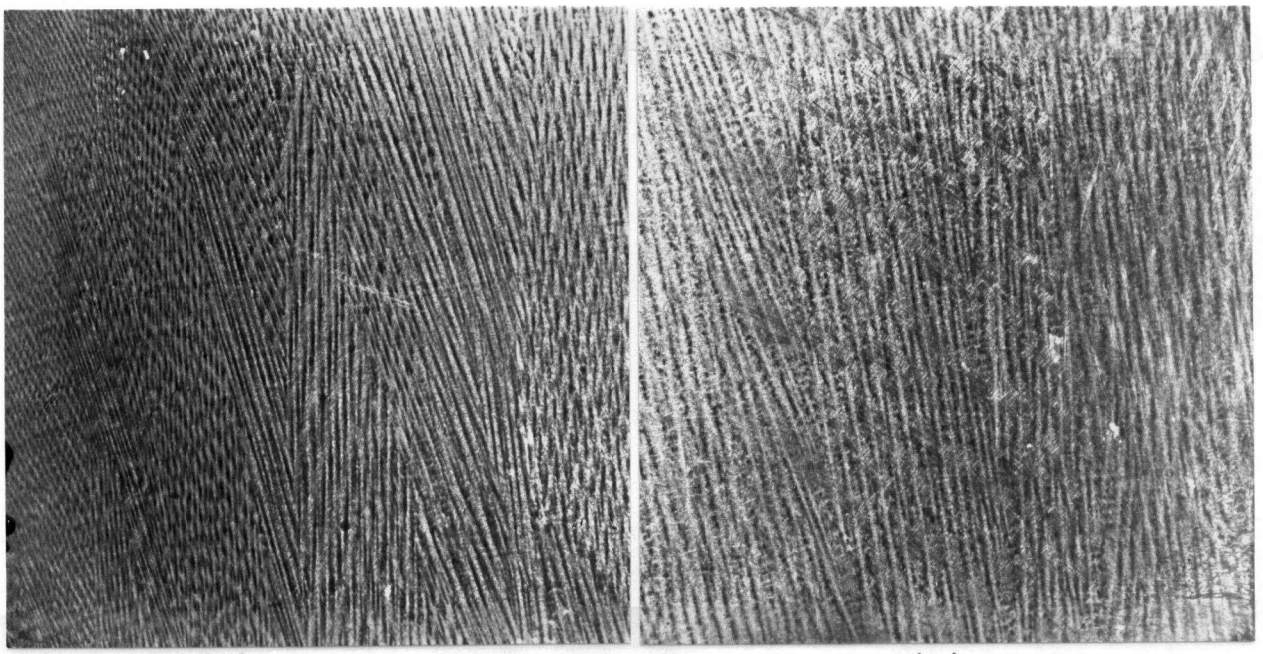

(a) 4 x

(b) 4 x

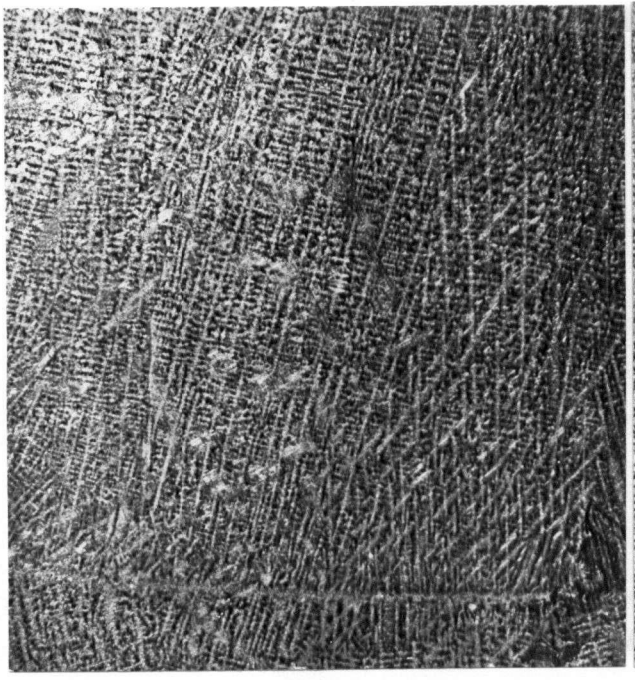

(c) 4 x

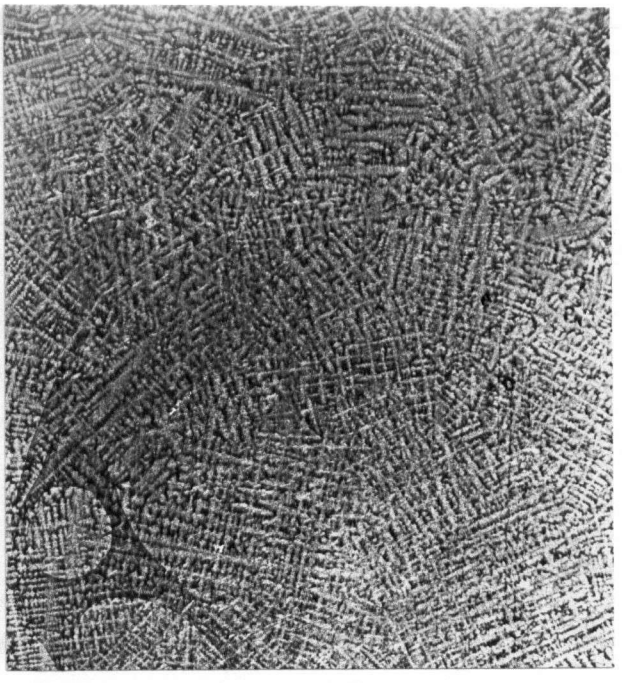

(d) 4 x

Figure 61. Dendritic structure of Valve No. 3.
(a) edge (b) mid-radius
(c) centre (d) top

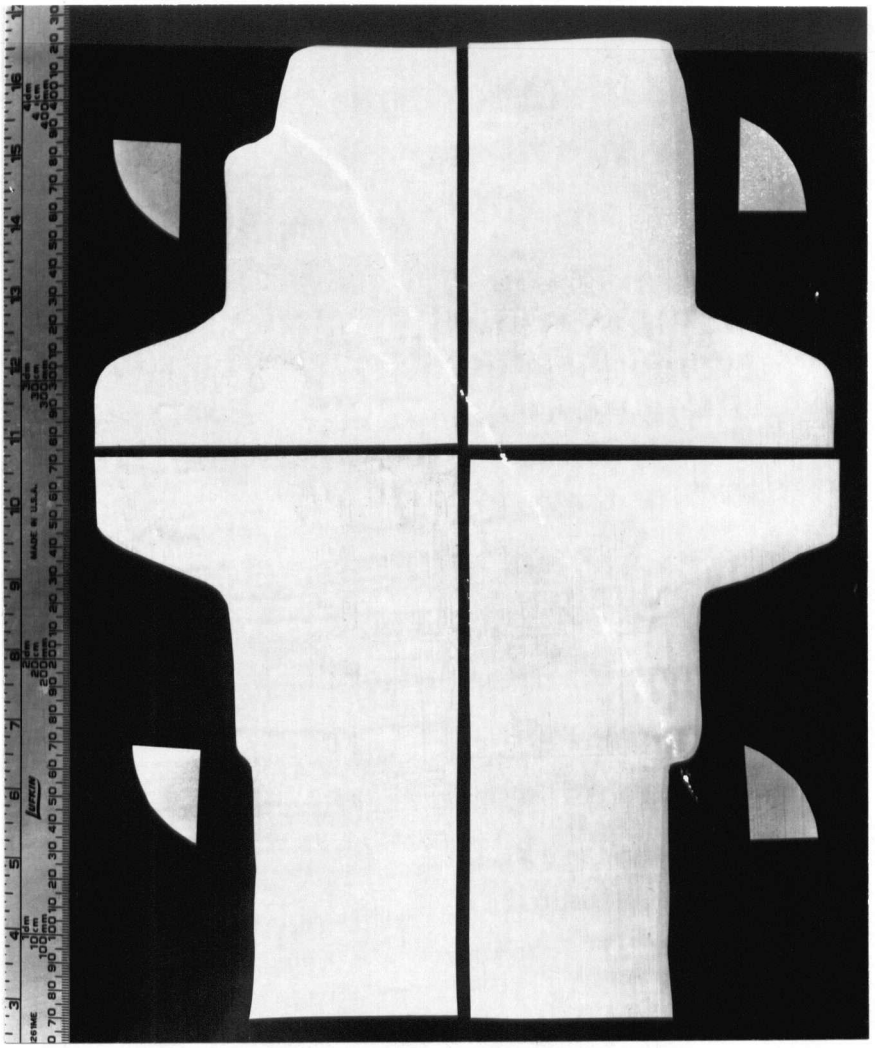

Figure 62. Sulphur prints of Valve No. 3.

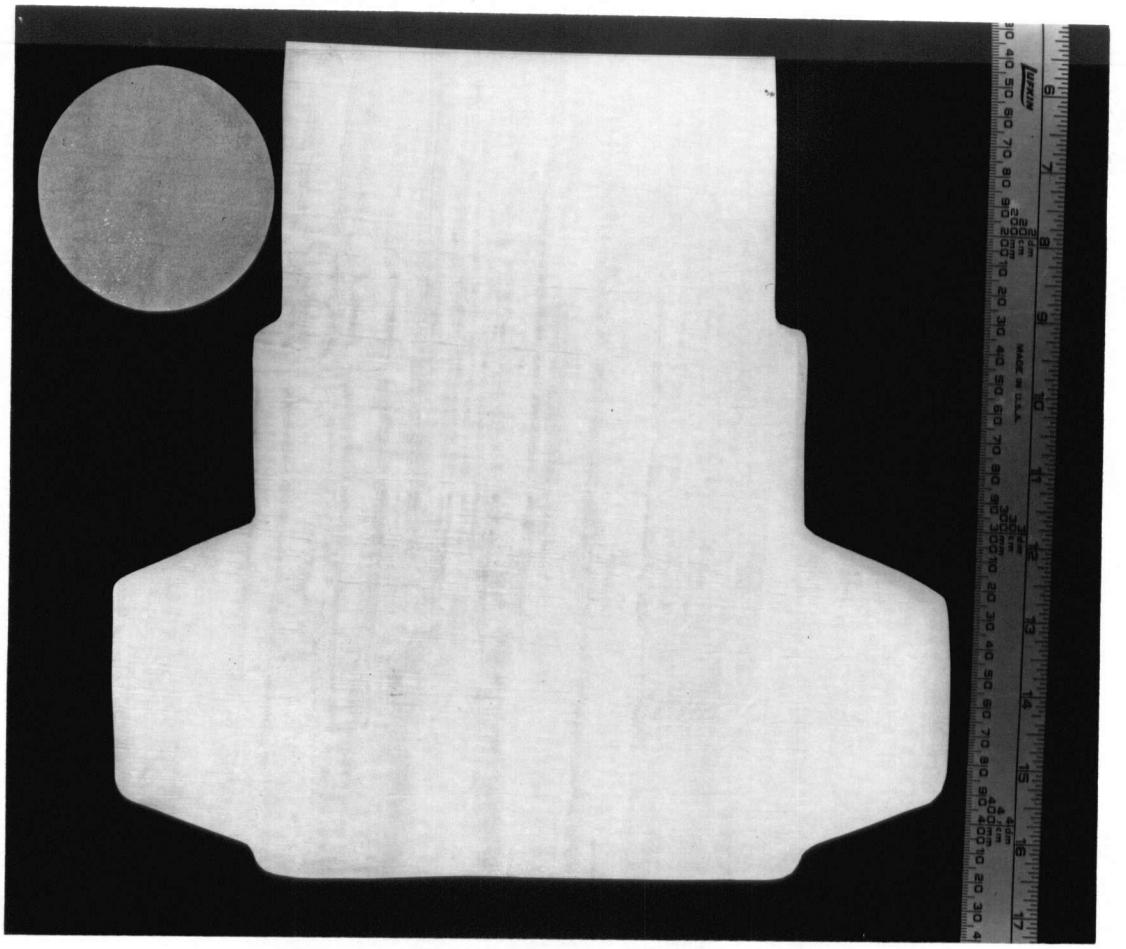

Figure 63. Sulphur Prints of Valve No. 8.

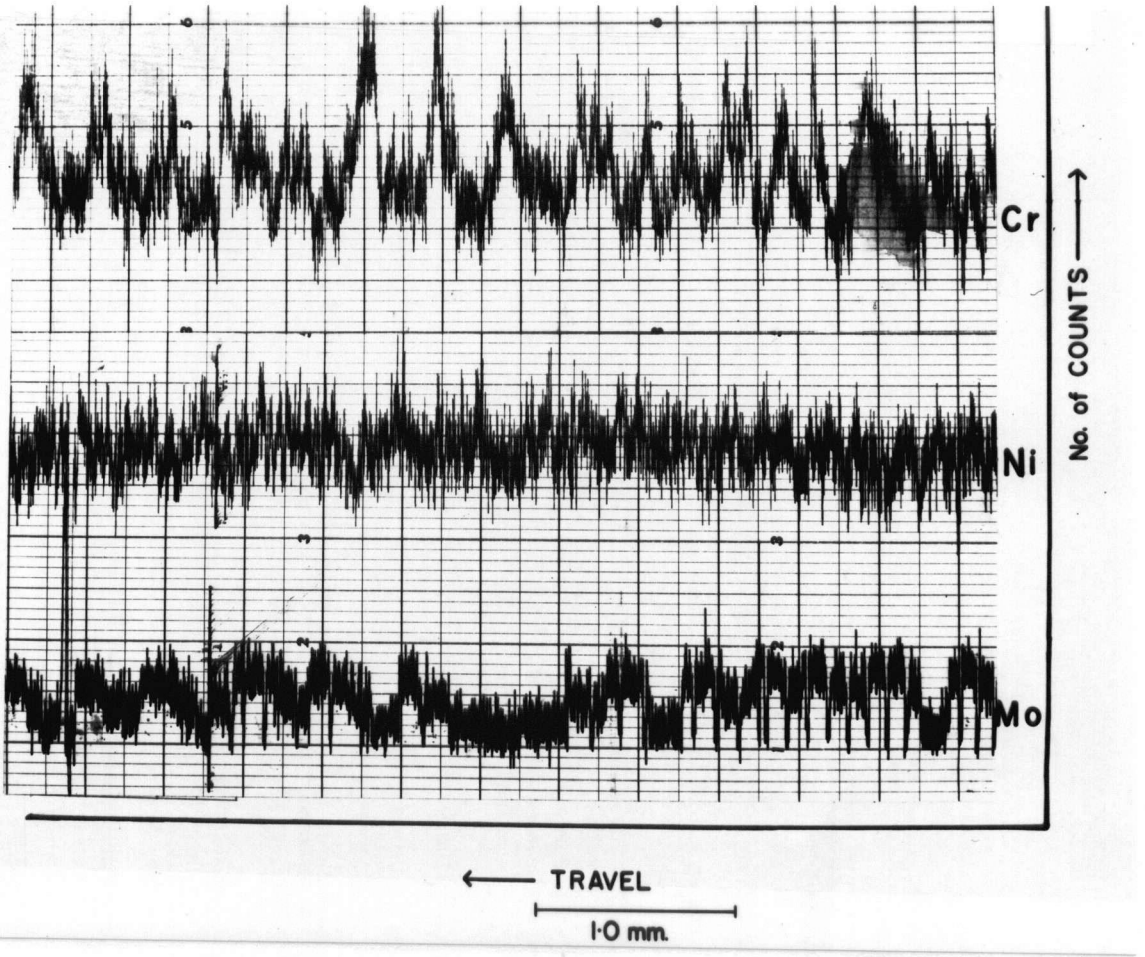

Figure 64. Variation of Cr, Ni and Mo across the dendritic direction in Valve No. 8.

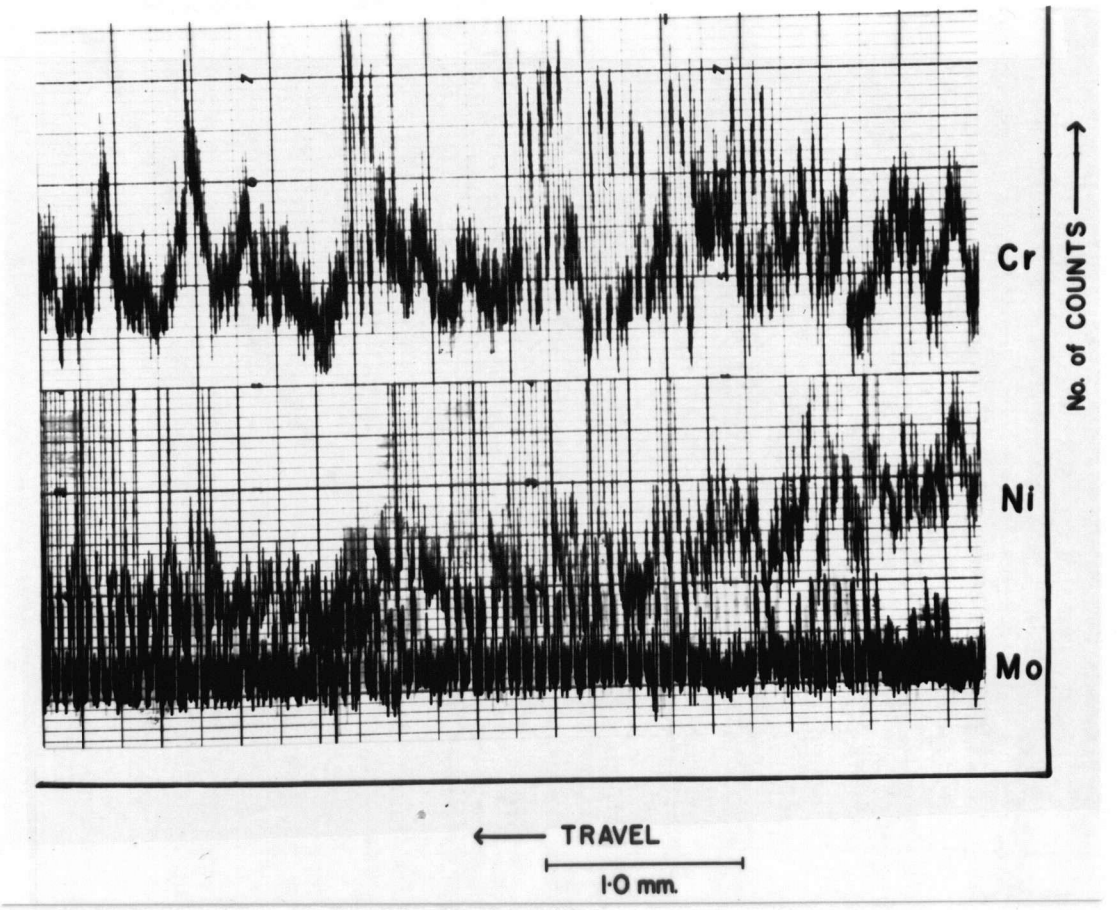

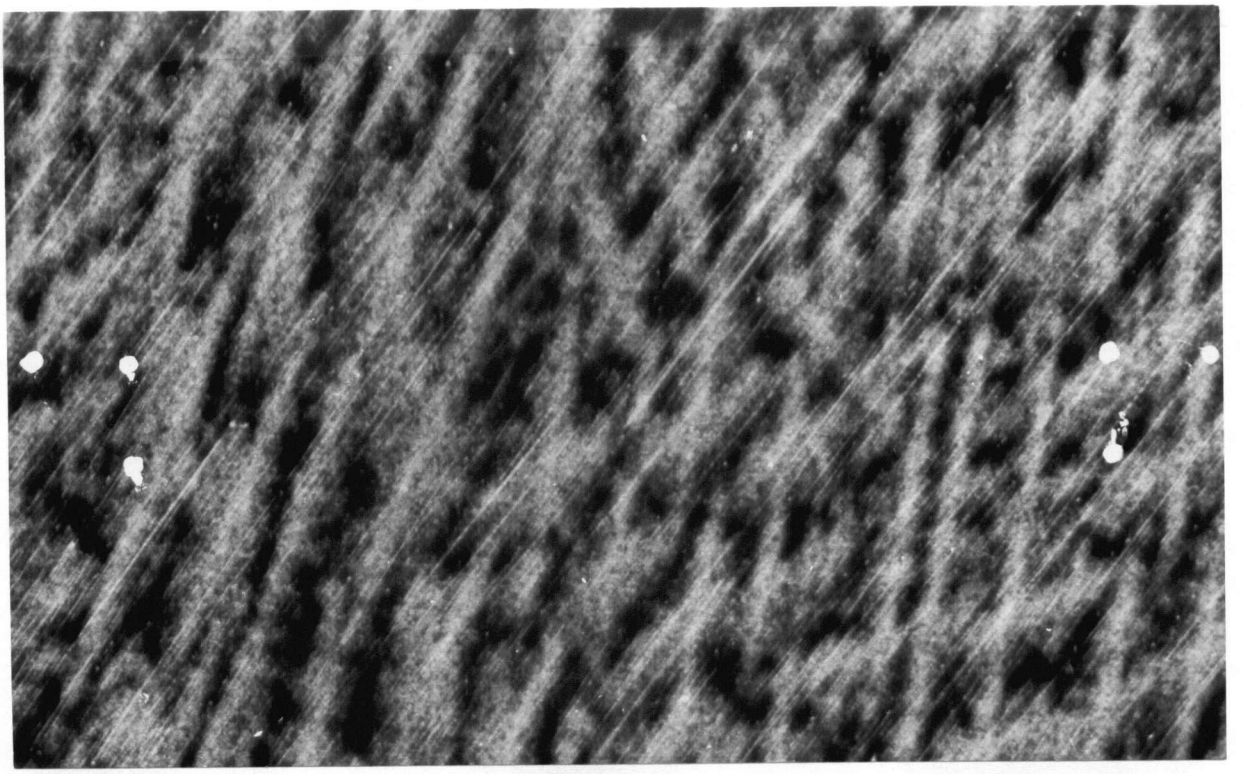

Figure 65. Variation of Cr, Ni and Mo across the dendritic direction in Valve No. 13.

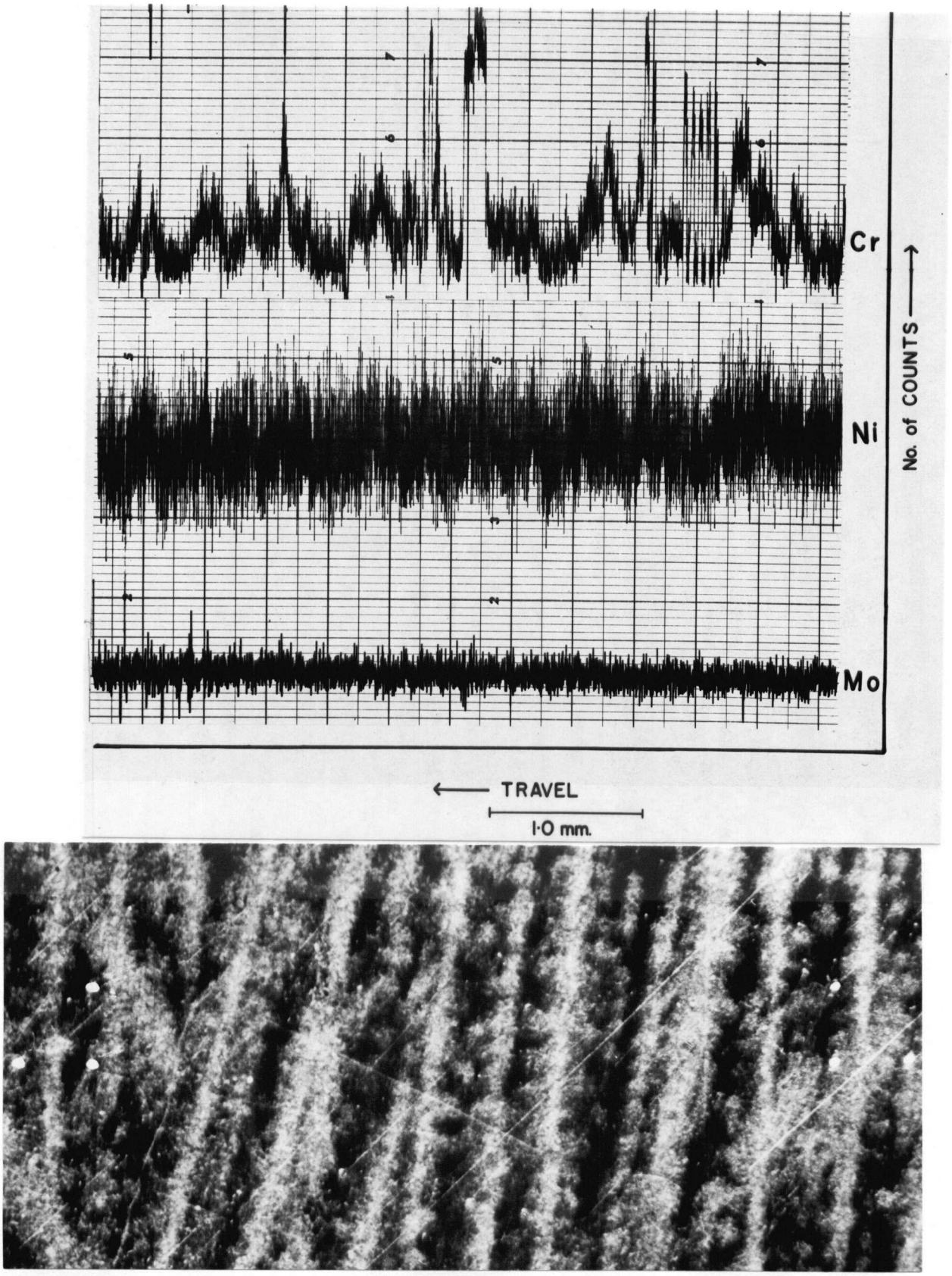

Figure 66. Variation of Cr, Ni and Mo across the dendritic direction in Valve No. 14.

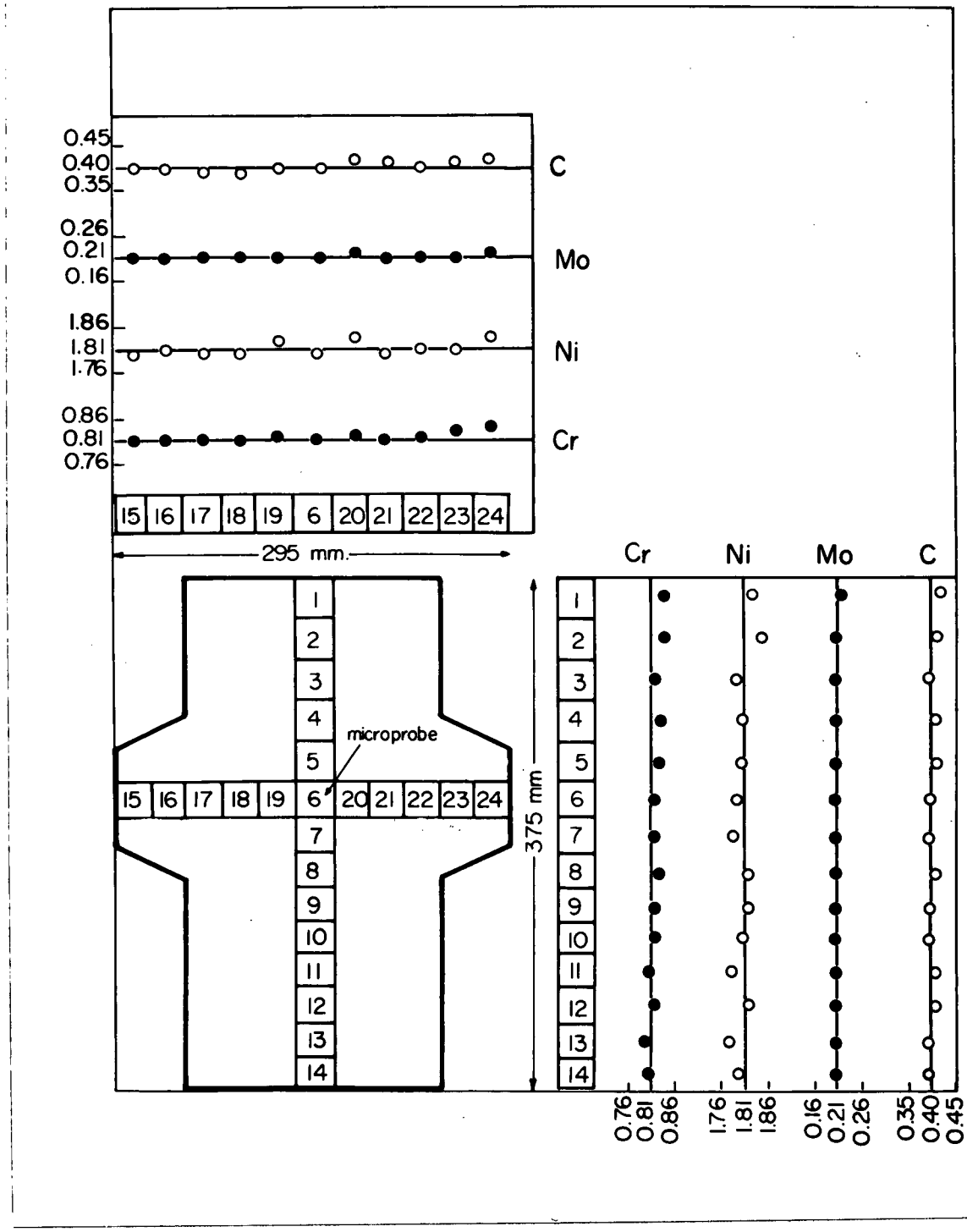

Figure 67. Composition variation in Valve No. 3.
(The solid line shows the overall average composition.)

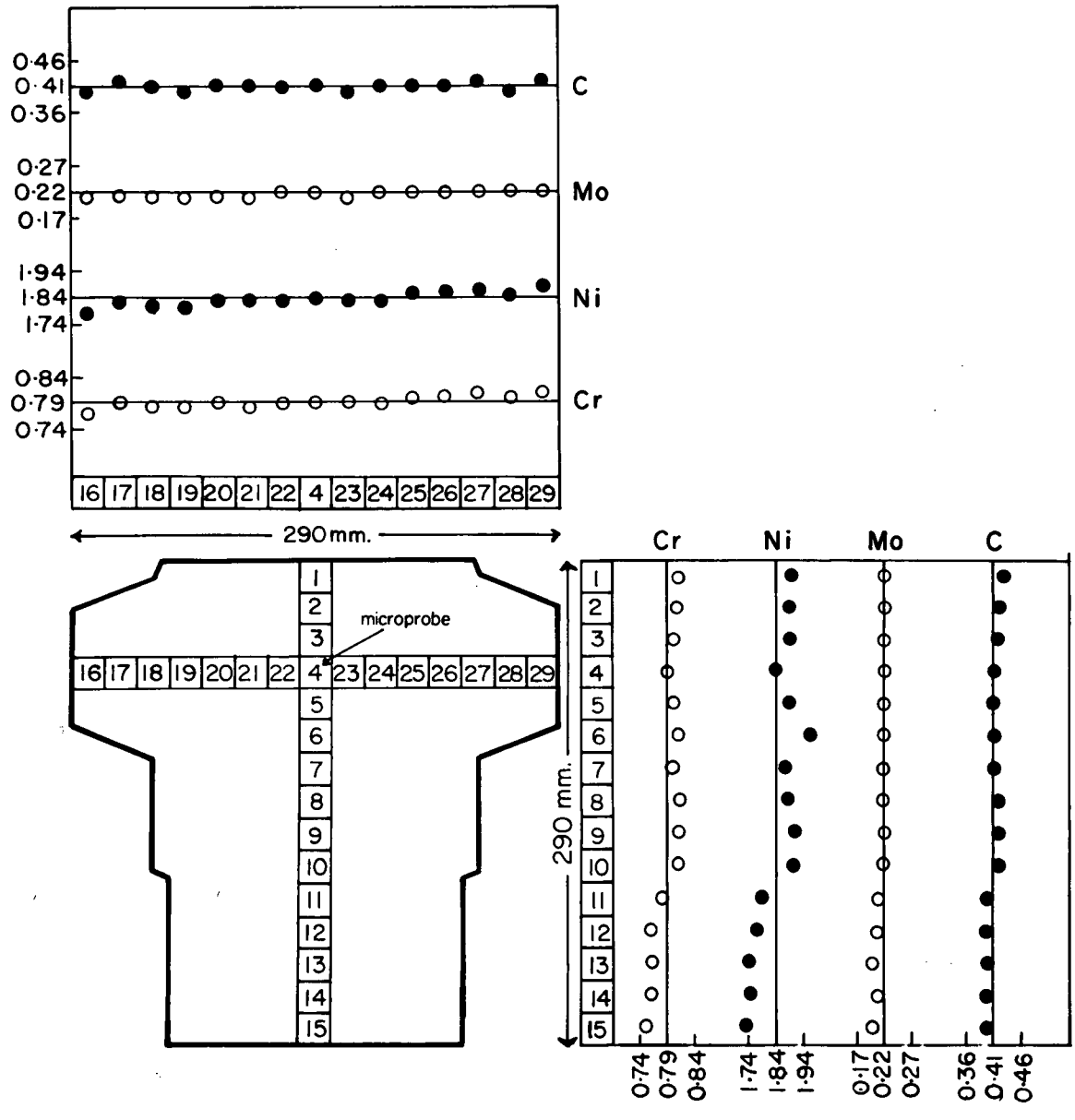

Figure 68. Composition variation in Valve No. 8.
(The solid line shows the overall average composition.)

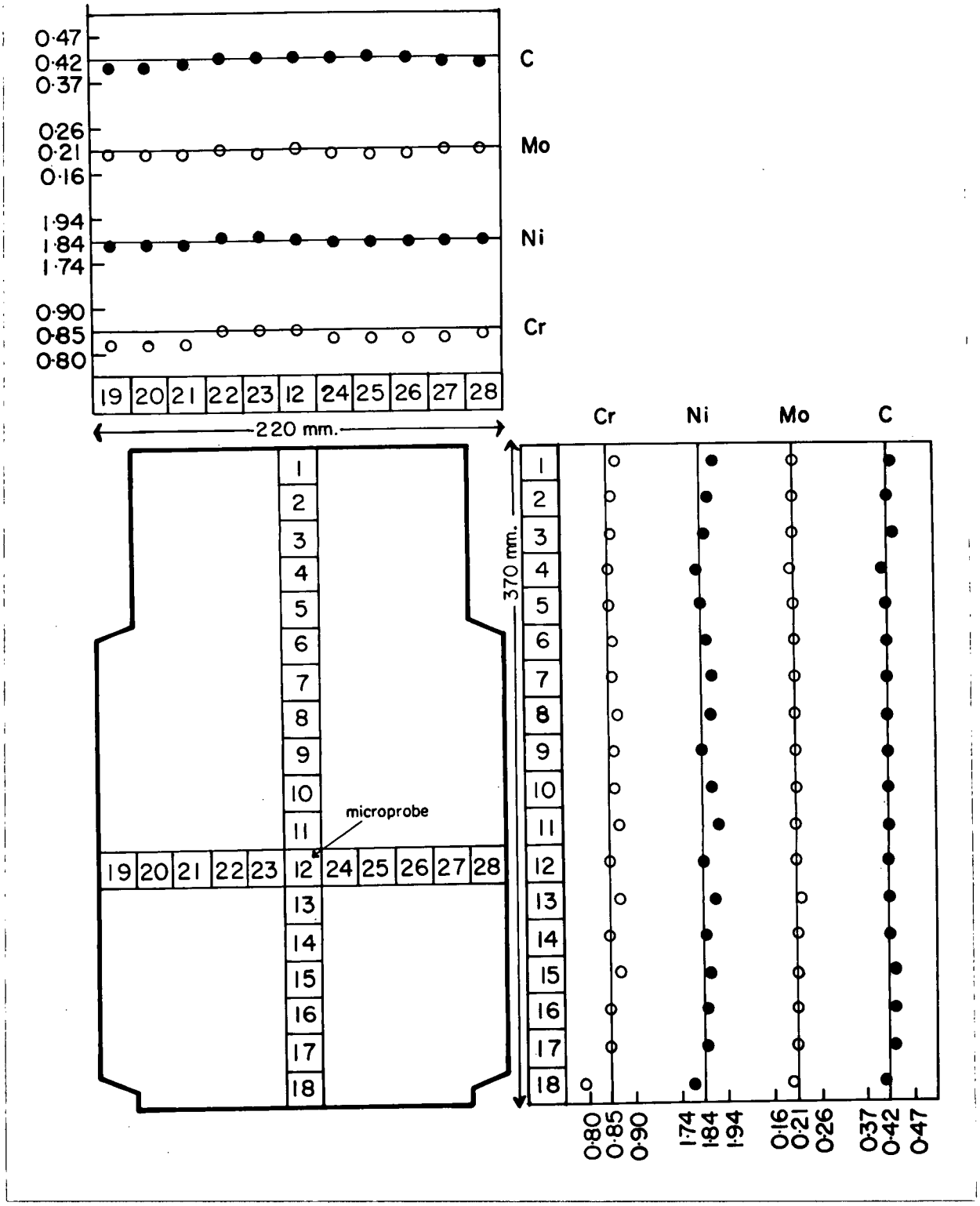

Figure 69. Composition variation in Valve No. 13. (The solid line shows the overall average composition.)

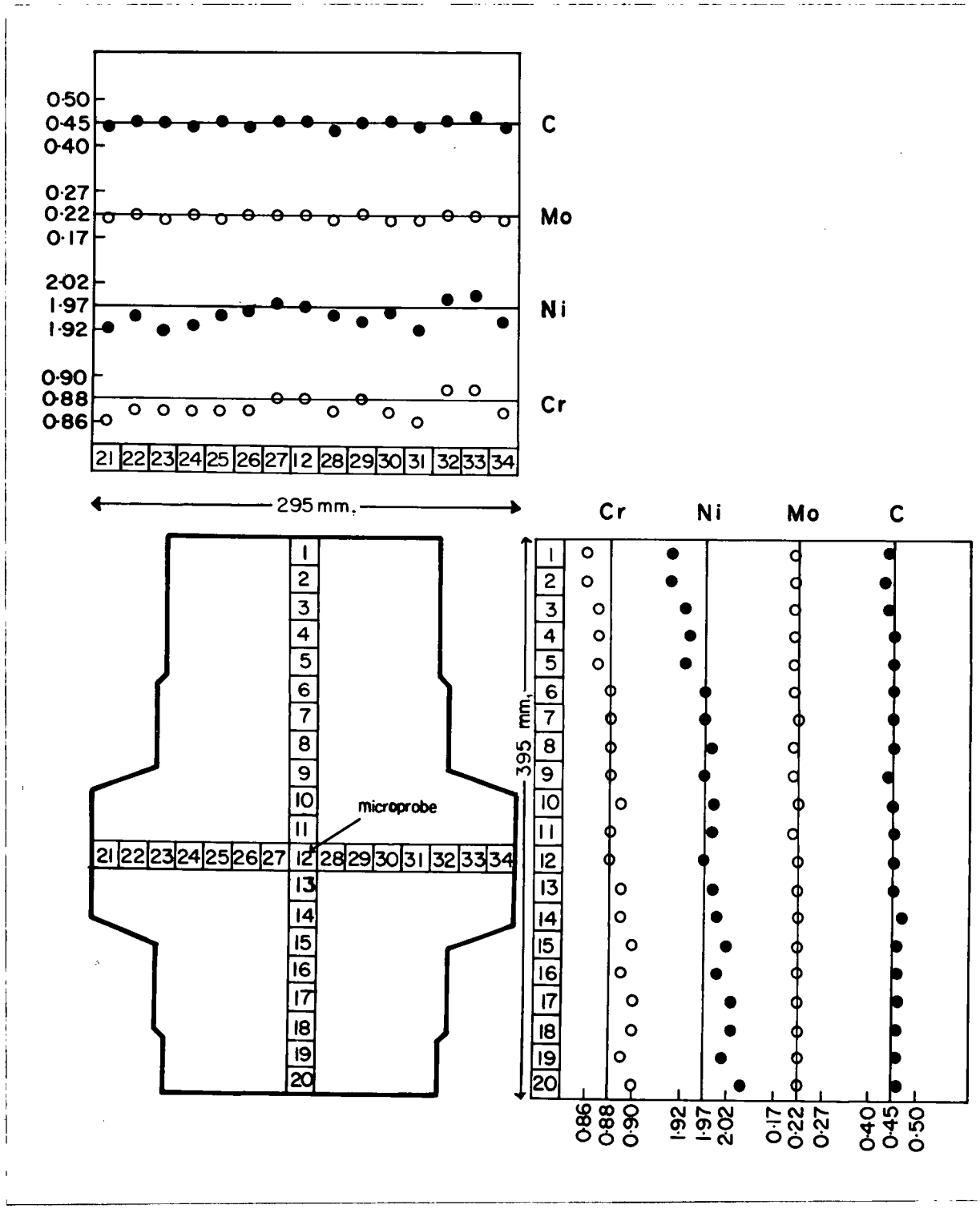

Figure 70. Composition variation in Valve No. 14.
(The solid line shows the overall average composition.)

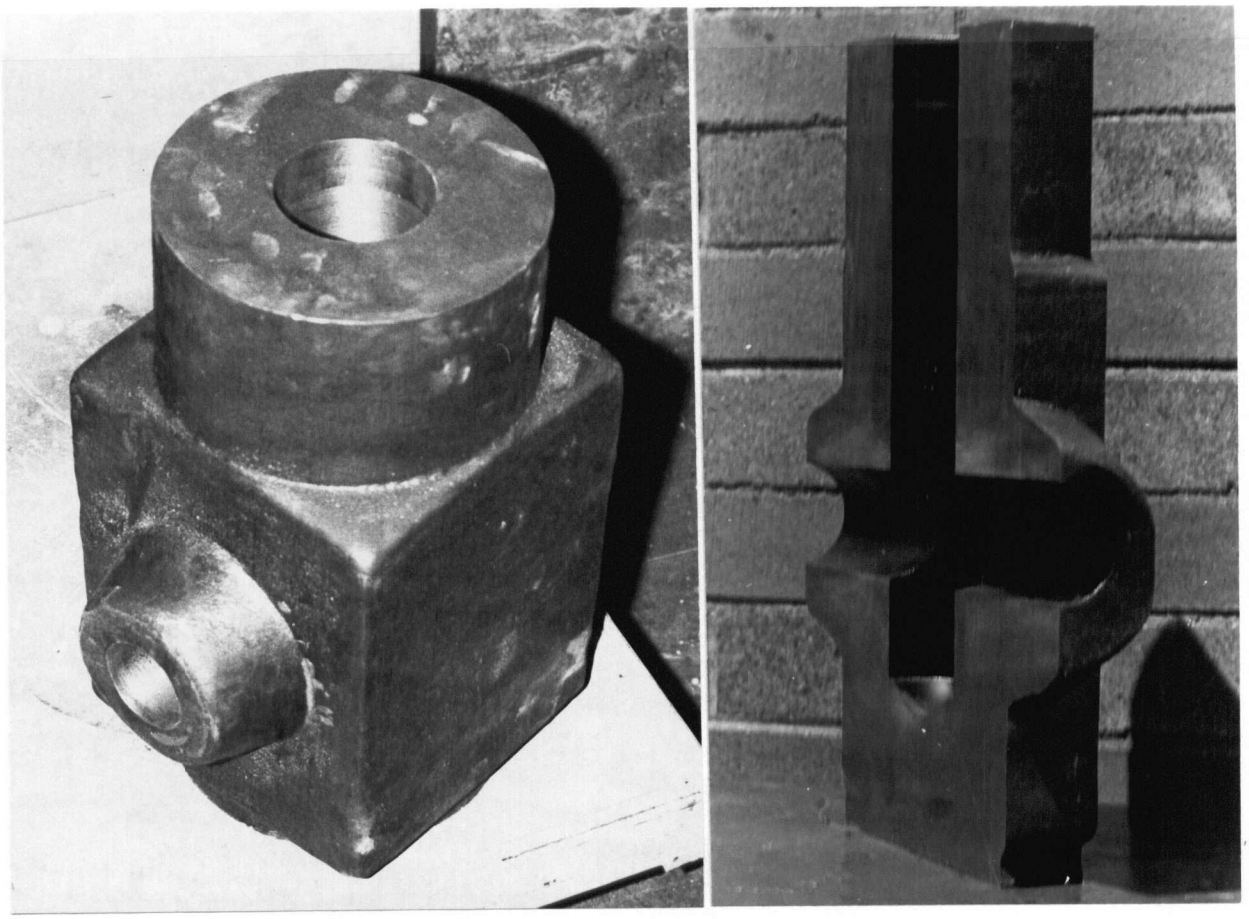

(a) (b)

Figure 71. Machined AISI 4340 ESC valve.

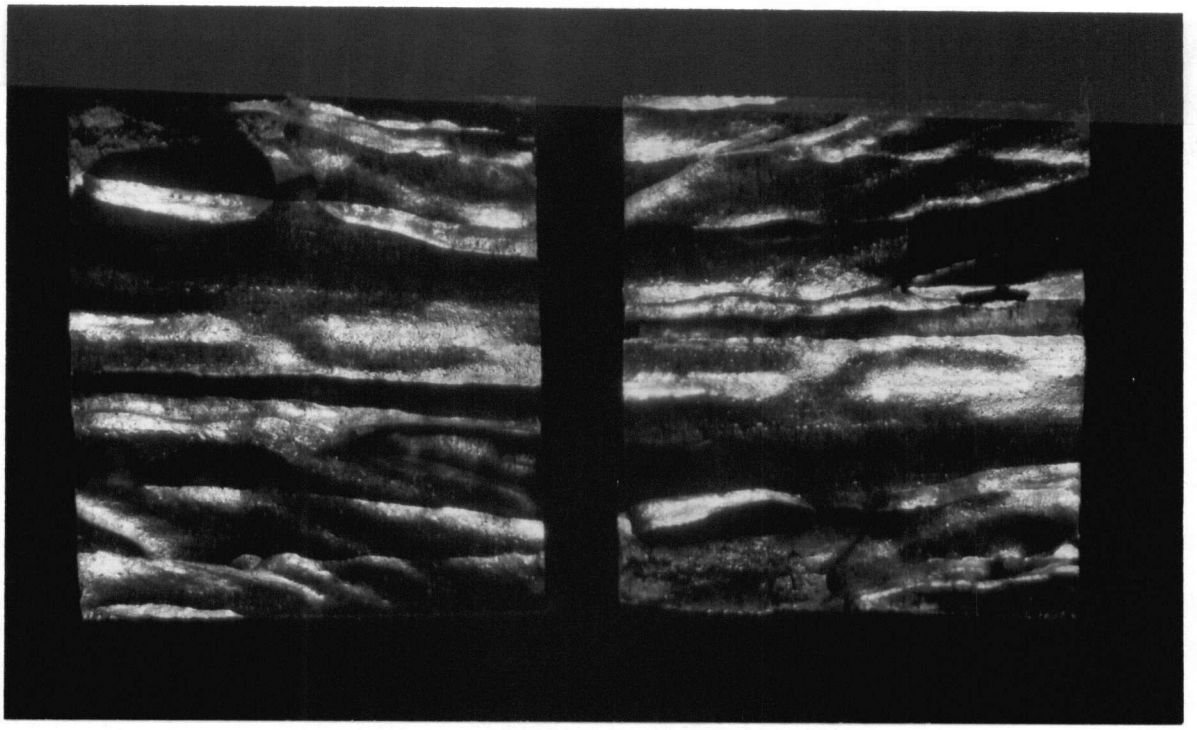

Figure 72. Separated surfaces along a crack in Valve No. 14.

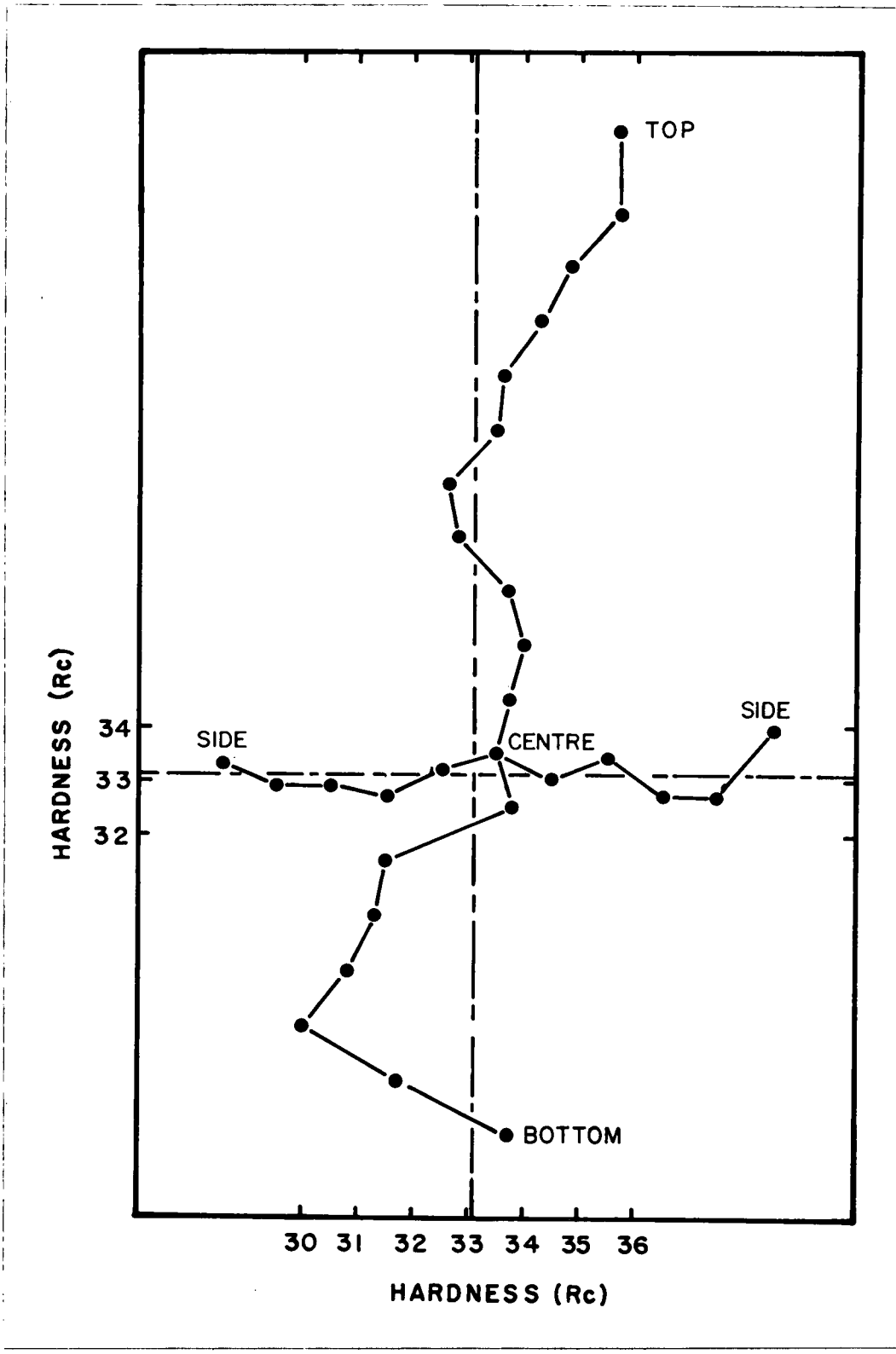

Figure 73. Hardness variation in heat-treated Valve No. 13.

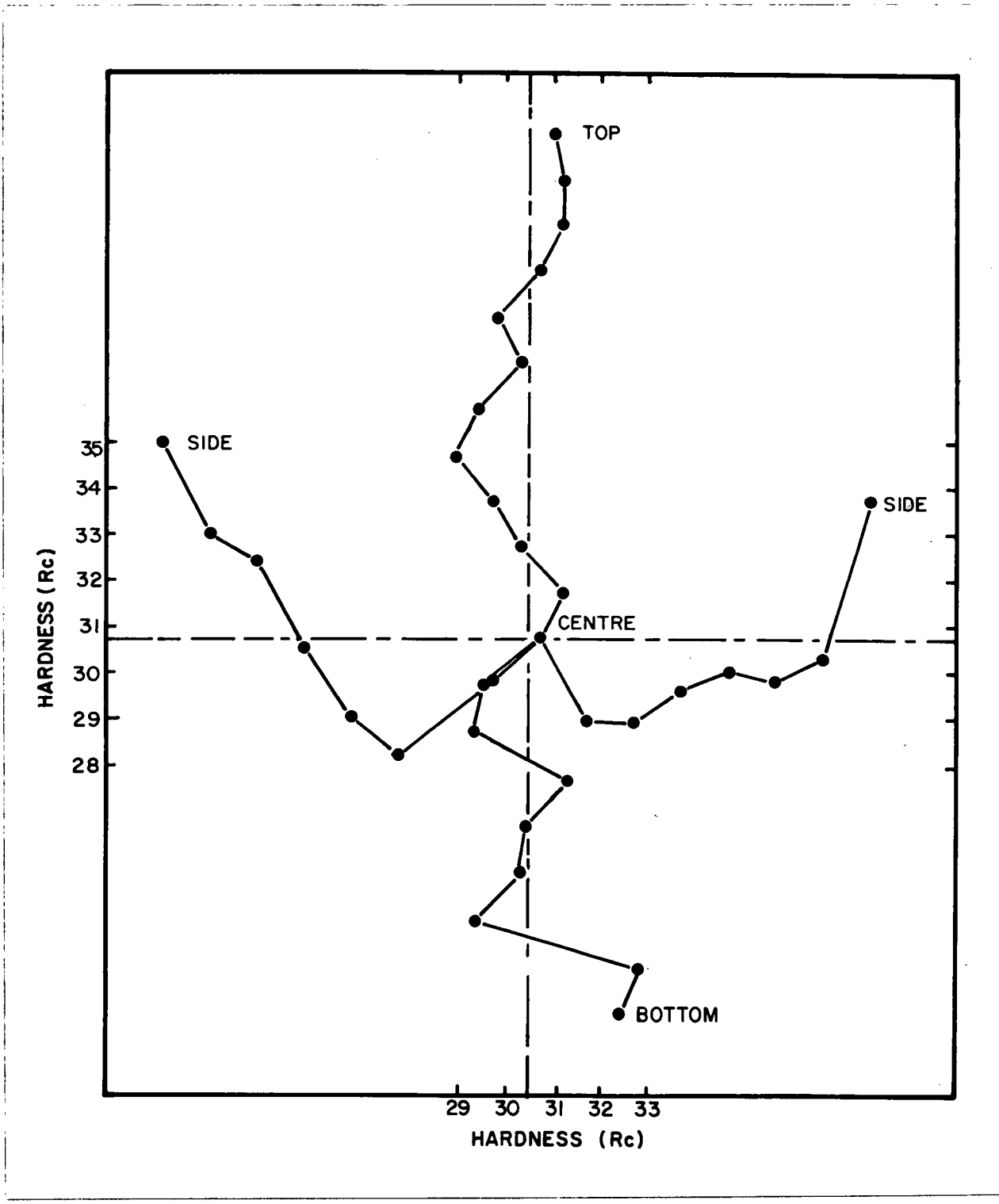

Figure 74. Hardness variation in heat-treated Valve No. 14.

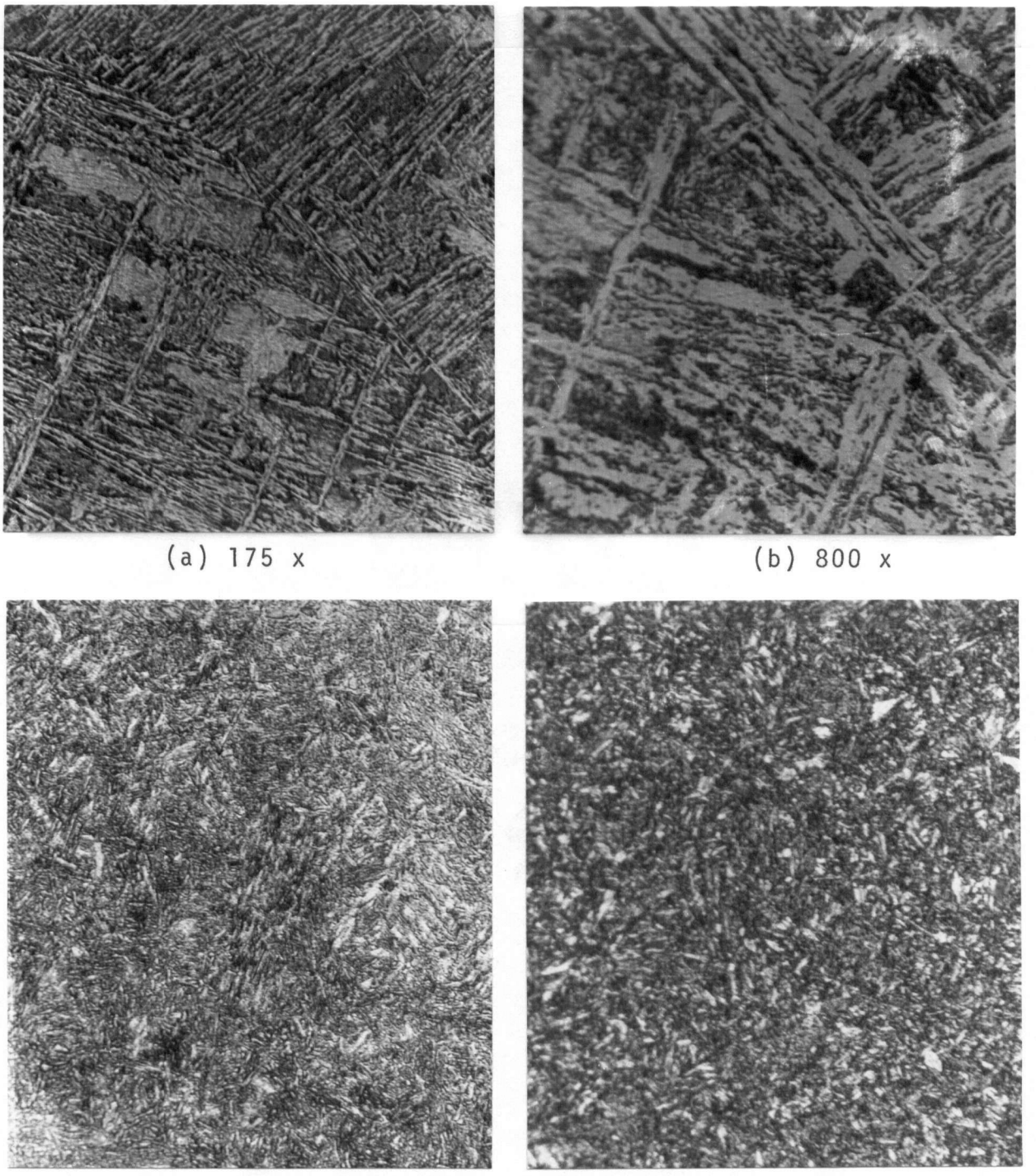

(a) 175 x

(b) 800 x

(c) 640 x

(d) 800 x

Figure 75. Microstructure AISI 4340 valve in as-cast and heat-treated conditions; electrode in heat treated condition.
(a), (b) and (c) - ESC Valve No. 8
(d) - Electrode

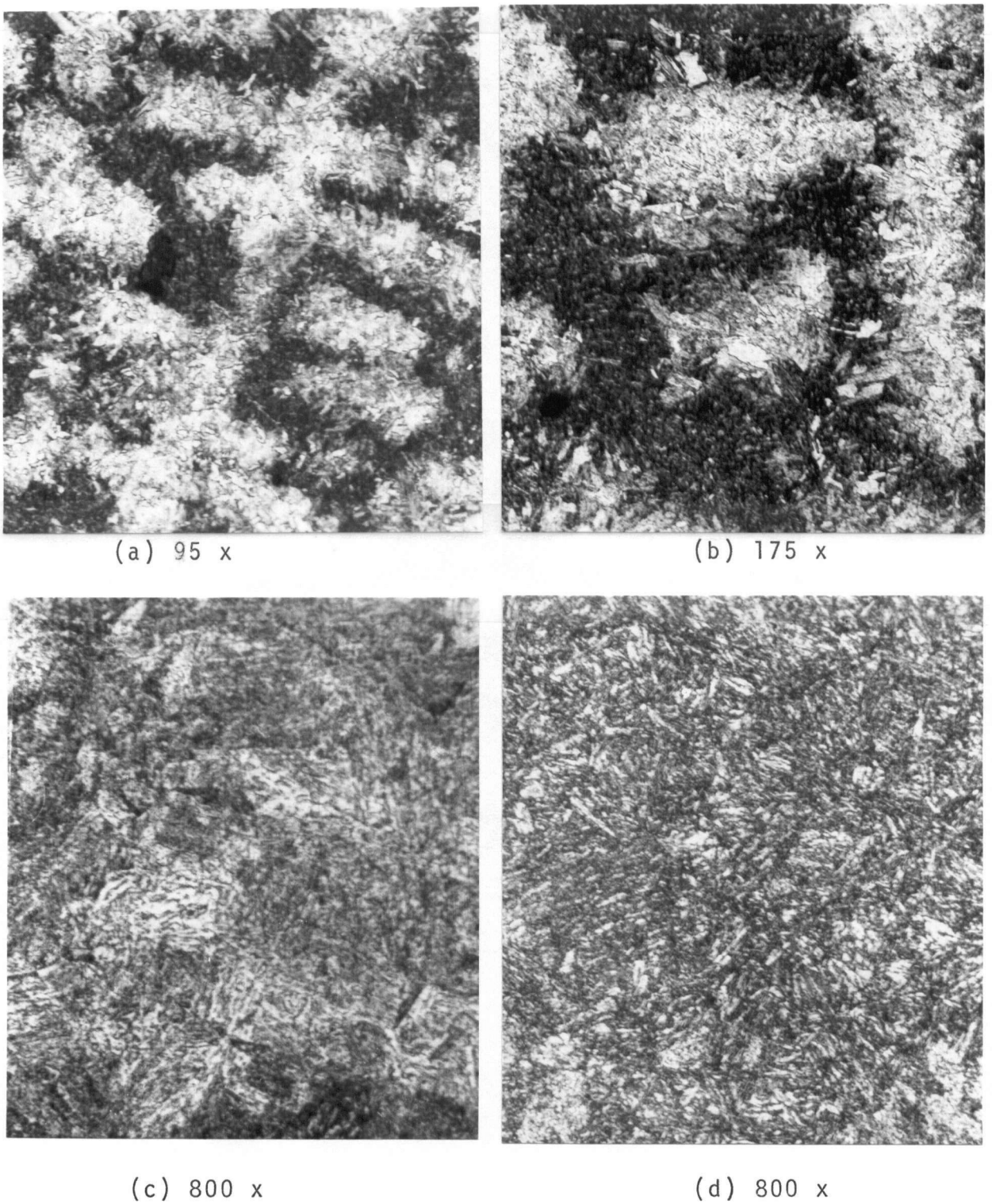

(a) 95 x

(b) 175 x

(c) 800 x

(d) 800 x

Figure 76. Microstructure of AISI 4340 ESC Valve No. 13 in heat-treated condition.
(b) - white areas - ferrite
- grey areas - bainite (shown in (c))
- black areas - Martensite (shown in (d))

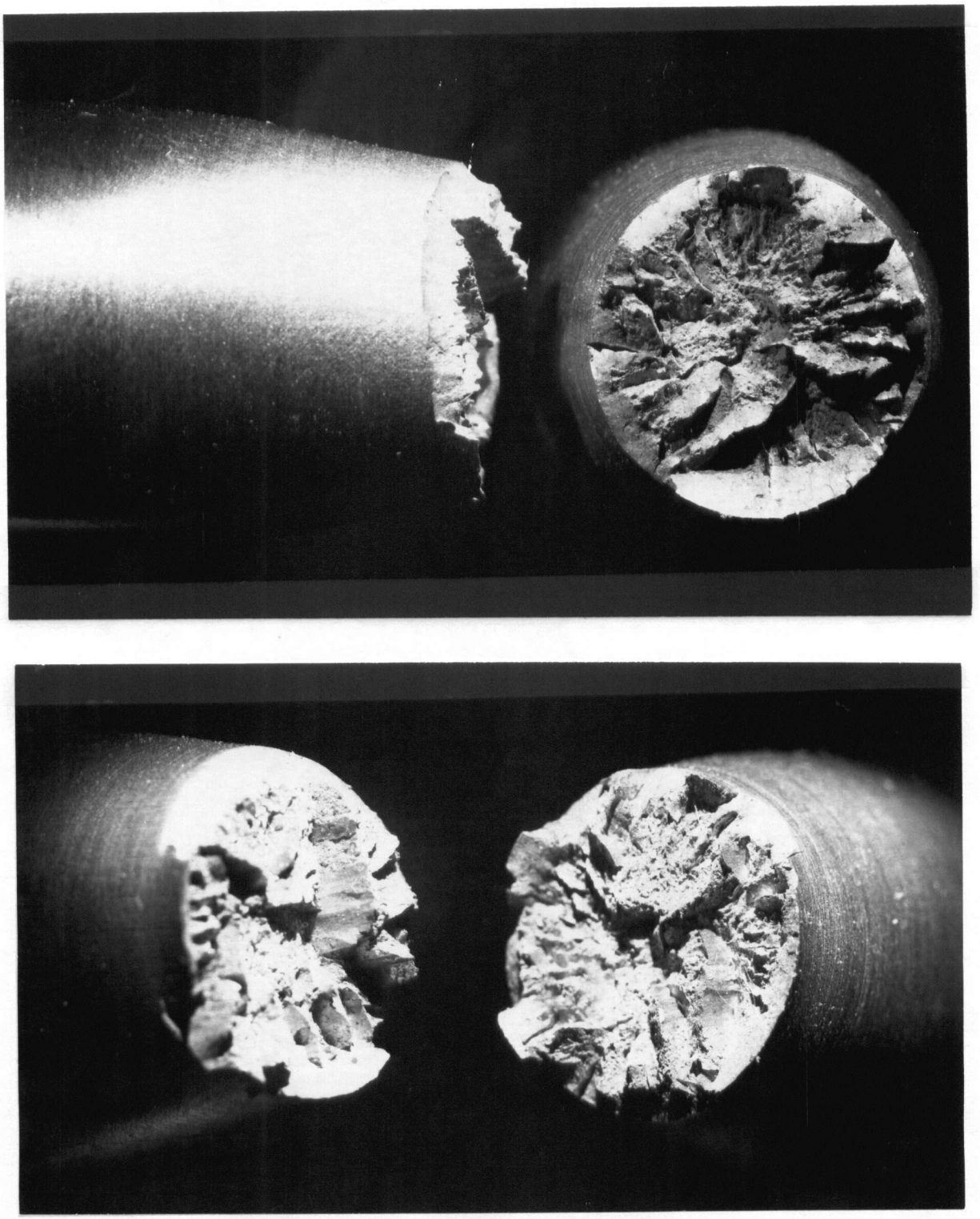

Figure 77. Fractographs of large tensile specimens of AISI 4340 from ESC Valve No. 8.

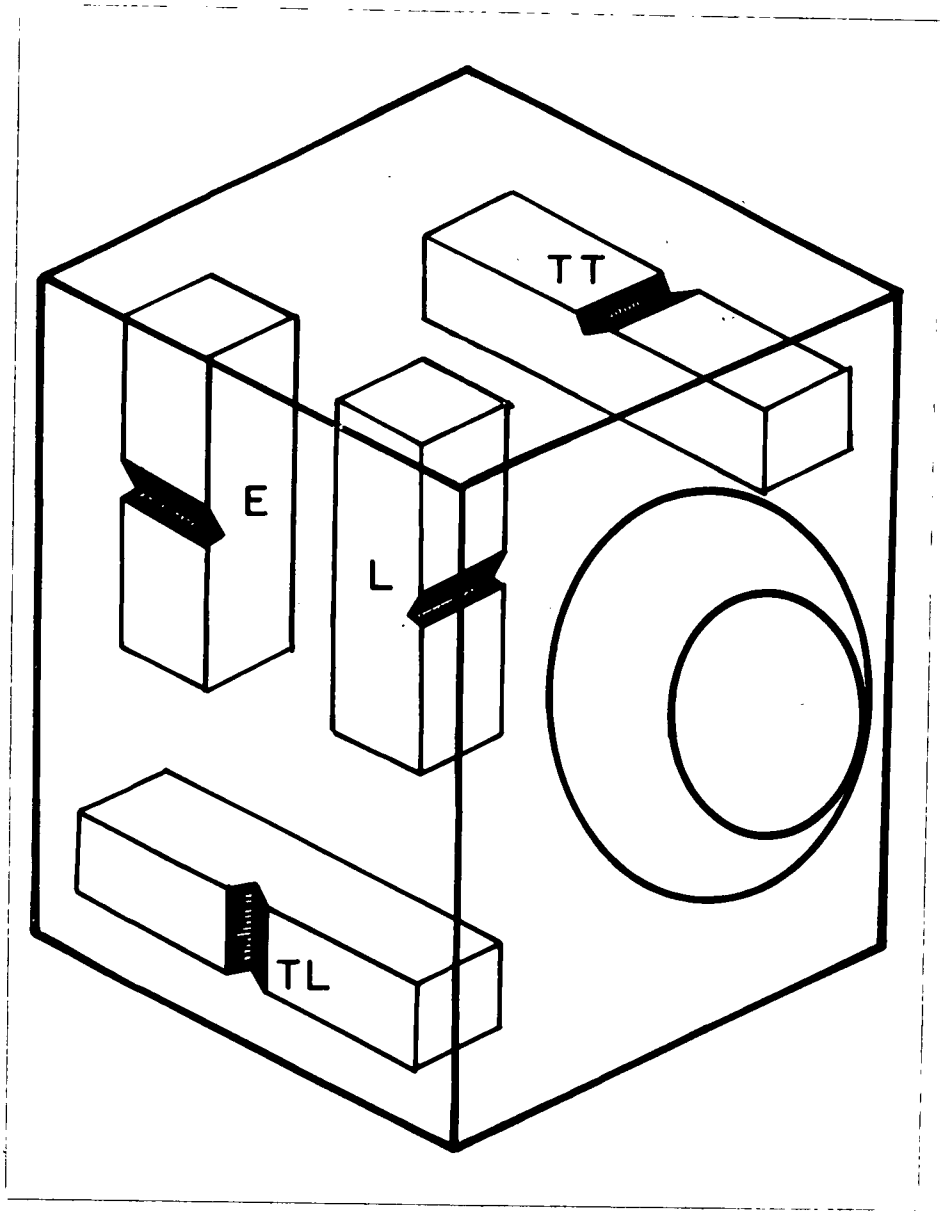

Figure 78. Orientation of the charpy specimens and the notch in Valve No. 8.

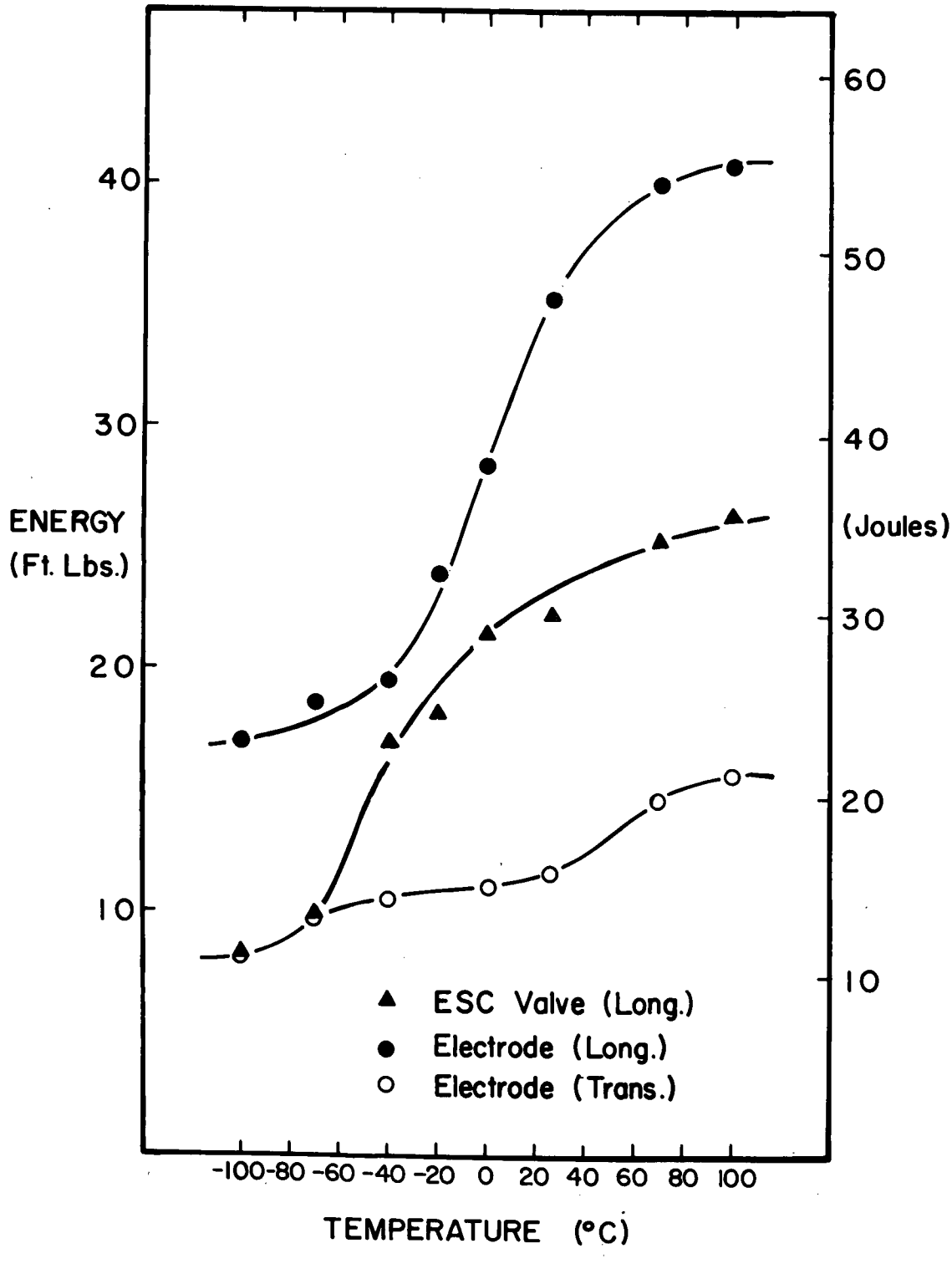

Figure 79. Ductile Brittle transition characteristics of Valve No. 3 and the electrode.
Heat Treatment: 1 hour at 845°C - oil quench.
Temper at 482°C to a hardness of 39 Rc.

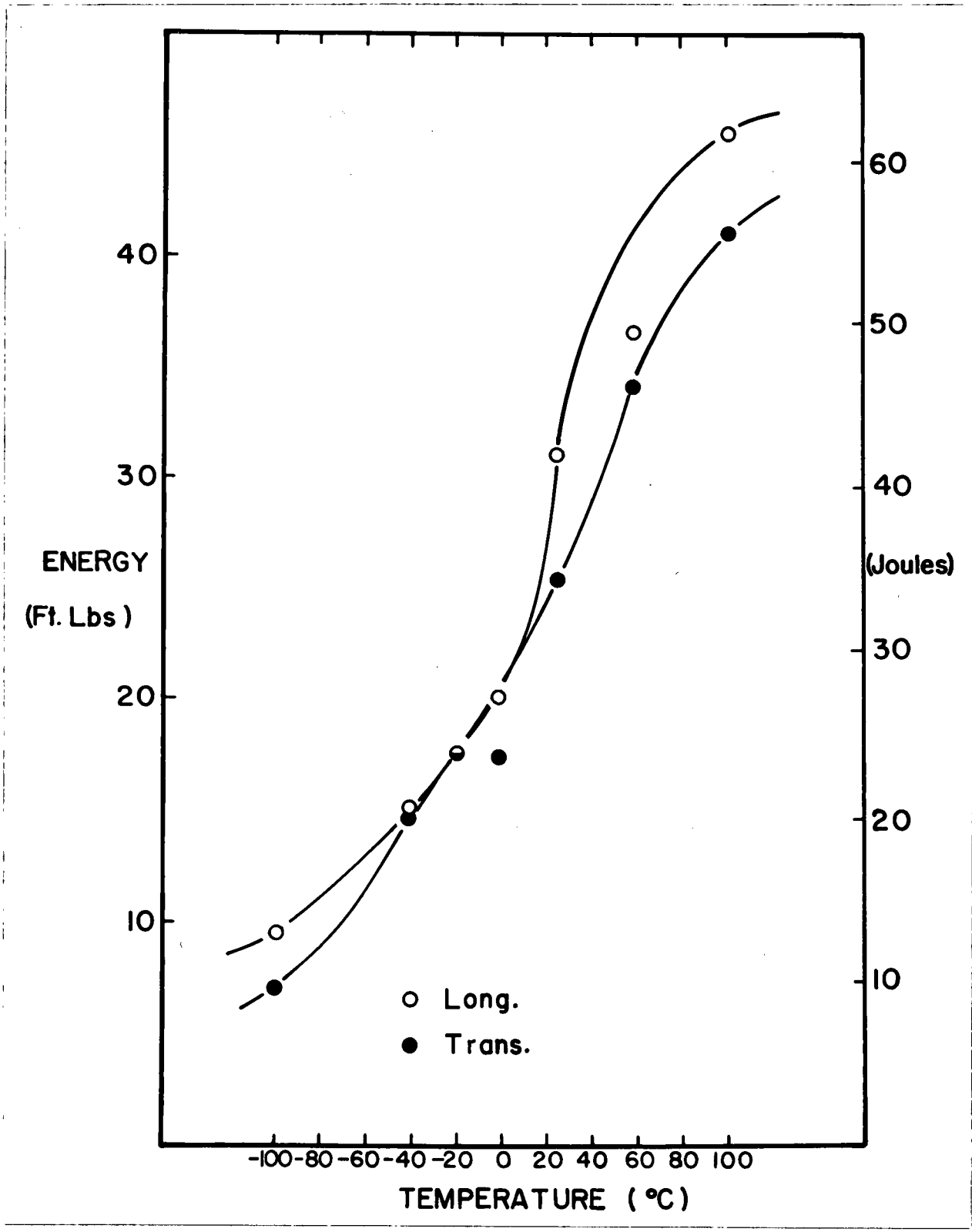

Figure 81. Ductile brittle transition characteristics of Valve No. 13.
Heat Treatment: 1 hour at 845°C - oil quench.
Temper at 560°C to a hardness of 35 Rc.

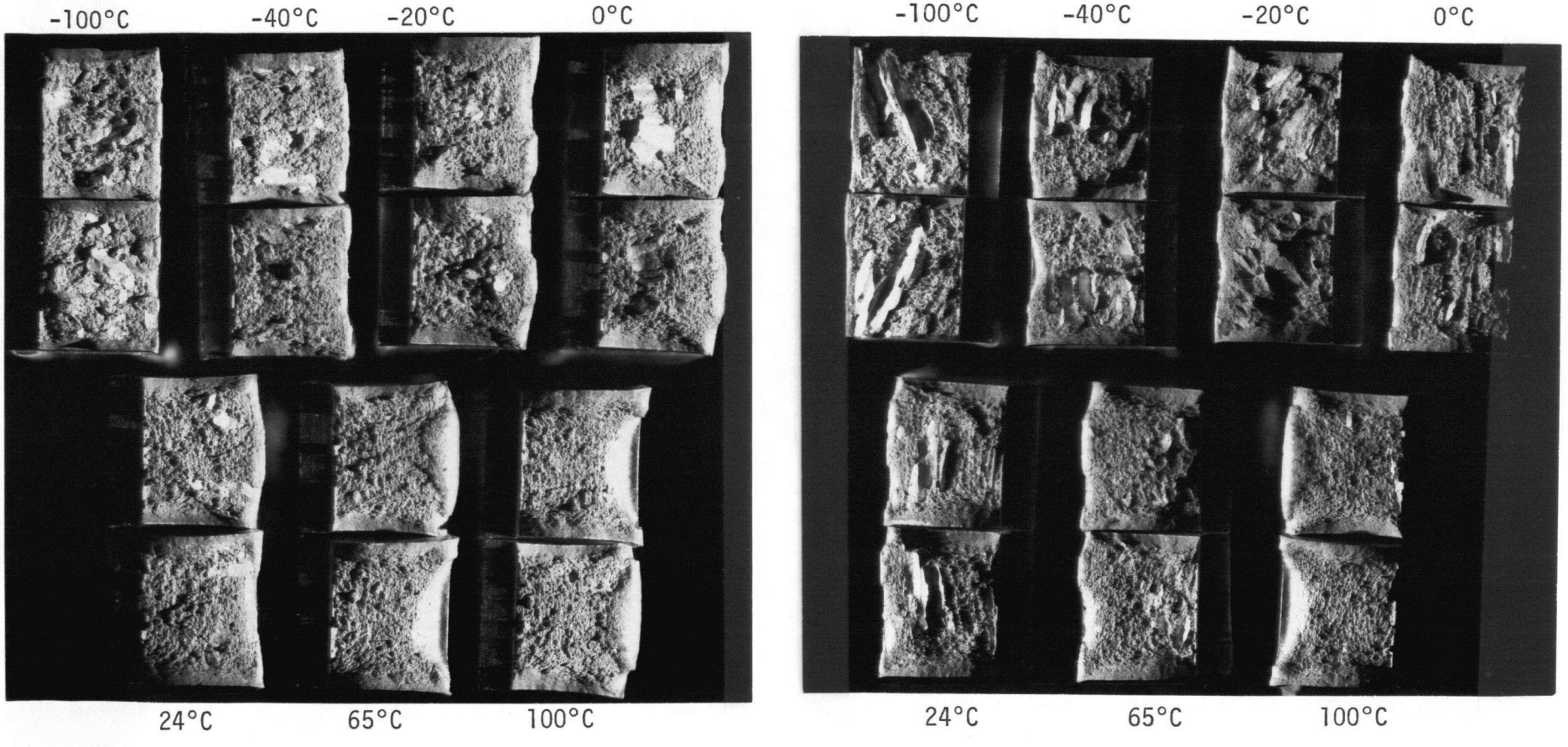

Figure 82. Optical fractographs of charpy specimens from Valve No. 8 tested at different temperatures and orientations.

a) - TT b) - TL

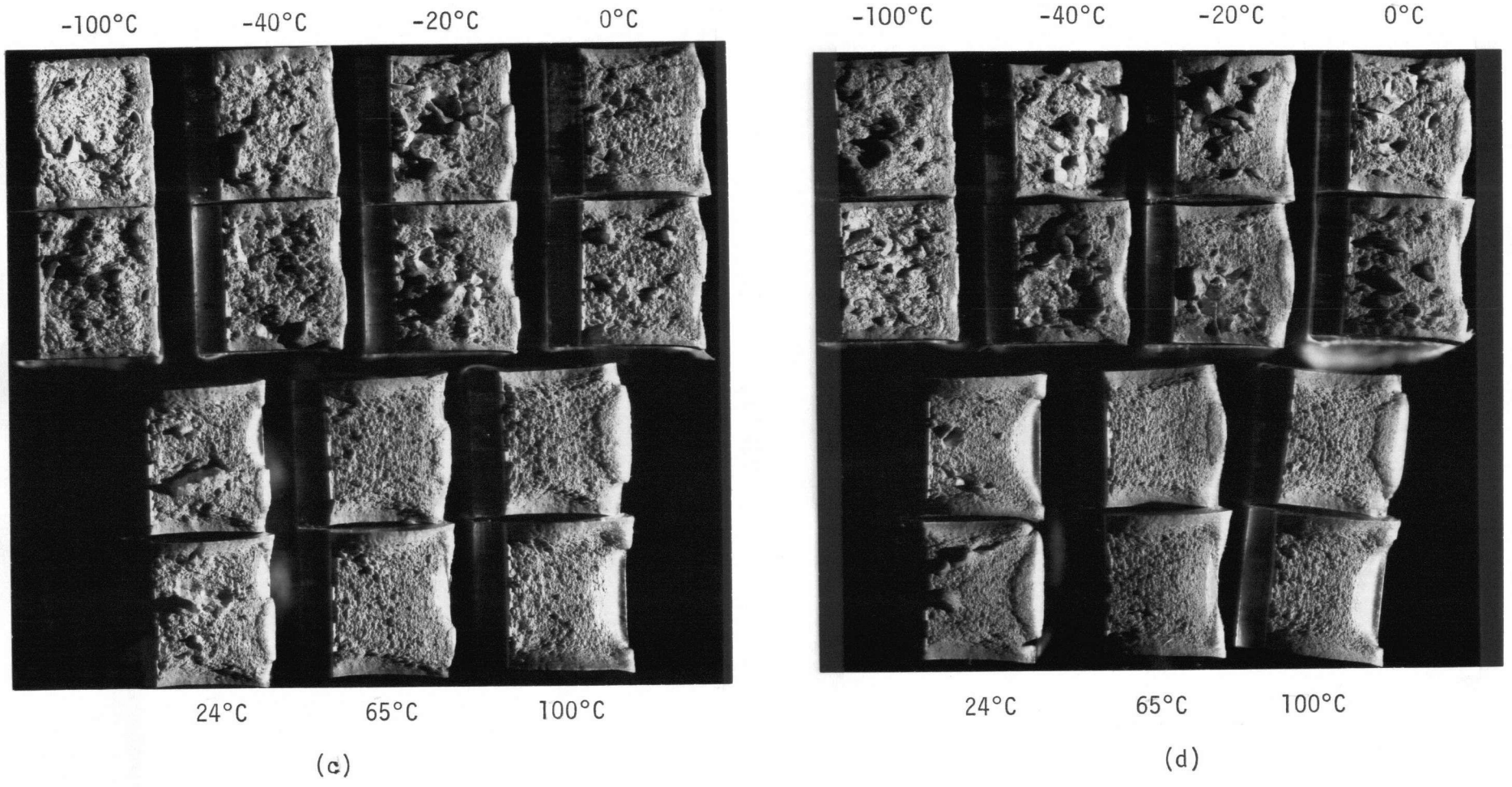

Figure 82. Optical fractographs of charpy specimens from Valve No. 8 tested at different temperatures and orientations.

c) - L d) - E

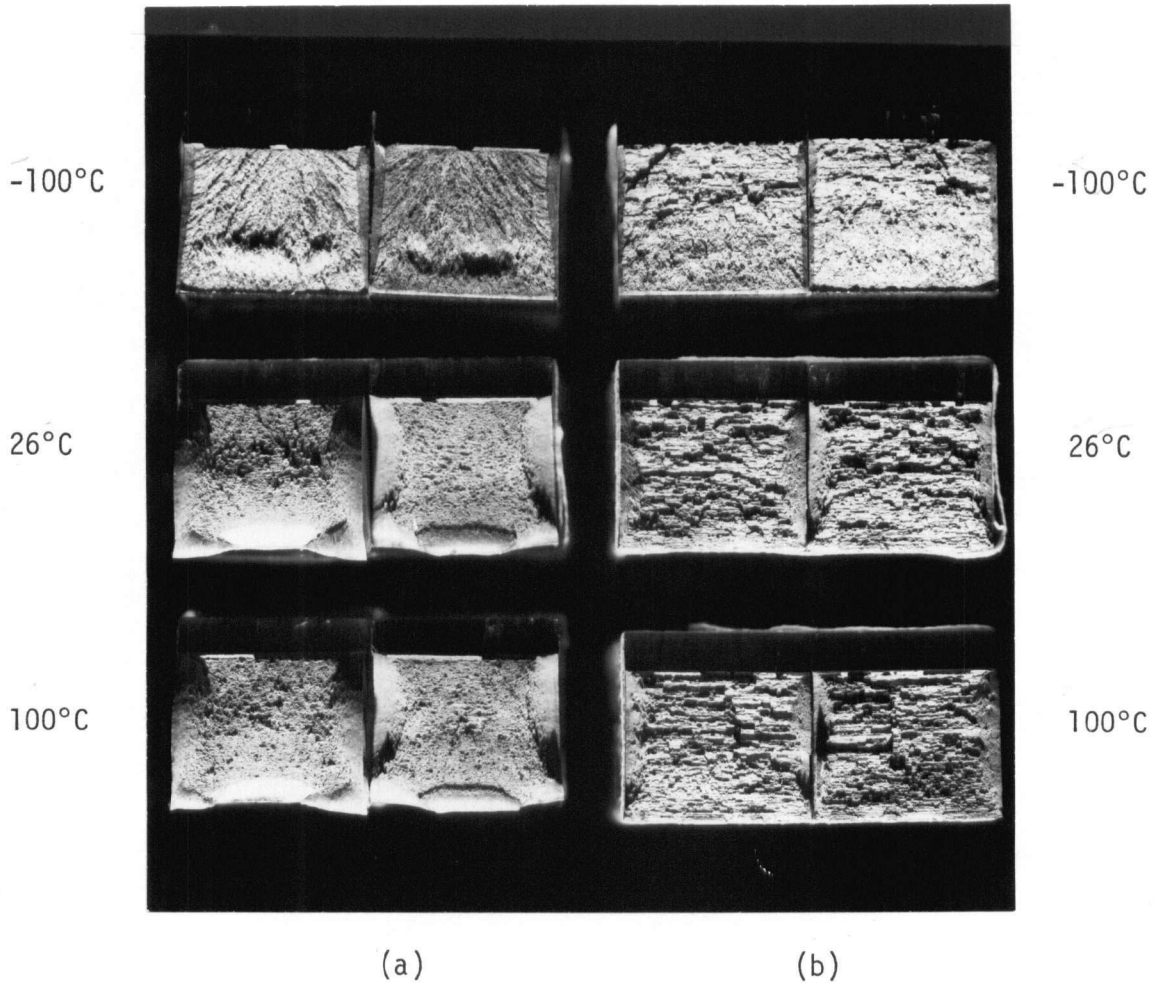

Figure 83. Optical fractographs of charpy specimens from the AISI 4340 electrode.
a) - Long. b) Trans.

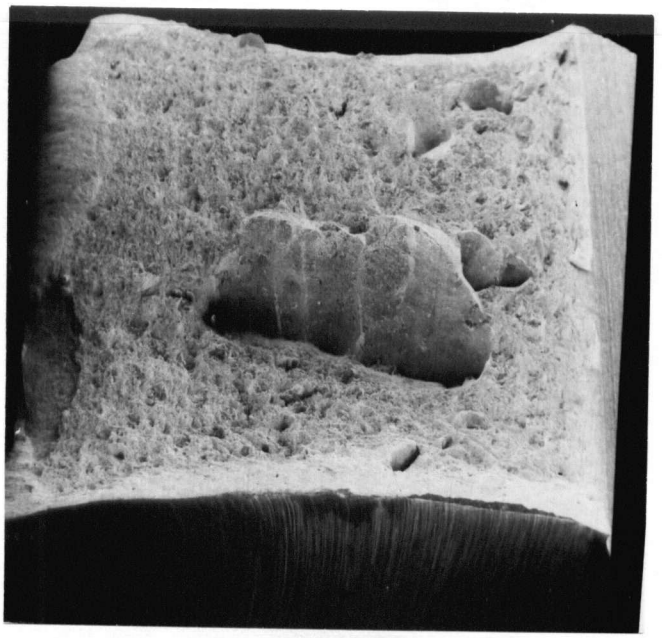

(a)

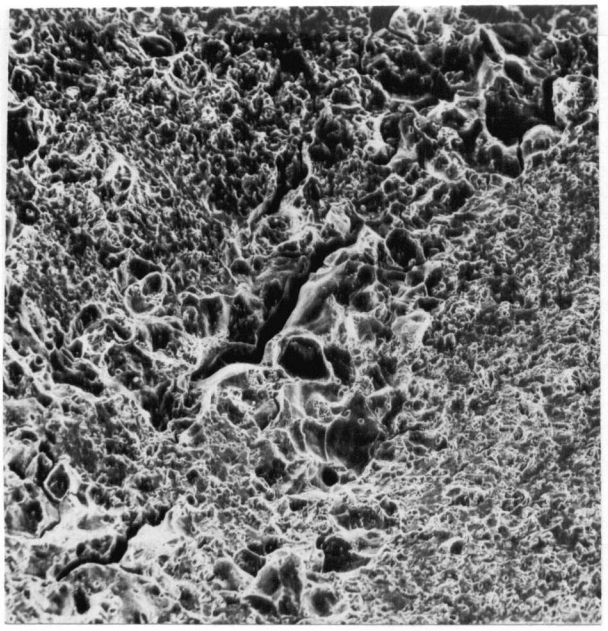

(b) 190 x

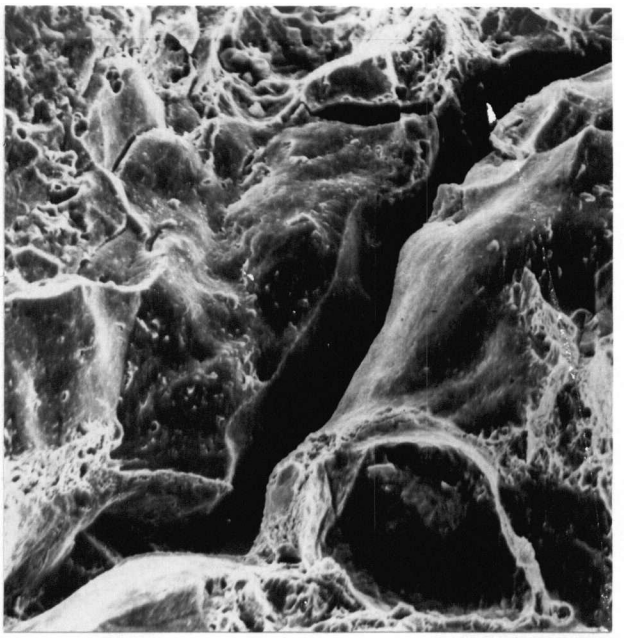

(b) 760x

Figure 84. SEM fractographs of charpy specimen
(a) ridge area
(b) micro-cracks.

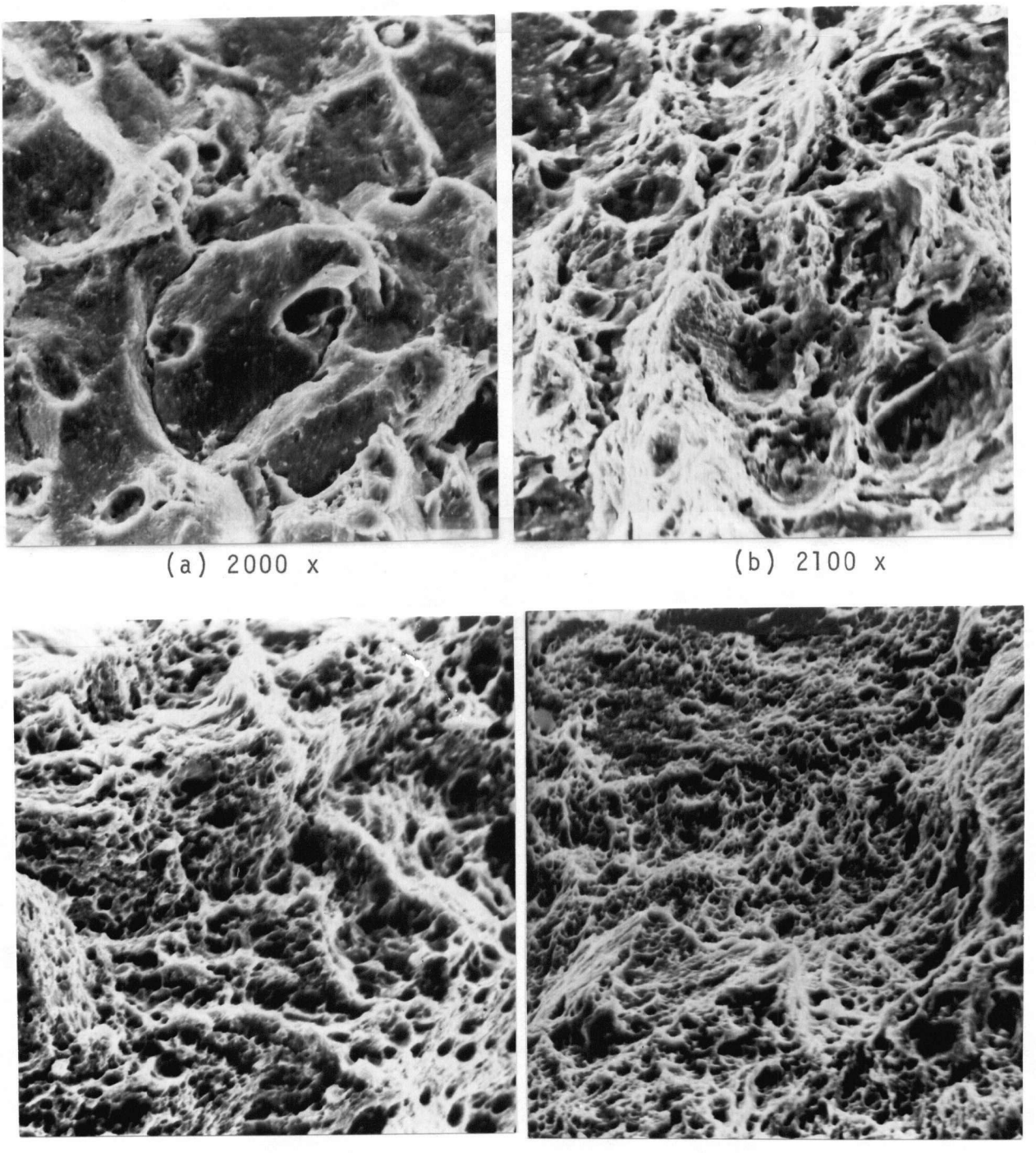

(a) 2000 x

(b) 2100 x

(c) 2100 x

(d) 2000 x

Figure 85. SEM fractographs of different regions of a charpy specimen.
(a) Area 1 (Ridge Area), 'Low Energy Fracture'.
(b) Area 2 (Base of the Ridge),'Intermediate Energy Fracture'.
(c) Area 3 (General Area), 'High Energy Fracture'.
(d) Area 4 (Shear Lip Area), 'High Energy Fracture'.

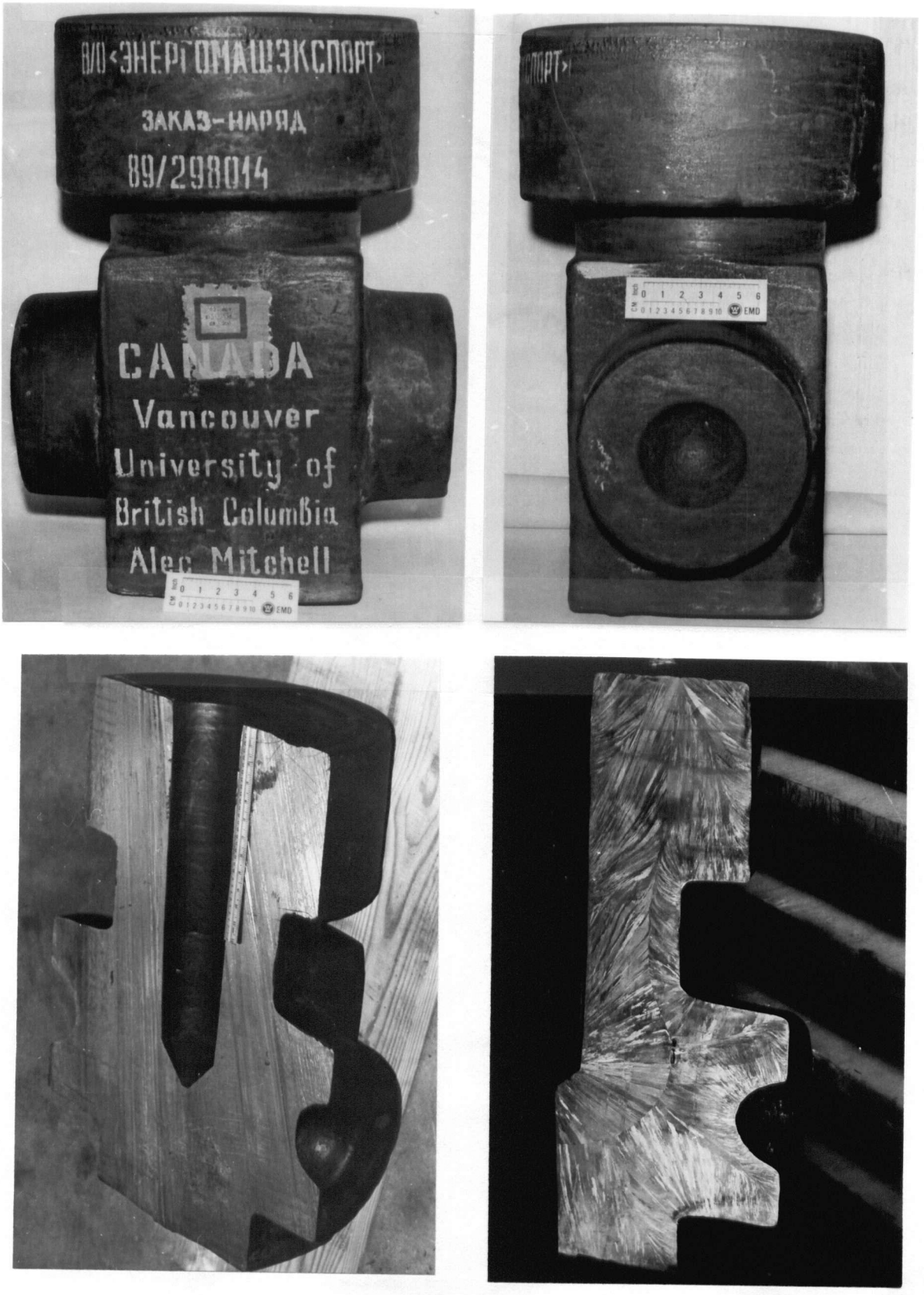

Figure 86. Soviet electroslag cast valve.

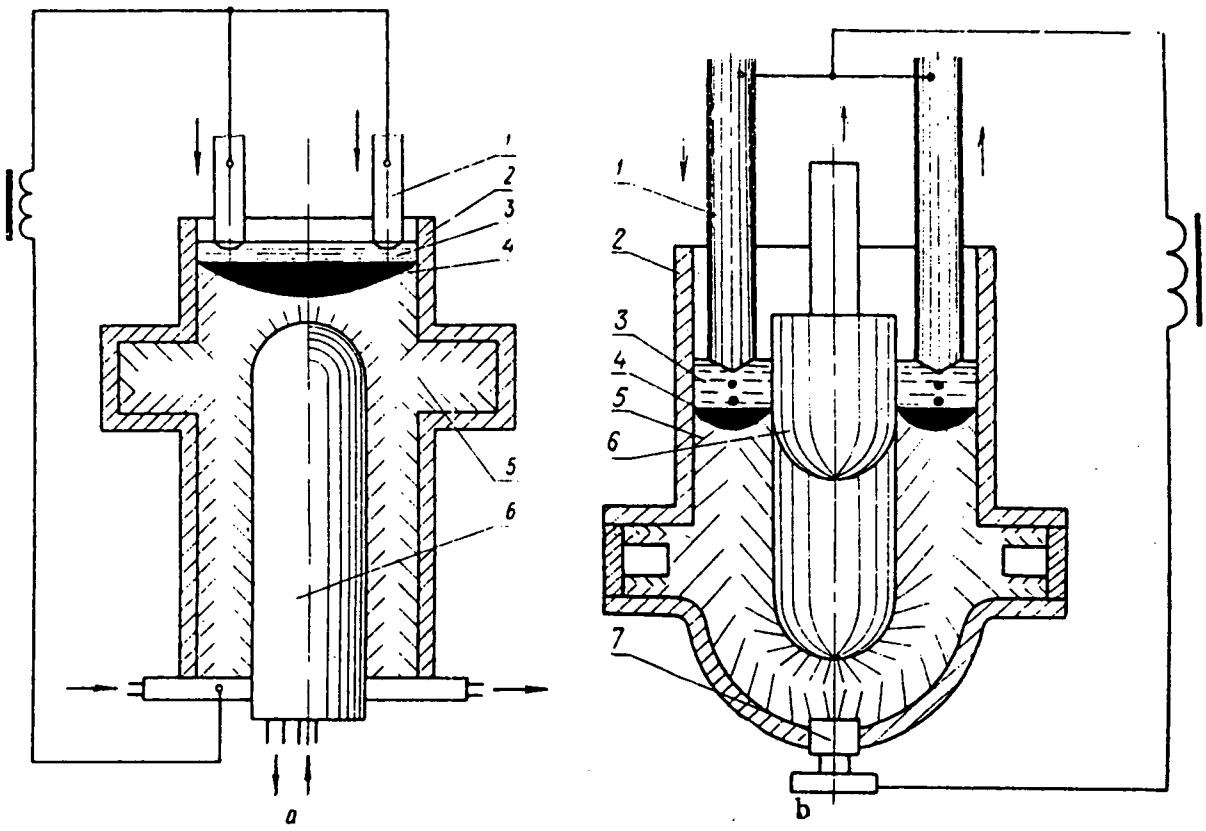

fixed (upside down) (a) and moving (b) core die

1-Consumable electrode; 2-Water-

cooled mold (crystallizer); 3-Slag bath; 4-Metal bath; 5-casting; 6-Die; 7-Seed charge.

Figure 87. Schematic of the methods used for making hollow ESC valves.[3]

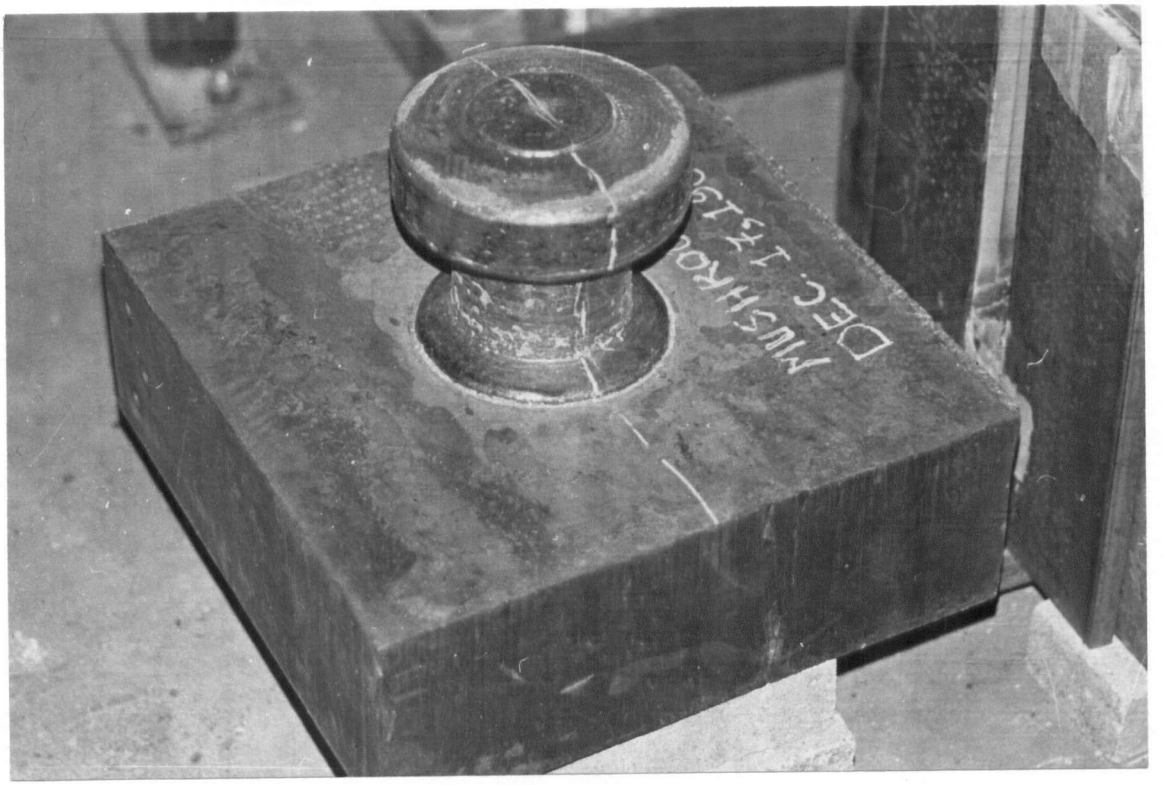

Figure 88. Electroslag casting of a flange for use in valve bodies.

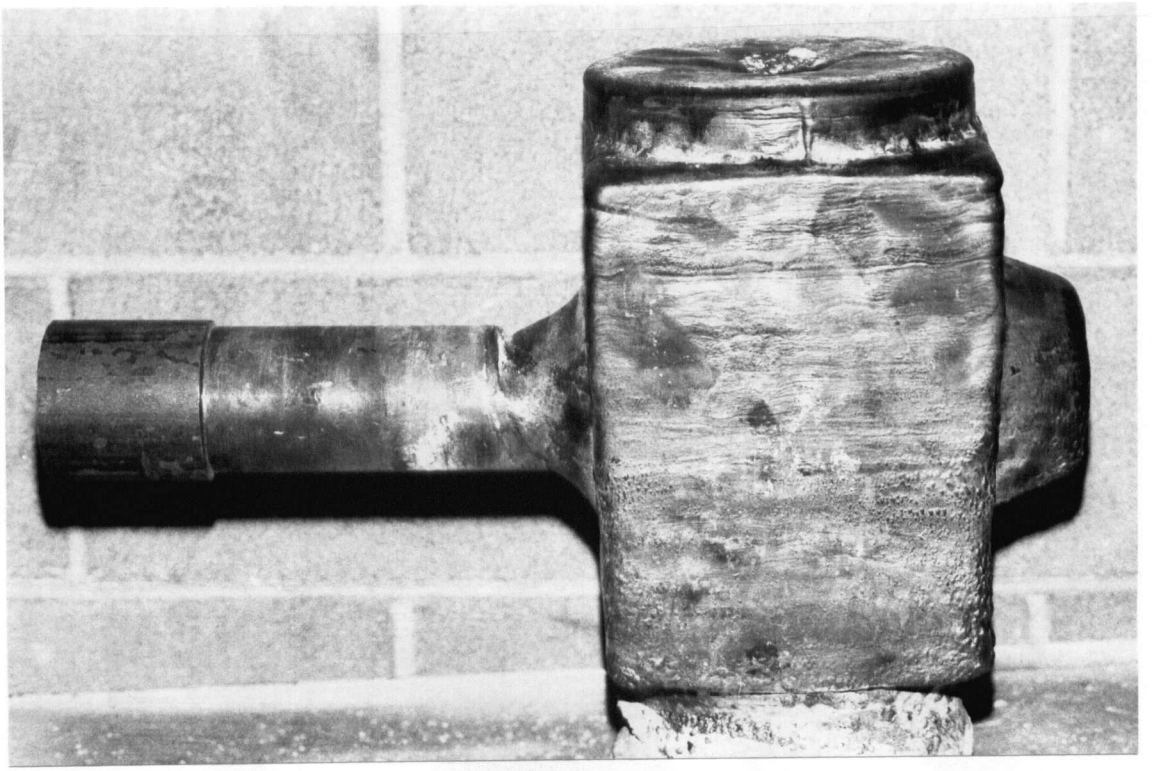

Figure 89. ESC valve with the welded insert.

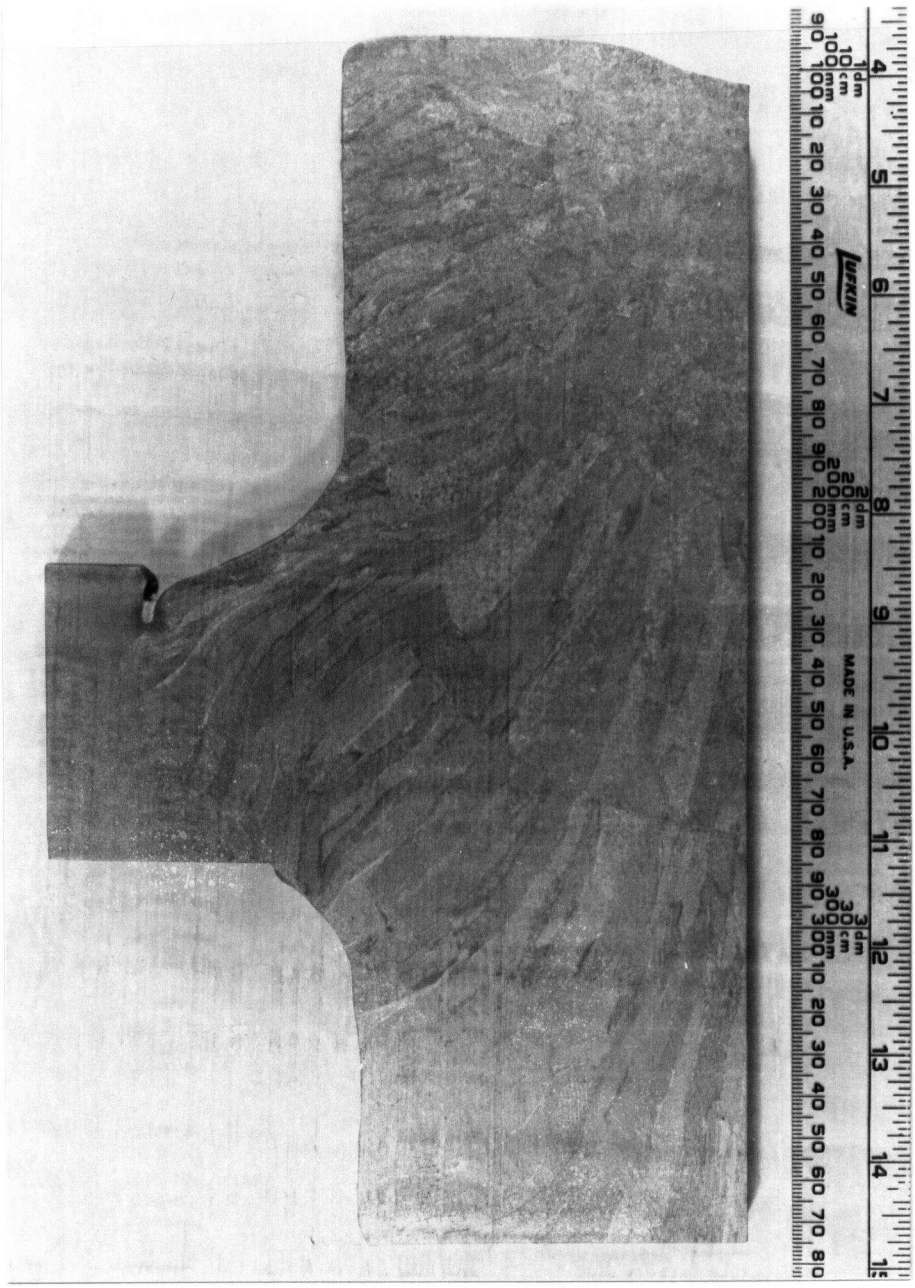

Figure 90. Macrostructure of the ESC valve with the welded insert.

DO NOT COPY LEAVES 197-212.

APPENDIX 1

ASME/ASTM SPECIFICATIONS

AMERICAN NATIONAL STANDARD ANSI/ASTM A 351 - 77

Used in USAEC-RDT Standards

Standard Specification for AUSTENITIC STEEL CASTINGS FOR HIGH-TEMPERATURE SERVICE[1]

This Standard is issued under the fixed designation A 351; the number immediately following the designation indicates the year of original adoption or, in the case of revision, the year of last revision. A number in parentheses indicates the year of last reapproval.

1. Scope

1.1 This specification[2] covers austenitic steel castings for valves, flanges, fittings, and other pressure-containing parts (Note 1) intended for high-temperature and corrosive service (Note 2).

NOTE 1—Carbon steel castings for pressure-containing parts are covered by Specification A 216, and low-alloy steel castings by Specification A 217.

NOTE 2—The committee formulating this specification has included 17 grades of materials extensively used for the present purpose. It is not the intent that this specification should be limited to these grades. Other compositions will be considered for inclusion by the committee as the need arises. Since these grades possess varying degrees of suitability for high-temperature and corrosion-resistant service, it is the responsibility of the purchaser to determine which grade shall be furnished; due consideration being given to the requirements of the applicable construction codes.

1.2 Eighteen grades of austenitic steel castings are included in this specification. Selection will depend on design and service conditions, mechanical properties, and the high-temperature and corrosion-resistant characteristics.

NOTE 3—The values stated in U.S. customary units are to be regarded as the standard.

2. Applicable Documents

2.1 *ASTM Standards:*

A 216 Specification for Carbon-Steel Castings Suitable for Fusion Welding for High-Temperature Service[3]

A 217 Specification for Martensitic Stainless Steel and Alloy Steel Castings for Pressure-Containing Parts Suitable for High-Temperature Service[3]

A 488 Recommended Practice for Qualification of Procedures and Personnel for the Welding of Steel Castings[4]

A 703 Specification for General Requirements Applicable to Steel Castings for Pressure-Containing Parts[3]

E 109 Dry Powder Magnetic Particle Inspection[5]

E 138 Wet Magnetic Particle Inspection[5]

E 165 Recommended Practice for Liquid Penetrant Inspection Method[5]

2.2 *Manufacturers Standardization Society of the Valve and Fittings Industry Standard:*

SP 55 Quality Standard for Steel Castings for Valves, Flanges and Fittings and Other Components (Visual Method)[6]

3. General Conditions for Delivery

3.1 Material furnished to this specification shall conform to the applicable requirements of Specification A 703, including the supplementary requirements that are indicated on the purchaser's order.

3.2 The post weld heat treatment requirements of Supplementary Requirement S11 may be specified when austenitic castings other than HK or HT are to be subjected to severe corrosive service.

---

[1] This specification is under the jurisdiction of ASTM Committee A-1 on Steel, Stainless Steel and Related Alloys and is the direct responsibility of Subcommittee A01.18 on Castings.

Current edition approved Oct. 28, 1977. Published December 1977. Originally published as A 351 - 52 T. Last previous edition A 351 - 76.

[2] For ASME Boiler and Pressure Vessel Code applications, see related Specification SA-351 in Section II of that code.

[3] *Annual Book of ASTM Standards*, Parts 1 and 2.

[4] *Annual Book of ASTM Standards*, Part 2.

[5] *Annual Book of ASTM Standards*, Part 11.

[6] Available from Manufacturers Standardization Society of the Valve and Fittings Industry, 1815 N. Fort Meyer Drive, Arlington, Va. 22209.

4. Ordering Information

4.1 The inquiry and order shall include or indicate the following:

4.1.1 A description of the casting by pattern number or drawing. Dimensional tolerances shall be included on the casting drawing.

4.1.2 Grade of steel.

4.1.3 Options in the specification.

4.1.4 The supplementary requirements desired including the standards of acceptance.

5. Process

5.1 Steel shall be made by the electric furnace process.

6. Heat Treatment

6.1 All castings shall receive a heat treatment proper to their design and chemical composition, except the HK and HT grades which shall be furnished in the as-cast condition.

6.2 Grade CD4MCu shall be heated to 2050°F (1120°C) for sufficient time to heat casting uniformly to temperature, furnace cooled to 1900°F (1040°C), held for a minimum of 15 min and quenched in water or rapidly cooled by other means so as to develop acceptable corrosion resistance.

6.3 The austenitic grades, except Grades HK and HT, shall be solution-treated by the manufacturer.

7. Chemical Requirements

7.1 The steel shall conform to the requirements as to chemical composition prescribed in Table 1.

8. Tensile Requirements

8.1 Steel used for the castings shall conform to the requirements as to tensile properties prescribed in Table 2.

9. Flanges

9.1 Flanged castings that have the flanges removed by machining to make welding end castings shall not be furnished under this specification.

10. Quality

10.1 The surface of the casting shall be examined visually and shall be free of adhering sand, scale, cracks, and hot tears. Other surface discontinuities shall meet the visual acceptance standards specified in the order. Visual Method SP 55 or other visual standards may be used to define acceptable surface discontinuities and finish. Unacceptable visual surface discontinuities shall be removed and their removal verified by visual examination of the resultant cavities.

10.2 When additional inspection is desired, Supplementary Requirements S5, S6, and S10 may be ordered.

10.3 The castings shall not be peened, plugged, or impregnated to stop leaks.

11. Repair by Welding

11.1 Repairs shall be made using procedures and welders qualified under Recommended Practice A 488.

11.2 Weld repairs shall be inspected to the same quality standards that are used to inspect the castings. When castings are produced with Supplementary Requirement S5 specified, weld repairs on castings that have leaked on hydrostatic test, or on castings in which the depth of any cavity prepared for repair welding exceeds 20 % of the wall thickness or 1 in. (25 mm), whichever is smaller, or on castings in which any cavity prepared for welding is greater than approximately 10 in.^{2} (65 cm^2), shall be radiographed to the same standards that are used to inspect the castings. When castings are produced with Supplementary Requirement S6 specified, weld repairs shall be inspected by liquid penetrant examination to the same standards that are used to inspect the castings.

NOTE 4—When austenitic steel castings are to be used in services where they will be subject to stress corrosion, the purchaser should so indicate in his order and such castings should be solution-heat treated following all weld repairs.

SUPPLEMENTARY REQUIREMENTS

The following supplementary requirements shall not apply unless specified in the purchase order. A list of standardized supplementary requirements for use at the option of the purchaser is included in Specification A 703. Those which are ordinarily considered suitable for use with this specification are given below. Others enumerated in A 703 may be used with this specification upon agreement between the manufacturer and purchaser.

S2. Destruction Tests.

S5. Radiographic Inspection.

S6. Liquid Penetrant Inspection.

S10. Examination of Weld Preparation.

S10.1 The method of performing the magnetic particle or liquid penetrant test shall be in accordance with Method E 109, Method E 138, or Recommended Practice E 165.

S11. Post Weld Heat Treatment.

S11.1 All austenitic castings, except Grades HK and HT, which have been subjected to weld repairs shall be given a post weld solution heat treatment.

TABLE 1 Chemical Requirements

Element, % (max, Except Where Range is Given)	CF3, CF3A	CF8, CF8A	CF3M, CF3MA	CF8M	CF8C	CH8	CH10	CH20	CK20	HK30	HK40	HT30	CF10MC	CN7M	CD4MCu
Carbon	0.03	0.08	0.03	0.08	0.08	0.08	0.10	0.20	0.20	0.25–0.35	0.35–0.45	0.25–0.35	0.10	0.07	0.04
Manganese	1.50	1.50	1.50	1.50	1.50	1.50	1.50	1.50	1.50	1.50	1.50	2.00	1.50	1.50	1.00
Silicon	2.00	2.00	1.50	1.50	2.00	1.50	2.00	2.00	1.75	1.75	1.75	2.50	1.50	1.50	1.00
Sulfur	0.040	0.040	0.040	0.040	0.040	0.040	0.040	0.040	0.040	0.040	0.040	0.040	0.040	0.040	0.04
Phosphorus	0.040	0.040	0.040	0.040	0.040	0.040	0.040	0.040	0.040	0.040	0.040	0.040	0.040	0.040	0.04
Chromium	17.0–21.0	18.0–21.0	17.0–21.0	18.0–21.0	18.0–21.0	22.0–26.0	22.0–26.0	22.0–26.0	23.0–27.0	23.0–27.0	23.0–27.0	13.0–17.0	15.0–18.0	19.0–22.0	24.5–26.5
Nickel	8.0–12.0	8.0–11.0	9.0–13.0	9.0–12.0	9.0–12.0	12.0–15.0	12.0–15.0	12.0–15.0	19.0–22.0	19.0–22.0	19.0–22.0	33.0–37.0	13.0–16.0	27.5–30.5	4.75–6.00
Molybdenum	...	...	2.0–3.0	2.0–3.0	...	...	...	...	...	...	...	0.50	1.75–2.25	2.0–3.0	1.75–2.25
Columbium	...	...	...	...	[A]	...	...	...	...	...	...	...	[B]	...	...
Copper	...	...	...	...	...	...	...	...	...	...	...	...	...	3.0–4.0	2.75–3.25

[A] Grade CF8C shall have a columbium content of not less than 8 times the carbon content but not over 100 %.
[B] Grade CF10MC shall have a columbium content of not less than 10 times the carbon content but not over 1.20 %.

TABLE 2 Tensile Requirements

	CF3	CF-3A[A]	CF8	CF-8A[A]	CF-3M	CF-3MA	CF-8M	CF8C	CH8	CH10	CH20	CK20	HK30	HK40	HT30	CF-10MC	CN7M	CD-4MCu
Tensile strength, min, ksi (MPa)	70 (485)	77 (530)	70 (485)	77 (530)	70 (485)	80 (550)	70 (485)	70 (485)	65 (450)	70 (485)	70 (485)	65 (450)	65 (450)	62 (425)	65 (450)	70 (485)	62 (425)	100 (690)
Yield strength,[B] min, ksi (MPa)	30 (205)	35 (240)	30 (205)	35 (240)	30 (205)	37 (255)	30 (205)	30 (205)	28 (195)	30 (205)	30 (205)	28 (195)	35 (240)	35 (240)	28 (195)	30 (205)	25 (170)	70 (485)
Elongation in 2 in. or 50 mm, min, %	35.0	35.0	35.0	35.0	30.0	30.0	30.0	30.0	30.0	30.0	30.0	30.0	10.0	10.0	15.0	20.0	35.0	16.0
Reduction of area, min, %	...	...	...	...	...	...	...	...	...	...	...	...	...	...	...	...	...	...

[A] The properties shown are obtained by adjusting the composition within the limits shown in Table 1 to obtain a ferrite-austenite ratio that will result in the higher ultimate and yield strengths indicated. Because of the thermal instability of Grades CF3A, CF3MA, and CF8A, they are not recommended for service at temperatures in excess of 800°F (425°C).
[B] Determine by either 0.2 % offset method or 0.5 % extension-under-load method.

AMERICAN NATIONAL STANDARD ANSI/ASTM A 182 - 77a

Endorsed by Manufacturers Standardization Society of the Valve and Fittings Industry
Used in USAEC-RDT standards

Standard Specification for FORGED OR ROLLED ALLOY-STEEL PIPE FLANGES, FORGED FITTINGS, AND VALVES AND PARTS FOR HIGH-TEMPERATURE SERVICE[1]

This Standard is issued under the fixed designation A 182; the number immediately following the designation indicates the year of original adoption or, in the case of revision, the year of last revision. A number in parentheses indicates the year of last reapproval.

1. Scope

1.1 This specification covers forged low alloy and stainless steel piping components for use in pressure systems. Included are flanges, fittings, valves, and similar parts to specified dimensions or to dimensional standards such as the ANSI specifications that are referenced in Section 2.

1.2 Other forgings for other applications may be made to this specification.

1.3 Thirty-three grades are covered including sixteen ferritic or martensitic steels and seventeen austenitic stainless steels. Selection will depend upon design and service requirements.

1.4 Supplementary requirements are provided for use when additional testing or inspection is desired. These shall apply only when specified individually by the purchaser in the order.

NOTE 1—The values stated in U.S. customary units are to be regarded as the standard.

2. Applicable Documents

2.1 *ASTM Standards:*

A 234 Specification for Piping Fittings of Wrought Carbon Steel and Alloy Steel for Moderate and Elevated Temperatures[2]

A 275 Magnetic Particle Examination of Steel Forgings[3]

A 370 Mechanical Testing of Steel Products[4]

A 509 Definition of a Steel Forging[3]

E 30 Chemical Analysis of Steel, Cast Iron, Open-Hearth Iron, and Wrought Iron[5]

E 165 Recommended Practice for Liquid Penetrant Inspection Method[6]

E 353 Chemical Analysis of Stainless, Heat-Resisting, Maraging, and Other Similar, Chromium-Nickel-Iron Alloys[5]

E 381 Rating Macroetched Steel[3,6]

2.2 *Manufacturers' Standardization Society of the Valve and Fittings Industry Standard:*[7]

SP 25 Standard Marking System for Valves, Fittings, Flanges and Unions.

2.3 *ASME Boiler and Pressure Vessel Code:*[8]

Section IX Welding Qualifications

SFA-5.4 Specification for Corrosion-Resisting Chromium and Chromium-Nickel Steel Covered Welding Electrodes

SFA-5.5 Specification for Low-Alloy Steel Covered Arc-Welding Electrodes

2.4 *American National Standards Institute Standards:*[9]

B16.5 Dimensional Standards for Steel Pipe Flanges and Flanged Fittings

---

[1] This specification is under the jurisdiction of ASTM Committee A-1 on Steel, Stainless Steel and Related Alloys, and is the direct responsibility of Subcommittee A01.22 on Valves and Fittings.

Current edition approved Oct. 28, 1977. Published December 1977. Originally published as A 182 - 35 T. Last previous edition A 182 - 77.

[2] *Annual Book of ASTM Standards*, Part 1.

[3] *Annual Book of ASTM Standards*, Part 5.

[4] *Annual Book of ASTM Standards*, Parts 1, 2, 3, 4, 5, and 10.

[5] *Annual Book of ASTM Standards*, Part 12.

[6] *Annual Book of ASTM Standards*, Part 11.

[7] Available from Manufacturers' Standardization Society of the Valve and Fittings Industry, 1815 N. Fort Myer Drive, Arlington, Va. 22209.

[8] Available from American Society of Mechanical Engineers, 345 E. 47th St., New York, N.Y. 10017.

[9] Available from American National Standards Institute, 1430 Broadway, New York, N. Y. 10018.

B16.11 Forged Steel Fittings, Socket Weld, and Threaded
B16.10 Face-to-Face and End-to-End Dimensions of Ferrous Valves

3. Basis of Purchase

3.1 Orders for material under this specification shall include the following information, as necessary, to describe adequately the desired material:

3.1.1 Name of forging,

3.1.2 ASTM specification number including grade,

3.1.3 Size and pressure class or geometry,

3.1.4 Quantity,

3.1.5 Test report if required, and

3.1.6 Supplementary requirements, if any.

4. Manufacture

4.1 The low-alloy ferritic steels may be made by the open-hearth, electric-furnace, or basic-oxygen process. The basic-oxygen process shall be limited to steels containing less than 2 % chromium.

4.2 The stainless steels shall be melted by one of the following processes: (*a*) electric-furnace (with separate degassing and refining optional); (*b*) vacuum-furnace; or (*c*) one of the former followed by vacuum or electroslag-consumable remelting. Grade XM-27 may be produced by electron-beam melting.

4.3 A sufficient discard shall be made to secure freedom from injurious piping and undue segregation.

4.4 The material shall be forged as close as practicable to the specified shape and size. Forged or rolled bar may be used without additional hot working for small cylindrically shaped parts within the limits defined by Specification A 234.

4.5 The finished product shall be a forging as defined by Definition A 509.

5. Heat Treatment

5.1 The ferritic grades and the martensitic grade shall be annealed, or normalized and tempered, except as permitted in 5.2. If furnished in the normalized and tempered condition, the tempering temperature for Grades F 1, F 2, F 11 and F 12 shall be not less than 1150°F (620°C). The minimum tempering temperature for Grades F 5, F 5a, F 6a Class 2, F 7, F 9, F 21, and F 22 shall be 1250°F (667°C). Grade F 6a Class 1 shall be tempered at not less than 1325°F (717°C); Grade F 6a Class 3 at not less than 1100°F (593°C); and F 6a Class 4 at not less than 1000°F (538°C).

5.1.1 Grade F 6a (martensitic) Classes 1 and 2 need be tempered only, provided the tempering temperature for Class 1 is not less than 1325°F (667°C) and for Class 2, not less than 1250°F (667°C).

5.1.2 Grade F 6NM shall be furnished in the normalized and tempered condition; the tempering temperature shall be not less than 1040°F (560°C) nor greater than 1120°F (600°C).

5.2 Liquid quenching followed by tempering shall be permitted when agreed to by the purchaser. The same minimum tempering temperature as specified in 5.1 shall be required for each grade. Parts that are liquid quenched and tempered shall be marked "QT" and shall be inspected for quench cracks by the magnetic particle method in accordance with Method A 275.

5.3 All austenitic material shall be furnished in the heat-treated condition. The heat treatment shall consist of heating the material to a minimum temperature of 1900°F (1040°C) and quenching in water or rapidly cooling by other means, except for grades F 321H, F 347H, and F 348H, which shall be solution treated at 1925°F (1050°C) min.

5.4 Heat treatment may be performed before machining.

6. Chemical Requirements

6.1 The steel shall conform to the requirements as to chemical composition for the grade ordered as listed in Table 1. For referee purposes, Methods E 30 or E 353 shall be used.

6.2 Grades to which lead, selenium, or other elements are added for the purpose of rendering the material free-machining shall not be used.

7. Cast or Heat (formerly Ladle) Analysis

7.1 An analysis of each heat of steel shall be made from samples taken preferably during the pouring of the heat and the results shall conform to Table 1.

8. Product Analysis

8.1 The purchaser may make a product

analysis on forgings supplied to this specification. Samples for analysis shall be taken from midway between the center and surface of solid forgings, midway between the inner and outer surfaces of hollow forgings, midway between the center and surface of full-size prolongations, or from broken mechanical test specimens. The chemical composition thus determined shall conform to Table 1 with the tolerances as stated in Table 2 or 3.

9. Mechanical Requirements

9.1 The material shall conform to the requirements as to mechanical properties for the grade ordered as listed in Table 4.

9.2 Mechanical test specimens shall be obtained from production forgings after heat treatment, or from separately forged test blanks prepared from the stock used to make the finished product. Such test blanks shall receive approximately the same working as the finished product. The test blanks shall be heat-treated with the finished product and shall approximate the maximum cross section of the forgings they represent.

9.3 For normalized and tempered, or quenched and tempered forgings, the central axis of the specimen shall correspond to the $^1/_4$ t plane or deeper position in the thickest section, t, of the represented forgings and the gage length shall be at least t distance from a second heat-treated surface. When section thickness or geometry interferes, the specimen shall be positioned as near as possible to the prescribed location.

9.4 For annealed ferritic and martensitic grades and also for austenitic stainless steels, the test specimen may be taken from any convenient location.

9.5 *Tension Tests:*

9.5.1 *Ferritic and Martensitic Grades*—One tension test shall be made for each heat in each heat treatment charge.

9.5.1.1 When the heat-treating cycles are the same and the furnaces (either batch or continuous type) are controlled within ± 25°F (± 14°C) and equipped with recording pyrometers so that complete records of heat treatment are available, then only one tension test from each heat of each forging type (Note 2) and section size is required instead of one test from each heat in each heat-treatment charge.

9.5.2 *Austenitic Stainless Steel Grades*—One tension test shall be made for each heat.

NOTE 2—"Type" in this case is used to describe the forging shape such as a flange, ell, tee, etc.

9.5.3 Testing shall be performed in accordance with Methods A 370 using the largest feasible of the round specimens. The gage length for measuring elongation shall be four times the diameter of the test section.

9.6 *Hardness Tests:*

9.6.1 Sufficient number of hardness measurements shall be made in accordance with Methods A 370 to assure that the forgings are within the hardness limits given for each grade in Table 4. The purchaser may verify that the requirement has been met by testing at any location on the forging provided such testing does not render the forging useless.

9.6.2 When the reduced number of tension tests permitted by 9.5.1.1 is applied, additional hardness tests shall be made on forgings or samples as defined in 9.2 scattered throughout the load (Note 3). At least eight samples shall be checked from each batch load and at least one check per hour shall be made from a continuous run. When the furnace batch is less than eight forgings, each forging shall be checked. If any check falls outside the prescribed limits, the entire lot of forgings shall be reheat treated and the requirements of 9.5.1 shall apply.

NOTE 3—The tension test required in 9.5.1 is used to determine material capability and conformance in addition to verifying the adequacy of the heat-treatment cycle. Additional hardness tests in accordance with 9.6.2 are required when 9.5.1.1 is applied to assure the prescribed heat-treating cycle and uniformity throughout the load.

10. Retreatment

10.1 If the results of the mechanical tests do not conform to the requirements specified, the manufacturer may reheat treat the forgings and repeat the tests specified in Section 9.

11. Finish

11.1 The forgings shall be free of scale, machining burrs which might hinder fit-up, and other injurious imperfections as defined herein. The forgings shall have a workmanlike finish and machined surfaces (other than surfaces having special requirements) shall have a surface finish not to exceed 250 AA

(arithmetic average) roughness height.

11.2 At the discretion of the inspector representing the purchaser, finished forgings shall be subject to rejection if surface imperfections acceptable under 11.4 are not scattered but appear over a large area in excess of what is considered to be a workmanlike finish.

11.3 *Depth of Injurious Imperfections*—Linear imperfections shall be explored for depth. When the depth encroaches on the minimum wall thickness of the finished forging, such imperfections shall be considered injurious.

11.4 *Machining or Grinding Imperfections Not Classified as Injurious*—Surface imperfections not classified as injurious shall be treated as follows:

11.4.1 Seams, laps, tears, or slivers not deeper than 5 % of the nominal wall thickness or 1/16 in. (1.6 mm), whichever is less, need not be removed. If these imperfections are removed, they shall be removed by machining or grinding.

11.4.2 Mechanical marks or abrasions and pits shall be acceptable without grinding or machining provided the depth does not exceed the limitations set forth in 11.4.1. Imperfections that are deeper than 1/16 in. (1.6 mm), but which do not encroach on the minimum wall thickness of the forging shall be removed by grinding to sound metal.

11.4.3 When imperfections have been removed by grinding or machining, the outside dimension at the point of grinding or machining may be reduced by the amount removed. Should it be impracticable to secure a direct measurement, the wall thickness at the point of grinding, or at an imperfection not required to be removed, shall be determined by deducting the amount removed by grinding from the nominal finished wall thickness of the forging, and the remainder shall be not less than the minimum specified or required wall thickness.

12. Repair by Welding

12.1 Weld repairs shall be permitted (see Supplementary Requirement S7) at the discretion of the manufacturer with the following limitations and requirements:

12.1.1 The welding procedure and welders shall be qualified in accordance with Section IX of the ASME Boiler and Pressure Vessel Code.

12.1.2 The weld metal shall be deposited using the electrodes specified in Table 5. The electrodes shall be purchased in accordance with ASME Specifications SFA-5.4 or SFA-5.5.

12.1.3 Defects shall be completely removed prior to welding by chipping or grinding to sound metal as verified by magnetic particle inspection in accordance with Method A 275 for the ferritic or martensitic grades, or by liquid penetrant inspection in accordance with Recommended Practice E 165 for ferritic, martensitic, or austenitic grades.

12.1.4 After repair welding, the welded area shall be ground smooth to the original contour and shall be completely free of defects as verified by magnetic-particle or liquid-penetrant inspection, as applicable.

12.1.5 The preheat, interpass temperature, and post-weld heat treatment requirements given in Table 5 shall be met.

12.1.6 Repair by welding shall not exceed 10 % of the surface area of the forging nor 33 1/2 % of the wall thickness of the finished forging or 3/8 in. (9.5 mm), whichever is less, without prior approval of the purchaser.

12.1.7 When approval of the purchaser is obtained, the limitations set forth in 12.1.6 may be exceeded, but all other requirements of Section 12 shall apply.

13. Marking

13.1 Identification marks consisting of the manufacturer's symbol or name, designation of service rating, the specification number, the designation, F 1, F 2, etc., showing the grade of material, and the size shall be legibly stamped on each forging or the forgings may be marked in accordance with Standard SP 25 of the Manufacturers' Standardization Society of the Valve and Fittings Industry, and in such position so as not to injure the usefulness of the forging.

13.1.1 Quenched and tempered ferritic or martensitic forgings shall be stamped with the letters QT following the ASTM designation.

13.1.2 Forgings repaired by welding shall be marked with the letter "W" following the ASTM designation.

13.1.3 When test reports are required, the

markings shall consist of the manufacturer's symbol or name, the grade symbol, and such other markings as necessary to identify the part with the test report (13.1.1 and 13.1.2 shall apply).

14. Inspection

14.1 The manufacturer shall afford the purchaser's inspector all reasonable facilities necessary to satisfy him that the material is being furnished in accordance with the purchase order. Inspection by the purchaser shall not interfere unnecessarily with the manufacturer's operations. All tests and inspections shall be made at the place of manufacture unless otherwise agreed upon.

15. Certification

15.1 For forgings made to specified dimensions, when agreed upon by the purchaser, and for forgings made to dimensional standards, the application of identification marks as required in 13.1 shall be the certification that the forgings have been furnished in accordance with the requirements of this specification.

15.2 Test reports, when required, shall include certification that all requirements of this specification have been met, the results of all required tests, and the type of heat treatment.

16. Rejection

16.1 Each forging that develops injurious defects during shop working operations or in service shall be rejected and the manufacturer notified.

17. Rehearing

17.1 Samples representing material rejected by the purchaser shall be preserved until disposition of the claim has been agreed upon by the manufacturer and the purchaser.

SUPPLEMENTARY REQUIREMENTS

The following supplementary requirements shall apply only when specified by the purchaser in the inquiry, contract, and order.

S1. Macroetch Test

S1.1 A sample forging shall be sectioned and etched to show flow lines and internal imperfections. The test shall be conducted according to Method E 381. Details of the test shall be agreed upon between the manufacturer and the purchaser.

S2. Product Analysis

S2.1 A product analysis in accordance with Section 8 shall be made from one randomly selected forging representing each size and type (Note 2) of forging on the order. If the analysis fails to comply, each forging shall be checked or the lot rejected. All results shall be reported to the purchaser.

S3. Heat Identification and Tension Tests

S3.1 In addition to the requirements of Section 9, the heat identification shall be marked on each forging and one tensile specimen shall be obtained from a representative forging from each heat at a location agreed upon between the manufacturer and the purchaser. The results of the test shall comply with Table 4 and shall be reported to the purchaser.

S4. Magnetic Particle Examination

S4.1 All accessible surfaces of the finished forging shall be examined by a magnetic-particle method. The method shall be in accordance with Method A 275. Acceptance limits shall be as agreed upon between the manufacturer and purchaser.

S5. Liquid Penetrant Examination

S5.1 All accessible surfaces shall be examined by a liquid penetrant method in accordance with Recommended Practice E 165. Acceptance limits shall be as agreed upon between the manufacturer and the purchaser.

S6. Hydrostatic Testing

S6.1 A hydrostatic test at a pressure agreed upon between the manufacturer and the purchaser shall be applied by the manufacturer.

S7. Repair Welding

S7.1 No repair welding shall be permitted without prior approval of the purchaser. If permitted, the restrictions of Section 12 shall apply.

S8. Heat Treatment Details

S8.1 The manufacturer shall furnish a detailed test report containing the information required in 15.2 and shall include all pertinent details of the heat-treating cycle given the forgings.

TABLE 1 Chemical Requirements

Identification Symbol	Grade	Composition, %								Columbium plus Tantalum	Tantalum, max	Titanium
		Carbon	Manganese	Phosphorus, max	Sulfur, max	Silicon	Nickel	Chromium	Molybdenum			
Ferritic Steels												
F 1	carbon-molybdenum	0.28 max	0.60–0.90	0.045	0.045	0.15–0.35	...	...	0.44–0.65	...	...	...
F 2[e]	0.5 % chromium, 0.5 % molybdenum	0.21 max	0.30–0.80	0.040	0.040	0.10–0.60	...	0.50–0.81	0.44–0.65	...	...	...
F 5[b]	4 to 6 % chromium	0.15 max	0.30–0.60	0.030	0.030	0.50 max	0.50 max	4.0–6.0	0.44–0.65	...	...	...
F 5a[b]	4 to 6 % chromium	0.25 max	0.60 max	0.040	0.030	0.50 max	0.50 max	4.0–6.0	0.44–0.65	...	...	...
F 6a	13 % chromium	0.15 max	1.00 max	0.040	0.030	1.00 max	0.50 max	11.5–13.5	...	...	...	...
F 6b	13 % chromium, 0.5 % molybdenum	0.15 max	1.00 max	0.02	0.02	1.0 max	1.0–2.0	11.5–13.5	0.40–0.60	Other Elements Cu 0.50 max		
F 6NM	13 % chromium, 4 % nickel	0.06 max	0.50–1.00	0.030	0.030	0.30–0.60	3.50–4.50	12.00–14.00	0.30–0.70	...	...	...
F 7	6 to 8 % chromium	0.15 max	0.30–0.60	0.030	0.030	0.50–1.00	...	6.0–8.0	0.44–0.65	...	...	...
F 9	9 % chromium	0.15 max	0.30–0.60	0.030	0.030	0.50–1.00	...	8.0–10.0	0.90–1.10	...	...	...
F 11	1.25 % chromium, 0.5 % molybdenum	0.10–0.20	0.30–0.80	0.040	0.040	0.50–1.00	...	1.00–1.50	0.44–0.65	...	...	...
F 12	1 % chromium, 0.5 % molybdenum	0.10–0.20	0.30–0.80	0.040	0.040	0.10–0.60	...	0.80–1.25	0.44–0.65	...	...	...
F 21	chromium-molybdenum	0.15 max	0.30–0.60	0.040	0.040	0.50 max	...	2.65–3.35	0.80–1.06	...	...	...
F 22	chromium-molybdenum	0.15 max	0.30–0.60	0.040	0.040	0.50 max	...	2.00–2.50	0.87–1.13	...	...	...
F XM-27[c]	27 chromium, 1 molybdenum	0.010 max	0.40 max	0.020	0.020	0.40 max	0.50 max	25.00–27.50	0.75–1.50	Other Elements N 0.015 max Cu 0.20 max		
F 429	15 chromium	0.12 max	1.00 max	0.040	0.030	0.75 max	0.50 max	14.0–16.0	...	...	...	...
F 430	17 chromium	0.12 max	1.00 max	0.040	0.030	0.75 max	0.50 max	16.0–18.0	...	...	...	...
Austenitic Steels												
F 304	18 chromium, 8 nickel	0.08 max	2.00 max	0.040	0.030	1.00 max	8.00–11.00	18.00–20.00	...	...	...	...
F 304H	18 chromium, 8 nickel	0.04–0.10	2.00 max	0.040	0.030	1.00 max	8.00–11.00	18.00–20.00	...	...	...	...
F 304L	18 chromium, 8 nickel, low carbon	0.035 max	2.00 max	0.040	0.030	1.00 max	8.00–13.00	18.00–20.00	...	...	...	...
F 304N[d]	18 chromium, 8 nickel, modified with nitrogen	0.08 max	2.00 max	0.030	0.030	0.75 max	8.00–10.50	18.00–20.00	...	...	...	...
F 310	25 chromium, 20 nickel	0.15 max	2.00 max	0.040	0.030	1.00 max	19.00–22.00	24.00–26.00	...	...	...	...
F 316	18 chromium, 8 nickel, modified with molybdenum	0.08 max	2.00 max	0.040	0.030	1.00 max	10.00–14.00	16.00–18.00	2.00–3.00	...	...	...
F 316H	18 chromium, 8 nickel, modified with molybdenum	0.04–0.10	2.00 max	0.040	0.030	1.00 max	10.00–14.00	16.00–18.00	2.00–3.00	...	...	...
F 316L	18 chromium, 8 nickel, modified with molybdenum, low carbon	0.035 max	2.00 max	0.040	0.030	1.00 max	10.00–15.00	16.00–18.00	2.00–3.00	...	...	...

TABLE 1 *Continued*

Identification Symbol	Grade	Composition, %								Columbium plus Tantalum	Tantalum, max	Titanium
		Carbon	Manganese	Phosphorus, max	Sulfur, max	Silicon	Nickel	Chromium	Molybdenum			
F 316N[d]	18 chromium, 8 nickel, modified with molybdenum and nitrogen	0.08 max	2.00 max	0.030	0.030	0.75 max	11.00–14.00	16.00–18.00	2.00–3.00	...	...	...
F 321	18 chromium, 8 nickel modified with titanium	0.08 max	2.00 max	0.030	0.030	1.00 max	9.00–12.00	17.00 min	...	...	...	[f]
F 321H	18 chromium, 8 nickel, modified with titanium	0.04–0.10	2.00 max	0.030	0.030	1.00 max	9.00–12.00	17.00 min	...	...	...	[f]
F 347	18 chromium, 8 nickel modified with columbium	0.08 max	2.00 max	0.030	0.030	1.00 max	9.00–13.00	17.00–20.00	...	[g]	...	...
F 347H	18 chromium, 8 nickel, modified with columbium	0.04–0.10	2.00 max	0.030	0.030	1.00 max	9.00–13.00	17.00–20.00	...	[h]	...	...
F 348	18 chromium, 8 nickel modified with columbium	0.08 max	2.00 max	0.030	0.030	1.00 max	9.00–13.00	17.00–20.00	...	[g]	0.10	...
F 348H	18 chromium, 8 nickel, modified with columbium	0.04–0.10	2.00 max	0.030	0.030	1.00 max	9.00–13.00	17.00–20.00	...	[h]	0.10	...
F XM-19	22 chromium, 13 nickel, 5 manganese	0.06 max	4.00–6.00	0.040	0.030	1.00 max	11.50–13.50	20.50–23.50	1.50–3.00	0.10–0.30	Other Elements N 0.20–0.40 V 0.10–0.30	
F 10	20 nickel, 8 chromium	0.10–0.20	0.50–0.80	0.030	0.030	1.00–1.40	19.00–22.00	7.00–9.00	...	...	...	...

[a] Grade F 2 was formerly assigned to the 1 % chromium, 0.5 % molybdenum grade which is now Grade F 12.

[b] The present grade F 5a (0.25 max carbon) previous to 1955 was assigned the identification symbol F 5. Identification symbol F 5 in 1955 was assigned to the 0.15 max carbon grade to be consistent with ASTM specifications for other products such as pipe, tubing, bolting, welding fittings, etc.

[c] Grade F XM-27 shall have a nickel plus copper content of 0.50 max %. Product analysis tolerance over the maximum specified limit for carbon and nitrogen shall be 0.002 %.

[d] Grades F 304N and F 316N shall have a nitrogen content of 0.10 to 0.16 %.

[e] Grade F 321 shall have a titanium content of not less than five times the carbon content and not more than 0.60%.

[f] Grade F 321H shall have a titanium content of not less than 4 times the carbon content and not more than 0.60 %.

[g] Grades F 347 and F 348 shall have a columbium plus tantalum content of not less than ten times the carbon content and not more than 1.00 %.

[h] Grades F 347H and F 348H shall have a columbium plus tantalum content of not less than 8 times the carbon content and nor more than 1.00 %.

TABLE 2 Product Analysis Tolerances for Low-Alloy Steels

Element	Limit or Maximum of Specified Range, %	Tolerance Over Maximum Limit or Under Minimum Limit for Size Ranges Shown, %[a]			
		100 in.² (6.45 × 10⁴ mm²), or less	Over 100 to 200 in.² (1.290 × 10⁵ mm²), incl	Over 200 to 400 in.² (2.581 × 10⁵ mm²), incl	Over 400 in.²
Manganese	to 0.90 incl	0.03	0.04	0.05	0.06
	over 0.90 to 1.00 incl	0.04	0.05	0.06	0.07
Phosphorus	to 0.045 incl	0.005	0.010	0.010	0.010
Sulfur	to 0.045 incl	0.005	0.010	0.010	0.010
Silicon	to 0.40 incl	0.02	0.02	0.03	0.04
	over 0.40 to 1.00 incl	0.05	0.06	0.06	0.07
Nickel	to 0.50	0.03	0.03	0.03	0.03
Chromium	to 0.90 incl	0.03	0.04	0.04	0.05
	over 0.90 to 2.10 incl	0.05	0.06	0.06	0.07
	over 2.10 to 3.99 incl	0.10	0.10	0.12	0.14
Molybdenum	to 0.20 incl	0.01	0.01	0.02	0.03
	over 0.20 to 0.40 incl	0.02	0.03	0.03	0.04
	over 0.40 to 1.15 incl	0.03	0.04	0.05	0.06

[a] Cross-sectional area

TABLE 4 Tensile and Hardness Requirements

Grade Symbol	Tensile Strength, min, ksi (MPa)	Yield Strength, min, ksi (MPa) (0.2 % offset)	Elongation in 2 in. or 50 mm, min, %	Reduction of Area, min, %	Brinell Hardness Number, max
Ferritic Steels:					
F 1	70 (483)	40 (276)	25.0	35.0	143-192
F 2	70 (483)	40 (276)	20.0	30.0	143-192
F 5	70 (483)	40 (276)	20.0	35.0	143-217
F 5a	90 (621)	65 (448)	22.0	50.0	187-248
F 6a Class 1	70 (483)	40 (276)	18	35.0	143-187
F 6a Class 2	85 (586)	55 (379)	18	35.0	167-229
F6a Class 3[e]	110 (758)	85 (586)	18	35.0	207-302
F 6a Class 4[e]	130 (896)	110 (758)	18	35.0	263-321
F 6b	110-135 (758-930)	90 (621)	16	45.0	235-285
F 6NM	110-135(758-930)	90 (621)	15	35.0	235-285
F 7	70 (483)	40 (276)	20.0	35.0	143-217
F 9	85 (586)	55 (379)	20.0	40.0	179-217
F 11	70 (483)	40 (276)	20.0	30.0	143-207
F 12	70 (483)	40 (276)	20.0	30.0	143-207
F 21	75 (517)	45 (310)	20.0	30.0	156-207
F 22	75 (517)	45 (310)	20.0	30.0	156-207
F XM-27	60 (414)	35 (241)	20.0	45.0	190 max
F 429	60 (414)	35 (241)	20.0	45.0	190 max
F 430	60 (414)	35 (241)	20.0	45.0	190 max
Austenitic Steels:					
F 304	75 (517)[a]	30 (207)	30	50	...
F 304H	75 (517)[a]	30 (207)	30	50	...
F 304L	70 (483)[a]	25 (172)	30	50	...
F 304N	80 (552)	35 (241)	30[c]	50[d]	...
F 310	75 (517)[a]	30 (207)	30	50	...
F 316	75 (517)[a]	30 (207)	30	50	...
F 316H	75 (517)[a]	30 (207)	30	50	...
F 316L	70 (483)[a]	25 (172)	30	50	...
F 316N	80 (552)	35 (241)	30[c]	50[d]	...
F 347	75 (517)[a]	30 (207)	30	50	...
F 347H	75 (517)[a]	30 (207)	30	50	...
F 348	75 (517)[a]	30 (207)	30	50	...
F 348H	75 (517)[a]	30 (207)	30	50	...
F 321	75 (517)[a]	30 (207)	30	50	...
F 321H	75 (517)[a]	30 (207)	30	50	...
F XM-19	100 (690)	55 (380)	35	55	...
F 10	80 (552)	30 (207)	30	50	...

[a] For sections over 5 in. in thickness, the minimum tensile strength shall be 70 ksi (483 MPa).
[b] For sections over 5 in. in thickness, the minimum tensile strength shall be 65 ksi (448 MPa).
[c] Longitudinal. The transverse elongation shall be 25 % in 2 in. or 50 mm, min.
[d] Longitudinal. The transverse reduction of area shall be 45 % min.
[e] No weld repair is permitted for these classes.

TABLE 3 Product Analysis Tolerances for Higher Alloy and Stainless Steels[a]

Elements	Limit or Maximum of Specified Range, %	Tolerance Over the Maximum Limit or Under the Minimum Limit
Carbon	0.030, incl	0.005
	over 0.030 to 0.20 incl	0.01
Manganese	to 1.00, incl	0.03
	over 1.00 to 2.00, incl	0.04
Phosphorus	to 0.040, incl	0.005
Sulfur	to 0.030, incl	0.005
Silicon	to 1.00, incl	0.05
	over 1.00 to 1.40, incl	0.10
Chromium	over 4.00 to 10.00, incl	0.10
	over 10.00 to 15.00, incl	0.15
	over 15.00 to 20.00, incl	0.20
	over 20.00 to 27.50, incl	0.25
Nickel	to 1.00, incl	0.03
	over 1.00 to 5.00, incl	0.07
	over 5.00 to 10.00, incl	0.10
	over 10.00 to 20.00, incl	0.15
	over 20.00 to 22.00, incl	0.20
Molybdenum	over 0.20 to 0.60, incl	0.03
	over 0.60 to 1.75, incl	0.05
	over 1.75 to 3.00, incl	.10
Titanium	all ranges	0.05
Columbium-tantalum	all ranges	0.05
Tantalum	to 0.10, incl	0.02
Cobalt	0.05 to 0.20, incl	0.01[b]
Nitrogen	to 0.16, incl	0.01

[a] This table does not apply to heat analysis.

[b] Product analysis limits for cobalt under 0.05% have not been established and the producer should be consulted for those limits.

TABLE 5 Repair Welding Requirements

Grade Symbol	Electrodes[a]	Recommended Preheat and Interpass Temperature Range; °F (°C)	Minimum Post Weld Heat-Treatment Temperature °F (°C)
Ferritic Steels:			
F 1	E 7018-A 1	200–400 (95–205)	1150 (620)
F 2	E 8018-B 1	300–600 (150–315)	1150 (620)
F 5	E 502-15 or 16	400–700 (205–370)	1250 (677)
F 5a	E 502-15 or 16	400–700 (205–370)	1250 (677)
F 6a	E 410-15 or 16	400–700 (205–370)	1400 (760)
F 6b	13 % Cr, 1½ % Ni, ½ % Mo	400–700 (205–370)	1150 (620)
F 6NM	13 % Cr, 4 % Ni	300–700 (150–370)	1050 (565)
F 7	E 7 Cr-15	400–700 (205–370)	1250 (677)
F 9	E 505-15 or 16	400–700 (205–370)	1250 (677)
F 11	E 8018-B 2	300–600 (150–315)	1150 (620)
F 12	E 8018-B 2	300–600 (150–315)	1150 (620)
F 21	E 9018-B 3	300–600 (150–315)	1250 (677)
F 22	E 9018-B 3	300–600 (150–315)	1250 (677)
F XM-27	26 % Cr, 1 % Mo	NR[c]	NR
F 429	E 430-16	400–700 (205–370)	1400 (760)
F 430	E 430-16	NR	1400 (760)
Austenitic Steels:			
F 304	E 308-15 or 16	NR	1900 (1040) + WQ[d]
F 304L	E 308L-15 or 16	NR	1900 (1040) + WQ
F 304H	E 308-15 or 16	NR	1900 (1040) + WQ
F 304N	E 308-15 or 16	NR	1900 (1040) + WQ
F 310	E 310-15 or 16	NR	1900 (1040) + WQ
F 316	E 316-15 or 16	NR	1900 (1040) + WQ
F 316L	E 316L-15 or 16	NR	1900 (1040) + WQ
F 316H	E 316-15 or 16	NR	1900 (1040) + WQ
F 316N	E 316-15 or 16	NR	1900 (1040) + WQ
F 321[b]	E 347-15 or 16	NR	1925 (1050) + WQ
F 321H[b]	E 347-15 or 16	NR	1900 (1040) + WQ
F 347	E 347-15 or 16	NR	1925 (1050) + WQ
F 347H	E 347-15 or 16	NR	1900 (1040) + WQ
F 348	E 347-15 or 16	NR	1925 (1050) + WQ
F 348H	E 347-15 or 16	NR	NR
F XM-19	XM-19W	NR	NR
F 10[b]	...	NR	

[a] Electrodes shall comply with ASME SFA 5.4 or SFA 5.5.
[b] Purchaser approval required.
[c] NR = not required.
[d] WQ = water quench.